ENGINEERING GEOLOGICAL INVESTIGATIONS

OF THE

WHARANUI EARTHFLOW

NORTHEAST MARLBOROUGH

A thesis
submitted in partial fulfillment
of the requirements for the Degree
of
Master of Science in Engineering Geology
in the
University of Canterbury
by

L. JASON MORRIS

University of Canterbury
1986

ABSTRACT

The Wharanui Earthflow, located 67 km south of Blenheim on the Kaikoura Coast, is of concern because of its proximity to State Highway 1. This thesis provides a detailed engineering geological assessment of its nature and movement to assist in determination of appropriate remedial measures. Field methods used in this study included engineering geological mapping, geophysical profiling, trench excavation, hand augering, and the installation of a comprehensive surface monitoring network.

The Earthflow descends 210 metres over a total length of 1 km, it ranges in width from 30 to 100 metres, and it has five distinct terminal lobes, only one of which is currently active. The lobes result from episodic movement of accumulated materials which are derived from adjacent feeder earthflows and from other types of slope movment occurring on the valley sides. These deposits consist of fine grained cohesive soils with a significant proportion of smectite clays. In-situ bedrock underlies the Wharanui Earthflow at depths of approximately 2 to 7 metres, and a number of shear surfaces have been identified in the earthflow deposits.

Localized zones of continuing movement are bounded by clearly defined basal and lateral shears, although monitoring showed little movement in the period since installation of the survey network, with displacements commonly less than 100 mm. Past movements have apparently exceeded 4.5 metres/year, and periods of displacement are related to cycles (5 year plus) of higher than average rainfall. Larger scale reactivation than is currently observed must be anticipated given the nature and quantities of debris in storage within the Earthflow, particularly in the upper portion.

Past remedial measures including drainage and planting have not successfully stabilized the Wharanui Earthflow. It is necessary that monitoring of the active

toe be continued on a regular basis, and recommended that a simple warning system be installed to indicate any sudden acceleration towards State Highway 1. Potential long-term solutions include drainage and planting, but a full geotechnical investigation and analysis is an essential pre-requisite to the design of any such remedial measures.

ACKNOWLEDGEMENTS

The following people and organisations are most sincerely thanked for the assistance given during the preparation of this thesis:

The Ministry of Works and Development, Blenheim, for financial assistance, and particularly Mr. Mike Peterson for his interest and help during the study. The people of the M.W.D., Christchurch, for allowing me to use their computer for survey triangulation.

My supervisors Mr. D.H. Bell and Dr. J.R. Pettinga for their guidance and editing of the thesis drafts.

Chris Thornley, Albert Downing, Glen Coates, Arthur Alloway, and Davy Jones of the University of Canterbury, Geology Dept. for their help in lots of things.

My classmates Julie, Roosell, Phil K., Mark, Phil G. and Doug for their encouragement, friendship, and sense of humour at work and at the class barbecues.

My great field assistants Russel Sanders, Mark Yetton, Phil & Lizzy Kelsey, Andrew Macfarlane, and especially Julie Mackwell for her tolerance and perseverance in locating grass covered survey points, cooking amazing garlic chicken, and for her warm companionship during the study.

Margaret and David Parsons for supplying wonderful accommodation while in the field.

Dee, Rob M., Mike & Julie, Phil K., Rob R., Pete, Sybil, and Andrea for their tremendous efforts when time was running out.

And to family and friends at home for staying close, even though thousands of miles away.

TABLE OF CONTENTS

CHAPTER THREE: SITE GEOLOGY AND GEOMORPHOLOGY

CHAPTER FOUR: EARTHFLOW DESCRIPTION AND MORPHOLOGIC DEVELOPMENT

APPENDICES

CHAPTER ONE

INTRODUCTION

1.1 SCOPE OF THESIS

The purpose of this project is to conduct detailed engineering geological investigations of the Wharanui Earthflow in order to 1) identify the nature and causes of movement, and 2) provide data pertinent to the determination and design of appropriate remedial measures.

The Wharanui Earthflow is located on the east coast of the South Island, Marlborough, New Zealand, approximately 67 kilometres northeast of Kaikoura and 62 kilometres south of Blenheim (Fig. 1.1). The "active" toe of the Earthflow lies within 25 metres of State Highway one and threatens disruption of this major transportation route (Figure 1.2). There has, however, been no movement which has forced closure of the highway at anytime.

The proximity of the Earthflow to the highway has caused the Ministry of Works and Development concern for many years. A drainage network was installed around the active toe in 1974 and upgraded in 1976 in an attempt to stabilize the toe. In addition, the Marlborough Catchment Board planted trees in 1978 in hopes of establishing a vegetative cover to 1) enhance interception of precipitation, and 2) increase regolith strength by introducing a root network, thus improving the stability. Neither the drainage scheme, nor the tree planting has been successful in arresting movement since the MWD began monitoring the Earthflow in 1976.

In 1984 the M.W.D., Blenheim, asked Mr. Brian Paterson of the New Zealand Geological Survey, Christchurch, to evaluate the Wharanui Earthflow and make recomendations concerning its stabilization. His report was the first

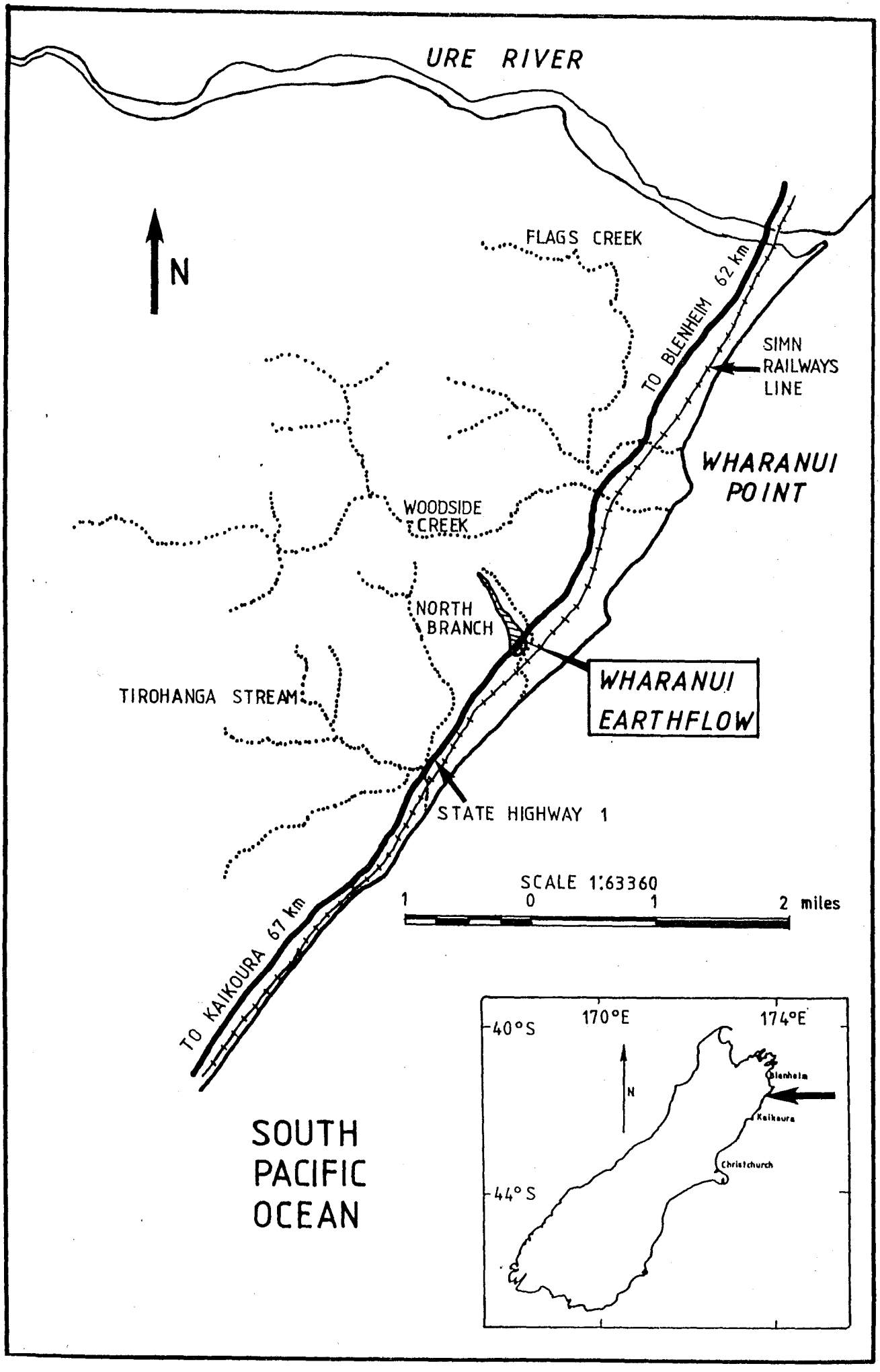

Figure 1.1 Locality Map of the Wharanui Earthflow.

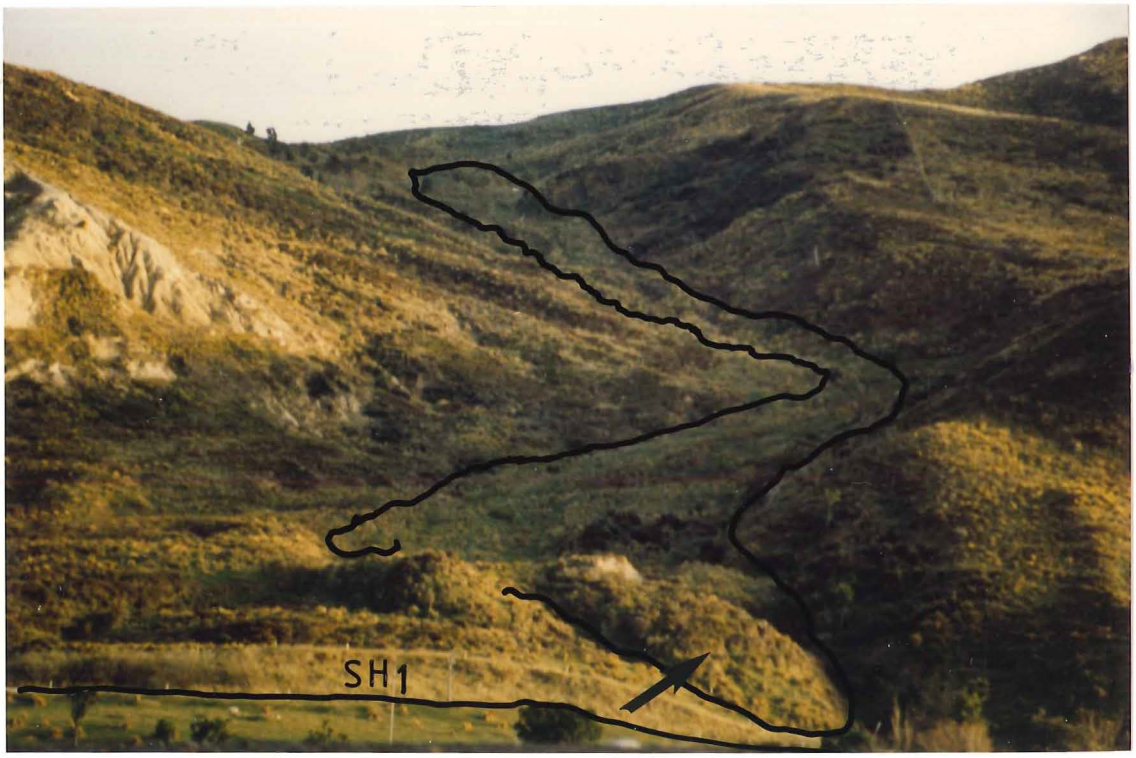

Figure 1.2 View looking northwest up towards the Wharanui Earthflow from the beach. The Earthflow boundaries are outlined and the active toe (arrowed) is 25 metres from State Highway 1 (S36 326E 454N).

engineering geological work concerned with the Wharanui Earthflow and called for further investigations which was the basis for the decision to make the Earthflow a thesis topic.

The Earthflow is not a life-threatening situation. The primary concern is to evaluate the landslide problem, with the ultimate objective of eliminating or reducing the hazard so that there is not a continual cost of maintenance, or at least maintenance costs are kept to a minimum.

1.2 REGIONAL GEOLOGIC SETTING

The Wharanui Earthflow is located within the structural/tectonic zone known as the East Coast Deformed Belt (Sporli 1980). This extends from East Cape of the North island southward through to Marlborough where it terminates in upper Cretaceous and Cainozoic covering strata which are complexly faulted and folded (Fig. 1.3). These strata are characterized by widespread fine-grained lithologies in which siliceous shale, chert, and micritic argillaceous limestone are dominant. Major structural features within the area include two dextral faults, the Clarence Fault and the Kekerengu Fault, which are boundaries for the Ben More block. The Ben More block consists of a complex north-east-plunging anticline, the Ben More Anticline, which is wrapped around a core of underlying indurated Mesozoic strata (Prebble 1980).

The cover lithologies were deformed by folding followed by dextral faulting on the northeast striking Kekerengu Fault (Prebble 1980). (Fig. 1.4). Minor faults in the area are the Deep Creek Fault, and a splinter off it, the Woodside Fault. Both the Deep Creek Fault and the Woodside Fault trend northwest-southeast and encompass a large "crush" zone between them. Most rocks within the zone are sheared and many are intensely fractured and crushed. The Woodside Fault is the predominant structural feature related to the Earthflow, which lies along its axis, and is a major factor influencing valley development where the flow

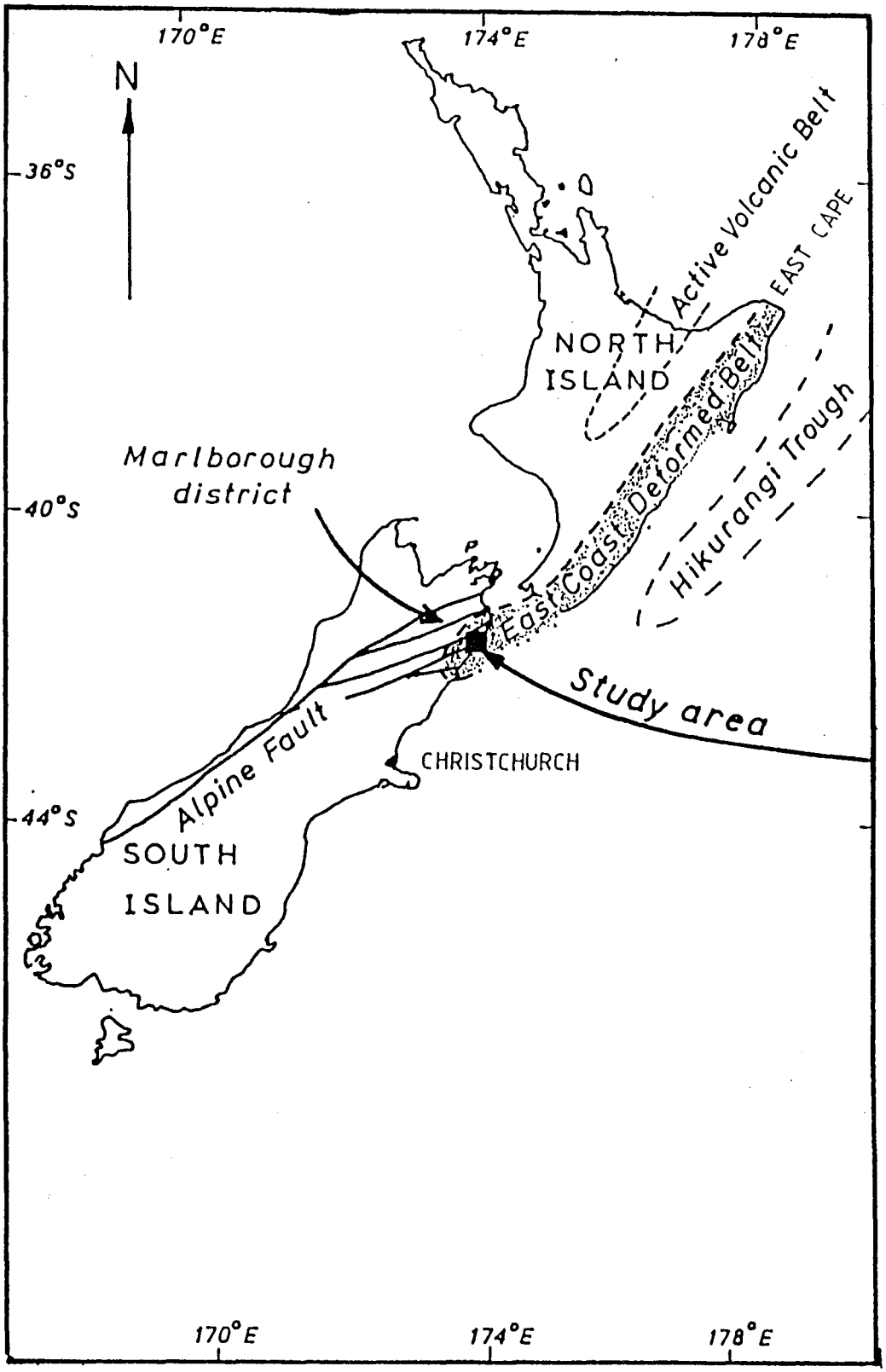

Figure 1.3 Locality Map showing the position of the study area within the East Coast Deformed Belt (from Prebble, 1980).

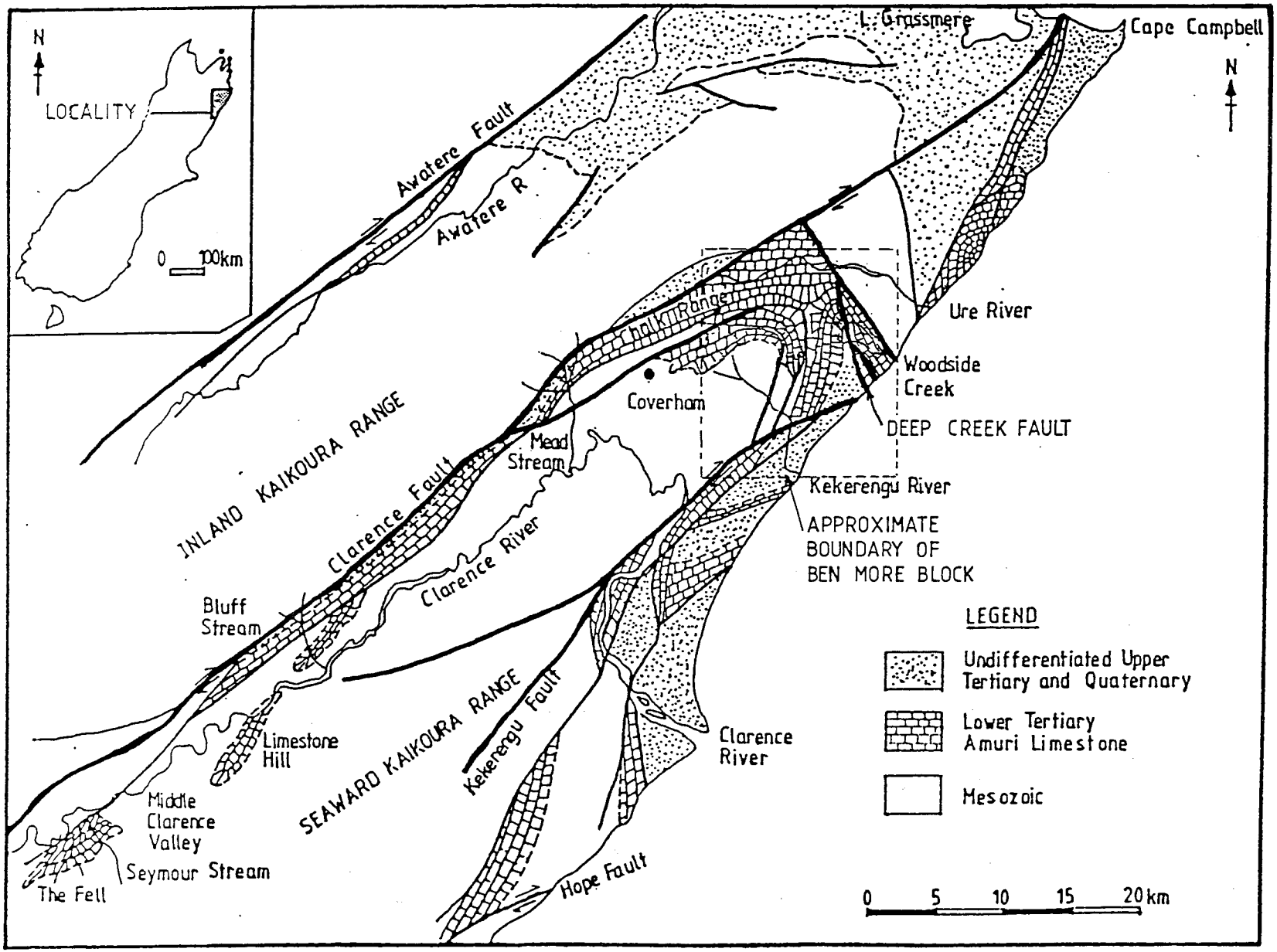

Figure 1.4 Generalised geological map of Marlborough (After Lensen, 1962; modified by Fergusson, 1985).

is located. The Deep Creek Fault is the boundary of an older stabilized landslide,the Ben More Earthflow, 500 metres southwest of the Wharanui Earthflow. (See Fig. 1, map pocket).

1.3 SITE DESCRIPTION

The thesis area is characterized by steep hills and ridges, deeply incised by streams and creeks. The most striking feature is Woodside Creek which has developed a deep joint controlled gorge incised within the Whangai Shale and the Amuri Limestone. Relief ranges from sea level to 288 metres (944 ft), Flags trig being the highest point.

Primary drainage systems besides Woodside Creek are the north branch of Tirohanga Stream, a minor stream south of "Flags" trig here named Delta Stream, and a small intermittent stream which flows from the Wharanui Earthflow valley here named Pipe Stream (see Fig 1.5). These systems discharge onto a narrow coastal strip where they have built small alluvial plains and fans. A 300 m wide beach plain of sand dune ridges and gravel separates the alluvial and debris fans from the present beach. See Fig. 1.5 and/or Fig. 1 (map pocket), for site geology and geomorphology.

The valley catchment of the Wharanui Earthflow is approximately 22 hectares, and the Earthflow itself comprises an area of approximately 5 hectares. It extends approximately 1 km from the headscarp to the "active" toe, and varies in width from 30 m to 100 m. It descends approximately 210 m along the length of the valley, and exibits a sinuous shape with the general flow direction being to the southeast.

In cross-section the valley of the Wharanui flow is asymmetric, with the eastern boundary a steep sided ridge, and the western boundary a long gently sloping ridge. Both of the ridges contribute debris material to the main flow body by several means, such as feeder flows, shallow regolith earth-slides, and erosion.

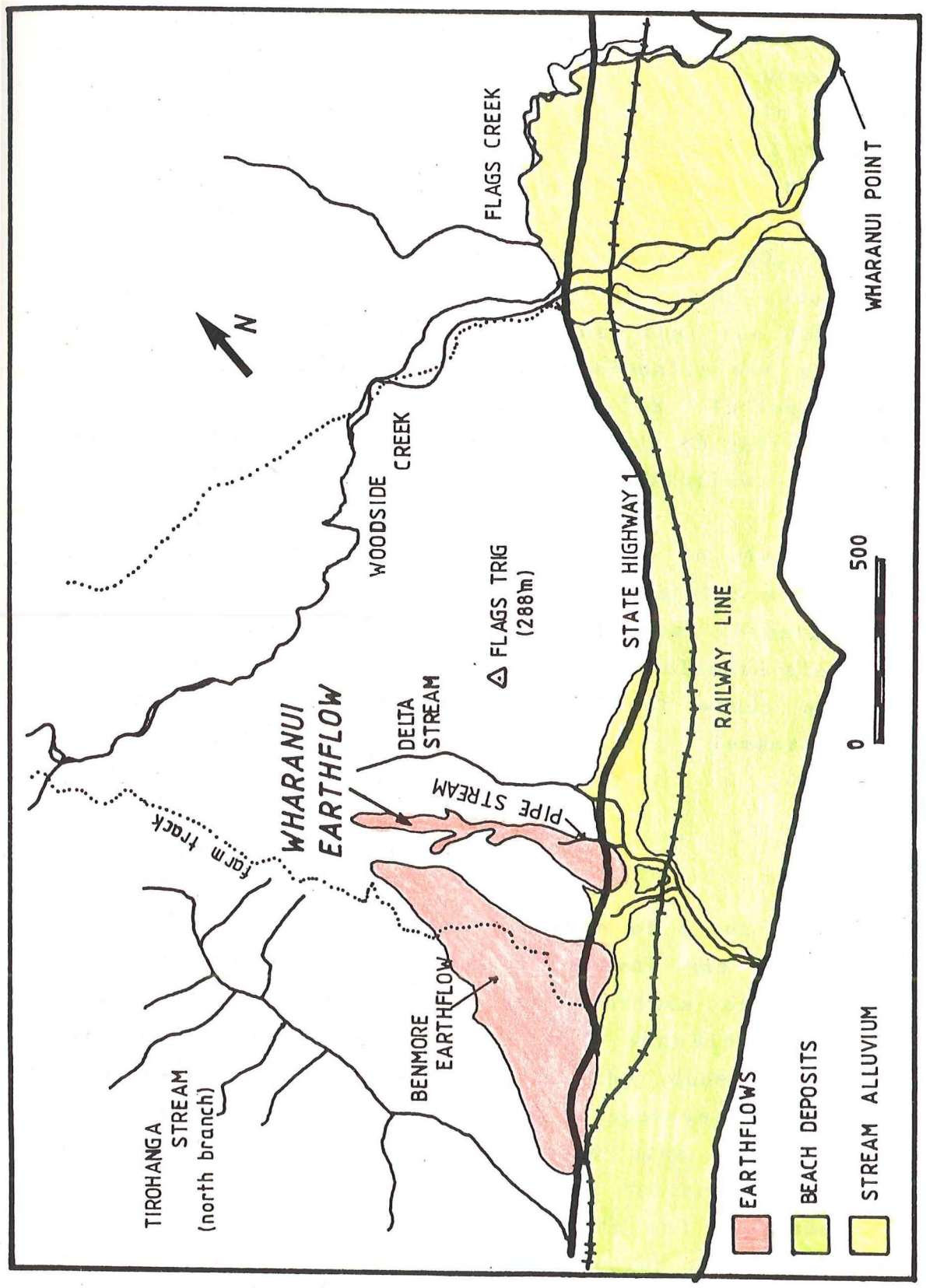

Figure 1.5 Primary drainage systems within the site showing areal extent of alluvial and beach deposits.

1.4 CLIMATE, VEGETATION, AND LAND USE

1.4.1 Climate

The two major influences upon the climate within the thesis area are the close proximity to the ocean and the hilly topography of the area. Rainfall within the thesis area averages 920 mm/year and is normally well distributed throughout the year. Figure 1.6 shows the yearly rainfall deviation from normal for the 44 year span from 1941-1985. Exceptionally wet months were January (1949, 1953, and 1961), March (1975 and 1980), April (1978), June (1950), July (1948), and August (1977). Note that the periods from 1947-1953 and 1974-1980 were exceptionally wet years; this will be discussed further in section 5.3.2 in regards to the effect of long term precipitation trends (5 years plus) upon the rate of movement of the Wharanui Earthflow.

The prevalent winds of the area in winter are cold southerlies but many of the southerly storms which hit the Kaikoura penninsula by-pass just offshore. Frosts are rare in the low altitude areas as the marine climate elevates the temperatures. In the summer prevalent winds are strong north westerlies or south westerlies. Temperatures are normally hot, frequently reaching 30^{o}C.

1.4.2 Vegetation

The beaches are almost barren of plant life until a zone is reached where sand or gravel has been somewhat consolidated. Here plant life consists of convolvulus, creeping sandsedge, pingao, and occasionally silvery Spinifex or Sand-grass. Where the dunes become more consolidated, other plants such as scab-weed and club-rush are common. The hills within the area are mostly well covered in silver tussock with some bracken fern, and some areas are covered in thick matagouri and Coprosma. Beech and broad leaf forests with such species as kowhai, red and white manuka, cream-wood, red maple and marbleleaf are found in parts of Woodside Creek, as are various unusual plant

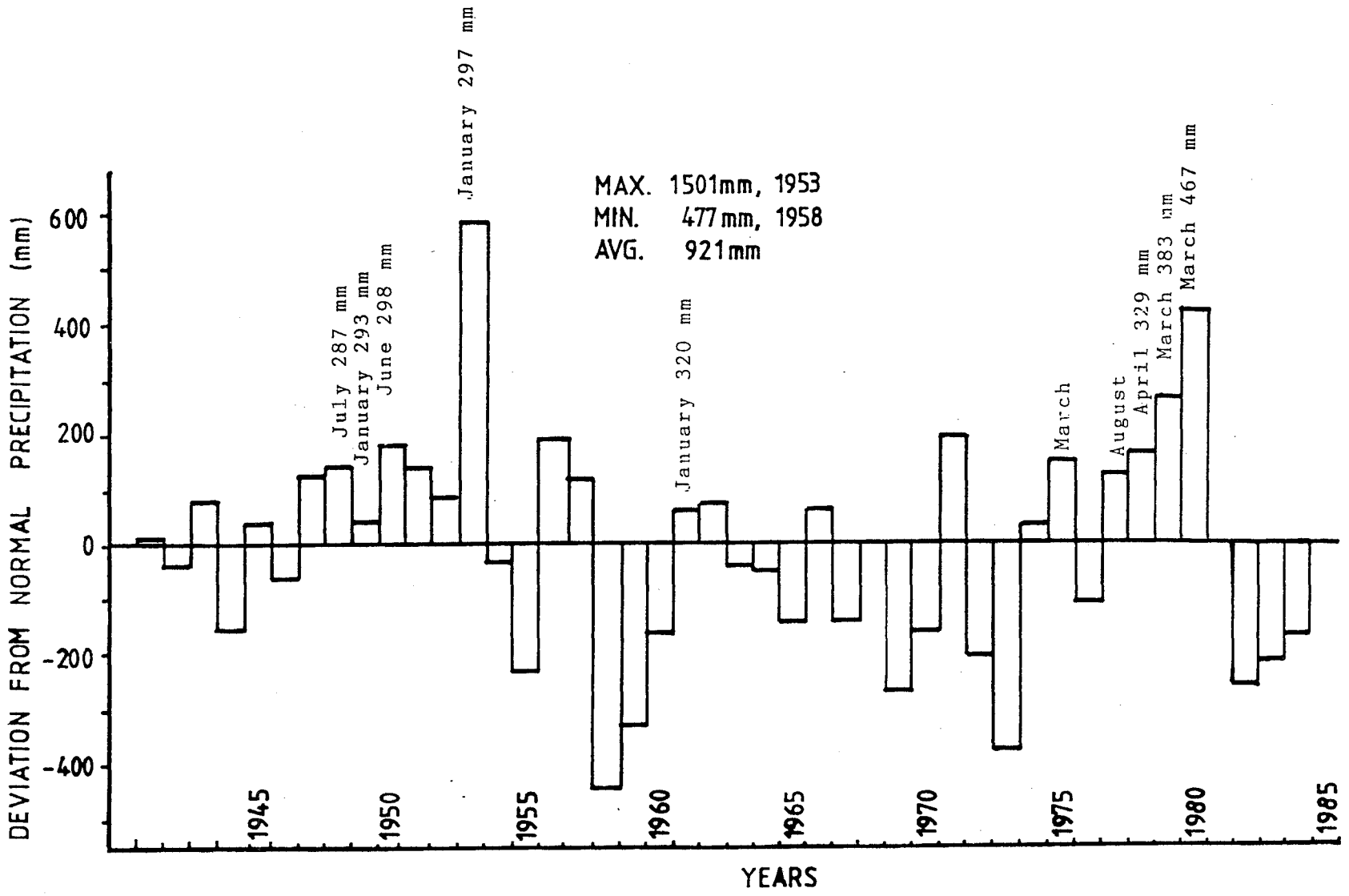

Figure 1.6 Rainfall data since 1941 showing the deviation from average precipitation, and months with excessive rainfall (rainfall data from Wharanui Station, 1.8 km north of Wharanui Earthflow).

species in the Gorge of Woodside Creek. These species usually found on the limestone cliffs of the gorge, are peculular to Marlborough and include willow-herbs, rare buttercups, Pink Broom, and blue bells.

1.4.2 Land Use

Primary land use in the thesis area is for grazing sheep and cattle. The Wharanui Earthflow itself is considered to be an area of prime grazing especially for pre-lamb ewes.

1.5 INVESTIGATION METHODOLOGY

1.5.1 Work Programme

The field investigation of the Earthflow included a geologic reconnaissance, an augering/sampling program, geophysical profiling and field instrumentation. The studies were planned to determine the probable earthflow mechanism(s) and to monitor any movement. Optimisation of available resources was necessary as there was limited funding for the project. Specifically the investigations included:

1. Detailed engineering geological mapping of the surrounding area at a scale of 1:5000; of the Earthflow at a scale of 1:1000; and of the toe area at a scale of 1:500.

2. Investigations of the subsurface conditions by hand augering, trenches and seismic traverses.

3. Installation of a comprehensive surface monitoring system with a primary network measuring movement along the length of the flow, and a secondary network measuring movement across tension cracks and scarps.

4. Installation of piezometers for pore pressure measurement, and to indicate subsurface movement.

5. Laboratory analysis of the materials comprising the Wharanui Earthflow to determine their composition and geotechnical characteristics.

6. Synthesis of data to establish principal causes of instability.

1.5.2 Fieldwork

Fieldwork began in June 1984 with the installation of base points for the survey network. This was followed by a topographic survey of the Earthflow for use as base plans for mapping at scales of 1:1000 and 1:500 and for planning the monitoring network.

A primary monitoring network which is intended to measure the type and rate of movement along the length of the flow was decided upon and installed. This was initially to be re-surveyed every 3 months, but a 3 month survey interval was deemed as unnecessary as there were no visible signs of activity, finally, the surveys were conducted at 6 month intervals.

A secondary monitoring network was installed in the active toe area of the flow so that the relative movement across tension cracks and scarps could be measured. Monitoring points were placed in a line across tension cracks in succession and relative vertical and horizontal displacements was measured. The purpose of this was to provide a qualitative knowledge of activity and enabled cumulative strain to be measured in the specific zone of interest.

After the monitoring networks were installed, detailed engineering geological mapping was completed which also provided survey base control.

Hand auger boreholes were used for subsurface sampling (disturbed), and to assist geophysical profiling in the determination of the depth to bedrock and subsurface geometry. In selected boreholes piezometers were installed so that groundwater pressure could be monitored, and as an indicator of subsurface movement from deformation of the piezometer standpipes.

Trenches were excavated so that an undisturbed profile of soil horizons could be examined and undisturbed samples could be extracted. Field description of engineering soils sampled during augering and logging of Trenches was completed using methods outlined by Bell and Pettinga (1984), and are presented on summary sheets in the map pocket (Fig. 6 and 7). In-situ shear strength determination of the materials were conducted during hand augering using a Genor shear vane .

1.5.3 Laboratory Studies

Laboratory analysis of materials involved within the flow was carried out on representative samples so that the materials' physical and hydraulic properties would enable interpretation of the failure mechanism(s). Originally triaxial shear strength testing was proposed, but this was not possible as suitable samples were unobtainable (discussed in Chapter 4).

Laboratory tests performed included:

1. natural moisture contents;
2. Atterburg limits;
3. sieve and hydrometer analysis for grainsize distribution;
4. linear shrinkage
5. whole sample and clay fraction mineralogy by X-ray diffraction; and
6. falling head permeabilty test.

Methods used in the laboratory programme are detailed

in Appendix 3 - 5, and discussed in Chapter Four.

1.5.4 Thesis Organization

The thesis has been organized into six chapters. Chapter Two is a Literature review of pertinent information regarding mass movement, with special reference to earthflows and their instrumentation. Chapter Three deals with the geology and geomorphology of the thesis area. Chapter Four discusses the morphology of the Wharanui Earthflow, the subsurface investigations, the material characteristics found in the laboratory programme, and proposes a model for Earthflow development and failure. Chapter Five describes the monitoring systems, the history of movement, the movement which occurred over the monitoring period, a discussion of stability and proposes remedial measures. Chapter Six contains the conclusions from the investigations.

CHAPTER TWO

A REVIEW OF EARTHFLOW TERMINOLOGY, MECHANISMS, AND INSTRUMENTATION

2.1 OBJECTIVES

The primary objective of this chapter is to give a brief summary of slope movement types, mechanisms, and classifications. Special attention is paid to earthflows, their morphology, and their mobilization. In a later chapter a model for the Wharanui Earthflow is developed, drawing in part from the mechanisms described herein.

The second part of this chapter is concerned with instrumentation used for the investigation of landslides in general and then focuses on the instrumentation used to study the Wharanui earthflow, the reasons for their selection, and their performance.

2.2 SLOPE MOVEMENTS

2.2.1 Introduction

Slope movement has been defined by Shuster (1978) as,

"the downward and outward movement of slope-forming materials - natural rock, soils, artificial fills, or combinations of these materials".

Lithology, structure, and tectonic setting are primary geological factors which predispose certain types of terrain to slope movement. The influence of rock structures (bedding planes, schistosity planes, folds, faults, and joints) are important in slope stability, as they may act as planes of failure. The importance of lithology alone in slope failures, even without the additional factors of unfavourable structure or oversteepened slope, is

demonstrated by many examples of slope movements associated with a particular type of rock or soil (ie. Norwegian quick clays, the London Clays, and Franciscan sedimentary complex of California). Other factors significantly influencing shallow slope movement are slope gradient, slope shape, and hydrologic properties of the soil.

2.2.2 Classifications

Slope movement classification systems usually attempt to catagorize material which has moved downslope in terms of similar morphology, material, and mechanism. One of the first classification schemes proposed was by Sharpe (1938) who classified slope movement based on type, material, and rate of movement. The Sharpe classification scheme is summarised in Fig. 2.1.

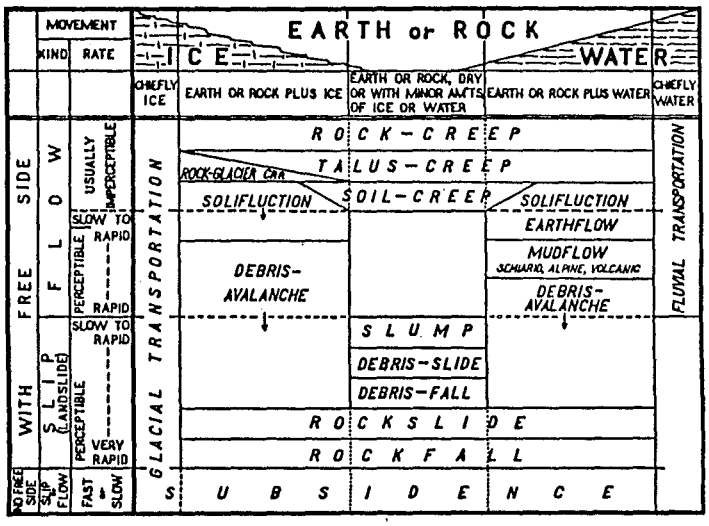

Figure 2.1 Sharpes' Classification (1938).

Since Sharpes' classification the subject has been intensively studied and there have been numerous proposals for classification schemes, [ie. Hutchinson, (1968); Zaruba and Mencl, (1969); Carson and Kirkby, (1972); Blong, (1973); Northey et al., (1974); and Varnes, (1958, 1978)].

Varnes (1958) proposed a slope movement classification based on mechanisms of failure, and type of material which he divided into 3 groups as slides, flows and

topples. He later modified the system (1978) to include falls and lateral spreads, as well as complex slope movements which are combinations of the principle types. An abbreviated version of the Varnes classification is shown in Fig 2.2.

TYPE OF MOVEMENT			TYPE OF MATERIAL		
			BEDROCK	ENGINEERING SOILS	
				Predominantly coarse	Predominantly fine
FALLS			Rock fall	Debris fall	Earth fall
TOPPLES			Rock topple	Debris topple	Earth topple
SLIDES	ROTATIONAL	FEW UNITS	Rock slump	Debris slump	Earth slump
	TRANSLATIONAL	FEW UNITS	Rock block slide	Debris block slide	Earth block slide
		MANY UNITS	Rock slide	Debris slide	Earth slide
LATERAL SPREADS			Rock spread	Debris spread	Earth spread
FLOWS			Rock flow (deep creep)	Debris flow	Earth flow (soil creep)
COMPLEX			Combination of two or more principal types of movement		

Figure 2.2 Abbreviated Version of Varnes Classification (1978).

Varnes further supplements the classification scheme with speed of movement which can vary from extremely rapid (3 m/second) to extremely slow (0.3 m/five years) Fig. 2.3.

The Varnes (1978) classification will be used in this study to define slope failures. However it should be noted that a rigid classification system is neither necessary nor desirable, as movement and materials vary from place to place and slope failure types will grade from one type to another.

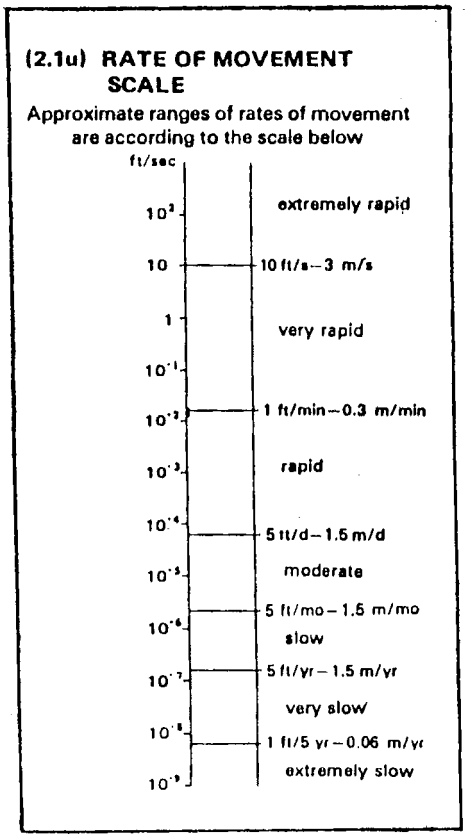

Figure 2.3 (from Varnes, 1978).

2.2.3 Movement Types Related To Study

The common types of slope movement occuring within the thesis area are slides, flows, and complex variations of the two.

Slides. In slides movement consists of shear strain and displacement along one or several surfaces that are visible or may be reasonably inferred within a narrow zone (Varnes 1978). Most of the slides within the thesis area are shallow (less than 1 m) translational slides, ie. slides predominantly along more or less planar or gently undulatory surfaces (Varnes, 1978). In the area studied these are shallow regolith "earth slides" of depths less than 1m, which normally occur within the residual regolith, or at the regolith bedrock interface. Such failures are generally rapid and normally occur due to high intensity rainstorms (Bell, 1976). Regolith becomes saturated and an increase in pore-pressures increases the shear stresses leading to failure.

Flows. In flows movement takes the form of a viscous fluid with spatially continuous deformation. This can result in bulging and other manifestations of plastic behaviour. Subaerial flows occuring in fine grained engineering soils such as sand, silt, or clay are classified as earthflows. The term "earthflow" as used in this thesis refers to the "drier and slower" type of earthflow described by Varnes (1978).

The term "earth" refers to soils in which 80% or more of the particles are smaller than 2 mm in diameter; it includes a range of materials from nonplastic sand to highly plastic clay (Varnes, 1978). "Debris flows" and "debris-slide-flow" combinations are slope movements commonly confused with earthflows and mudflows but differ in several ways, the major distinction being grainsize. "Debris" refers to soils in which 20-80% of the particles are larger than 2 mm in diameter (Varnes, 1978).

2.3 MATERIALS AND MORPHOLOGY OF EARTHFLOWS

2.3.1 Lithologies Associated With Earthflows

Bedrock lithologies from which earthflows derive are varied including stiff fissured clays, flysh, altered and weathered volcanic rocks, tectonic melange, glacial till, and poorly consolidated shale, mudstone, and sandstone. Keefer and Johnson (1983) tabulated earthflow bedrock types from various parts of the world, and these are shown in Table 2.1.

In addition to those listed it should be noted that in New Zealand earthflows commonly occur in Upper Cretaceous and Cenozoic "soft rock" sedimentary formations. In particular earthflows are associated with smectite mudstones. Some of these earthflows other than the Wharanui Earthflow include:

1) The Mikonui Earthflow, which lies on the Kaikoura coast (east coast, South Island), 3 km south of Oaro. This earthflow occurs within smectite mudstones of Upper Cretaceous age (Grocott, 1977).

2) The Waerenga-o-kuri Earthflow located in the Waerengaokuri Basin (east coast, North Island). This earthflow occurs within blue-grey smectite mudstones of Eocene age (Bishop, 1968).

3) The Blue Slip which is a complex earth-slump-flow which occurs within the smectite mudstones of Middle Eocene age (Macpherson, 1952).

4) Within the Poverty Bay East-Coast Region are numerous earthflows associated with various lithologies including smectite mudstones, argillites, sandstones, and shale (Smith, 1974).

EARTH-FLOW MORPHOLOGY, MATERIALS, AND SETTINGS

—Bedrock in areas containing abundant earth-flow deposits outside the San Francisco Bay region

Area	Bedrock	Reference
Redwood Creek basin, northern California.	Franciscan assemblage (upper Mesozoic): Unmetamorphosed argillaceous rocks and slightly metamorphosed highly sheared sedimentary rocks.	Harden and others (1978).
Van Duzen River basin, northern California.	Franciscan melange (Mesozoic and early Cenozoic): Highly sheared clayey siltstone.	Kelsey (1977).
Eel River basin, northern California.	Franciscan Group of Cooksley (1964) (upper Mesozoic): Interbedded black shale, graywacke, and conglomerate; folded, faulted, and locally intruded by serpentinite; deeply weathered to abundant clay.	Cooksley (1964).
Western Cascade Range, Oregon.	Volcaniclastic rocks, lava flows, ash flows, and intrusive rocks (Tertiary), highly altered to form clay and saprolite; earth flows are particularly common where soft volcaniclastic rocks are capped by harder lava flows and (or) ash flows.	Swanson and James (1975), Swanson and Swanston (1977), Swanson and others (1980).
Northwestern Wyoming and adjacent parts of Montana and Idaho.	Soft shale and claystone (upper Mesozoic to Eocene) with interbedded sandstone and siltstone containing minor amounts of conglomerate, limestone, and coal; much of the shale and claystone is highly plastic and bentonitic. Glacial till (Quaternary)	Bailey (1972).
Gardiner area, Montana.	Dacite breccia (Eocene) containing abundant highly plastic bentonite---------- Landslide Creek Formation (Upper Cretaceous): Conglomeratic sandstone interbedded with bentonitic mudstone and claystone.	Fraser and others (1969).
Upper Ohio River Valley; Ohio, West Virginia, Pennsylvania, and Kentucky.	Clay, clay-shale, and coal (Pennsylvanian and Permian): Earth flows are particularly abundant where rock creep has formed impermeable layers with dips parallel to slopes; many earth flows form at sags in impermeable layers.	Sharpe and Dosch (1942).
Barbados----------	Shale, mudstone, and sandstone (Tertiary)----------	Prior and Ho (1972).
Panama Canal Zone.	Cucaracha Formation (early Miocene): Sandy claystone, very poorly cemented and very closely fractured, deeply weathered to soil containing abundant kaolin, mica, chlorite, and iron oxides; rock disintegrates after oven drying at 100°C and reexposure to water.	National Academy of Sciences (1924).
Dunedin district, New Zealand.	Abbotsford mudstone (Cretaceous): Glauconitic mudstone----------	Benson (1940).
Razorback Range, Australia.	Wianamatta Group (Triassic): Shale interbedded with lithic sandstone----------	Dunkerley (1976).
Antrim coast, northern Ireland.	Decomposed claystone, chalk, basalt, marl (Triassic), and glacial till (Quaternary): Earth flows occur only where Triassic strata dip steeply inland owing to disturbance by rotational slumping; steep dip allows ground water to percolate along bedding planes.	Prior and others (1968).
Coastal cliffs in southeastern England.	London clay (Eocene), Barton clay (Eocene), and Hamstead beds (Oligocene): Stiff fissured overconsolidated clay with interbedded silt and fine sand.	Ward (1948), Hutchinson (1970), Hutchinson and Bhandari (1971), Barton (1973), Bromhead (1978).
Coastal cliffs in Denmark.	Mo clay and Lille Baelt clay (Eocene): Stiff fissured overconsolidated clay containing some volcanic tuff and diatomaceous beds.	Prior (1977).
Okoličné area, Czechoslovakia	Flyschoid strata of Zakopane facies (Paleogene): Claystone containing lesser amounts of sandstone; earth flows form where confined aquifers occur.	Fussgänger and Jadrŏn (1977).
Carpathian Mountains, Czechoslovakia.	Soft tectonically disturbed flysch, sandstone, and pelitic and argillaceous shale (Paleogene). Tuff, agglomerate, coal, and poorly consolidated clay, silt, sand, and gravel (Neogene).	Záruba and Mencl (1969).

Table 2.1

2.3.2 Morphologic Features

Morphologically an earthflow has distinctive features which are a result of the materials involved and slope geometry. Earthflows generally occur along relatively gentle slopes or depressions and display basal and lateral shear failure along distinct and often "slickensided" planes of failure (Keefer and Johnson 1983). An earthflow itself may be either tongue or tear-drop shaped. The "toe" lies at the point most distant from the head, refered to as the "distal margin" of an earthflow. Its length from head to toe is normally considerably greater than its depth (Fig. 2.4).

Material is provided from "zones of depletion". Zones of depletion are generally at the head or crown of the flow, where material is continually added to the mass. Normally in the zone of depletion the earthflow surface is at a lower elevation than the ground on either flank. In the "zone of accumulation" the surface of an earthflow bulges above the undisturbed ground on either flank. In profile earthflows generally show a sinusoidal form with the zone of depletion being concave upward and zone of accumulation convex upward. This is thought to result from earthflow movement where thinning of the earthflow near the head is followed by thickening near the toe (Fig. 2.4) (Keefer and Johnson, 1983).

In the zone of accumulation it is common for lateral ridges to form in one of three ways: (1) pushed up as a pressure ridge, (2) overflow of earthflow material on to the adjacent ground surface, and (3) a toe overrides the former ground surface then stops and if later remobilized part of the deposit may be left in place forming lateral ridges (Fig. 2.5).

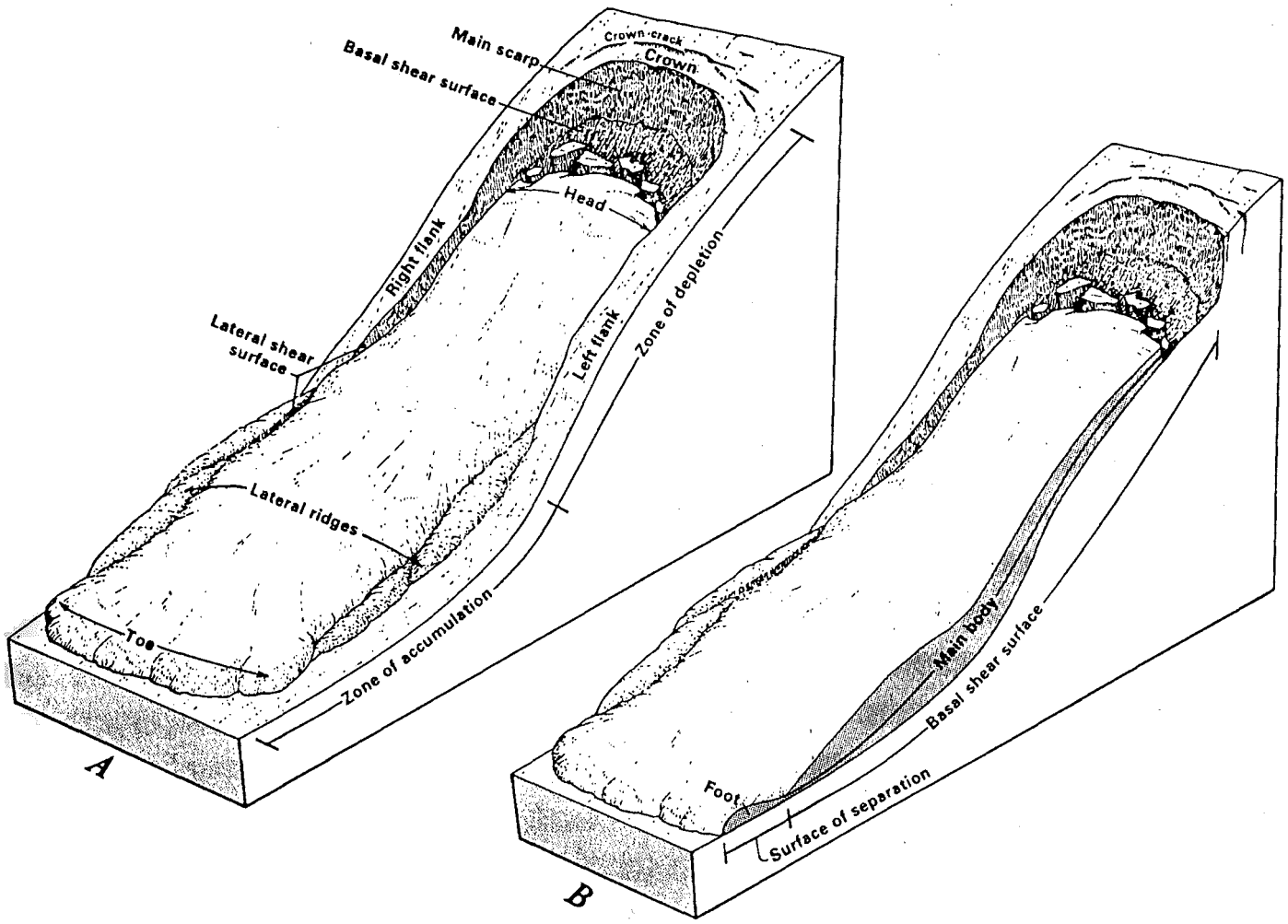

Figure 2.4 Schematic block diagram of an idealized earthflow. A - Surface features. B - Subsurface features. (from Keefer and Johnson, 1983).

An earthflow generally moves as a coherent body but is disrupted by numerous cracks formed from internal differential movements, and drag along the flanks, or desiccation. Lateral shears are often slickensided and when weathered, their trace can be recognized as scarps along the flanks, sometimes connecting with the main scarp. Subsurface features include basal shear surfaces which are pervasively slickensided. Although generally linear the basal shear surface may be rough containing 'asperities'.

The distal margin is usually marked by a steep bulging rounded toe only slightly wider than the body even though it's not laterally confined.

If drainage along the flow becomes entrenched gullying usually occurs whereby erosion can cause significant removal of material.

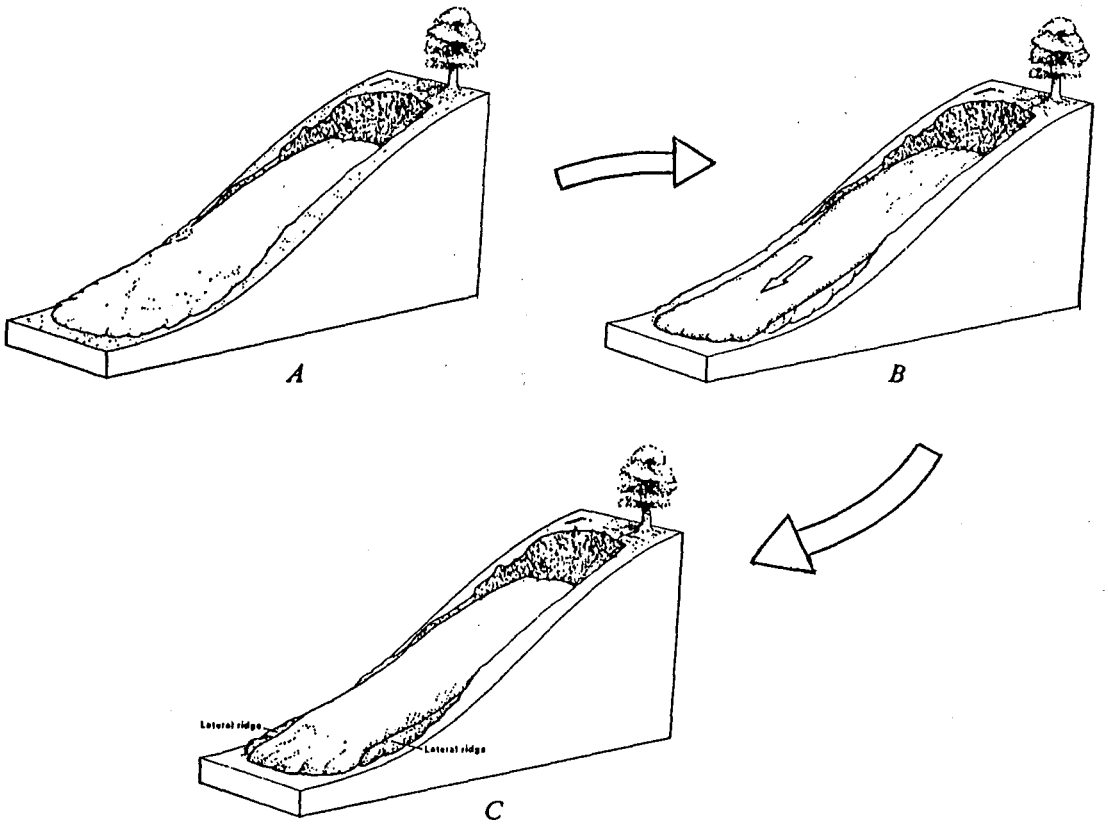

Figure 2.5 Formation of lateral ridges when toe overrides former ground surface. (from Keefer and Johnson 1983)

2.3.3 Slope Inclinations

The slope inclinations on which earthflows occur have been measured in several localities. Keefer and Johnson (1983) measured slope inclination in the Orinda, California, area and Davilla Hill, California, area and found that 99 % of all earthflows occur only on slopes steeper than 15 and 12 degrees respectively, and no earthflows occurred on slopes less than 10 and 8 degrees respectively. In the Gros Ventre mountains of Wyoming the minimum inclination for earthflows is 2 degrees (Baily, 1972); along the coast of southeast England the minimum inclination is 4 degrees

(Hutchinson and Bhandari, 1971). Smith (1974) found that in the Poverty-Bay East Coast region, (New Zealand) earthflows can develop on slopes of less than 5 degrees but most earthflows developed on slopes between 10 to 25 degrees.

2.3.4 Earthflow Complexes

An earthflow complex may contain several earthflow lobes as well as other types of slope movement deposits. Most earthflow deposits occur as parts of earthflow complexes (Keefer and Johnson, 1983). Earthflow complexes may consist of coalescing channels, they may cover large areas with hummocky disrupted topography, or may be a single sinuous channel as in the Wharanui Earthflow.

Many earthflow complexes are active only intermittently over many years or even several centuries (Hutchinson et al., 1974). Within a complex an earthflow may be formed by older deposits, but may not have the same boundary as the older earthflows. The new flows will commonly leave behind remnants of older irregular earthflows as scarps and new lateral shears cut across old boundaries of earthflow deposits.

2.4 MOBILIZATION OF EARTHFLOWS

2.4.1 Initial Mobilization

The mobilization of earthflows has been found by Keefer and Johnson (1983) to occur when pore-water pressures increase in the soil. Pore-water pressure increases can occur by either a rise in the water table from infiltration, or rapid undrained loading of debris discharged from feeder slides or other earthflows (Hutchinson and Bhandari, 1971).

Engineering soils which contain clay minerals of the swelling variety (ie. smectite and chlorite) become dessicated during periods of low precipitation, form cracks, and are subjected to negative pore-pressures. When high precipitation occurs, water infiltrates into the cracks and

saturates the near surface material. The negative pore-pressures are dissipated and tend to draw water into the soil causing it to swell, whereupon the strength is reduced. (Terzaghi and Peck, 1967, Wu and Sangrey, 1978). With continued moderate precipitation local zones of perched water form, growing as precipitation continues. When the groundwater rises to a point where pore-pressures are increased and exceed the local threshold value, the earthflows become mobilized.

The initial mobilization of an earthflow can be expressed in terms of a slope stability analysis. In the analysis the shear resistance of the soil is given by the Coulomb failure criterion, modified by Terzaghis' theory of effective stress accounting for the effects of pore-water pressure. This explains how rising pore-water pressure can induce mobilization (Hutchinson et al., 1974, Keefer and Johnson, 1978).

A slope stability model would take into account slope inclination, unit weight and strength parameters of the soil, maximum pore-water pressure generated, and the geometry of the mobilized mass. All the parameters are interrelated and changes in one parameter will affect values of the other parameters. Hence an earthflow may stop moving if the inclination decreases, or if the pore-water pressure decreases due to drainage or evaporation, which explains why an earthflow will stop moving despite a uniform slope.

2.4.2 Movement After Mobilization

The slope stability model can explain mobilization but once the earthflow has been mobilized, several additional factors must be considered. A model must be consistent with measurements of velocity, observations of the morphology, shear surfaces and associated zones of disturbance, and measurements of the distribution of displacements within earthflows (Keefer and Johnson, 1983).

Earthflow velocity may be a slow movement that

persists for several days, months, or years; or less commonly be a surge which lasts a few minutes. Most earthflows are of the slower persistent type.

Over the years earthflows have been observed to move slowly, but with varying velocities (Bishop, 1968; Hutchinson et al., 1974; Harden et al. 1978; Keefer and Johnson, 1978). As expected they often move faster during periods of high precipitation rather than during dry periods. However the correlation with rainfall can be more complex and dependant upon several factors.

Several earthflows have been continuously monitored and movement was found to take place in four different patterns. In the first example movement was found to take place at relatively constant velocity with short periods of acceleration and deceleration, (Fig. 2.6 A). In the second example movement is at relatively constant velocity, (Fig. 2.6 B). In the third example movement of the monitored earthflow was notably "stick-slip", where the earthflow would advance at relatively low velocities for hours then abrubtly surge forward at relatively high velocities (Fig. 2.6 C). The fourth example is that of a major surge, in which the earthflow would advance several metres/min due to rapid loading under conditions generating excess pore-pressures; the surges would suddenly begin and gradually decelerate (Fig. 2.6 D).

2.4.3 Distribution of Displacement

Most earthflows have distinct boundary shears which are planar or gently curved, though they may contain local asperities. Surface and subsurface measurements show that most movement occurs within these boundaries. Although some internal deformation occurs, the movement adjacent to lateral shears predominates. Internal deformation can be indicated by displacement profiles. Some deformation may be from discrete internal shear zones similar to those at the boundaries. However internal deformation due to flow within the material also occurs.

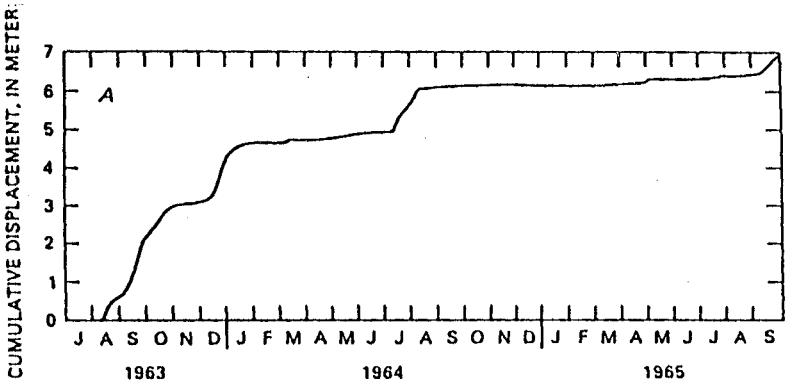

A - Waerenga-o-kuri Earthflow, New Zealand, (from Campbell, 1966).

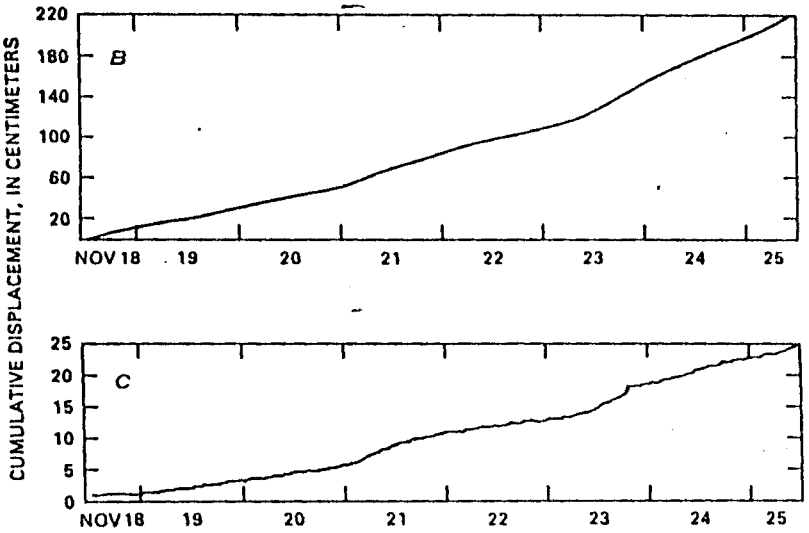

B - Earthflow 1, C - Earthflow 2, Minnis North, northern Ireland, (from Prior and Stephens, 1972).

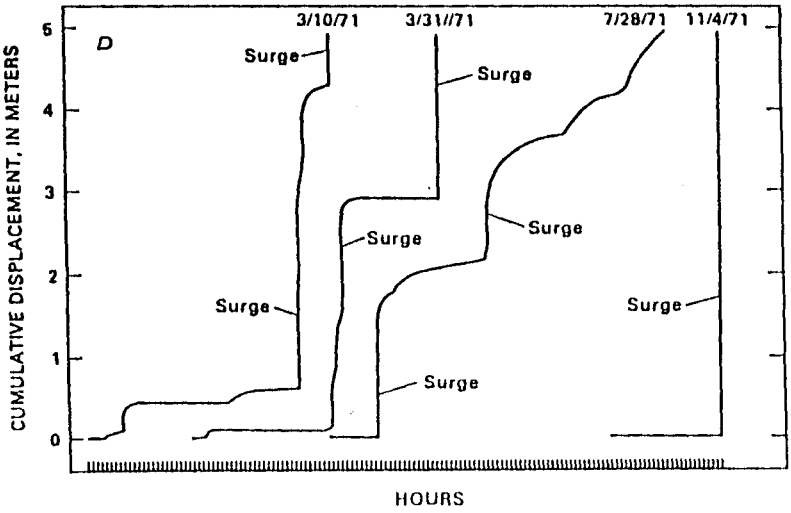

D - Earthflow 1, Minnis North, northern Ireland, (from Hutchinson et al., 1974).

Figure 2.6 Movement patterns of earthflows monitored with continuous recording devices.

Measurements of movement on earthflows which have had subsurface monitoring have shown that most of the displacement measured at the ground surface took place very close to the basal shear surface (Fig. 2.7). Three examples are cited below.

1) In the study of the Davilla Hill Earthflow (California) by Keefer and Johnson (1983), subsurface displacements were measured using a stack of wooden disks placed in an augered borehole. The disks were subsequently excavated and showed that 94% of the movement was within 13 mm of the basal shear surface.

2) In an earthflow at Beltinge, (England), Hutchinson (1970) used a borehole inclinometer to measure subsurface displacement. He found that 89-95% of the displacement measured at ground surface took place within 200 mm of the basal shear surface.

3) At the Mikonui earthflow, Oaro, (New Zealand), Grocott (1977) used a borehole inclinometer to determine subsurface displacement and found that 87-95% of displacement occurred within 200 mm of the basal shear surface, .

2.5 INSTRUMENTATION

2.5.1 Introduction

Field Instrumentation has long been used for providing design data in the correction of landslides. There are many case histories of landslides where remedial measures were successfully carried out, in part due to information provided from the monitoring (Tueller, 1965; Wilson, 1974; Munoz, 1974; Durr 1974; Thomson, 1975;). There are also cases where monitoring of movement has prevented loss of life and property when imminent failure was apparent (McCauley, 1980). The information acquired by

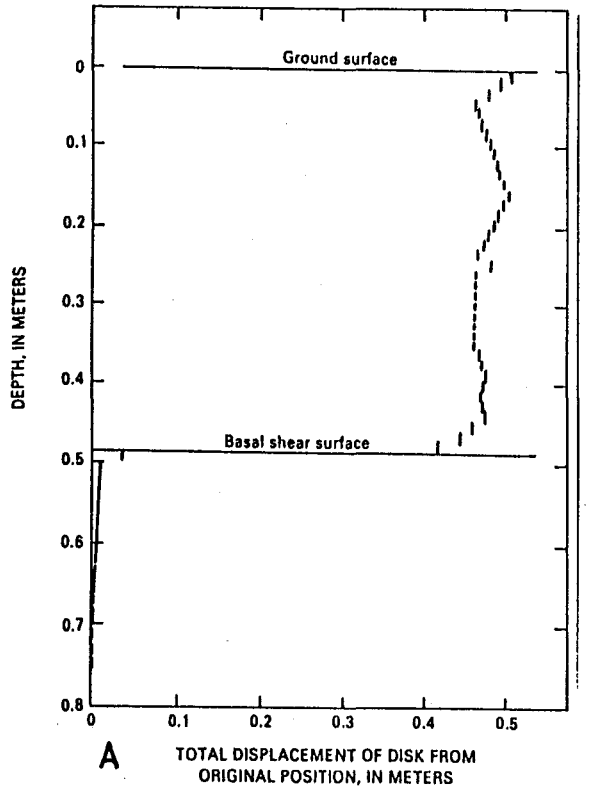

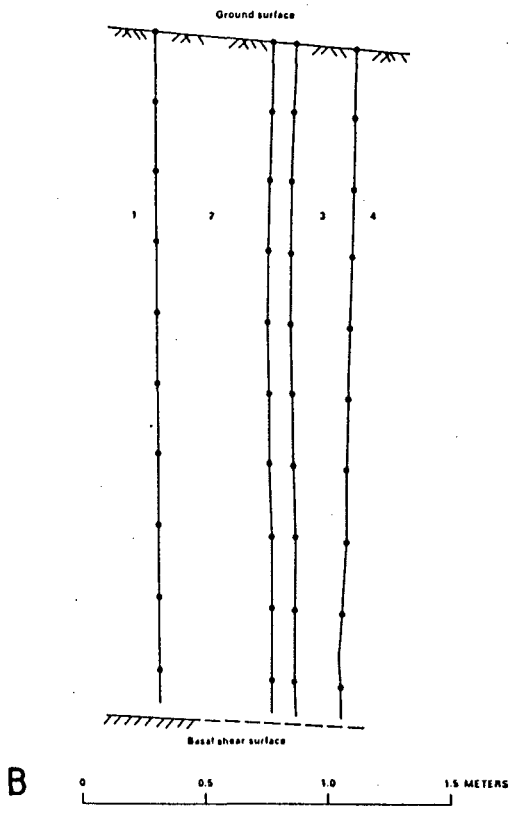

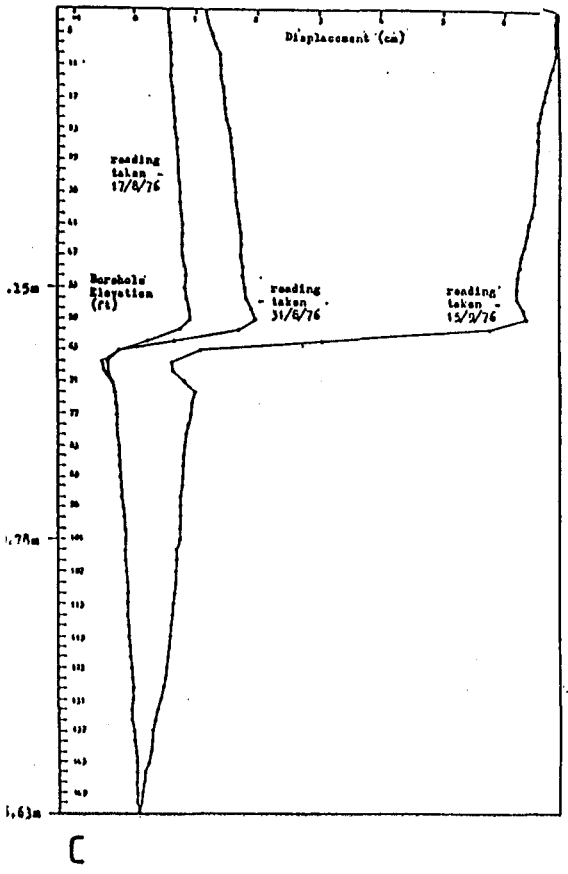

Figure 2.7 Subsurface Displacement profiles of earthflows.

A - Davilla Hill Earthflow, California; movement of buried wooden disks (from Keefer and Johnson 1983).

B - Beltinge, England, line 1 is initial position of inclinometer tube April 28, 1964; line 4 is position on June 11, 1964 (from Hutchinson, 1970).

C - Mikonui Earthflow, Oaro, New Zealand; movement of inclinometer tube (from Grocott, 1977).

instrumentation or monitoring of landslides includes:

1. determination of the depth, and shape of the sliding surface;
2. determination of the absolute lateral and vertical movements;
3. determination of the rate of sliding (accelerating or decelerating);
4. the activity of marginally stable slopes;
5. groundwater levels or pore-pressures;
6. and evaluation of the effectivness of various control measures.

Monitoring movement of the Wharanui earthflow is a primary objective of this project. To accomplish this, standard types of instrumentation were incorporated for the study.

The role of specific types of instrumentation is thoroughly treated in literature, (British Geotechnical Society, 1974; McCauley, 1980; Munoz, 1974; Shannon, 1962; Transportation Research Board, 1974; Wilson, 1962; Wilson, 1978; and Sowers 1978), and will not be discussed here. However, a background of the types of instrumentation used in studying the Wharanui earthflow, and their selection will be briefly discussed.

2.5.2 Types of Instrumentation

The types of instrumentation commonly in use are survey grid systems, crack width monitors, borehole extensometers, piezometers, and in-situ shear testing (Wilson and Mikkelsen 1978).

Survey Systems. In active slides, surface movements are commonly monitored to determine the areal extent of slide activity, the rate of movement, and movement patterns. Electronic distance measurement (EDM), optical instrument surveys and tape measures are commonly used for this purpose. Stable marks located outside the slide area are

used as reference points so that lateral and vertical movements can be indicated.

The use of survey grids is best for the monitoring of slower continuous movements as in the Wharanui earthflow. Rapid failures that stabilize after initial movement are not subject for survey grids.

A Wild DI3 EDM and a T16 theodolite were used for installation and monitoring of a survey network on the Wharanui earthflow due to the accuracy obtainable and their ease of use (Discussed in Chapter 5, and Appendix 9).

Crack Width Monitoring. Measurements of crack widths can provide simple qualitative knowledge of landslide activity. The movement on cracks give indications of the increasing size and activity of a landslide. Crack width monitoring can be done by direct measurement of points on opposite sides of the cracks. Measurement of both the horizontal and vertical component are useful for indicating the relative movements. A device constructed at the University of Canterbury was used on the Wharanui Earthflow which is accurate to 1 mm and gives information on both lateral and vertical separation (refer to Chapter 5 and Appendix 9).

Borehole Extensometers. Borehole extensometers are used to monitor internal soil or rock mass deformation by measurement of changes in the lengths of drill holes or sections of drill holes. These were not considered for use, as expense would have been prohibitive.

Inclinometers. One of the most important contributions to the study of landslides has been the use of inclinometers. Inclinometers have become one of the most common forms of instrumentation. They are used to locate zones of movement at depth (Tice 1974). Constraints on funding prevented these from being used in this investigation. Piezometers are used indirectly for this purpose.

Piezometers. The measurement of pore-water pressure is one of the most important aspects of instrumentation. As discussed earlier the influence of water on mobilization of earthflows is paramount. Therefore measuring of the pore-water pressures can indicate when they are becoming excessively high, prior to movement. Piezometers used for measuring pore-water pressures at various depth include: open standpipe, Casagrande, Pneumatic, and electric types (Terzaghi and Peck, 1967; Wilson and Mikkelsen, 1978).

Shortcomings of the devices are primarily due to the environment in which they are installed. Pinching of the tube, improper sealing, clogging of parts, electrical malfunctions, or improper choice may render the piezometer inoperative or useless.

Because of the low permeability of the Wharanui earth flow deposits (10^{-8}m/s to 10^{-9}m/s) the soils are more suited to the use of pneumatic or electric piezometers as response times to pore water pressure changes are almost instantaneous. Installing an open standpipe would be useless as Terzaghi (1967) noted that there would not be enough volume of water and that they may, "so radically alter the pressure near the point of measurement that the results of the observation are utterly misleading or the time required to reach 90% equilibrium may be intolerably long."

However funding and practicality would not allow either pneumatic or electric piezometers to be installed. Instead Casagrande piezometers were chosen for their simplicity, low cost, no maintenance, and their adequate performance.

The Casagrande Piezometer essentially consists of a pervious ceramic tip imbedded at the depth which water is to be measured and a riser pipe to the surface (see Appendix 6 for construction of piezometers). This type of piezometer will not give instantaneous values but its response time is approximately 1 day depending upon the soil mass

permeability (Fig. 2.8). This was considered adequate, as the piezometers were to be permanent installations, and fluctuations of pressure were not likely to be significant. What was required was a general indication of groundwater levels and pressures.

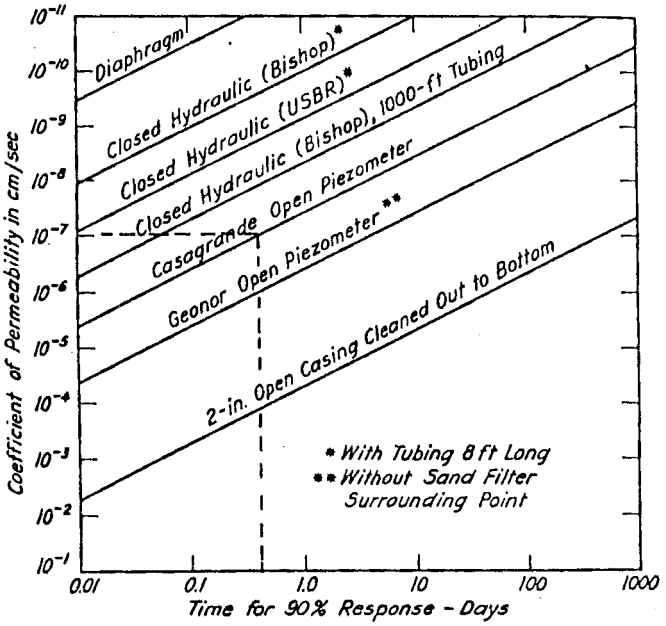

Figure 2.8 Approximate response times for various types of piezometers (from Terzaghi and Peck, 1967).

2.6 SUMMARY

Many classification schemes for slope movements have been proposed, the Varnes (1978) scheme is used in this study. The Varnes classification of slope movements is based on mechanisms of failure, type of material, and rate of movement.

Earthflows are distinguished from other types of movement by their morphology, materials, and rate and kind of movement. Principal characteristics of earthflows are: tongue or teardrop shape; a rounded, bulging toe; a sinusoidal longitudinal profile; lateral ridges; and discrete boundary surfaces. Earthflows are commonly associated with other slope movements which may coalesce into earthflow complexes.

Initial mobilization of earthflows is due to rising pore-water pressures which increase stresses and reduce shear strength. Movement is generally slow and persistent but velocities may vary greatly over time and depend largely on precipitation and boundary conditions. With drainage, evaporation, or a decrease in slope angle, movement will cease.

Instrumentation of earthflows can give vital information regarding the type of movement mechanism, the rate of movement and the susceptability towards future movement. This is primarily achieved through the use of survey grid systems, inclinometers, and piezometers.

With regards to the Wharanui Earthflow, a preliminary study of the materials, the morphology, and the rate of movement led to the determination of the type of instrumentation to be used in the site investigation programme. Instrumentation provides new data from which the failure surface may be defined and groundwater conditions revealed. This information is used to aid in determining potential remedial measure designs.

CHAPTER THREE

SITE GEOLOGY AND GEOMORPHOLOGY

3.1 INTRODUCTION

Consideration of the geology of the regional area is essential in order to understand the development of the Wharanui Earthflow and as background for more detailed mapping of the site. The examination of the regional geological history (Appendix 1) can draw attention to important geological features not actually recognizable at the site.

The objectives of this chapter are to:

2) describe the nature, distribution, and structural relationship of the bedrock units within the site, and
3) discuss the geomorphic development of the site with respect to geologic controls.

The "site" refers to the area surrounding the Wharanui Earthflow, boundaries of which are the north branch of Tirohanga stream to the southwest of the flow, and Woodside Creek to the northeast of the flow (Fig. 3.1 and Fig 1 in the map pocket).

3.2 PREVIOUS WORK

Hector (1886), Hutton (1874), and Mckay (1886) were the first to publish accounts on the regional stratigraphy of Marlborough. Since then many workers have been involved with the general geology and stratigraphy of the Marlborough area. The Kekerengu River to Ure River area was mapped by Prebble (1976) and this study is of particular interest as the Wharanui Earthflow lies within its area (Fig 3.1). Prebble's work is used as a basis for the regional

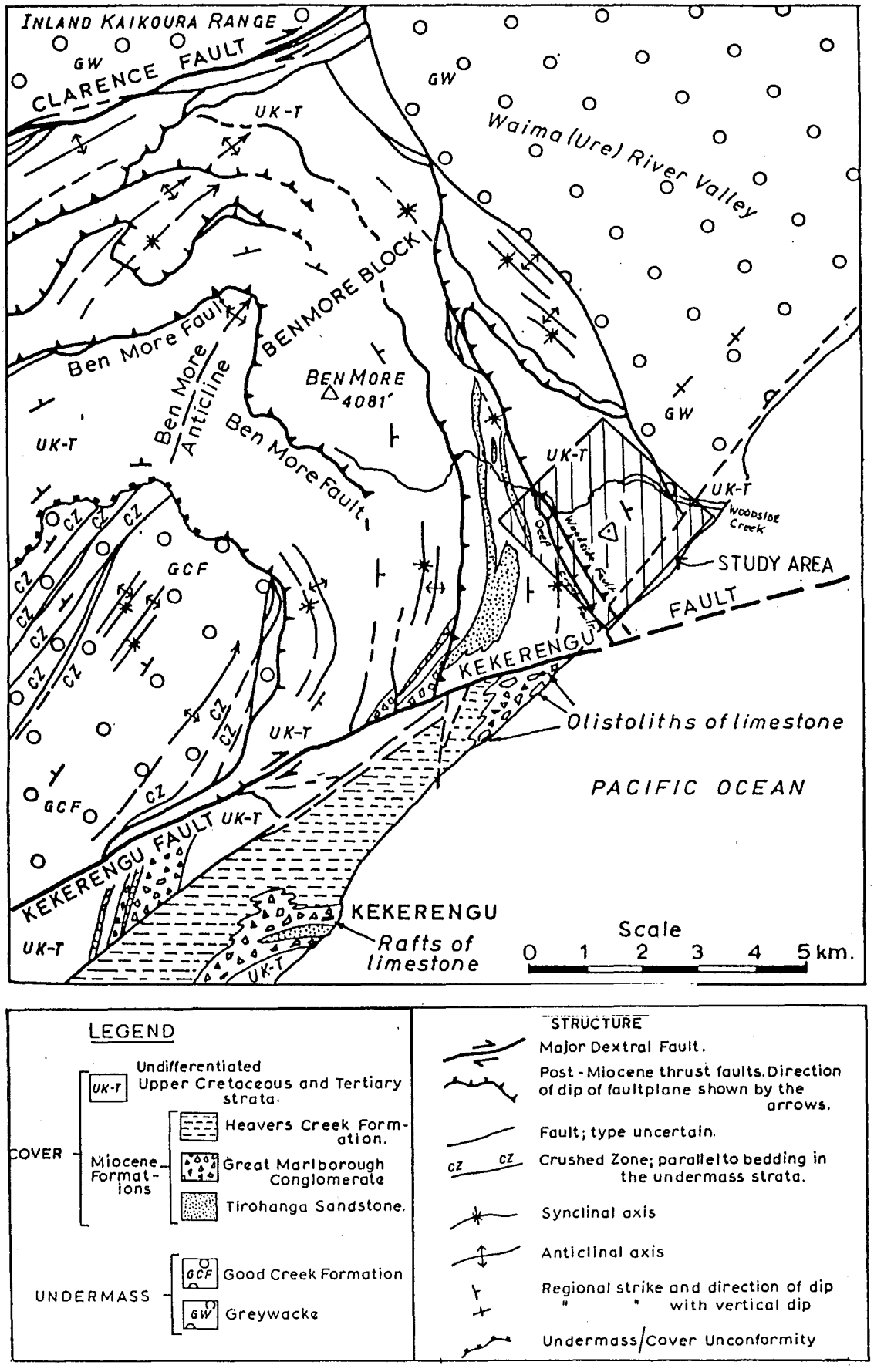

Figure 3.1 Location of site with respect to regional geology (from Prebble, 1980).

geological history. A brief outline of the history is presented in Appendix 1.

The only previous worker to look specifically at the Wharanui Earthflow was Paterson (1984). His inspection of the Wharanui Earthflow was conducted at the request of the Ministry of Works, Blenheim, to ascertain 1) the principal causes of instability, 2) suggestions for further investigations, and 3) to suggest remedial measures.

3.3 BEDROCK GEOLOGY

3.3.1 Field Methods

Engineering geological mapping of the site was conducted at a scale of 1:5000. Since no suitable topographic plots were available for mapping at that scale, aerial photograph enlargements were prepared from:

New Zealand Aerial Mapping
Survey no. 3839 D/9 - D/12, 1975,
Survey no. 5097 A/18 - A/21, 1978, and
Survey no. 5759 N/6 and N/7, 1980.

Transparent overlays were used to map on, and information from these was transfered to a large compilation sheet (Fig. 1 in the map pocket). A summary map of the site geology is shown in Fig 3.2.

Grid references listed for figures are either taken from NZMS 1, S36 or NZMS 260, P30. Those taken from S36 are noted as such. Grid references from P30 are simply listed with eastings and northings without refering to the map number.

Three geological sections of the site were drawn using data compiled from tape and compass traverses (Fig. 2 in the map pocket). These traverses were walked along lines approximately perpendicular to strike so that sections are as near to true dip as possible.

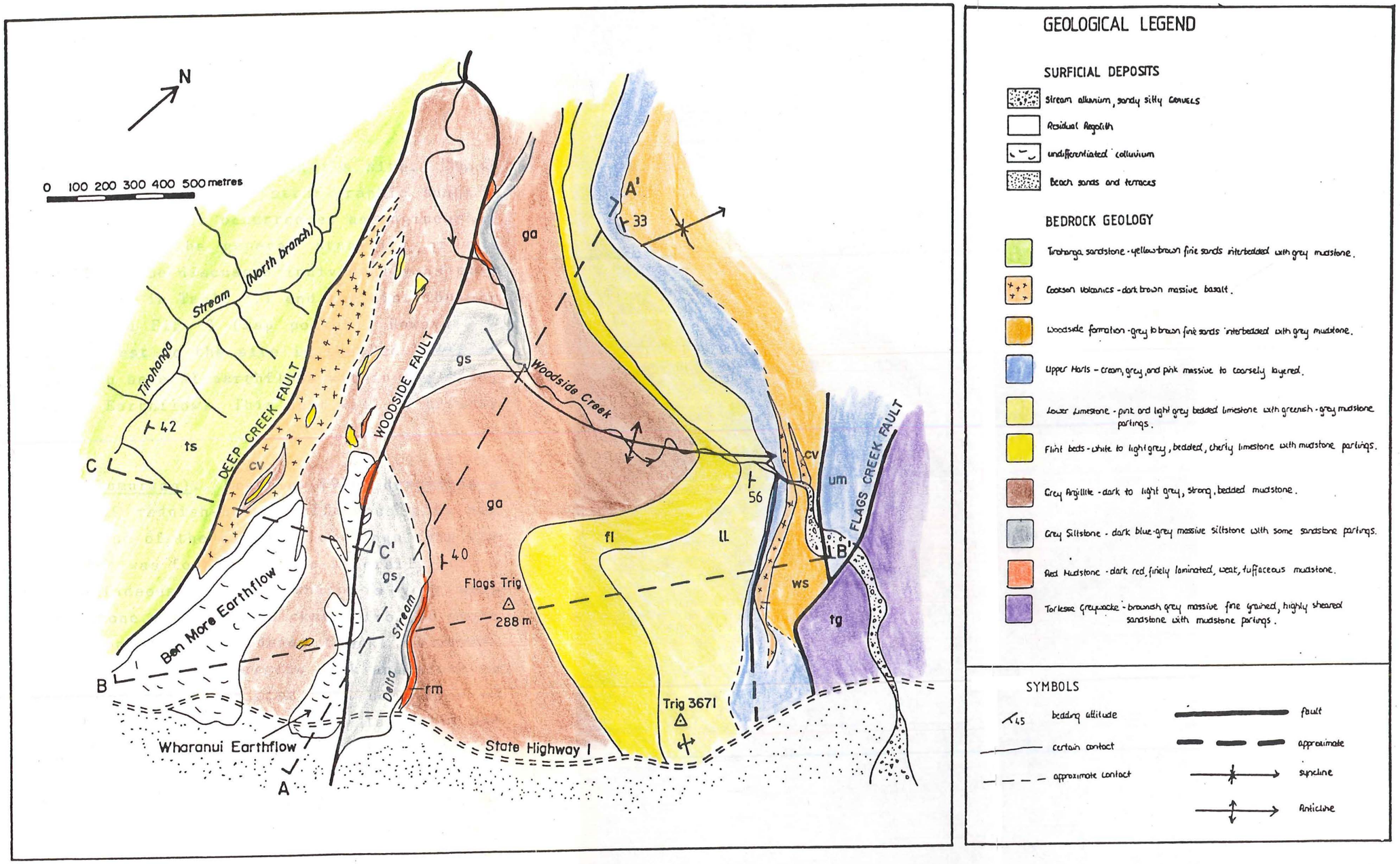

Figure 3.2 Summary sketch map of site geology showing structural features and lines of sections of Fig. 2 (in the map pocket).

The Bell & Pettinga (1983) engineering geological descriptive system was adopted because of the simple and concise terminology. Their classification was especially useful for logging of augerholes and was chosen over other schemes, as descriptions in the field were easier to compile. (See Appendix Two).

3.3.2 Mapping Units

Ten mapping units were used within the site. These are shown in Table 3.1 which gives a stratigraphic summary of the lithology, including their occurrence, an engineering geological description, and the general stability of the units. The units will not be discussed individually as they are sufficiently described in Table 3.1 and the distribution is shown in Fig. 3.2 and Fig. 1 (map pocket). However, a unit of particular interest to the site is the Red Mudstone which is associated with several earthflows within the site, including the Wharanui Earthflow. This unit will be briefly discussed below.

Red Mudstone (Haumurian). Prebble (1976) describes a "five foot thick bed of reddish-brown tuffaceous grit and conglomerate" at the base of the cliff below Flags Trig (in Delta Stream). This bed was found to grade laterally into a dark red volcanic tuffaceous mudstone which is very weak (Fig. 3.3). This mudstone varies in thickness from 30 cm in Delta Stream to 1.5 metres in Woodside Creek. However, exposure is very poor as it is inherently weak and prone to slumping. All exposures are associated with some type of slope movement. In Woodside Creek it is finely laminated and has a high silt and clay content (sample S63 - 14 % sand, 43 % silt, and 43 % clay). On The Northeastern ridge of the Wharanui Earthflow, near the headscarp, there is a bed of tuffaceous volcanic breccia. This breccia has been mapped as part of the Red Mudstone. Both the red tuffaceous mudstone and the volcanic breccia contribute a considerable amount of material to the Wharanui Earthflow.

TABLE 3.1

MAPPING UNIT	EXPOSURE LOCALITY	ENGINEERING GEOLOGICAL DESCRIPTION	GEOMORPHIC CHARACTERISTICS	STRATIGRAPHIC RELATIONSHIP
TIROHANGA SANDSTONE Otaian to Altonian (Miocene)	the north branch of Tirohanga stream	Moderately weak, yellowish-brown finely laminated, coarsely layered to massive, medium to fine grained slightly calcareous SANDSTONE; moderately weak olive-grey mudstone interbedded; very widely spaced joints.	This relatively soft sandstone siltstone sequence weathers easily to residual regolith, is highly erodible, and a has some tunnel gullies on moderate slopes. Surficial regolith failures are prevelant on steep slopes.	Faulted contact with Cookson Volcanics along Deep Creek fault.
COOKSON VOLCANICS Landon (Oligocene)	Lower Woodside creek, 720 metres upstream from State Highway 1 bridge and along Deep creek fault.	Highly weathered, weak, dark brown massive porpheritic BASALT; fine grain groundmass with feldspar and some quartz phenocrysts.	The weak, highly weathered volcanics are susceptible to slumping with poor exposure in failures.	Baked contacts with the Woodside formation where the Cookson volcanics are intruded and interfingered; and faulted contacts between the Tirohanga Sandstone along Deep Creek fault.
WOODSIDE FORMATION Waipawan to Heretaungan (Eocene)	Lower Woodside Creek 700 metres upstream from State Highway 1 bridge.	Slightly weathered, moderately weak to moderately strong, dark greenish-brown coarsely layered to massive, fine to very fine grained slightly glauconitic SANDSTONE, interbedded with moderately weak finely layered mudstone; widely spaced closed joints, some small faults.	Regolith from weathering is highly susceptible to slumping. Good exposure in fresh failures.	Baked lower contact with Cookson Volcanics and interfingered or conformable with Lower Marls; upper contact faulted Greywacke.
UPPER MARLS Waipawan to Heretaungan (Eocene)	40 metres below gorge entrance in slump failure and above the bluffs of the Woodside gorge.	Slightly to moderately weathered, moderately strong, light cream to grey and pink, moderately bedded, finely to coarsely layered, MARL; some orange staining, spheroidal weathering; close to very closely spaced joints, occasional tight folds, contorted and sheared.	The Marls are highly susceptible to weathering with little other outcrop than in failures and slumps.	Conformably underlies the Woodside formation except where Cookson Volcanics intrude.
LOWER LIMESTONE Haumurian to Dannevirke (Cretaceous-Tertiary boundary)	Well exposed at Woodside Creek lower gorge entrance and on State Highway 1, 700 metres south of Woodside creek overbridge.	Slightly weathered to unweathered, very strong to extremely strong, pink and white to light grey, well bedded, coarsely layered to massive LIMESTONE with some chert lenses; greenish-grey mudstone partings; wide to extremely wide spaced joints.	Minor rock falls along joint and bedding plane intersections, tends to form bluffs where exposed.	Conformable contact with Upper Marls in most areas, possible fault contact at gorge entrance.
FLINT BEDS Haumurian (Late Cretaceous)	Well exposed in Woodside creek, 170 metres upstream from gorge entrance and in bluffs of the Woodside gorge. Some blocks of float of the highly sheared altered Flint beds occur between Woodside and Deep Creek faults.	Unweathered, extremely strong, white to light grey, well bedded, very coarsely layered siliceous LIMESTONE with very dark grey to black lenses of chert from 5-20cm thick; greenish grey siltstone partings. Moderate to widely spaced joints; minor faults and folds.	Minor rockfalls along joint and bedding plane intersections, tends to form bluffs where exposed.	Conformably lies below the Lower Limestone and above the Grey Argillites.
GREY ARGILLITES Haumurian (Late Cretaceous)	Well exposed in Woodside creek lower gorge begining 285 metres upstream from gorge entrance, and along cliff face south of Flags trig.	Slightly weathered to moderately weathered, moderately strong to strong, dark grey to light grey and cream coloured, micaceous, siliceous, sub-fissil, finely layered, well bedded ARGILLITE; closely to moderately spaced joints; dark reddish brown staining and some yellow sulphurous efforesence; some moderately strong thin partings of fine grained sandstone and some thick beds of sandstone interfinger.	This unit differs from the Grey Siltstone in that it is harder, does not erode as, easily and tends to form ridges and bluffs. It is relatively stable except where it is highly sheared within crush zones.	This unit occurs in two seperate sequences with the Grey Siltstones and Red Mudstones interfingered between them. Conformably underlies the Flint Beds of the Amuri.
GREY SILTSTONE Haumurian (Late Cretaceous)	In Woodside creek, in Delta Stream below Flags trig and in failures on ridges parallel to Wharanui earthflow.	Slightly weathered to highly weathered, moderately weak to moderately strong, dark blueish and brownish grey massive SILTSTONE; with nodular weathering appearence and closely spaced joints. Thin brown fine grained sandstone partings, and some sandstone dikes; minor folds and faults, steeply dipping to the northeast.	This unit is much weaker and more erodible than the Grey Argillites, forming a weathering profile prone to regolith failure on steep (>25 degree) slopes.	Conformably lies between two sequences of the Grey Argillites.
RED MUDSTONE Haumurian (Late Cretaceous)	Poorly exposed southwest of Flags trig in bluffs and in Woodside creek near Woodside fault. Occurs in single beds 30 cm to 1.5 m thick.	Slightly weathered to moderately weathered, weak to very weak, dark red very finely laminated,thickly bedded, tuffaceous MUDSTONE, locally includes red volcanic tuffaceous breccia.	The nature of the materials make it prone to major slope failure. Many of the earthflows and slumps within the area contain a high proportion of this material.	Conformably interbedded with Grey Argillites and Grey Siltstones.
TORLESSE GREYWACKE Motuan (Early Cretaceous)	Lower Woodside creek just upstream from State Highway 1 bridge	Slightly weathered, very strong,light brownish-grey, massive poorly bedded fine grained SANDSTONE; closely jointed with some highly sheared mudstone partings and cannon ball concretions up to 15cm diameter. Steeply dips to the north.	The greywacke has formed steep ridges and has a shallow covering of residual regolith. Alluvial terraces overlie much of the greywacke.	Faulted contact with Woodside formation.

Figure 3.3 Red Mudstone - thin bed (30 - 40 cm) of red tuffaceous mudstone exposed in slump above Delta Stream. The Red Mudstone thickens to the west in Woodside Creek to 1.5 m and contains some volcanic breccia in other areas (S36 328E 426N).

3.3.3 Nomenclature

The informal stratigraphic subdivisions and member names of lithologies of Prebble (1976) and Hall (1964) are generally used in this thesis, but some significant changes in names and divisions have been made. Changes within the Whangai Shale and Flags Formation were necessary so that important variations within these lithologies could be distinguished at the scale of mapping. The changes made are shown in a schematic summary column (Fig. 3.4) and include:

1. Grouping the very strong, argillaceous, mudstones of the Whangai Shale and the Flags Formation sandstones, which interfinger with them, into one unit; the sandstones are a minor lithology within the unit which predominantly consists of material which is argillaceous, and is referred to as the GREY ARGILLITES;

2. Distinguishing the moderately weak, dark grey, siltstone within the Flags Formation, from the sandstone due to the siltstones local predominance and weathering differences; this unit is called the GREY SILTSTONES;

3. Distinguishing a red tuffaceous mudstone (discussed above) which appears in 30 cm to 1.5 m beds within the Grey Siltstone and the Grey Argillites. This red mudstone has important lithological characteristics which make it highly susceptible to slope movement; this unit is called the RED MUDSTONE; and

4. Not distinguishing between all members of the Amuri Limestone because of similarities within the unit or members too thin to be mappable within the site.

3.3.4 Structure

The Woodside Fault and the Deep Creek Fault (Prebble, 1976) are the main structural features within the site. These are two southeast-trending subparallel thrust faults. The Woodside Fault splinters off from Deep Creek Fault and

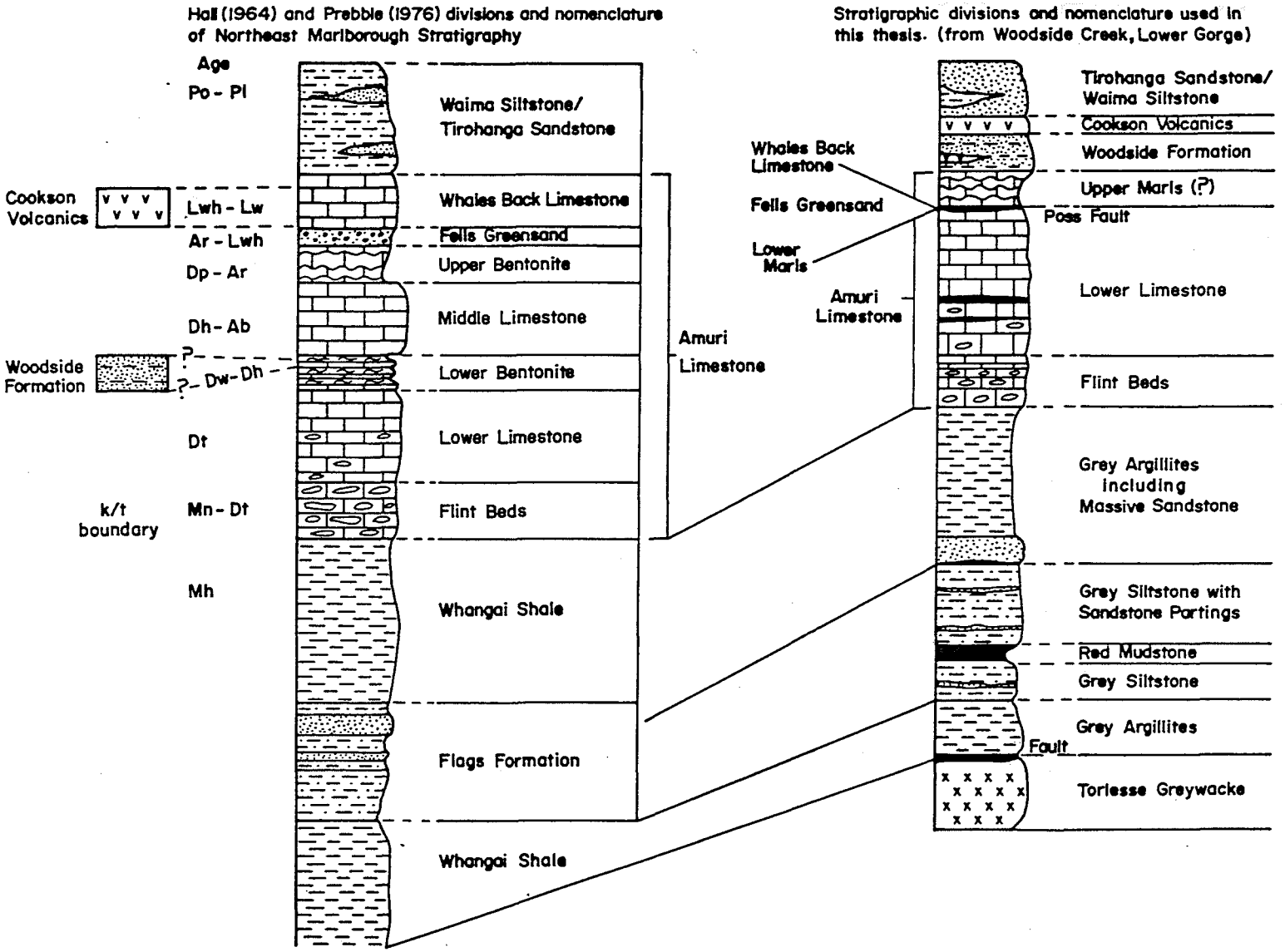

Figure 3·4: Schematic summary stratigraphic columns showing nomenclature of Prebble (1976) and Hall (1964) and correlation to stratigraphy of the site.

they both terminate against the Kekerengu Fault (Fig. 3.1).

At the northern end of the faults Prebble (1976) notes the acute junction "encloses a tightly folded, steeply plunging syncline which is partly overturned." Within Woodside Creek both faults are at least partially obscure, being covered by slope movement deposits. The Woodside Fault is covered in deposits derived from the Red Mudstone, and the Deep Creek Fault is covered partially in earthflow deposits derived from the Upper Marls.

The southern end of the faults are obscured by Recent coastal deposits.

Deep Creek Fault. The Deep Creek Fault dips steeply eastward at approximately 80° thrusting Tirohanga Sandstone, which dips 40 - 45° to the northeast, beneath the Cookson Volcanics. Prebble (1976) estimated the net vertical slip to be at least 1400 metres. Cookson Volcanics on the eastern side of the Fault are crushed and sheared but the Tirohanga Sandstone on the western side does not appear to have undergone alteration of any kind. The crushed zone is at least 30 metres wide, but delineating the true width is not possible as outcrops are obscured by slope movement deposits (ie. Ben More Earthflow). Within the zone are slivers of sheared Grey Argillites and Flint Beds, some of which have baked contacts with the Cookson Volcanics. Separating the crushed Cookson Volcanics from the Tirohanga Sandstone is a thin layer of fault gouge (cream-coloured clay) which is possibly derived from the Upper or Lower Marls. The Fault is considered to be approximately of Southland age (Mid-Miocene).

Woodside Fault. The Woodside Fault dips steeply, as does the Deep Creek Fault, but in a slightly more northeasterly direction. On the eastern side of the Woodside Fault, Grey Siltstone dips 40 - 45° to the northeast. To the west, the Fault is notable by a large shear zone which is 30 - 80m wide in exposure. Within the shear zone Grey Argillites are the dominant lithology but there are several

other lithologies within the zone including Cookson Volcanics, Lower Limestone (Fig. 3.5) , and Flint Beds . Bedding attitudes are generally indistinguishable within the shear zone, but there is evidence that some overturning has occured during the faulting as highly sheared Grey Argillites overlie crushed Flint Beds. This is visible at the base of the southwestern ridge, which is parallel to the Fault zone. The Fault is considered to be approximately the same age as the Deep Creek Fault.

Between the two faults there is very little bedrock exposure, as most of the area is overlain by earthflow deposits (the Benmore Earthflow covers an area 200 - 500 m wide and 1000 m long between the two faults) or is covered in vegetation. A few minor outcrops occur on a ridge line between the faults. This ridge runs from the head of the Ben More Earthflow to Woodside Creek (Fig. 1 in the map pocket) and is primarily composed of Lower Limestone and Grey Argillite. Between each of these outcrops the bedding orientation changes and minor faults have been inferred.

Northeast of the Woodside Fault the Grey Argillites and Amuri Limestone have undergone folding resulting in a steeply plunging anticline which trends to the northeast. Woodside Creek has incised along the path of the axis of the anticline as it has been the zone of least resistance in the strata (Fig. 3.2).

In the northeastern area of the site, just before the Woodside Creek lower gorge entrance, a fault trace oriented northwest - southeast is recognizable on aerial photographs. Exposure of the fault zone is obscured by slope movement debris. On the western side of the fault Lower Limestone dips 56^{o} to the northeast (into the fault) and on the eastern margin there are tightly folded and sheared Upper Marls. The Upper Marls have baked contacts with the Cookson Volcanics. The Cookson Volcanics are interfingered with the Woodside Formation which dips 44^{o} to the northeast.

Flags Creek Fault. The southern end of the Flags

Figure 3.5 Shearing of Lower Limestone within the Woodside Fault zone. Shears are filled with greenish - grey gouge derived from interbedded mudstone (S36 320E 470N.

Creek Fault (Prebble, 1976) passes just inside the site area. This vertical fault is a major boundary separating the Woodside Formation of Waipawan age (Tertiary strata) from Torlesse Greywacke of Motuan age (Early Cretaceous). The Fault is characterized by a crushed zone 30 to 60 m wide.

3.4 SURFICIAL DEPOSITS

3.4.1 Introduction

Surficial deposits within the area consist of residual regoliths, colluvium, stream alluvium, and beach deposits. These deposits are here considered to be engineering soils defined by Varnes (1978) as,

"... any loose, unconsolidated, or poorly cemented aggregate of solid particles, generally of natural mineral, rock, or inorganic composition and either transported or residual, together with any interstitial gas or liquid."

Surficial deposits mantle all of the site, excluding the bluffs and scarps. They form coverings several meters thick. The regoliths and colluvium are particularly prone to mass movement on steep slopes.

3.4.2 Residual Regoliths and Colluvium

Residual regoliths are engineering soils which form from the in-situ weathering of bedrock, and develop predominantly from rocks which are moderately weak (see Appendix 2 for terminology) and tend to weather easily. The profile from soil to the weathered bedrock is gradational and is usually less than one metre thick within the thesis area.

Residual regoliths are found in most of the site with the thickest covering (up to 2 m thick) found in the Tirohanga Sandstone, Woodside formation, and the Grey Siltstone. These residual soils overlying bedrock are

susceptible to shallow surficial failures (normally less than 1.5 m) on slopes steeper than 20^{o}.

The colluvial deposits within the site are derived from regolith failures on the steeper slopes. Colluvium deposits are found in valleys and depressions and are generally associated with earthflows where mass wasting causes soil materials to build up. There is an extensive distribution of colluvium as there are numerous earthflows and shallow earth slides within the field area. Colluvial deposits of The Wharanui earthflow are discussed in Chapter Four.

3.4.3 Stream Alluvium and Beach Deposits

Recent river and stream alluvium is derived from Woodside Creek, Tirohanga Stream, Delta Stream, and Pipe Stream. These streams have discharged their load on the coast to form a narrow discontinuous strip of alluvial deposits, comprising both small fans and beach terraces. This narrow alluvial strip on the coast separates the earthflow deposits from the beach dunes and terraces (Fig 1.5). The stream alluvium and beach deposits are Recent sediments. Much of the alluvium was deposited prior to and during the deposition of earthflow lobes and is interfingered with both the beach terraces and the earthflow deposits (Fig 3.6). The interfingering of sediments is a result of post-glacial eustatic changes in sea level as well as regional uplift.

The beach is up to 540 metres wide, and is increasing in width through uplift and progradation. This has resulted in the streams cutting through the old sand dunes and beach terraces so that narrow channels of alluvium are found from the old beach dunes to the present day beach. The existing shoreline is approximately 650 metres from the Wharanui Earthflow.

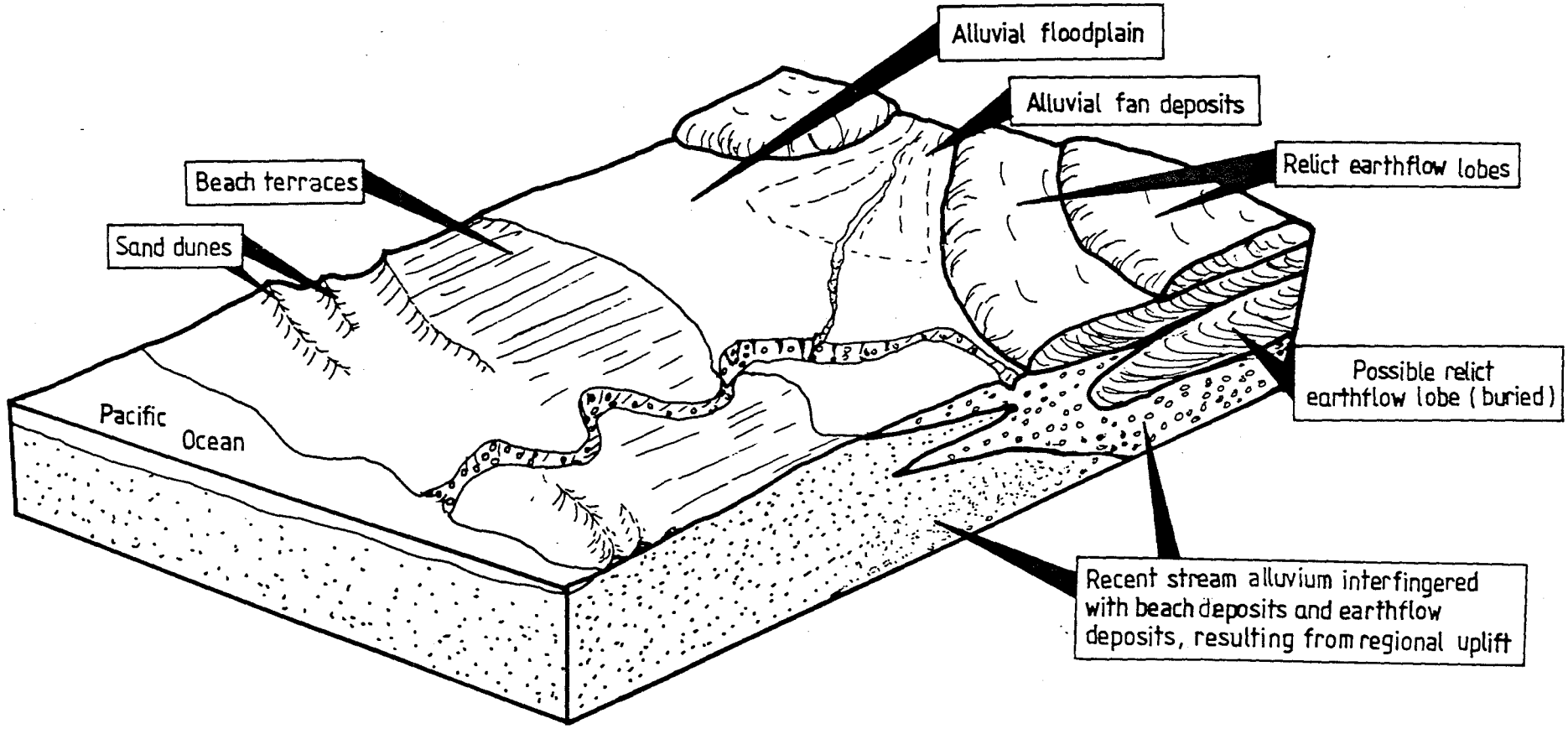

Figure 3.6 Schematic diagram of Recent alluvial and beach deposits interfingered with earthflow deposits. Interfingering is a result of uplift and progradation of the shoreline.

3.4.4 Wharanui Earthflow Formation.

The Wharanui Earthflow Formation is here defined as the soils and rocks associated with the Wharanui Earthflow. It is made up of a composite of the lithologies previously discussed in section 3.3.1. The primary lithologies associated with the Earthflow include the Grey Argillites, Grey Siltstones, and Red Mudstones. The soils associated within the Earthflow are derived from these lithologies and are transported to the Earthflow by slope movement processes.

The Wharanui earthflow lies on the edge of a large shear zone resulting from the Woodside Fault. The Earthflow lies within a valley which is controlled by this faulting.

The northeastern ridge predominently consists of the Grey Siltstone (Fig. 3.7). Along the ridge bedding is not easily distinguished as outcrops are poor, but in some fresh scarps bedding has been exposed and is striking subparallel to the flow, dipping approximately 40-45 degrees to the northeast. This corresponds to bedding found in Delta Stream on the opposite side of the ridge (Fig. 3 in the map pocket).

In the upper corner of the ridge near the headscarp are exposures of brownish-red tuffaceous volcanic breccia. The ridge has developed a colluvial covering along much of its length, the colluvium being derived from this volcanic breccia.

The southwestern ridge is primarily composed of the Grey Argillites which have weathered to a buff colouring. This unit is marked by its intensely sheared nature (Fig. 3.8), and large siliceous concretions within the argillite (Fig. 3.9). These rocks are strong when fresh, but their highly sheared nature makes them susceptible to weathering, and failures within the weathered profiles are common (Fig. 3.10). Bedding attitudes are not distinguishable as they have been crushed and intensely sheared.

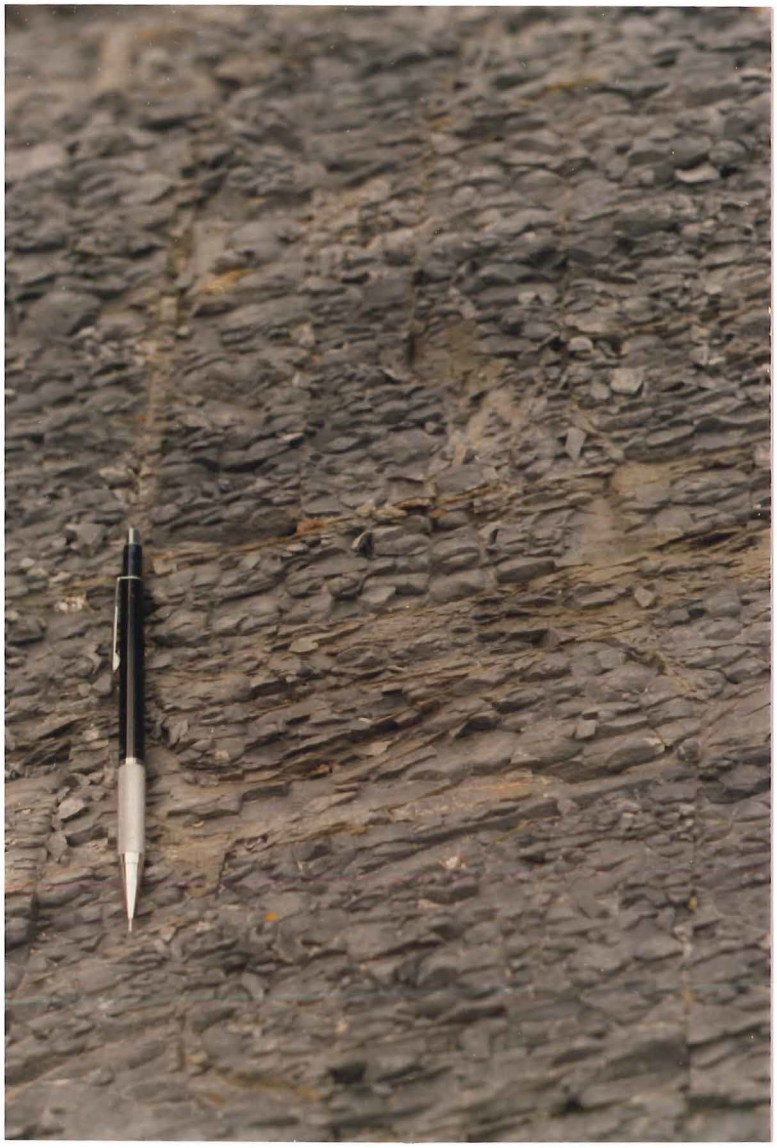

Figure 3.7 Grey Siltstone - exposure is in Woodside Creek (S36 314E 480N) note nodular weathering pattern and closely spaced joints. Pencil is 150 mm long.

Figure 3.8
Highly sheared Grey Argillites on south-western ridge above Wharanui Earthflow. Shovel is 60 cm long (S36 320E 460N).

Figure 3.9 Large spherical concretions within the Grey Argillites (S36 457E 322N).

Figure 3.10 Earthslide within residual regolith, derived from highly sheared Grey Argillites at the base of the southwestern ridge. Failure occured along the regolith - bedrock interface (8480E 7470N).

At the upper end of the flow the ridge consists of limestone and volcanics. These are blocks of "float" which are not in stratigraphic succession, and probably have been thrust in place from the Woodside Fault.

The valley deposits consist of colluvium almost entirely derived from the Grey Argillites, Grey Siltstone, and Red Mudstone. These are discussed fully in Chapter Four.

Grey Siltstone underlies the colluvium and is relatively continuous for the length of the flow. Excavations with the backhoe to the base of the earthflow enabled some bedrock samples to be obtained. Hand speciman and thin section examination of the samples showed that the bedrock was sheared with some alteration due to faulting. The Grey Siltstone is composed of very fine grained sand and coarse silt in a supporting mud matrix. It contains secondary pyrite mineralization and calcite veining. The altered siltstone forms the base of the earthflow and is relatively impermeable. (See section 4.4.2 Subsurface Investigations).

3.5 GEOMORPHOLOGY

3.5.1 Introduction

To aid in describing the field area, it has been divided into 3 sectors. The southwestern sector includes the area from the north branch of Tirohanga Stream to Woodside Fault; the central sector, from Woodside Fault to Woodside gorge; and the Northeastern sector from Woodside gorge to the State Highway 1 bridge. (See Fig 3.2 and/or Fig. 1 in map pocket).

3.5.2 Southwestern Sector

This sector of the site from the north branch of Tirohanga Stream to Woodside Fault is, geologically, the most complex of the sectors. The combination of weak

lithologies, unfavourable structures, and steep terrain (slopes up to 36°) has resulted in a large number of slope failures above the north branch of Tirohanga Stream. Instability is predominantly from shallow (less than 1 m deep) regolith failures derived from the Tirohanga Sandstone. This unit has developed a trellised drainage pattern reflecting jointing within the rock mass. The main stream channel has an orientation of approximately 160° and tributary streams are oriented approximately 70°. Drainage entrenched along discontinuities resulted in erosion and subsequent valley development. The valleys have become catchments for debris derived from regolith failures, and the accumulating debris have resulted in deposits which are susceptible to movement in the form of earthflows.

The headscarps of these earthflows occur along the Deep Creek Fault where the Tirohanga Sandstone contacts the Cookson Volcanics. A thin clay seam can be found in some outcrops separating the two. The clay forms an aquiclude at the contact, resulting in a line of seepage and springs located along the fault. The seepage areas and springs provide water at the head of the earthflows so that pore-pressure and material weight are increased. This results in an increase in stresses which may result in instability (see Fig. 3.11).

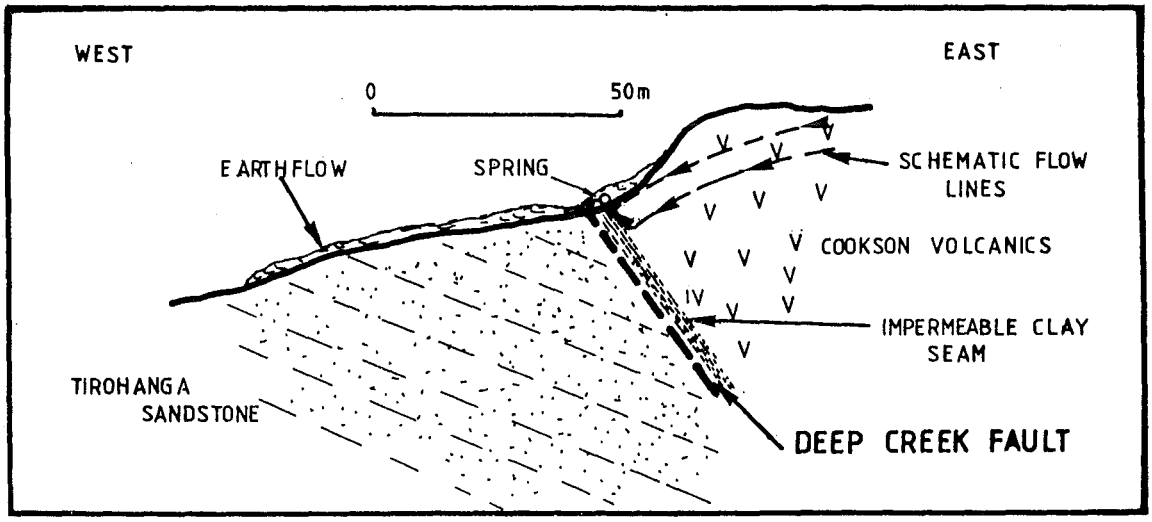

Fig. 3.11 Schematic section showing spring hydrology.

The area between the Deep Creek Fault and the Woodside Fault is generally hummocky, much of it being covered by earthflow deposits. These include the "Ben More" Earthflow, the Wharanui Earthflow, and numerous other smaller earthflows. These are classified as very slow to slow moving earthflows on the Varnes (1978) scale of movement, except the Ben More Earthflow which is presently stabilized and completely revegetated. These earthflows are made up of materials derived from the Upper Marls, the Red Mudstone, and the Grey Siltstone.

The most active earthflow within the site occurs adjacent to the Woodside Fault and flows into Woodside Creek (Fig. 3.12). Recently it has been active and movement caused material to dam Woodside Creek for a short time (David Parsons pers. comm.) (Fig. 3.13). This earthflow shows many of the features described in Chapter Two. Relevant features include pronounced lateral shears, pressure ridges, ridges with slickensided surfaces, and a bulging toe which is tear-drop shaped. Due to the steep slope (22^{o}), the very wet cohesive soils, and the continual removal of support by Woodside Creek, the earthflow appears to be continually active. During examination springs were noted in the headscarp, the material was very wet and could not support the authors weight. This earthflow has very similar material properties to the Wharanui earthflow. The major differences are in flow morphology and activity, which can be partially attributed to slope angle.

3.5.3 Central Sector

This sector's most prominent feature is the lower gorge of Woodside Creek where bluffs are formed along the creek due to the competent, strong rocks of the Grey Argillites and Amuri limestone (Flint beds and Lower Limestone, Fig 3.14). This gorge is formed along the core of a steeply plunging anticline, and stress induced discontinuities along the core, (ie. joints and small faults) formed the path of least resistance so a drainage

Figure 3.12 Active earthflow in southwestern sector, flowing into Woodside Creek within Woodside Fault zone. Note prominent headscarp and lateral ridges (S36 312E 403N).

Figure 3.13 Toe of earthflow in 3.12 dammed Woodside Creek in June, 1985.

Figure 3.14 Limestone bluffs above the lower gorge of Woodside Creek, view looking east towards Wharanui Point (arrowed) S36 320E 480N.

network became entrenched along the structure.

Flags trig is the highest point and lies along the crest of a ridge which extends along the width of the sector. This ridge is formed from well indurated Grey Argillites and Amuri Limestone which dips 30-45 degrees to the northeast.

Slopes are relatively stable in this sector as compared to those of other sectors, even where they become very steep (up to 42°). Minor rockfalls within the Lower Limestone were the only evidence of slope instability in the sector. These occur due to the intersection of defects.

3.5.4 Northeastern Sector

The northeastern sector's most dominant feature is Woodside Creek, where upon leaving the gorge it flows into a relatively broad stream channel over 100 m wide, narrowing just before the State highway 1 bridge A high bed load of limestone gravel in the creek contributes to road and rail bridges experiencing considerable aggradation problems.

Widening of the valley from the gorge is controlled by the lithology after this point. The ridges to the north and south sides of the creek in this area are steep-sided, up to 42 degrees, and are made up of predominantly weak to moderately weak rocks. These rocks include the Woodside Formation, Upper Marls, Cookson Volcanics, and Torlesse Greywacke. All of these lithologies weather to form a residual regolith covering, usually less than 1 m thick which is potentially unstable on the steep slopes (Fig. 3.15). Regolith failures in the form of translational slides are common, and the colluvium derived from the failures accumulates in the gullies and small depressions to form earthflows.

The southern ridge is narrow and steep sided with numerous translational earth-slides occurring at the

Figure 3.15 View looking east at south ridge above Woodside Creek (Wharanui Point is just outside top right corner of photo) S36 335E 478N.

weathered regolith-bedrock interface.

On the northern ridge there are many slumps and failures on the ridge sides within the Upper Marls and Cookson Volcanics. Several faults pass through this ridge including one minor fault and one major fault (Flags Creek Fault). The minor fault and the Flags Creek Fault are boundaries for for a sliver of the Upper Marls (Fig. 1, in the map pocket). The fault zones are partially obscured by earthflow deposits derived from the Upper Marls. On the western side of the Flags Creek Fault, a crushed zone approximately 20 m wide has resulted in a the formation of a gully along the weakend zone. Within the Upper Marls, large deep seated slumping (up to 5 metres deep) is observed. The top of the northern ridge is flat and the presence of alluvial deposits with some colluvium suggests that it was once a base level for a stream course. Other elevated terraces on the banks of Woodside Creek were noted as well. This and other evidence presented by Prebble (1980) suggest that there has been active Quaternary faulting and a high rate of uplift within the area.

CHAPTER FOUR

EARTHFLOW DESCRIPTION AND MORPHOLOGIC DEVELOPMENT

4.1 OBJECTIVES

The primary objectives of this chapter are to describe the Wharanui Earthflow in terms of its;

1) surface morphology,
2) subsurface geology and hydrology, and
3) geotechnical characteristics.

The surface morphology was mapped at a scale of 1:1000 and is presented in Fig. 3 (map pocket). Subsurface investigations were carried out to determine the inter-relationships of the soil types within the earthflow, the groundwater regime, and the subsurface geometry including delineation of basal shear surfaces and depth to bedrock. Laboratory characterization of the Earthflow deposits was carried out to determine physical and hydraulic properties of the soil types to aid in predicting their behaviour.

From the above information, interpretations have been made concerning the sequential development of the Earthflow, and a developmental model of the Earthflow is proposed.

4.2. SURFACE MORPHOLOGY

4.2.1 Field Surveys.

Morphologic features of the Wharanui Earthflow complex were surveyed and mapped using a Wild DI3 distomat and T-16 theodolite, and supplemented by aerial photograph interpretation (photograph numbers are listed in Chapter Three, section 3.3.1). Topographic plans were prepared at scales of 1:1000 using a 2 metre contour interval for the

whole Earthflow (Fig. 3), and at 1:500 with a 1 metre contour interval for the toe area (Fig. 4). These plans were used for mapping the flow in detail, and for presenting the monitoring data (discussed in Chapter Five). Mapping of individual earthflow deposits was carried out between June and August 1984. The following descriptions refer to the Earthflow complex at that time.

4.2.2 General Features.

The Wharanui Earthflow is located within a narrow valley on the Kaikoura coast. The Earthflow has a length of approximately 1 km from the headscarp to the distal margin and an elevation difference of approximately 210 m along its length. The area of the valley from ridge to ridge is approximately 22 ha, and the Earthflow itself comprises an area of approximately 5 ha. The flow has a sinous shape in plan view, with the direction of movement generally to the southeast (Refer to Fig. 4.1 and Fig. 3 in the map pocket).

In the upper portion of the valley there is an arcuate headscarp and the valley opens up into a basin with a symmetrical cross-section. In the lower portion of the valley, before it opens out onto the coastal plain, the valley sides have a markedly asymmetrical profile as the northeastern ridge has developed a steep slope (greater than 25 degrees), whereas the southwestern ridge is typically a more gentle slope (approximately 15 degrees).

The Earthflow has been divided into 3 sections for the purposes of description, and these are 1) the 'zone of depletion', 2) the 'main body', and 3) the 'zone of accumulation' (Fig 4.1). Descriptions of each section follows.

4.2.3 Zone of Depletion

The 'zone of depletion' (Fig 4.1) is characterized by both fresh and revegetated scarps. The scarps are the result of rotational slumps up to 3 m deep, and of shallow

translational slides less than 1 m in depth. Degraded back-tilted blocks are present on the slopes of the headscarp, whilst the headscarp itself is moderately to steeply inclined (25 - 35 degrees) and has an arcuate shape in plan view resembling an amphitheatre. The base of the headscarp is marked by a sharp break in slope which flattens out into a basin of approximately 0.5 hectares, where some ponding of water occurs (Fig. 4.2).

The northeastern ridge adjacent to the headscarp is steep (25°) and is mantled by tuffaceous volcanic breccia and colluvium up to 3 metres deep. Within these materials shallow (less than 1.5 m deep) translational slides or deeper seated (up to 2.5 m) rotational slumps are observed. No mass movement features were noted on the southwestern ridge in the headscarp area.

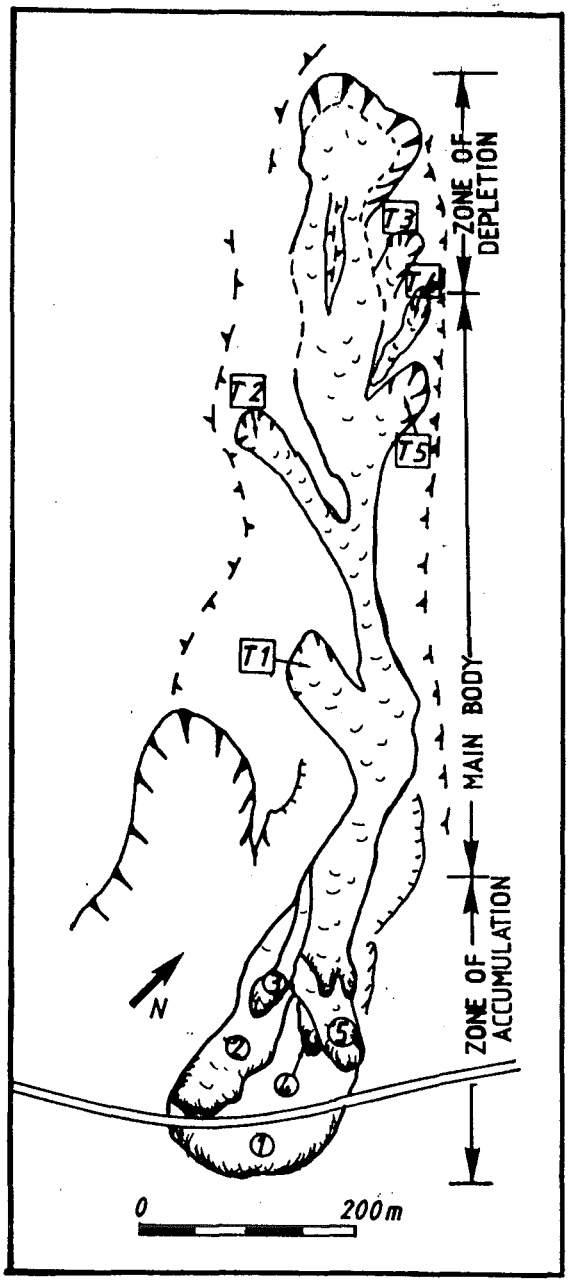

Fig. 4.1 Plan view of Wharanui Earthflow showing extent of each 'zone', and feeder flows.

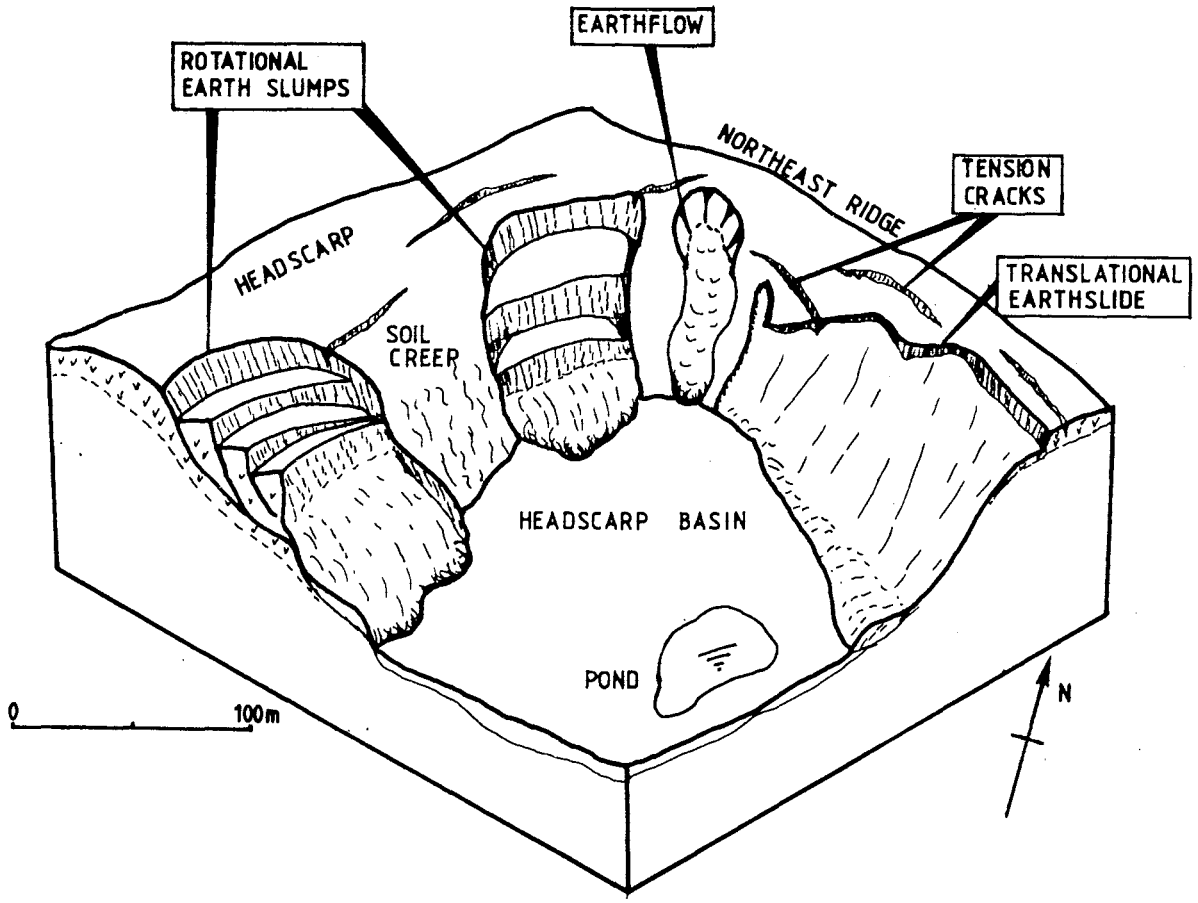

Fig 4.2 Schematic diagram of Zone of Depletion.

4.2.4 Main Body

The main body of the flow as defined here involves an area of approximately 2.5 ha, and stretches from the zone of depletion to the zone of accumulation (Fig. 4.1). It is confined to a narrow valley floor which varies in width from approximately 30 to 100 metres, and which is slightly sinusoidal in shape (Fig. 4.1). The average gradient is approximately 13 degrees. The features within the main body are discussed separately below.

1. Pressure Ridges. Pressure ridges are features found in areas where either two or more channels merge, or where the Earthflow is confined. An area of converging channels occurs below the headscarp basin where a central ridge, which is stable, divides the Earthflow into two

channels. These channels later coalesce to form a single channel at the end of the ridge (Fig. 4.3 and 4.4). Along the flanks of this ridge there are well defined lateral pressure ridges up to .75 m high (Fig. 4.5). Other prominent pressure ridges have formed at the mid section of the main body where the flow is at its narrowest point. In this location the Earthflow is only 20 metres wide, and pressure ridges have formed within the confined area.

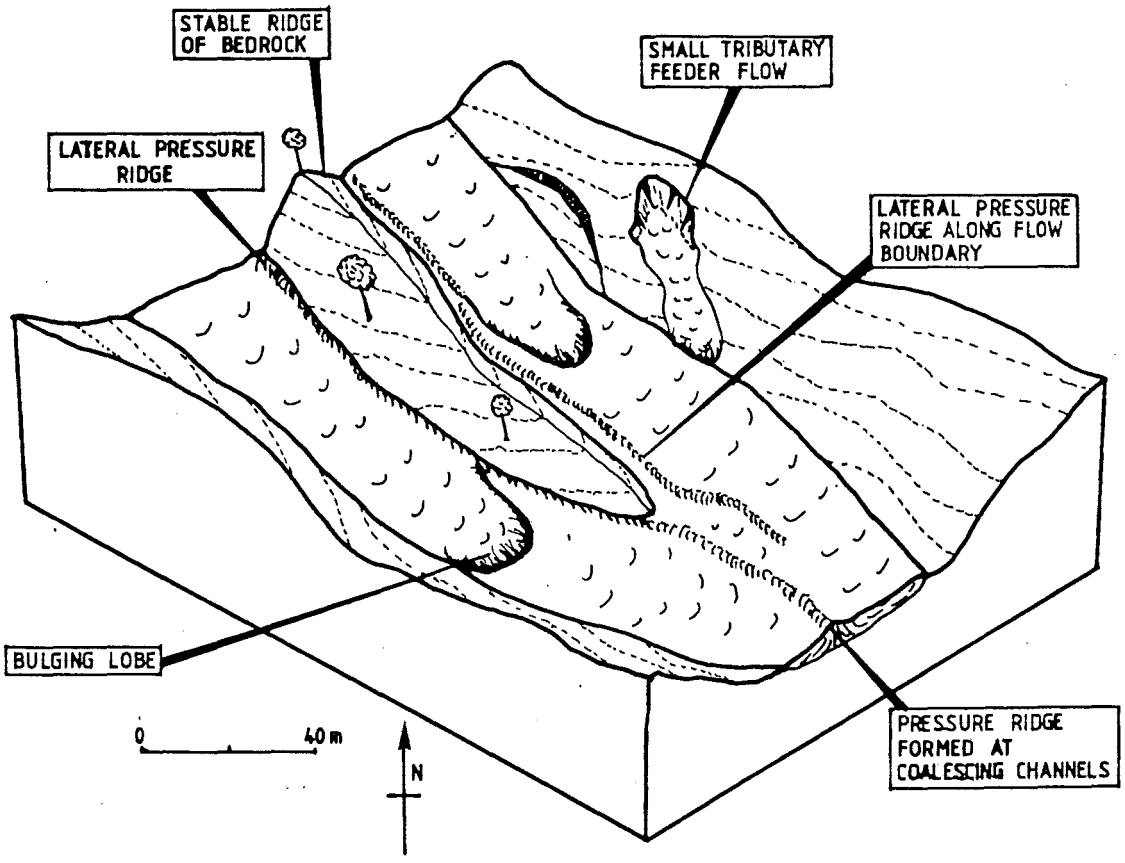

Fig 4.3 Schematic diagram of coalescing channels which have formed pressure ridges.

2. Tributary Earthflows and Earth-slides. There were five tributary earthflows mapped which join the main body of the Wharanui Earthflow (T1 - T5, Fig. 4.1). Each of these earthflows has its own locally developed headscarp and is analogous in morphology to a stream tributary. Some of the earthflows appear to be stabilized and completely revegetated whilst others show recent signs of movement which include very hummocky, pervasively crevassed chaotic ground surfaces.

Figure 4.4 Stable ridge shown with coalescing earthflows (arrowed). Lines show outline of boundary shears. View is looking south from 8200E 7900N.

Figure 4.5 Lateral pressure ridge formed alongside stable ridge pictured above. Ridge is up to .75 m high. View is looking southeast from 8200E 7250N.

On the southwestern ridge there are few earth-slides as defined by Varnes, but two noteworthy earthflows were observed. The first of these (T1) is essentially revegetated, the ground surface is relatively undisturbed and only the headscarp and lateral shears remain as prominent features. The second tributary earthflow (T2) is characterized by a hummocky ground surface with large open tension cracks. The three tributary earthflows (T3 - T5) on the northeastern ridge all occur in the upper portion of the main body, and orginate within the tuffaceous volcanic breccia.

There are numerous earth-slides which occur along the northeastern valley side, and these are typically translational earth-slides less than 1 metre deep. They occur at the regolith bedrock interface of the Grey Siltstone (Fig 4.6 and 4.7), and are the primary type of slope movement related to this lithology.

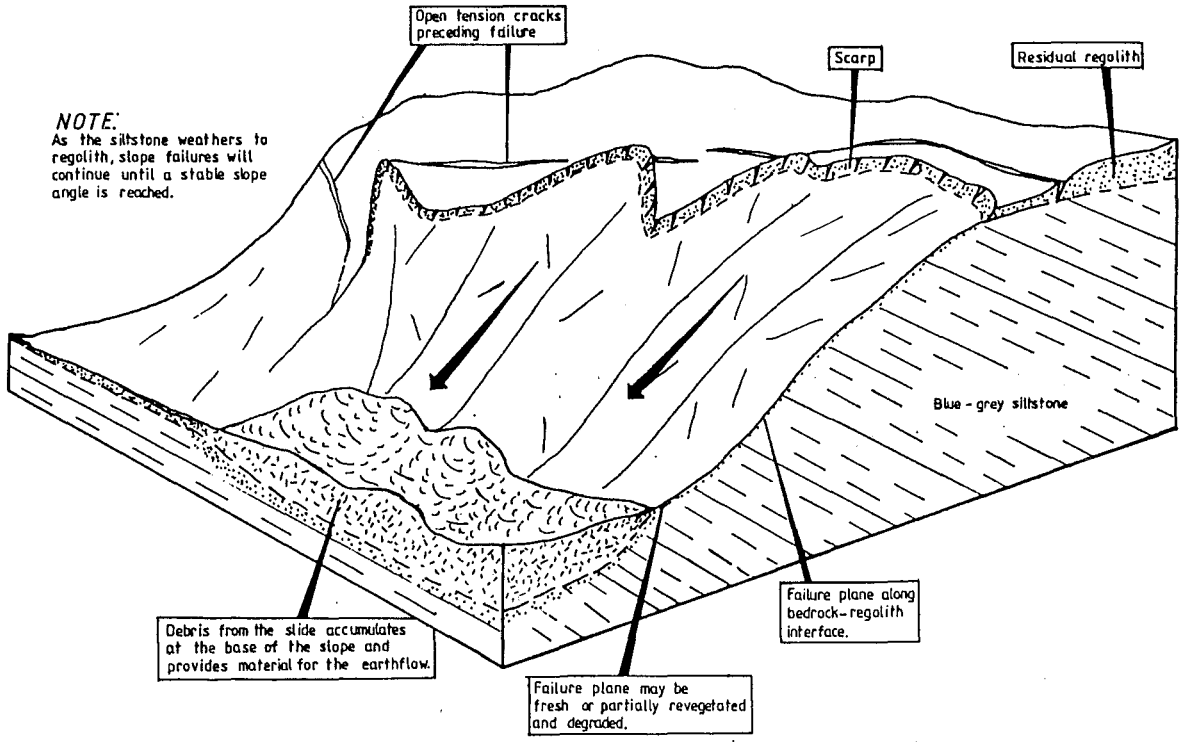

Figure 4.6 Schematic diagram of shallow earth-slide, typical of northeastern ridge above Earthflow.

Figure 4.7 Shallow translational earthslide typical of those on the northeastern ridge above Wharanui Earthflow. View is looking northeast from 8500E 7600N.

3. Bulges. Within the main body of the flow distinct bulges or lobes have formed. In plan view the bulges are rounded and concave sourceward; in profile they are convex upwards displaying fissures, hummocky ground, and broken turf mats. The bulges typically override the former ground surface and are underlain by a surface of separation (Fig. 4.8). They appear to have been active intermittently, as some bulges are degraded and revegetated and others show more recent activity (eg. little vegetation has developed on the more recent bulges, see Fig 4.9 and 4.10).

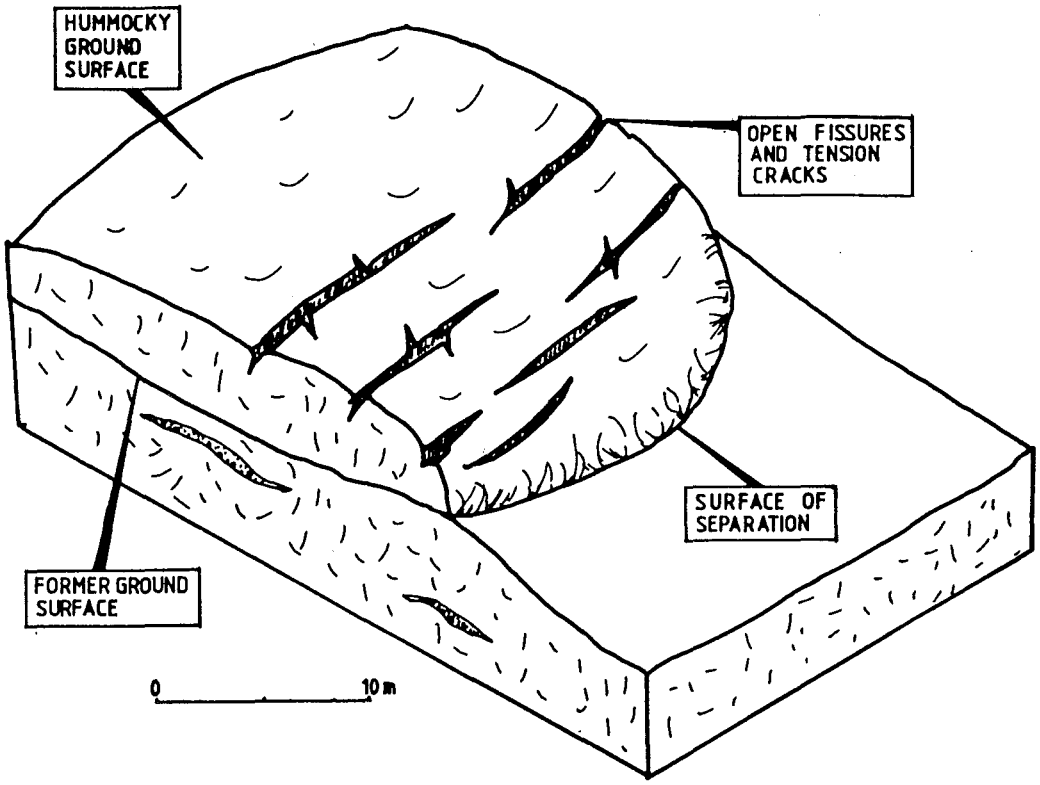

Fig. 4.8 Schematic diagram of typical bulge.

4. Gullies. Gullies begin at the mid-section of the main body and extend for over 200 metres (refer to Fig. 3 in the map pocket). They are up to 1.8 metres deep and are a relatively continuous for the length of the mid-section, forming a significant drainage network. The gullies are at their deepest where the slope angle is greatest, approximately 15 degrees, but reduce and eventually end where the slope angle has decreased to 12.5 degrees or less. There are some other minor gullies which have become entrenched within depositional lobes, but these are small

Figure 4.9 Hummocky broken ground surface typical of bulges within the Wharanui Earthflow. These turf mats are degrading as vegetation becomes established (8595E 7500N).

Figure 4.10 More recent lobe movement is demonstrated in another earthflow within the site. Note the lack of vegetation in contrast to Fig. 4.9 and the highly disrupted ground surface. View looking downslope where the earthflow toe occasionally blocks Woodside Creek (S36 312E 483N).

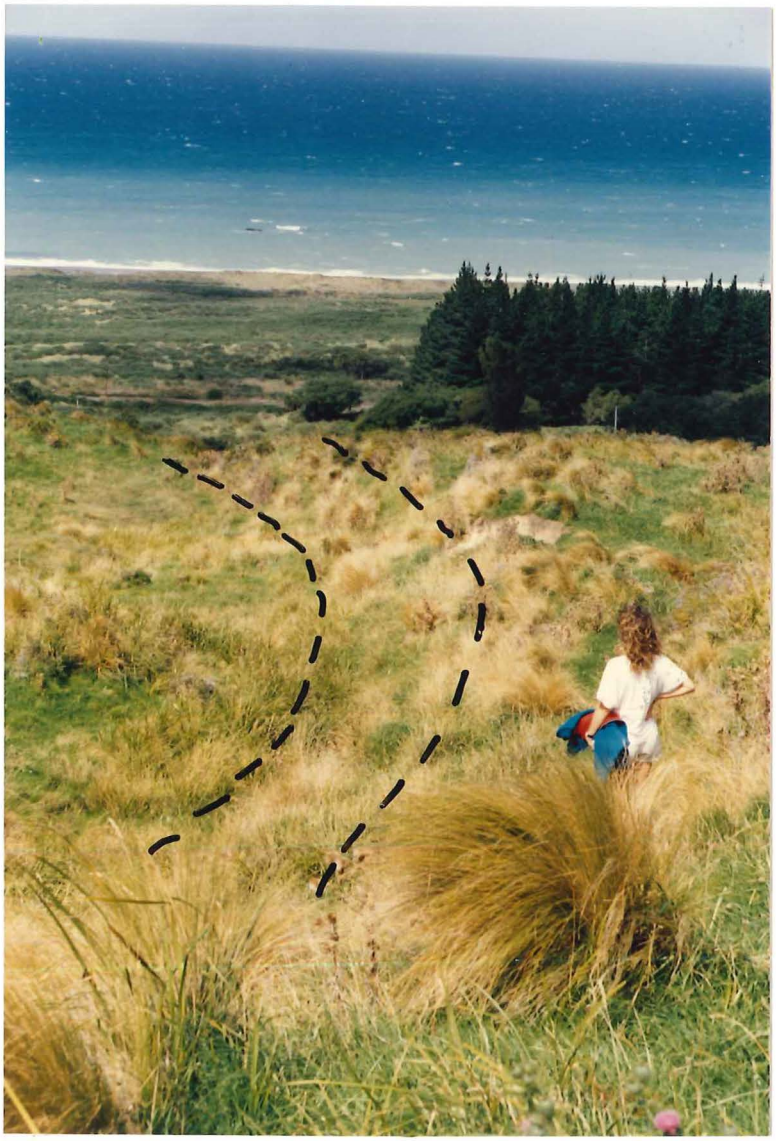

Figure 4.11 Degraded Lateral shear scarp (dashed outline) approximately 1.5 m high in the zone of accumulation. View looking south from 8550E 7490N.

discontinuous localized gullies and do not form a significant drainage pattern.

5. Lateral Shears. Lateral shears indicate the extent of present flow activity and are obvious features along the length of most of the flow. They have a very similar morphology to pressure ridges, but they occur at the lateral limits of the flow. They generally form ridges of approximately 0.5 metres high and are visible on both flanks of the Earthflow. In the lower portion of the main body, the Earthflow has truncated an older debris lobe and a lateral shear scarp has formed which is up to 1.5 metres high (Fig 4.11). It is currently revegetating and shows no signs of recent movement (eg. fresh slickensided surfaces, or displaced ground surface).

4.2.5 Zone of Accumulation

The zone of accumulation is dominated by five distinct tear-drop shaped terminal lobes (numbered 1 to 5 in Fig 4.12). The largest of these, lobe 1, extends across State Highway 1 forming a tongue approximately 150 metres wide. Lobes 2 to 5 overlie lobe 1 in a depositional sequence with lobe 3 overlying lobe 2. Lobe 4 and lobe 5 both overlie lobe 1, having been deposited to the east of lobe 2 and lobe 3. The lobes generally decrease in size upslope.

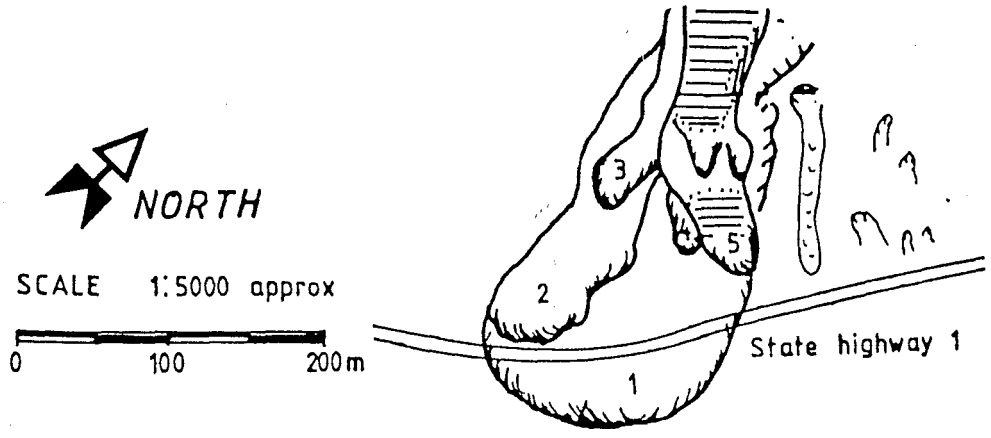

Fig. 4.12 Number and position of terminal lobes.

Figure 4.13 Terminal face of lobe five, with scarplets and active gully erosion on the flanks. View is looking northwest (upslope) from 8710E 7390N.

Lobes 1 to 4 are differentiated from lobe 5 by their vegetation development and absence of cracks and scarplets. Lobe 5 has a steep (approximately 25 degree) terminal face, is strongly convex in cross-section, and is characterized by tension cracks, scarplets and steep sided gullies on the lateral margins (Fig 4.13). Although covered by vegetation on the frontal surface little vegetation has established in the gullies .

On the flank of lobe 5 gully erosion has downcut into lobe 1, exposing the deposits within the lobe. These deposits exhibit multiple shear surfaces arranged like imbricate thrust faults (Fig 4.14).

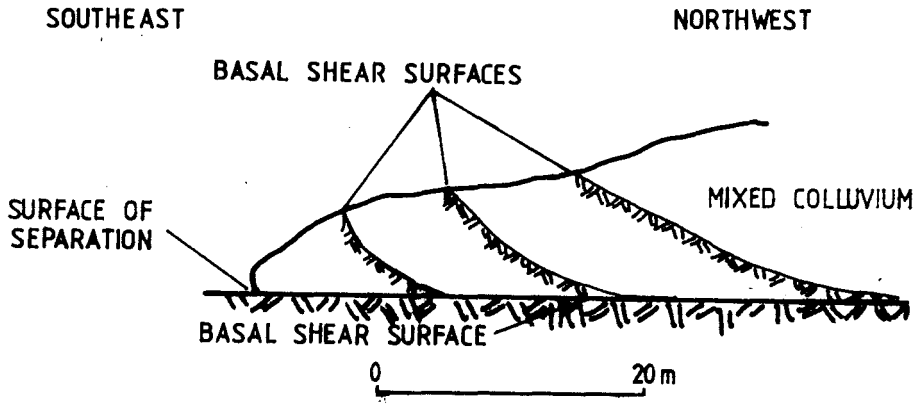

Fig. 4.14 Schematic diagram of multiple shear surfaces within Lobe One as seen in an adjacent gully.

4.3 SUBSURFACE INVESTIGATIONS

4.3.1 Methods Used

Subsurface investigations began in September 1984 using a hand auger, and a total of 20 boreholes were completed to depths varying from 1 to 6.8 metres (see Summary Sheets in map pocket for detailed logs). In addition to hand augering, 2 backhoe trenches were excavated, 5 seismic refraction traverses were made across the flow, and 1 for a length along the flow centreline.

Groundwater level monitoring began in March 1985 using Casagrande type piezometers. Five piezometers were installed in selected auger holes (see Appendix 6).

4.3.2 Augering

Of the 20 hand auger holes drilled, one was below lobe 5 (A1), one was on the northeast ridge in regolith (A10), two were in feeder zones (A18 & A19), and 16 were located on the flow surface (refer to Fig. 3 in the map pocket for hole locations). Fifteen of the auger holes were drilled into bedrock (13 in Grey Siltstone and 2 in Red Mudstone) identified as the base of the Earthflow. Evidence which supports the siltstone being the base includes:

1. a similar lower profile in each of the 15 holes, consisting of moist grey clayey silts which rapidly graded (within 100-200 mm) into Grey Siltstone or the Red Mudstone that could not be penetrated with the hand auger.

2. seismic profiles which generally corresponded with the depths from the augering (see 4.3.4).

3. bedrock was reached at 4.0 metres in Trench 1 (refer 4.3.3).

Summary logs of each auger hole are presented in Figs. 6 and 7 in the map pocket. The graphic logs give details about the soils of the Earthflow deposits including sample intervals, shear vane testing, moisture content, and water levels within each hole. Augering indicated that depth of the colluvium was between 2 and 5 metres for most of the flow length and more than 7 metres at the toe (refer to Long-Section Fig. 3 in the map pocket).

Representative 'disturbed' samples were collected from the various soil types for laboratory testing and characterization. These are discussed in section 4.4.

4.3.3 Trench Excavations

Two backhoe trenches (test pits) were excavated within the Wharanui Earthflow (see Fig. 4.15 for location). The first trench was excavated from the northeastern ridge

across the lateral shear and into the main body of the flow. Depth of the trench was up to 4 metres. The excavation was nearly perpendicular to the flow movement direction, thus providing a transverse cross section through the deposits. The second trench, up to 3.8 metres deep, was excavated on the southwestern side of the Earthflow margin, and into the main body of the flow.

Trench 1. Observations within the first trench were limited due to unsafe conditions at the time of excavation. The trench could not be entered to allow close examination, as there were sudden wall failures within the Grey Siltstone at the northern end of the trench, as well as bulging of trench walls at the southern end (Fig. 4.16).

The excavation into the ridge revealed the Grey Siltstone was moderately to highly weathered, moderately weak, coarsely layered, and sheared. The trench was excavated through the Siltstone and into the Earthflow materials.

The lateral shears while pronounced on the surface were obscured below the ground surface and only a gradational zone could be delineated. The zone consisted of sheared Grey Siltstone grading into a grey silty 'pug'. This pug is considered to be due to shearing associated with movement along the Woodside Fault.

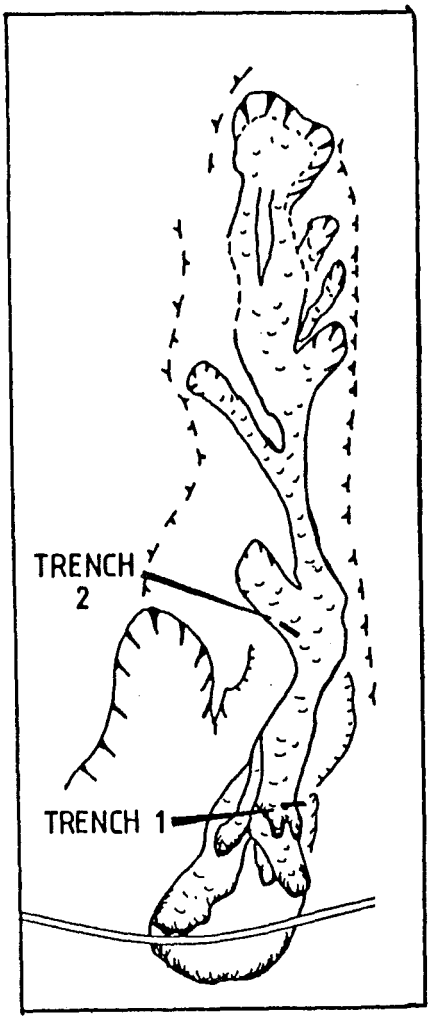

Figure 4.15 Locality of Trenches.

Figure 4.16 Excavation of Trench 1 showing collapse within sheared siltstone at northern end (lower part of photo) and bulging of walls at southern end (upper part of photo). The collapsing walls made entry into the trench impossible. Note water flowing into the trench (arrowed). (8600E 7505N).

Within the trench, Earthflow material consisted of yellowish brown clayey silts with lenses of red clay and grey silts. Contacts between the colluvial types were sharp but irregular. (see trench log Fig 4.17).

In the trench bedrock was encountered for a length of 2 metres along the base of the trench. However, soon after reaching the bedrock, the excavation had to be terminated due to the walls bulging. The bedrock along the base consists of strong, greyish green, intensely sheared siltstone, with secondary calcite veining and pyrite crystallisation. This alteration is thought to be associated with the Woodside Fault.

Water was observed flowing into the trench at approximately 10 litres/min (visual estimate), from a rubbly layer (described as a sandy gravelly silt) which was at a depth of 3 metres. This lense shaped rubbly layer was perched above the bedrock and enveloped within the fine grained cohesive soils.

Trench 2. As with the first trench, the second trench was unstable upon excavation, and detailed examination was limited. While core samples were being extracted from the trench, tension cracks were noticed which were indicative of imminent failure and only four core samples could be extracted. Subsequently a large block of material slumped into the trench, though not as rapidly as had occurred in the first trench (Fig 4.16).

At approximately 1.4 metres depth within the trench a shear zone was noted. Below the shear zone the soil is a homogenous greenish-grey to bluish-grey clayey silt with some fine sand lenses (Fig. 4.18). Above the shear zone, colluvium is chaotically mixed, with highly irregular contacts between the colluvial soils (Fig. 4.19). Bedrock was not reached during excavation of this trench. The blue-grey clayey silts below the shear zone are thought to be in-situ soils as there were no shear surfaces located, nor was there any other evidence of movement such as mixing

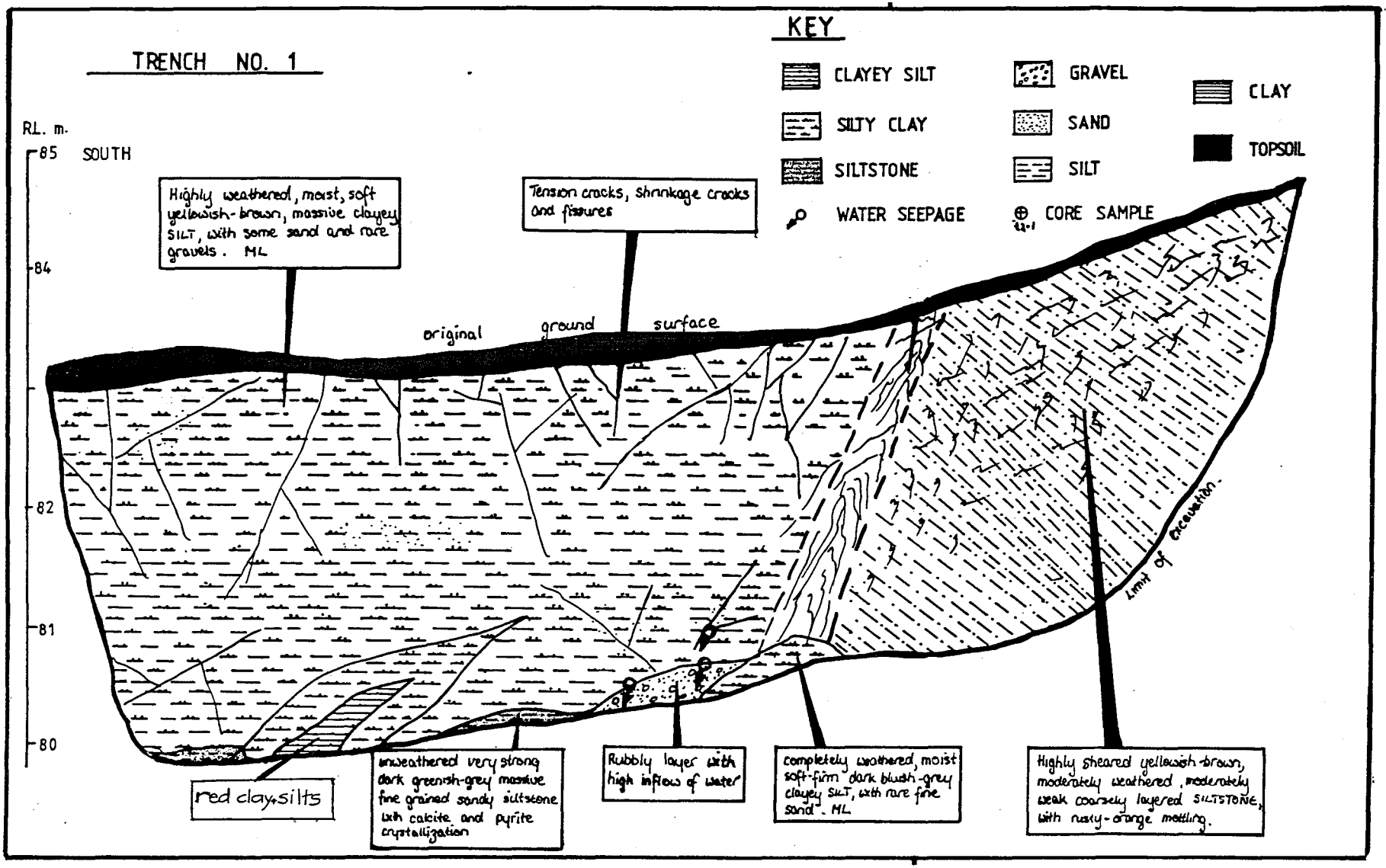

Fig. 4.17 Log of Trench 1

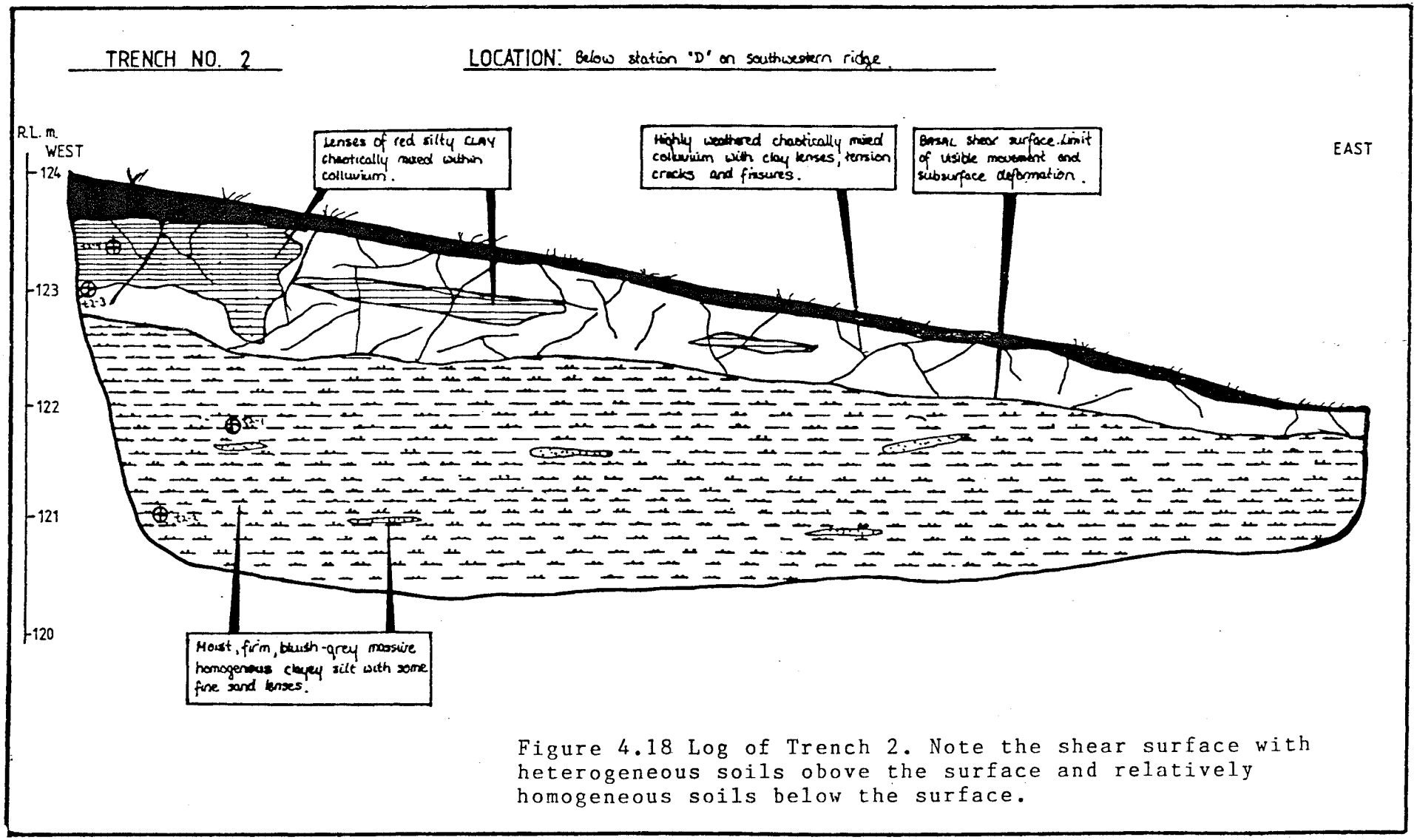

Figure 4.18 Log of Trench 2. Note the shear surface with heterogeneous soils obove the surface and relatively homogeneous soils below the surface.

Figure 4.19 View looking down into Trench 2. Note irregular contact between red silty clay and yellowish brown clayey silt (dashed). Below the mixed colluvium the grey clayey silt is relatively homogeneous and apparently undisturbed. (8515E 7600N).

of soil types.

It was anticipated that during trench excavations suitable undisturbed samples could have been extracted for use in triaxial strength testing to facilitate a stability analysis, however this could not be achieved. Although detailed logging and sampling could not be performed due to the unstable conditions within both trenches, it did not prevent important observations from being made of significant features within the Earthflow deposits and of the base of the Earthflow.

Major features of the Earthflow material and mass determined in the trenches were:

1. three major soil types chaotically mixed within the Earthflow deposits;
2. bedrock underlying the Earthflow material at a depth of approximately 4 metres.
3. the existence of semi - confined aquifers with groundwater flow; and
4. A basal shear surface within 2 metres of the ground surface.

4.3.4 Subsurface Profile

Five seismic refraction traverses were used to construct general subsurface profiles (See Fig. 3 in the map pocket for location). Seismic refraction plots show the Earthflow soil material to range in depth from 2 to 5 metres with seismic velocities of approximately 350-380 m/s. The bedrock underlying the flow had seismic velocities from 1600-2600 m/s. (See Appendix 8 for methods employed).

The earthflow complex generally consists of mixed colluvium overlying grey siltstone. Data from hand auger boreholes, seismic refraction traverses, and trenches were used in compilation of long sections and cross sections shown in Fig. 3 in the map pocket. Two cross-sections are presented (Figs. 4.20 and 4.21) as typical subsurface profiles. All seismic profiles are shown in Appendix 8.

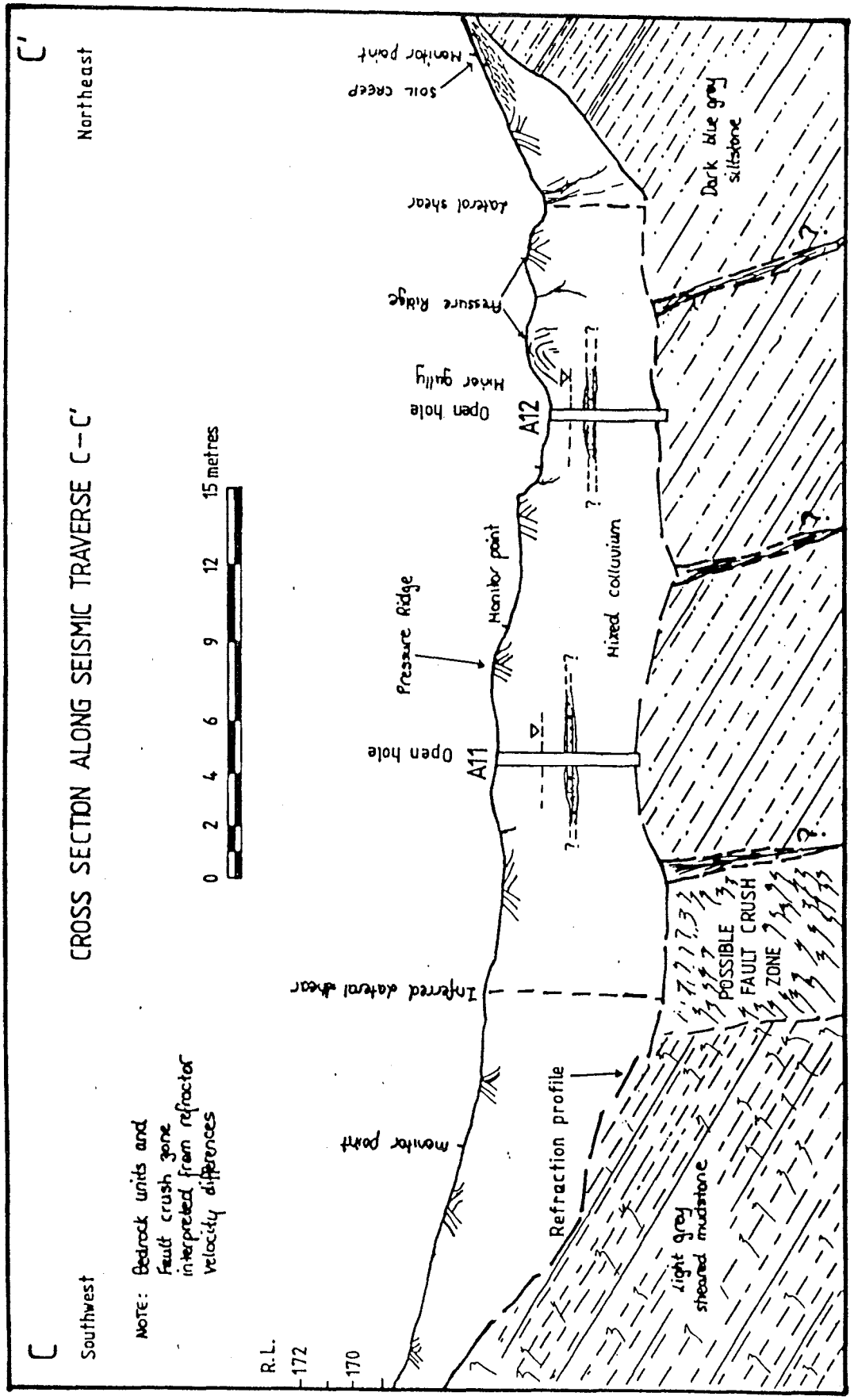

Figure 4.20 Interpreted profile along seismic profile C - C' showing refraction profile compared to the augering depths. Lithology and the faults are interpreted from seismic velocity variations within the bedrock (see Fig. 1 in the map pocket for location).

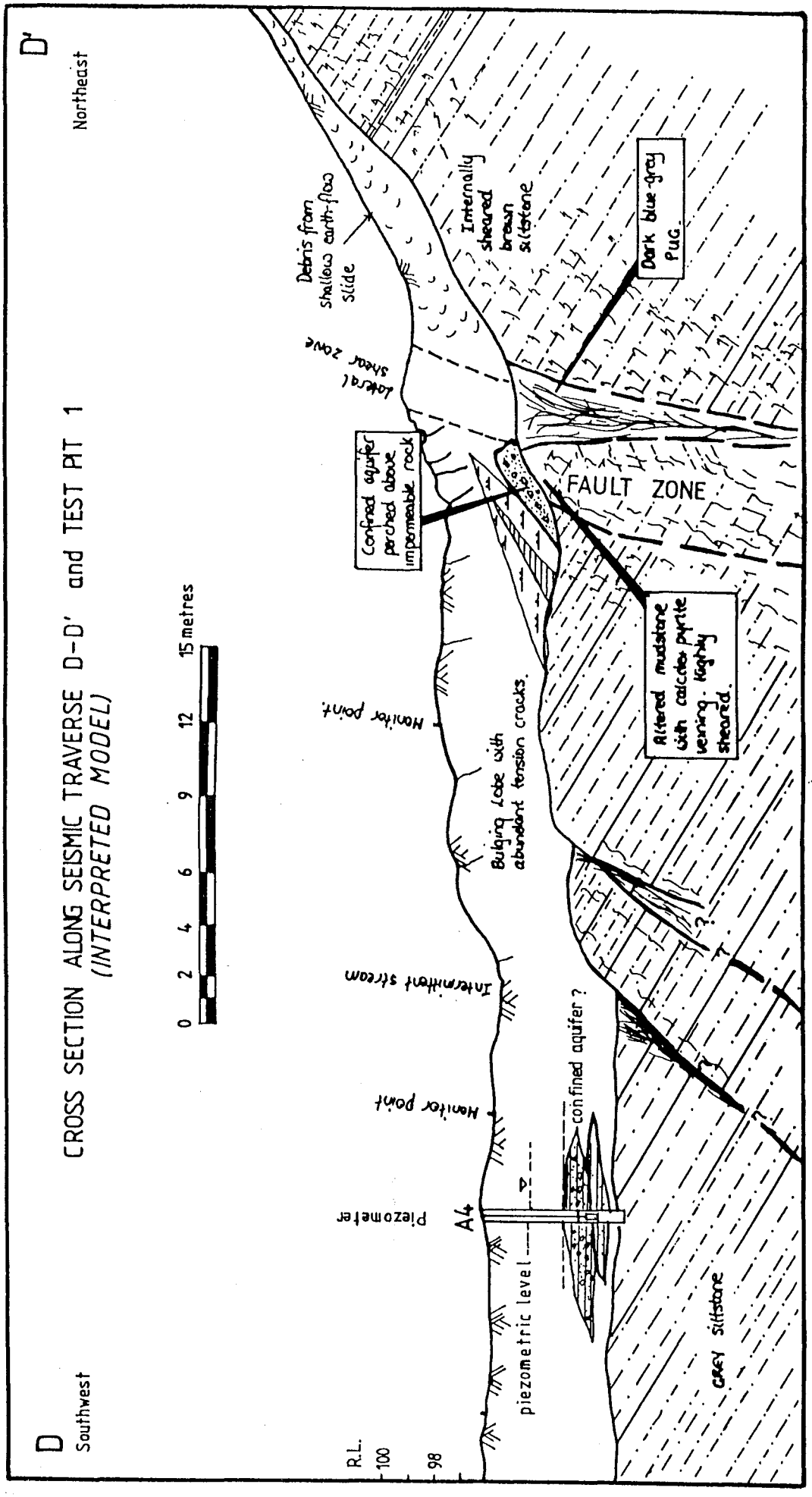

Figure 4.21 Interpreted profile along D - D' showing location of confined aquifer, and fault zone as determined by Trench 1.

Lithological boundaries between soil and bedrock may be either gradational, occuring over an interval of 100 - 200 mm, or distinct where there is a sharp break between the soil - bedrock interface.

The bedrock profile is relatively linear for the length of the flow, but is not a smooth surface. As has been stated earlier in Chapter Two, the Wharanui Earthflow overlies the axis of the fault. Seismic interpretation indicates that the bedrock below the Earthflow is faulted in cross-section resulting in displaced blocks. These displaced blocks are shown schematically in Fig. 4.20. The Fault is shown to have a crushed zone in Fig. 4.21. This was interpreted from a sudden velocity drop of 1913 m/s (Grey Siltstone) to 1174 m/s (interpreted crush zone) followed by an increase in velocity to 2636 m/s denoting a lithological change which is thought to be the Grey Argillites (see Appendix 8).

4.3.5 Groundwater

The groundwater regime of the Wharanui Earthflow is not well defined. Within the earthflow there are two contrasting soil groups which influence the hydrology:

(1) the cohesive fine grained soils which dominate the earthflow material; and
(2) rubbly soil lenses which occur within the cohesive soils.

Fig. 4.22 shows a schematic representation of the rubbly lenses within the fine grained soils and they appear to be confined or semi-confined aquifers as they are enveloped within soils of very low permeability. There are an indeterminate number of these aquifers within the colluvial deposits.

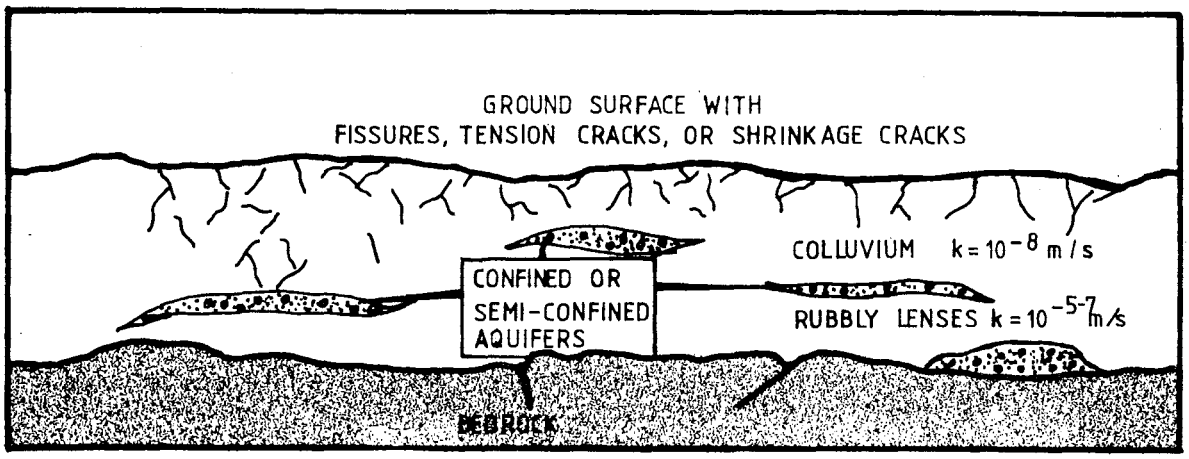

Fig. 4.22 Schematic representation of confined aquifers (rubbly lenses) within cohesive soils along flow axis.

Recharge of the groundwater occurs by infiltration. When the soil is dry, dessication cracks are more or less open so that at the start of infiltration the soil has a high hydraulic conductivity. As precipitation saturates the soil by infiltration, the clays and colloids swell so that the fractures close, thus there is a diminishing hydraulic conductivity.

The soil moisture content is an important factor affecting the groundwater recharge. If there is a deficiency in soil moisture content, then recharge of aquifers will not take place as any infiltration would recharge the soil moisture. The soil moisture must increase to a value beyond the field capacity so that water will drain downward to the groundwater table (Davis and DeWiest 1966).

Laboratory tests on the cohesive soil material gave permeabilities of approximately 10^{-10}m/s (see Appendix 7). In-situ falling head permeability tests were carried out within the piezometers and gave soil mass permeabilities of 10^{-8} - 10^{-9}m/s (see Appendix 7). The rubbly lenses consisting of silt, sand, and gravel are estimated from data in Freeze and Cherry (1977, p. 29) to have permeabilities of

10^{-5} - 10^{-7}m/s.

Casagrande type piezometers were installed in five auger holes (A1, A3, A4, A5, & A8) to monitor groundwater fluctuations (see Fig. 3 in the map pocket for location). Refer to Appendix 6 for construction details and Chapter Two for a discussion of piezometer selection and performance.

The piezometers were installed in the zones where water was observed flowing into the borehole. They were installed only in these zones as they had sufficient volumes of water to generate reasonable response times. If they were installed in the cohesive soils there would not have been sufficient water volume to obtain any readings at all as the soils are of such low permeabilities.

It was not possible to take frequent readings nor was it necessary as the objective was to gain a general idea of groundwater levels. The piezometer readings were taken in March, May, and August. Depth of piezometric level from the ground surface is shown in Table 4.2, and Fig. 4.23 correlates individual piezometric fluctuations to rainfall. A few uncased auger holes also had water in them, levels were measured and are presented in Table 4.3.

PIEZOMETER READINGS

Date	Water Level Below Ground Surface (metres)				
	A1	A3	A4	A5	A8
8/3/85	3.46	1.09	1.35	1.16	1.80
24/5/85	3.1	1.32	2.37	2.09	1.33
28/8/85	2.75	0.85	1.20	1.98	0.88

Table 4.2 Piezometric Level Measurements.

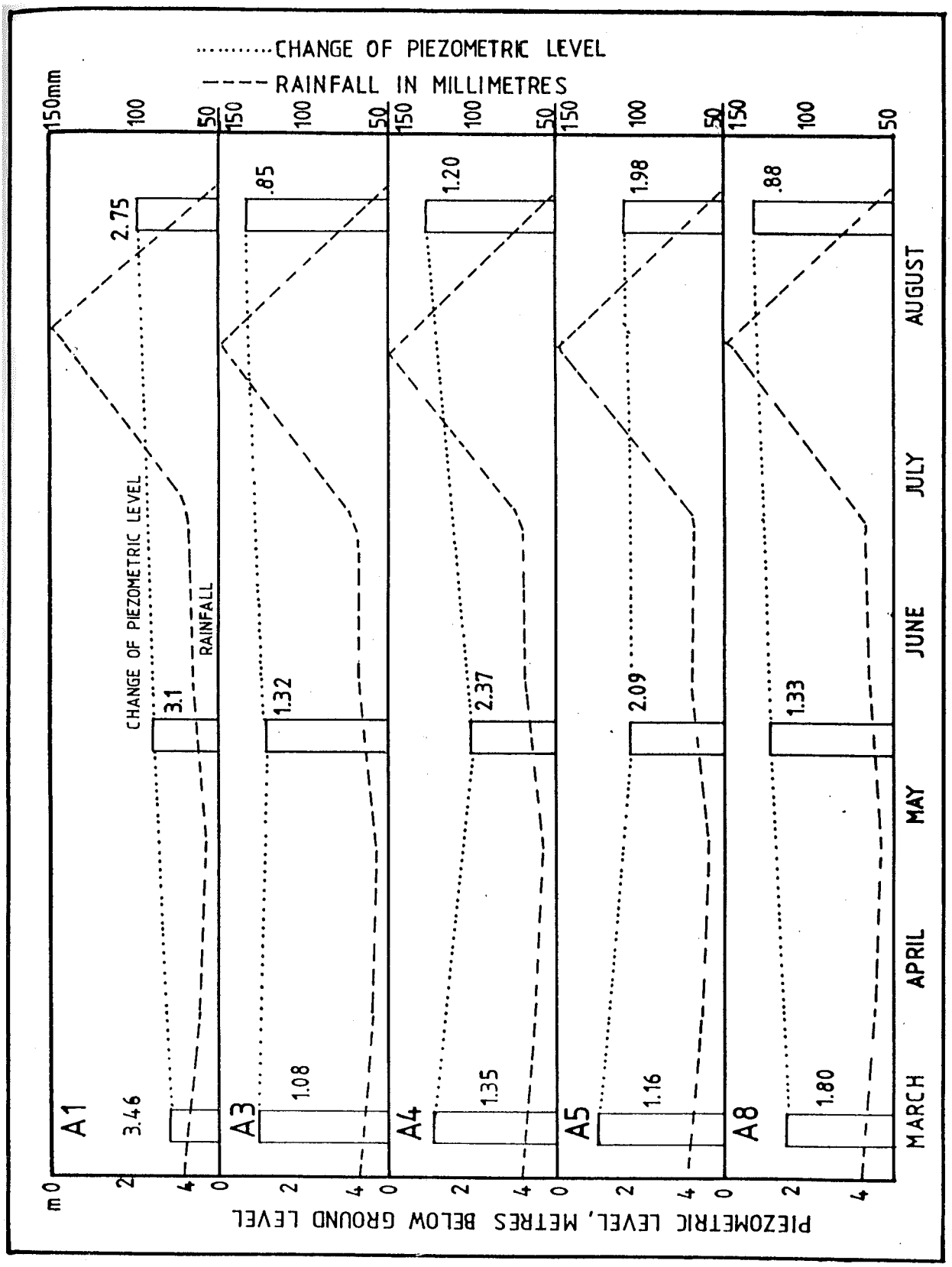

Figure 4.22 Correlation of piezometric levels to rainfall.

OPEN HOLE READINGS

Date	Water Level Below Ground Surface (metres)				
	A20	A11	A12	A13	A15
8/3/85	3.72	2.06	3.24	0.30	3.64
24/5/85	1.2	1.75	-	0.48	2.60

Table 4.3 Open Hole Water Level Measurements.

4.4 GEOTECHNICAL PROPERTIES

4.4.1 Strength Testing

In-situ shear vane testing was carried out in 5 Auger holes during drilling. A Geonor shear vane accurate to + 10% was used to determine undisturbed and remoulded undrained shear strength values at approximately .5 m intervals. A full discussion of shear vane testing is discussed by Andresen (1981). Results are shown in Fig. 4.24. (Refer to Fig. 6 in the map pocket for correlation to lithology).

Fig. 4.24 shows a general correlation between shear strength and moisture content. Low shear strength values are measured for materials with high moistrue contents and high shear strength values for low moisture contents. Undrained shear strength showed no relationship to depth. Remoulded shear strength values were lower for all profiles tested.

A distinct zone of low shear strength values consistent with a basal shear surface was not delineated during these investigations.

4.4.2 Laboratory Testing

Laboratory testing of colluvium obtained by augering and from test pits was carried out by the author. Determinations of moisture content, dry density, linear

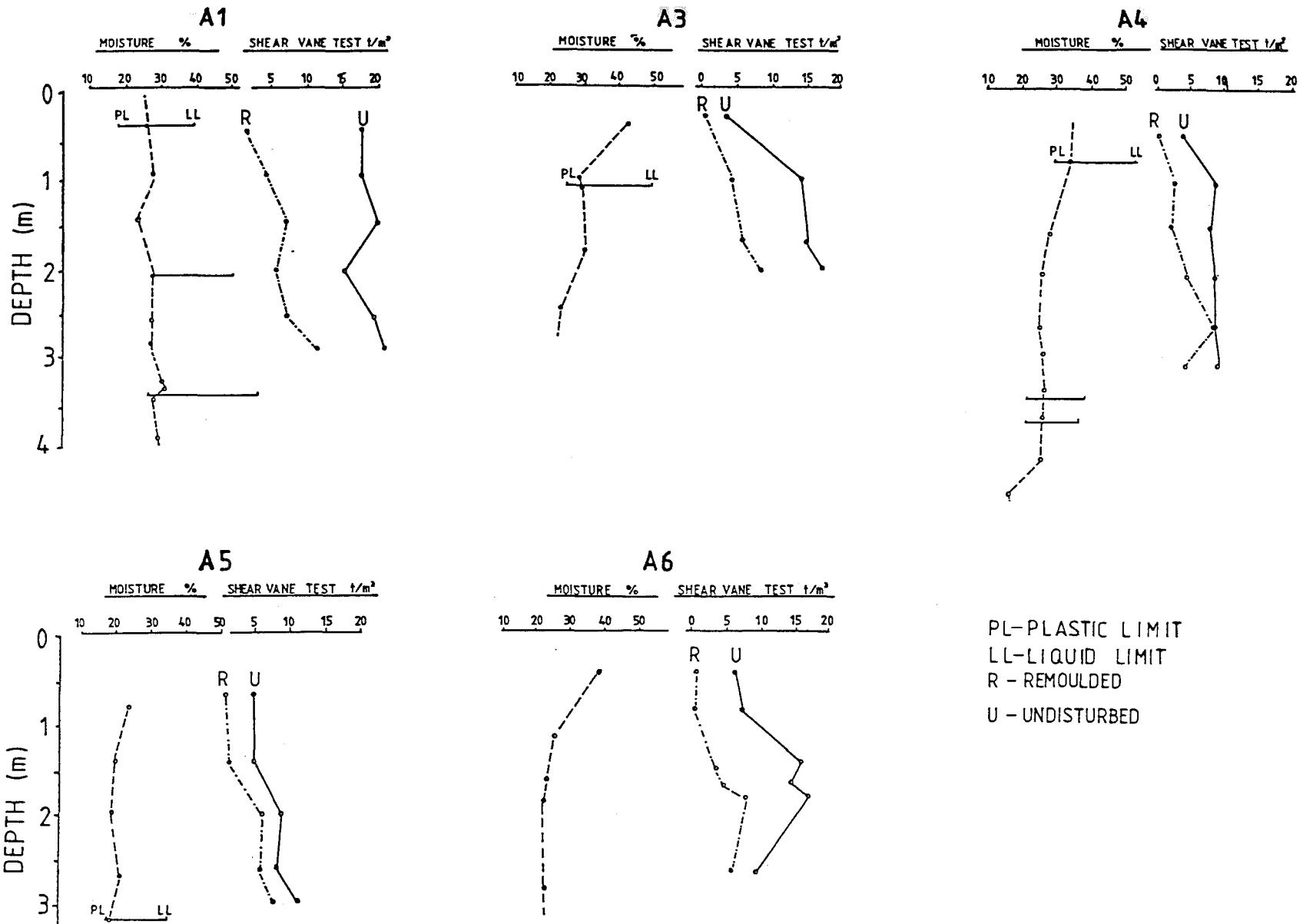

Figure 4.24 Correlation of Shear vane values to moisture content. Geology of the logs is shown in Fig. 6 in the map pocket.

shrinkage, and Atterberg limits were performed using N.Z. Standards 4402 part 1: 1980. Grainsize analysis was conducted using standard sieve and hydrometer methods outlined by Lewis (1981). Permeabilities were determined using a Laboratory permeameter designed by Hawley and Northey (1981) and modified to suit the equipment available at the University of Canterbury. Clay mineralogy was determined using a Phillips X-ray diffractometer. Laboratory strength testing was not carried out as there were no suitable samples available from shear surfaces.

The materials analysed were representative samples of the cohesive soils dominating Earthflow deposits which could generally be divided into four distinguishable groups. These groups initially were categorized in the field by colour as it was the primary visual distinction. Gradations of colour exist, but there is a dominant colour in each sample. The four categories of materials include:

1. red silts and clays;
2. grey clayey silt;
3. yellowish-brown clayey silt; and
4. cream sandy clays.

The cream sandy clay was found in only one auger hole (A18) and was approximately 100 mm thick.

Results of laboratory tests are presented in Table 4.4, and discussed below.

4.4.3 Discussion and Interpretation of Results.

1. Grainsize Distribution. In fine grained cohesive soils, such as those found within the Wharanui Earthflow, the clay mineralogy is likely to be the single most important factor determining operties. In addition to clay mineralogy, other factors such as grainsize distribution, non-clay mineral composition, organic material, and geologic history will control the engineering properties of clays and soils.

RED SILTS AND CLAYS

Sample	Depth (m)	Natural Moisture Content %	PARTICLE SIZE			ATTERBERG LIMITS				Linear Shrinkage %
			Clay %	Silt %	Sand %	Liquid Limit %	Plastic Limit %	Plasticity Index	Activity	
A3-6	3.1-3.30	22.90	35.0	55.0	10.0	50	23	27	0.77	-
A6-4	4.4-4.50	29.80	32.0	38.5	29.5	43	21	22	0.48	-
*A8-1	0.4-0.90	28.40	32.0	38.5	29.5	56	24	32	0.81	13.90
*A8-3	1.9-2.40	29.60	36.5	39.5	24.0	49	21	28	0.64	12.60
*A13-3	1.9-2.30	31.35	37.0	40.5	23.0	49	25	24	0.56	13.30
A15-2	1.5-2.00	32.80	33.5	40.5	26.0	-	-	-	-	-
A15-3	3.2-4.00	31.40	53.0	28.5	18.5	71	28	43	0.81	11.30
*A20-1	1.6-2.10	33.40	44.0	39.0	17.0	78	29	49	1.02	10.80
*A20-2	3.1-3.50	34.40	38.0	45.0	17.0	70	24	46	1.10	18.10
*A20-3	4.1-4.50	30.80	35.0	47.5	35.0	54	22	32	0.91	11.50
GREY CLAYEY SILTS										
A3-9	5.8-6.30	25.00	33.5	53.0	13.50	48	22	26	0.78	-
*A4-1	0.6-0.80	35.00	27.5	40.0	32.50	55	31	24	0.76	-
A5-6	3.0-3.20	18.80	33.0	55.0	12.50	36	17	18	0.54	-
A9-1	0.2-1.00	12.30	37.0	58.0	5.00	41	17	24	0.64	10.80
*A11-3	3.0-4.00	18.00	20.0	42.5	37.50	35	17	18	0.70	7.80
T2-1	2.5	14.70	38.0	47.5	14.50	-	-	-	-	-

YELLOWISH-BROWN SILTY CLAYS

Sample	Depth (m)	Natural Moisture Content %	PARTICLE SIZE			ATTERBERG LIMITS				Linear Shrinkage %
			Clay %	Silt %	Sand %	Liquid Limit %	Plastic Limit %	Plasticity Index	Activity	
A1-1	0.5-0.55	-	20.0	53.0	27.0	39	22	17	0.85	-
A1-4	2.1-2.24	24.10	36.5	53.5	10.0	51	24	27	0.73	-
*A1-10	3.4-3.55	28.30	23.0	43.0	34.0	58	26	32	0.91	-
A3-3	1.1-1.20	30.10	32.0	47.0	21.0	54	25	29	0.91	-
A3-7	5.0-5.40	18.50	32.0	61.0	7.0	41	21	20	0.63	-
*A4-5	3.1-3.30	28.60	39.5	46.0	14.5	40	23	17	0.41	-
*A4-6	3.4-3.60	28.20	31.0	38.0	31.0	40	23	17	0.42	-
*A11-2	1.8-2.50	23.70	30.0	53.0	17.0	39	21	18	0.56	7.70
CREAM SILTY CLAYS										
A18-3	2.5-2.70	40.23	54.0	34.0	12.0	80	26	54	1.00	20.40
S14	-	-	50.0	36.5	13.5	88	30	58	1.16	19.90

*Denotes samples sieved prior to determinations of Atterburg Limits.
The activities for these samples were calculated minus the sand fraction greater than 425μ.

Table 4.3 Summary Table of grain-size, in situ moisture content, Atterberg Limits, and linear shrinkage from representative samples at Wharanui Earthflow.

Fig. 4.25 shows envelopes of grainsize plots for three types of the colluvium. The yellowish-brown clayey silts are not shown as they are the oxidized equivalent to the grey clayey silt and have a very similar grainsize distribution (see Appendix 3).

The grainsize curves show there is a reasonably high proportion of clay within Earthflow materials. As can be seen from the grainsize envelope the cream smectites have the highest percentage of clay (54 %) and the narrowest range of variability. The red silts and clays contain from 32 to 53% clay, 28 to 55 % silt, and 10 to 35 % sand. The grey clayey silts contain from 20 to 38 % clay, 42 to 53 % silt, and 5 to 37 % sand.

2. Atterberg Limits. The red silts and clays are moderately to highly plastic (PI of 27 - 49 %), classified as MH to CH in Unified Soil Classification System. The grey clayey silts and the yellowish-brown clayey silts are similar soil types of low to moderate plasticity (PI of 17 - 31 %), and classified as ML in the Unified Soil Classification System. The cream sandy clay is a highly plastic soil (PI of 56 %), and CH in the Unified Soil Classification System.

The Atterberg Limits define properties of the whole soil but these plastic properties are mainly determined by the amount and type of clay minerals present. The results of the tests therefore depend on the proportion of clay mineral in the soil, as well as on its nature (Scott 1980). This can be defined as the 'activity' of the soil where activity is:

Plasticity Index / % by weight of clay size particles.

The activity is therefore a useful indication of the clays physical properties of a clay material, as well as a general indication of the clay minerals present. Other factors influencing activity include particle size, soluble salts,

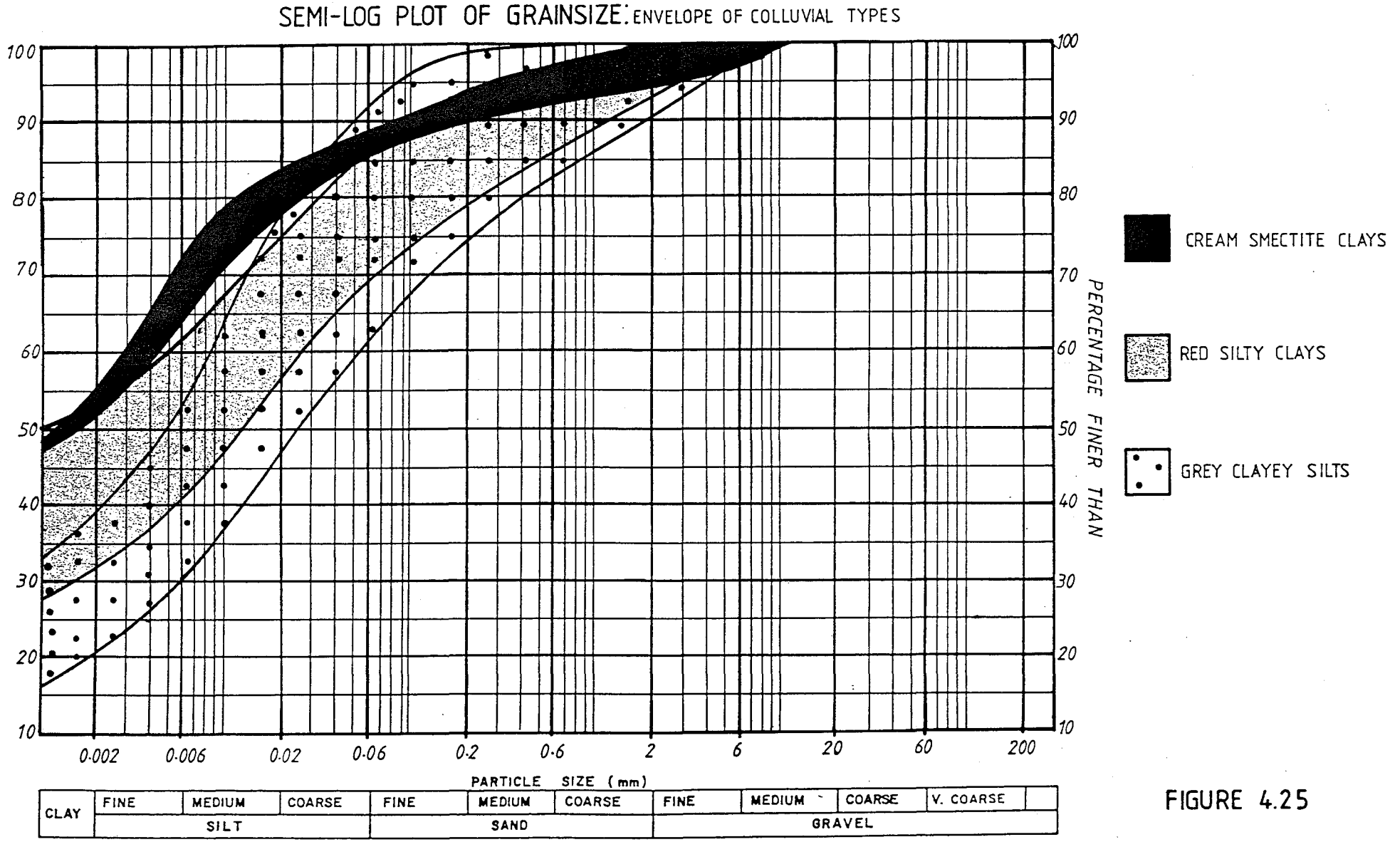
SEMI-LOG PLOT OF GRAINSIZE: ENVELOPE OF COLLUVIAL TYPES
100
90
80
70
60
50
40
30
20
10
0·002
0·006
0·02
0·06
0·2
0·6
2
6
20
60
200
PARTICLE SIZE (mm)
PERCENTAGE FINER THAN
CLAY
FINE
MEDIUM
COARSE
FINE
MEDIUM
COARSE
FINE
MEDIUM
COARSE
V. COARSE
SILT
SAND
GRAVEL
CREAM SMECTITE CLAYS
RED SILTY CLAYS
GREY CLAYEY SILTS

FIGURE 4.25

and organic liquids.

Skempton (1953) divided activity into three groups:
Group 1 - Inactive with activity less than .75
Group 2 - Normal with activity .75 to 1.25
Group 3 - Active with activity greater than 1.25

Most samples fall into group 1 or group 2. In soils with high activity there is generally a high water holding capacity, low permeability, low resistance to shear, with cohesion largely responsible for strength. Low activity soils have little cohesion and internal friction is largely responsible for strength (Grim, 1962).

3. Clay Fraction Mineralogy. X-ray diffraction was used to identify the clay minerals present within each soil type (see Appendix 4). Oriented slide mounts of representative samples were prepared by taking a sample of the .002 mm and finer fraction from settling columns during hydrometer analyses. The mounts were X-rayed normally, treated with glycerol and re-run, then heated for 1 hour at 550°C, and re-run again. The methods are discussed and diffractograms are shown in Appendix 4. Quantitative clay mineral analysis was not carried out, however peak area and heights were used to approximately compare and contrast the abundance of clay minerals within and between representative soil types.

Results of the analyses show that the grey clayey silts and yellowish-brown clayey silts contained illites and kaolinites with traces of smectites. The red clays and silts contained illites, kaolinites, and smectites. The cream sandy clays had traces of kaolinite and illite with a high proportion of smectites (Ca variety).

4. The Influence of Smectites. The smectites present within the soils largely affect the hydraulic and mechanical properties. Smectite is a swelling clay and large increases (as much as 400 % in some varieties) in volumes can take place with water absorption. While smectites are not a major

constituent within the soils there are enough present to have an influence on the material properties.

The linear shrinkage values obtained for the cream smectites are the highest, at approximately 20 %, followed by the red silts and clays at 13 %, and the grey clayey silts at 9 %. The higher shrinkage values reflect a higher proportion of smectites present.

Shrinkage cracks are a principal manifestation of smectites. Shrinkage cracks form upon drying of the soils and are responsible for augmenting an otherwise low infiltration rate, particularly on slopes where vegetation is less (Fig. 4.26). This occurs when shrinkage cracks form on slopes, and precipitation follows, entering directly into the cracks. Anderson (1984) found that even after closure of shrinkage cracks there is a permanent increase in permeability of the soil mass.

4.5 EARTH FLOW DEVELOPMENT MODEL

4.5.1 Introduction

A hypothetical model for development of the Earthflow complex has been derived from interpretation of the geological and geomorphological observations, and from limited geotechnical data. The model is used to explain the mechanism of failure and the sequential development of the Earthflow complex. This model involves four stages:

1. Initial valley development;
2. Derivation of material
3. Failure mechanism; and
4. Movement sequences and development of earthflow morphology.

4.5.2. Initial Valley Development

The Wharanui Earthflow lies within a narrow valley of which the geomorphic development has largely been controlled

Figure 4.26 Shrinkage cracks formed within grey clayey silt colluvium. Exposure within gully on lateral margin of the earthflow. Spade is 60 cm long (8652E 7440N).

by the Woodside Fault. The valley has developed essentially parallel to the strike of the Fault where the rocks were weakened from crushing and shearing. The present valley morphology has been influenced by weathering, erosion, and mass movement of both sheared rocks within the fault zone, and bedrock adjacent to the zone. A summary map of the morphology is shown in Fig 4.27.

The valley asymmetry discussed in section 4.2.1 is thought to reflect the structural relationship and lithological differences between the Grey Siltstone of the northeastern ridge and the Grey Argillites of the southwestern ridge (Fig 4.28). These are discussed below.

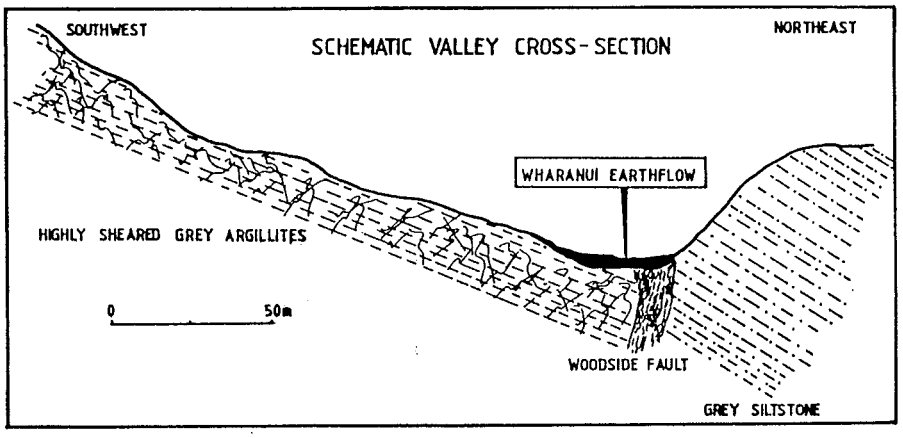

Fig. 4.28 Schematic section showing valley asymmetry and dip of strata.

The lithology of the southwestern ridge is predominantly Grey Argillites. These rocks are moderately strong to very strong (field determination of strength defined by Bell and Pettinga, 1984), but are intensely crushed and sheared. Water infiltrates into the fractures, which has the effect of accelerating weathering processes. The chemical and physical breakdown of this lithology has resulted in a mantle of regolith several metres thick.

Regolith on most of the southwestern ridge is stable, indicating that a stable angle of repose has been reached at approximately 15°. However, there is a steep terminal face at the southern end of this ridge where complex failures in the sheared Grey Argillites are continuing (Fig 4.27). These complex failures are predominantly controlled by the

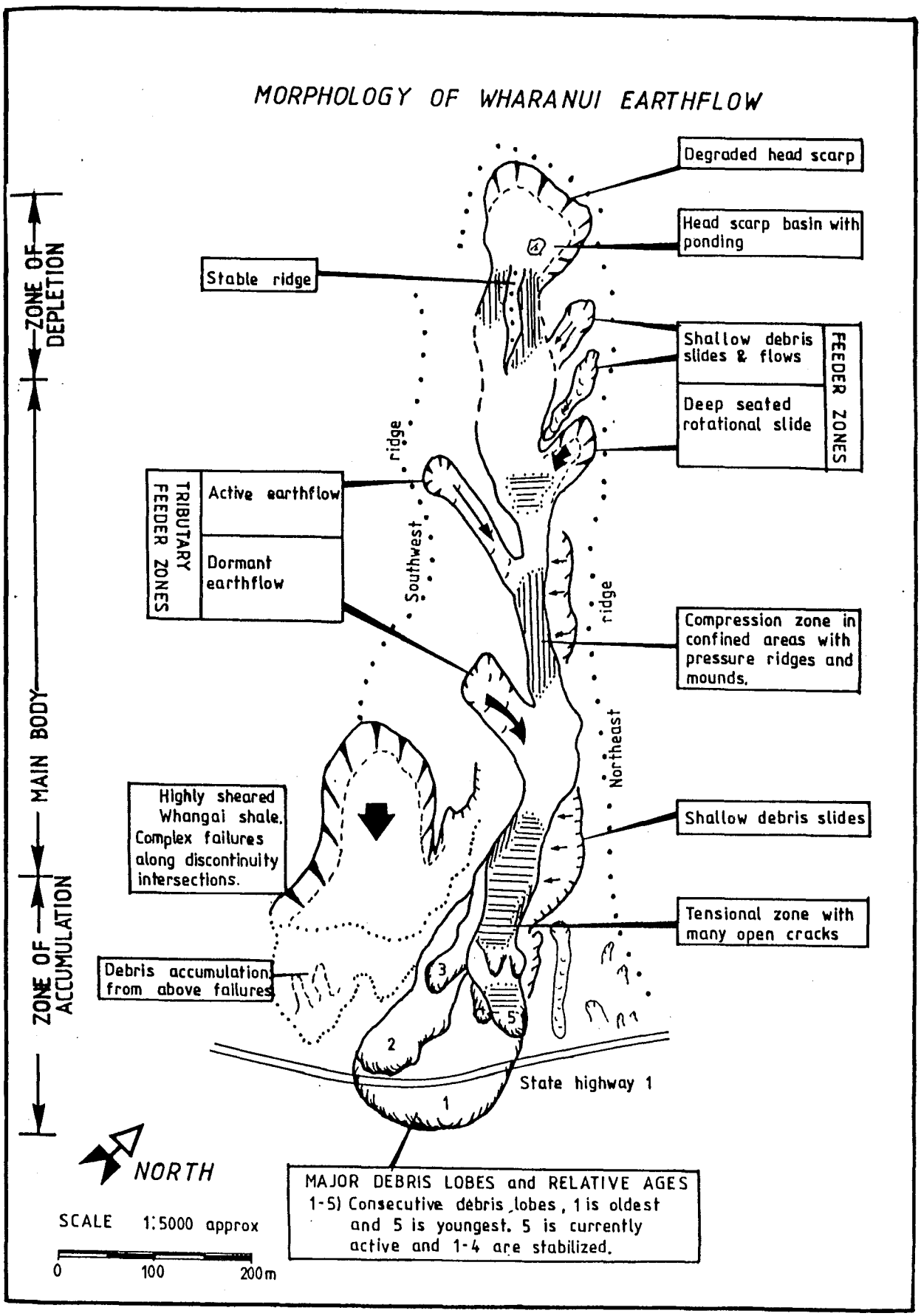

Figure 4.27 Summary morphology map of the Wharanui Earthflow.

intersection of unfavourable discontinuities, along shear planes and bedding planes. Shallow-seated regolith slumps (< 1.5 m deep) also occur on the lower slopes of this face, but debris from these failures are outside the boundaries of the Wharanui Earthflow.

The northeastern ridge is essentially a fault escarpment with the Grey Siltstone striking approximately parallel to the valley and steeply dipping (35 - 45°) to the northeast. This has resulted in a slope exceeding 25° along the northeastern ridge, which is underlain by Grey Siltstone, which is weaker than the Grey Argillites but has not been intensely sheared. The Grey Siltstones are prone to slaking as expansive clay minerals (smectite) within the siltstone break down the rock fabric through continued wetting and drying cycles. The weathering of this siltstone has resulted in a regolith covering of up to 1.5 metres thick.

4.5.3. Derivation of Materials

Earthflow materials within the valley floor are principally derived from mass movement of colluvium within the regolith and tuffaceous volcanic breccia on the valley sides. These failures are described in Section 4.2.3.

The materials have collected in the valley to form deposits approximately 2 to 7 metres thick. These soil deposits are generally fine grained, high in silt and clay content, with some sand and gravels, and generally have soil mass permeabilities of 10^{-8}m/s.

The rubbly lenses, described in section 4.3.5 (Groundwater), are thought to have developed from alluvial deposits (stream and swamp) which have subsequently been buried by earthflow movements. When the Earthflow is in a period of little activity erosional processes exceed the rate of deposition and movement. Coarse grained sediment from gully erosion may collect in depressions or in channels whereas fines may be washed away. Subsequent mobilization

of the earthflow would bury these coarse grained sediments enveloping them in the finer grained matrix. This implies that movement occurs intermittently within the Earthflow complex. Some of these rubbly lenses were observed in a gully along the flanks of lobe 5.

4.5.4 Failure Model

On the basis of field and laboratory investigations it is apparent there are a number of interdependent factors which combine to form the engineering geological model. These factor inter-relationships are schematically shown in Fig. 4.29.

1. Geological and geomorphological pre-conditions include the weak materials which mantle the over-steepened northeastern valley side. The slopes are too steep for regolith to remain stable. (The material on the southwestern valley side appears to have reached a stable angle of repose).

2. High intensity precipitation can trigger regolith failures on the slopes depositing material on the valley floor.

3. The volume of material deposited in the upper portion creates a driving force for material in the lower portion of the flow.

4. Relatively high precipitation must occur for long periods (5 years plus, as will be discussed in Chapter Five) for water to infiltrate into the very low permeability soils. The eventual increase in moisture content results in an increase in the unit weight and a decrease in the shear strength, and when the load threshold value is exceeded the material moves down the valley.

5. Movement of material downslope relieves the surcharge pressures (lateral pressures) created by the deposition from the valley walls. This in turn releases

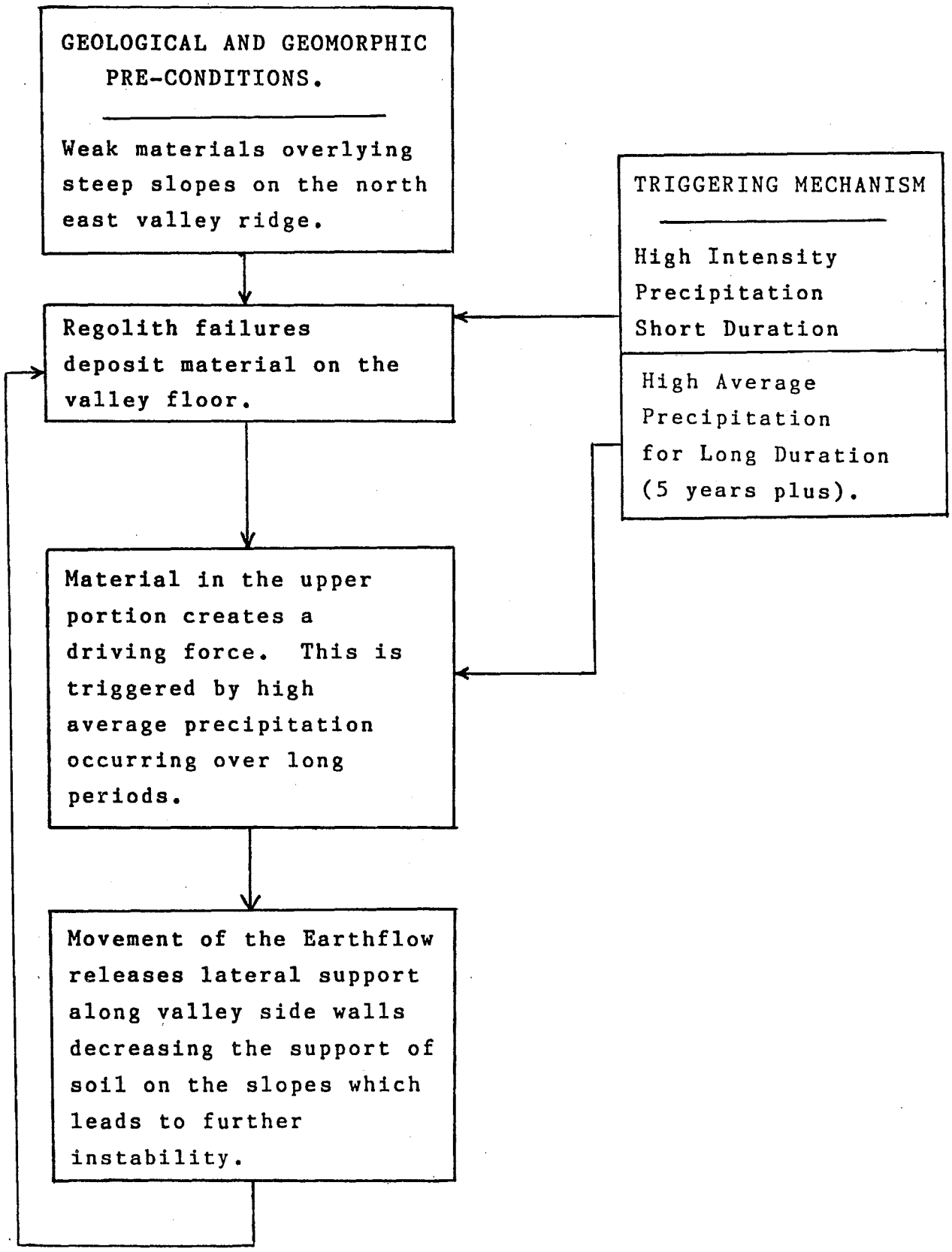

Figure 4.29 Schematic flow diagram of failure model.

support of the soils on the valley sides thereby initiating new instabilities.

Basal Shears. Although there is evidence to suggest significant internal deformation (ie. chaotic mixing of soil types), movement is primarily along basal and lateral shears within the Earthflow. The basal shear zone of the Wharanui Earthflow is not a single plane where movement occurs, eg. at the soil - bedrock interface, but there are shear surfaces at varying depths and extent which are associated with the intermittent activity of different parts of the Earthflow at different times. Evidence for this includes:

1. In the zone of accumulation stratified deposits are visible within a depositional lobe indicative of separate events of movement. Each of these events would then have a separate basal shear, at least in the zone of accumulation (refer to section 4.2.4, Fig. 4.12).

2. A basal shear zone was located within trench 2 at 1.4 metres. This shows that basal shear does occur above the bedrock - soil interface.

3. The mobilization and remobilization of small bulges within the body of the flow would create a basal shear for that specific lobe. Therefore, basal shear zones within the Earthflow complex as a whole would vary spatially (horizontally and vertically) (refer to long section Fig. 3 in the map pocket).

4.5.5 Movement Sequences

The Earthflow complex involves many earthflows occuring within the sinuous valley floor. Individual lobes and bulges are evidence that activity has been intermittent throughout the Earthflows' history. The common remobilization of older earthflow deposits indicates that changes which take place in the soil when the earthflow stops moving are not irreversible, therefore the earthflow

deposits are susceptible to renewed movement. The renewed movement would be subject to mobilization in the same manner that initial mobilization occured.

The low gradient of approximately 13° has been a significant influence on stability and has been a major factor in the slow, intermittent activity of the earthflow.

The earthflow complex has evolved to its present form by periods of episodic mobilization and stabilization of various parts of the complex. The first major mobilization probably occured centuries ago or possibly thousands of years ago making it very young geologically. Lobe one rests on very young stream alluvium deposited since the last glaciation. Specific age determinations were not possible.

The zone of depletion is notable in that 5 lobes have been preserved (described in section 4.2.4) and the sequential development of these is clear. Fig 4.27 shows the position and relative ages of these, 1 is the oldest and 5 is the youngest.

The first two lobes were deposited successively on top of lobe 1 flowing to the south, but lobe 4 and 5 appear to have been redirected to the east truncating the older debris lobes. Each of the debris lobe apears to have stabilized prior to another lobe accumulating on top of it It is lobe five which is the present threat to State Highway 1.

CHAPTER FIVE

EARTHFLOW STABILITY AND REMEDIAL OPTIONS

5.1 INTRODUCTION

The primary objectives of this chapter are to:

1) discuss the stability of the Wharanui Earthflow including the history of movement prior to, and during this study;

2) review and recommend remedial options with the aim of preventing movement onto State Highway 1.

To assess the current stability of the Wharanui Earthflow two survey systems were installed to monitor flow movement (see Appendix 9). These systems are referred to as to as the 'primary network' and the 'secondary network', and are used in this study to define:

1. patterns of movement,
2. areas of instability,
3. provision of a base grid for mapping of scarps, ground cracks, and seeps.

In addition to survey networks the subsurface movement was indicated by deformation of piezometer riser pipes.

5.2 PRIMARY MONITORING NETWORK

5.2.1 Methods

The primary network, installed in August 1984, was designed to monitor absolute flow movement with monitoring points placed both parallel and perpendicular to the axis of

the Earthflow. Monitoring points consisted of 1/2 and 3/4 inch steel pipe driven in the ground surface. These were surveyed using a Wild DI3 distomat and a T16 theodolite. It should be noted that a survey error of +20 mm is recognized; this is discussed in Appendix 9.

Two surveys were completed after initial installation, the first was in March 1985 and the second in September 1985. Fig. 5 in the map pocket shows the location of each monitoring point of both networks. The total movement and direction of movement of each point is shown on the map using vectors. The initial and final coordinates of each point are listed in Appendix 9 and on Fig. 5.

5.2.2 Movement Since Installation of the Network

Movement for the period of observation was not great enough to delineate the nature of movement for the whole earthflow (see Fig 5 in the map pocket). Some areas seemed to exibit a 'rigid plug' type of movement where a portion of the Earthflow moved along discreet shear boundaries, whilst other areas did show signs of internal deformation inferred from surface measurements (Fig. 5).

The earthflow movement can be considered in 3 sections divided into the zone of depletion, the main body and, the zone of accumulation (see Fig. 5.1).

1. Zone of Depletion. The zone of depletion had the least amount of movement of any section on the Earthflow. Only 3 points had any movement at all including f1, f8, and f9 which moved 53 mm, 38 mm and 45 mm respectively. Movement on all points was to the southeast (ie. downslope towards State Highway 1).

2. Main Body. Generally the main body (Fig. 5.1) had the most movement of the Earthflow. However, the upper portion of the main body had very little activity, and movement which did occur appeared to be inconsistent with the rest of the flow. The upper portion had a few points

with a relatively high magnitude of movement, D23 and G8 which moved 316 mm and 338 mm respectively. This movement is thought to be from localized displacements such as opening of tension cracks or movement of small blocks of earth within the Earthflow mass. A tributary earthflow (T2 Fig. 5.1) had some activity but movement was generally less than 100mm. Movement in the rest of the upper area was very little.

Movement was restricted in the middle portion to one point, D16, in a locally active area of the Earthflow (see Fig. 5, map pocket). This point, located on a pressure ridge, moved 390 mm, which is the highest movement recorded for any one point during the monitoring. Reactivation appears to be caused by removal of lateral restraint associated with gully erosion at the edge of the adjacent pressure ridge.

The area around the pressure ridge is marked by fresh tension cracks forming an arcuate scarp. Fig. 5.2 shows a sketch of the pressure ridge and the direction of movement which has taken place. Fresh tension cracks are visible on the ground surface where the mass moved. Failure is probably caused from a localized shallow sliding movement and is not associated with any major reactivation of the Earthflow. It is significant in that it demonstrates how the Earthflow has intermittently active localities.

In the lower half of the middle portion movement averaged 110 mm. In this area the earthflow appears to be moving like a rigid plug with a generally moving downslope in a south westerly direction. This type of flow would involve some internal deformation but most of the movement occurs along discrete shear zones, either on the flanks or within the main body of the flow (Fig. 5, map pocket).

3. Zone of Accumulation. The zone of accumulation displayed little movement. At the distal margin, movement on the toe was recorded at 29 mm, just slightly more than the survey error of 20 mm. Horizontal movement of up to 80

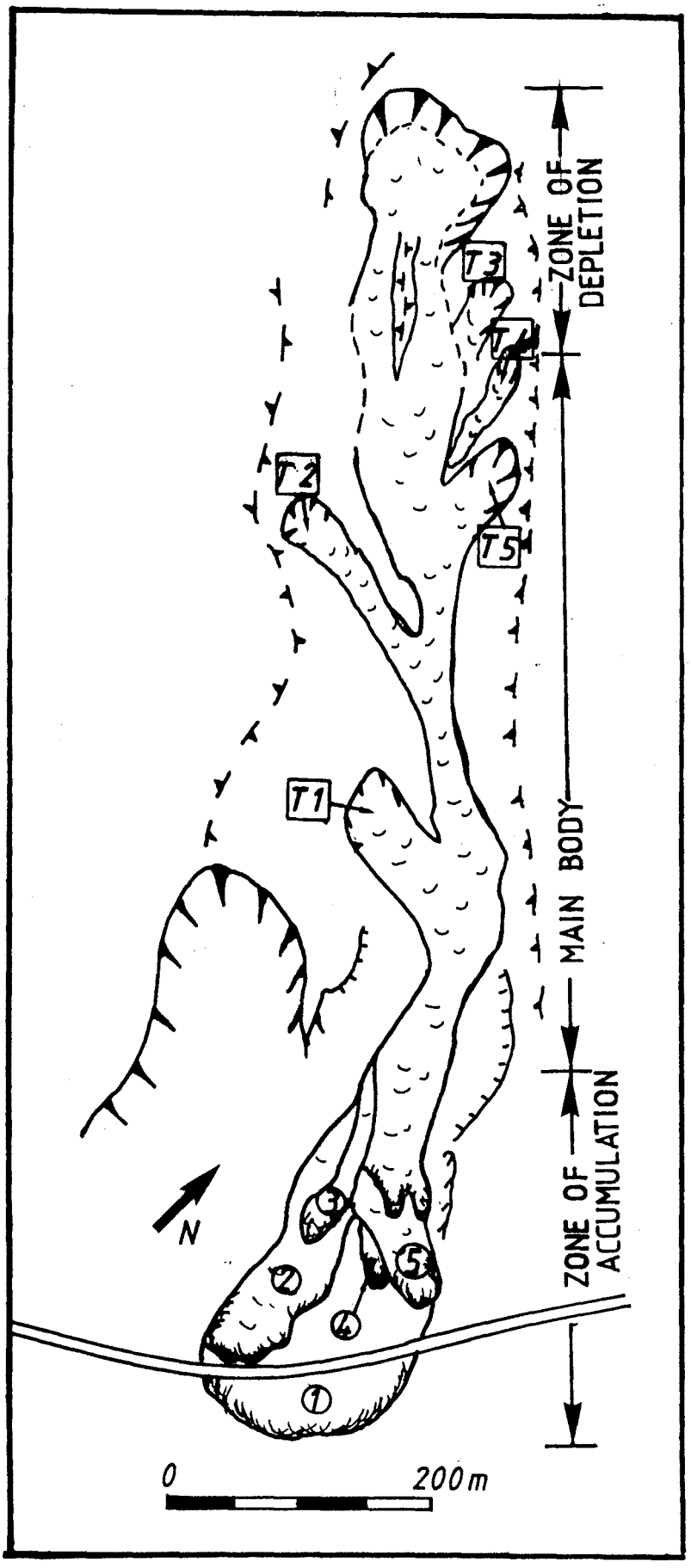

Figure 5.1 Sketch of Earthflow showing the locality of the zone of depletion, the main body, and the zone of accumulation. The main body had the most movement for the period of study averaging 100 mm.

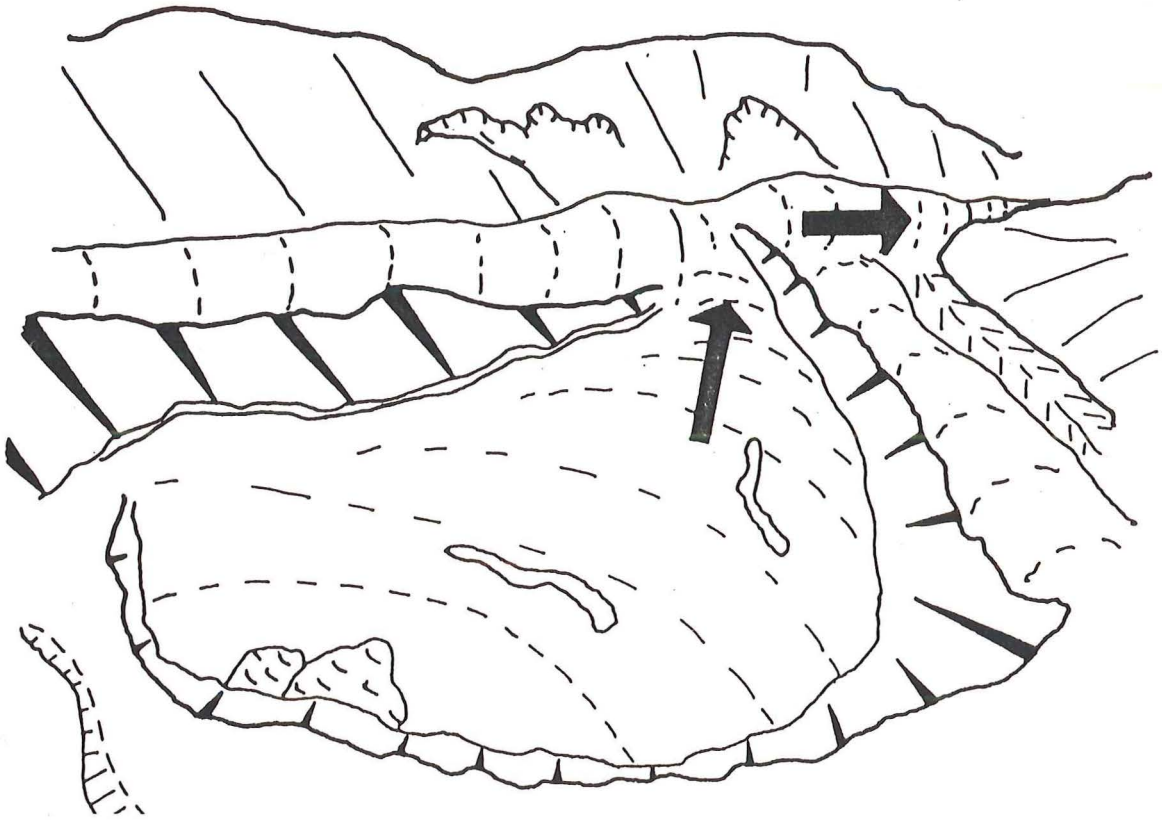

Figure 5.2 Sketch of the area surrounding the zone of local instability shown above. Note that tension cracks are fresh and movement appears to be initiated from gully erosion removing lateral support from the flow body. Arrows denote direction of flow movement.

mm was surveyed on the older apparently "stable" lobes 1 and 3, (Fig. 5) suggesting that they may not be completely stable. However, it must be noted that stock movement (cattle and sheep) around the survey points could easily account for this amount of movement.

5.2.3 Growth of Area Involved

Growth of the landslide has not been evident by monitoring. The last major event which triggered movement on the ridge sides of the Earthflow was in March 1980, when 500 mm of precipitation occurred in 3 days. Aerial photos after the storm event show extensive slope failures. The areas which supplied the debris are currently stable. The scarps are degrading and becoming revegetated. Many of the features associated with movement ie., lateral shears and broken crevassed ground, are not as prominent as on fresh earthflows in the area with steeper gradients.

It is certain that the ridge slopes have the potential for further instability as there are open tension cracks on the slopes above the Earthflow, and with an increase in pore pressure from an intense rainfall, regolith failure is likely.

5.3 SECONDARY MONITORING NETWORK

5.3.1 Purpose

The secondary monitoring network was designed to supplement the primary network by creating a quick and simple means of detecting readings. The secondary network is not meant to replace the primary network, since it will not provide absolute movement data, but provides relative movement data across tension cracks and scarps indicating increases or decreases in movement.

5.3.2 Methods

Pipes were driven into the ground in succession on

opposite sides of multiple tension cracks which had developed on the 'active' toe (lobe 5), or across scarps within the toe area (see Fig. 5.3 for location of monitoring points). A total of six lines (Alpha, Beta, Sigma, Phi, Omega, and Delta) were placed in the immediate vicinity of the toe or on the toe itself in November 1984. Each line of points was re-measured in March 1985 (survey 1), May 1985 (survey 2), and August 1985 (survey 3) and vertical and horizontal changes were recorded (see appendix 9). This was accomplished using a crack width monitor (Fig. 5.4), designed and constructed at the University of Canterbury, which could measure movement to within 1 mm (see Appendix 9 for full details concerning the use, performance, and an evaluation of the device).

5.3.3 Discussion of Movement

Table 5.1 gives a summary of cumulative changes after survey 3. As can be seen, few points had any significant movement, and much of movement which did occur could be attributed to the shrinkage or swelling characteristics of the soil. Distance changes which occurred between points were often not a permanent increase or decrease, but were temporary, the points returning to their original position.

The secondary monitoring reflects the low movement rates observed from the primary network during the study period. However, the duration of available records is insufficient to substantiate a correlation between the two networks.

5.4 HISTORY OF MOVEMENT

5.4.1 Movement Since 1947

The Wharanui Earthflow has probably been active intermittently for thousands of years, as discussed in Chapter 4, section 4.5.4. It is not possible to establish exactly what time or at what rate the five major lobes were deposited in their respective positions (Fig. 4.27).

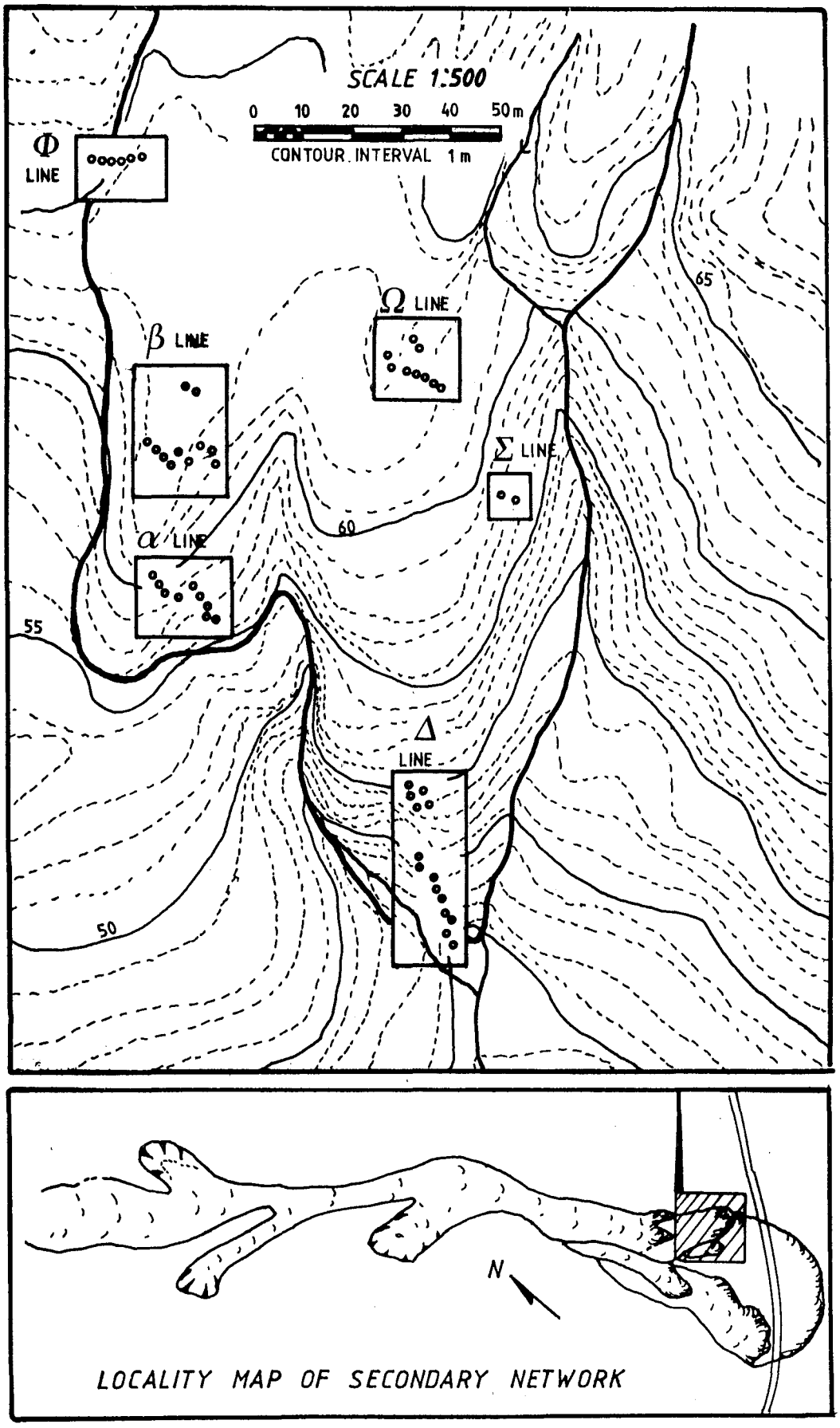

Figure 5.3 Locality of secondary monitoring network and points within the network.

Figure 5.4 Crack width monitor used to measure movement between tension cracks and scarps.

SUMMARY OF CRACK WIDTH MONITORING
ALL MEASUREMENTS IN MILLIMETERS

ALPHA LINE

Point span	Horiz. length	Cum. chg.	Vert. length	Cum. chg.
1-2	990.0	-15.5	843.5	+11
2-3	980.0	+2.0	258.5	-5.0
3-4	880.0	+1.5	320.5	+6.0
5-6	851.0	+5.0	284.5	-6.0
6-7	947.0	+1.0	489.5	+5.0
7-8	857.0	+14.0	95.5	+6.0
8-9	898.5	-8.5	533.5	+1.0

BETA LINE

Point span	Horiz. length	Cum. chg.	Vert. length	Cum. chg.
1-2	957.0	-4.5	263.5	0.0
2-3	969.0	+6.0	103.5	+0.5
3-4	977.0	+2.5	172.5	+5.5
4-5	926.0	-22.0	365.5	-2.0
5-6	841.0	-2.0	291.5	-5.0
7-8	893.0	+7.0	331.5	+7.0
8-9	869.0	-31.5	377.5	-2.5
10-11	833.0	-13.0	491.5	+2.0

SIGMA LINE

Point span	Horiz. length	Cum. chg.	Vert. length	Cum. chg.
1-2	851.0	-14.5	650.0	-1.0

PHI LINE

Point span	Horiz. length	Cum. chg.	Vert. length	Cum. chg.
1-2	930.0	-0.5	697.0	+2.5
2-3	973.0	+6.5	373.5	+27.5
3-4	897.0	-1.5	193.5	-29.5
4-5	1020.0	+ 2.0	373.5	+9.0
5-6	993.0	-4.0	254.5	+7.0

OMEGA LINE

Point span	Horiz. length	Cum. chg.	Vert. length	Cum. chg.
1-2	855.0	-13.0	420.5	+2.0
3-4	943.0	-43.0	492.5	-21.0
4-5	743.0	+14.0	359.5	+22.0
5-6	767.0	+2.0	116.5	-14.0
8-9	894.0	-10.5	450.5	+6.0

DELTA LINE

Point span	Horiz. length	Cum. chg.	Vert. length	Cum. chg.
1-2	PEG NO. 1 DISAPEARED			
3-4	893.0	+4.0	704.0	+1.0
4-5	866.0	-35.0	757.0	-0.5
5-6	851.0	+27.0	420.5	+2.0
6-7	930.0	-24.5	779.0	-0.5
8-9	918.0	+1.0	559.0	-1.0
10-12	872.6	+6.0	502.5	-3.0
12-14	996.0	-0.5	539.5	-0.5
11-13	791.0	-2.0	510.5	+2.0

ble 5.1 Summary of Crack Width Monitoring showing final rizontal and vertical distances between points, and the mulative change over the survey period.

However, the recent history of lobe 5, regarded here as the active lobe, is relatively clear. Aerial photographs from 1947 were used to interpret the position of lobe 5 at that time (aerial photo survey no. 1383/1 to 3, 1947). Fig. 5.5 shows that in 1947 the extent of lobe 5 was 59.5 m from State Highway 1, compared to 25 m presently or a cumulative movement of 34.5 m. This is an average movement rate of approximately .91 m/year. However, the earthflow does not move at a slow constant rate, but has periods of relatively higher and lower movement activity. These periods of activity are closely related to long term rainfall patterns (3-5 years) as will be shown.

5.4.2 Correlation Of Movement With Rainfall

The period of study was at the end of a five years of low rainfall. The lack of precipitation over this time has been the major influence in the lack of movement on the Earthflow for the study period and for the last five years.

Monitoring of the Earthflow was begun by the M.W.D. in 1976. Note that the strong correlation between precipitation and movement at the toe (Fig. 5.6) There was approximately 9 metres of movement recorded between 1976 to 1980. The most movement (4.62 m) occured in 1980, corresponding to the highest rainfall of the period.

While the correlation of movement to rainfall is clear, it is not a simple case of high rainfall generating high movement rates. As can be seen in Fig. 5.7, rainfall data over the last 40 years has shown the 7 year period from 1974 through 1980 to be exceptionally wet, with all but one year (1976) above the normal. Thus movement results from the cumulative effect of wet weather over a period of years. Movement has dropped markedly during the years since 1980 as rainfall has been below average.

The total movement since 1947 is shown in Fig. 5.7. The graph shows rainfall to be highest in the periods from 1947-1953 and 1975-1980. It is likely that the 1947-1953

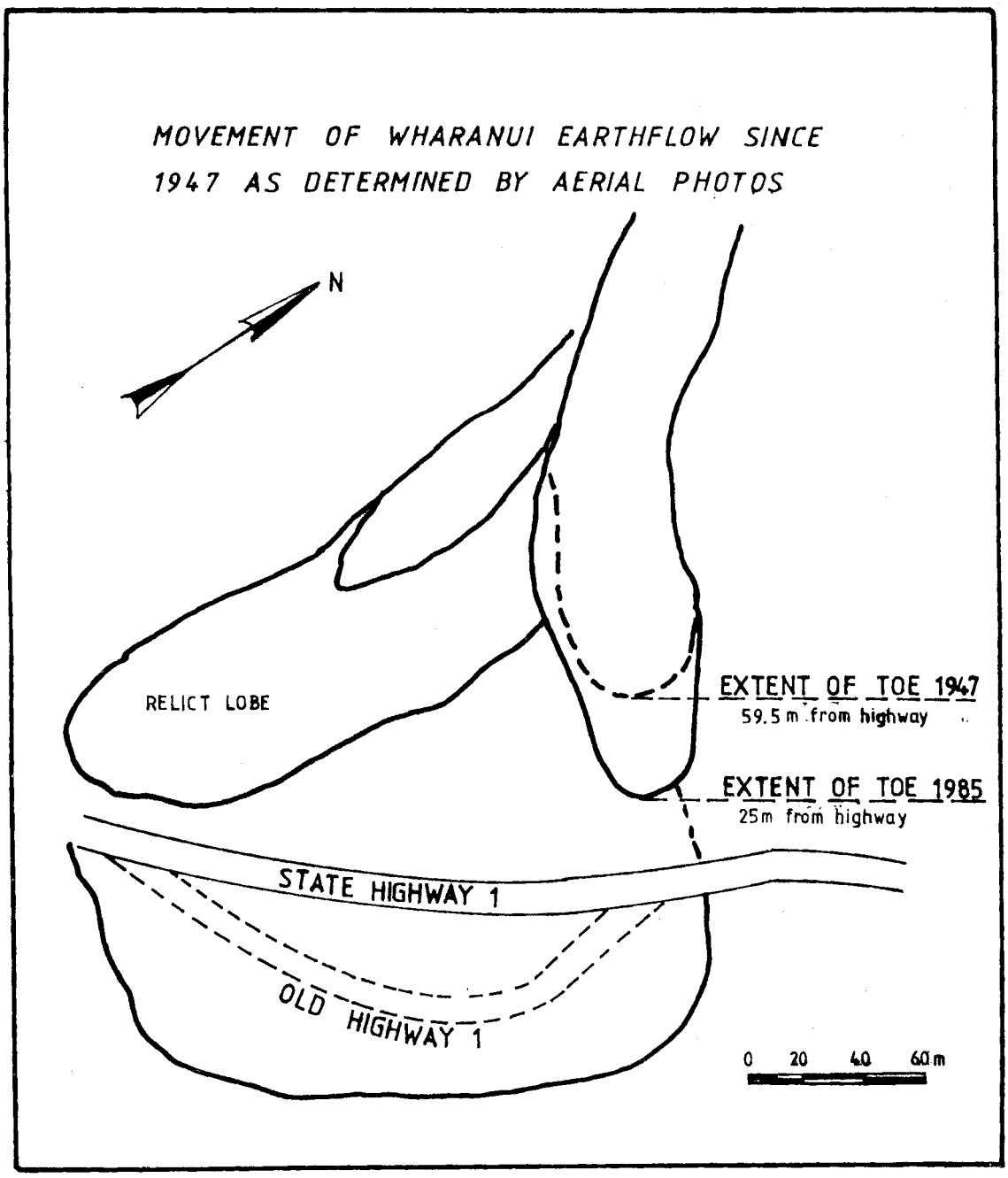

Figure 5.5 Extent of the active toe in 1947 as interpreted by aerial photos and the location in 1985.

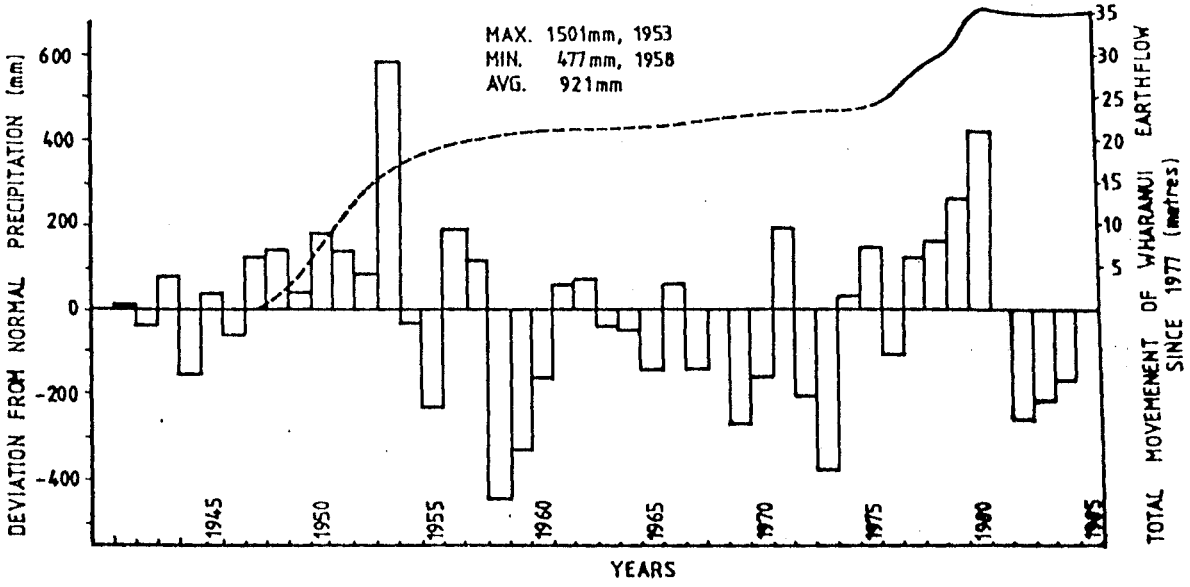

;ure 5.6 Correlation of rainfall to movement from 1947 to 1985.)ashed line is probable movement before monitoring began in 1976, ;olid line is measured movement since monitoring began.

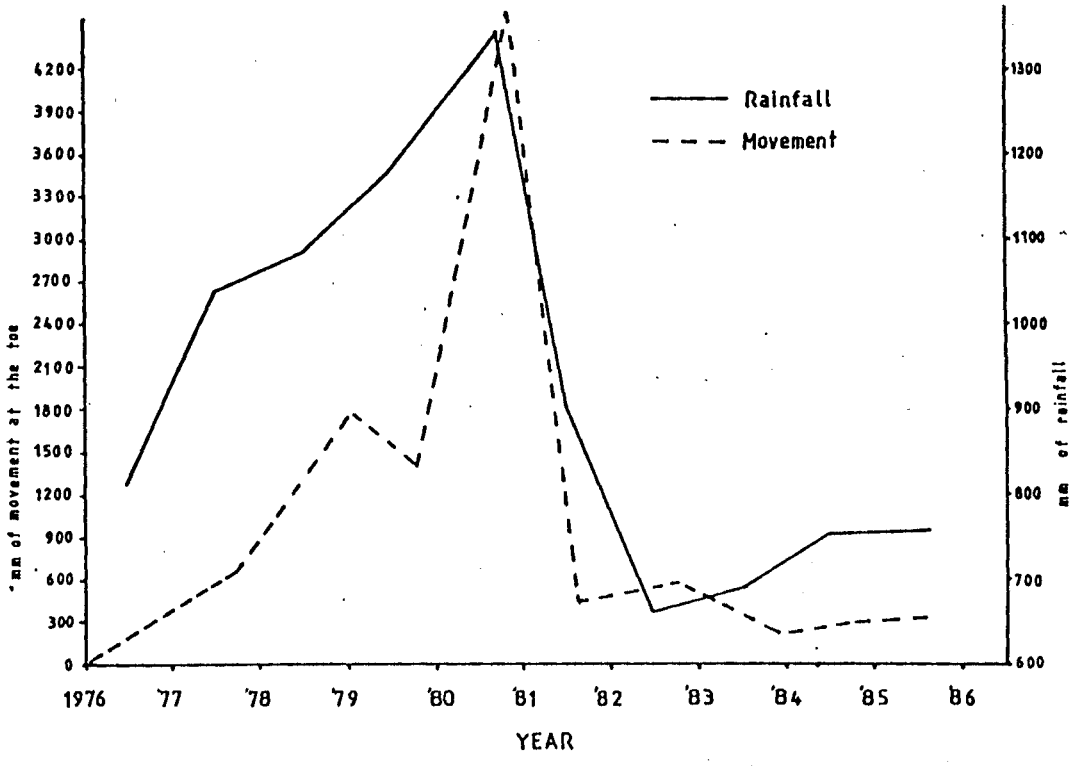

igure 5.7 Correlation of movement and rainfall at the active toe, from 1976 to 1985.

period had a similar movement curve to the 1976-1980 period, because the successive years of high rainfall in the first period are similar to the second period where relatively high movement was recorded. This can not be confirmed. The intervening years from 1954-1975 probably had considerably lower rates of movement.

5.5 SUBSURFACE MOVEMENT

Although inclinometers were not available for this study, the piezometers installed did give limited information on subsurface movement. This was simply done while measuring the water levels. As movement occured there was also deformation of the standpipe riser at depth. This made insertion of the water measuring device difficult and was indicative of either a separate failure surface at that point or some pressure which deformed the riser at that point.

The 'tight spots' were encountered in 3 of the 4 piezometers on the flow itself, and occured at depths of 0.9m in A3, 2.1m in A4, and 1.6m in A5. A8 did not have any deformation of the standpipe riser.

5.6 STABILITY ASSESSMENT

5.6.1 Quantitative Evaluation

Slope failure occurs when mobilizing (driving) forces exceed material strength. Factors which complicate this relationship are:

1. variations in material shear strengths;
2. pore pressure distribution variability;
3. heterogeneity of material due to layering and discontinuities; and

The problem of slope stability is essentially a limit equilibrium problem. Outlines of the principles underlying limit equilibrium analysis and the roles of computed factors

of saftey are presented in Lamb & Whitman (1969) and Morgenstern & Sangrey (1978).

A quantitative stability analysis was not carried out on the Wharanui Earthflow for two reasons ie. the heterogeneity of Earthflow deposits, and insufficient geotechnical information.

1. Heterogeneity of Earth flow deposits

A deterministic types of stability analysis (ie. infinite slope analysis, circular slip surface analysis and, non circular slip analysis) imply that soil and hydrologic properties are known with a good deal of precision (Sidle, 1985). The problem with applying a quantitative stability analysis on natural slopes is primarily due to large unknown spatial varibility of the deposits on a slope. The deposits within the Wharanui earthflow are chaotically distributed with variable water contents, strength parameters, and unknown aquifers which do not create an ideal situation for a limit equilibrium analysis. This high degree of anisotropy and heterogeneity in soil properties within the earthflow could lead to major errors in factor of saftey calculations.

2. Insufficient Geotechnical Information

A stability analysis requires adequate subsurface data from the zone of movement. Augering did not reveal a specific zone in which movement occured. There were softened zones in which a shear surface was likely, but this could not be substantiated, nor could undisturbed samples be obtained for strength testing. In the trenches, as was stated earlier, detailed examination was not possible and samples could not be extracted from the shear zone seen in trench 2, because of the failure of the trench walls. This meant that no samples were avalable for strength testing. Hence a stability assesment can only be a subjective appraisal taking into account the earthflows' mechanism of failure and any influences which trigger movement such as precipitation and seismicity.

5.6.2 Seismic Hazard

Seismic activity may initiate rapid mass movement or be responsible for triggering and reactivating slower types of movement such as the Wharanui Earthflow. Small mass movements of soil materials occur in both moderate and large earthquakes. For example in the 1964 Alaskan earthquake more than 2,000 slides and avalanches occured within a 5,000 km^2 area around the epicentre. Keefer (1984) indicated that earthquakes affect an area and induce landslides directly proportional to the magnitude of earthquakes, increasing from 0 km^2 at a magnitude of 4.0 to approximately 500,000 km^2 at magnitude of 9.2.

Although Earthquakes of low magnitude can trigger rock falls, rock slides, soil falls, and disrupted soil slides; the generation of deep seated slumps and earthflows are generally initiated by stronger and longer duration earthquakes (Voight & Pariseau, 1978).

The ability of earthquakes to trigger landslides at a distance depends on many factors including (1) the stability of potential sliding mass, (2) orientation of potential failures in relation to the earthquake epicenter, (3) vegetation and land use, and (4) direction of seismic wave propagation, earthquake magnitude, focal depth, seismic wave attenuation, and after shock distribution (Voight & Pariseau, 1978).

One of the direct effects of seismic wave propagation is horizontal acceleration of earth materials and structures. (Lambe & Whitman, 1969). This acceleration in large earthquakes or near the epicenter of moderate earthquakes is often 0.1 to 0.5 times gravitational acceleration and may in some instances equal or exceed gravitational acceleration. The main effect of this horizontal acceleration on slope stability is to alter the distribution of forces in a mass equivalent to a temporary steepening of slope. Additionally, seismic waves subject soils to cyclic loading and unloading. Stress fluctuations

can produce irreversible changes in pore-water pressures resulting in long or short-term changes in soil strength. Zaruba & Mencl (1969) pointed out that earthquake shocks can disturb and destroy intergranular bonds and cause decreased cohesion and/or internal friction.

The Wharanui earthflow could be subject to acceleration and reactivation of movement if an earthquake was strong enough to induce horizontal acceleration which was capable of altering soil mass parameters as discussed above.

5.6.3 Future Extent of Flow

Movement of the Wharanui earthflow will continue downslope towards the road along its present course. The main question which cannot be answered is, how long will it take? During the past five years rainfall has been very low. However a year or two with higher than average rainfall, or a strong earthquake could initiate mobilization which could move the toe of the earthflow to the highway or beyond. The chance of movement could substantially be reduced with appropriate remedial measures, but these would have to be more effective than those installed and operated from the 1974-1980 period (refer to Appendix 10).

5.7 REMEDIAL OPTIONS

5.7.1 Potential Remedial Measures

Potential remedial measures for the Wharanui Earthflow include:

1. surface and subsurface drainage,
2. planting trees to aid in evapotranspiration,
3. diversion of the Earthflow,
4. relocation of the Highway,
5. coping with the situatuion as it now exists.

Each of these potential remedial measure design

schemes are shown in Fig. 8 (map pocket). The recommendations are given with knowledge that the total stabilization of the Wharanui Earthflow may not be an economically viable proposition.

5.7.2 Surface Drainage

As has been shown in section 5.3, long term precipitation trends can be directly related to earthflow movement. Therefore any stabiliztion scheme should include drainage of the surface waters. The existing drainage scheme, in its present state, has been proven to be unsuitable (refer to Appendix 10 for previous remedial works).

Sufrace drainage channels should reduce groundwater infiltration and recharge from precipitation by promoting rapid runoff and removal of water from the Earthflow surface. This would prevent surface ponding of water in the slopes.

5.7.3 Subsurface Drainage

Counterfort drains across the Earthflow could intercept significant sub-surface water, effectively reducing pore-pressures. Trenches could be excavated 3-5 metres deep to the assumed bedrock-Earthflow interface and perforated novacoil laid down and backfilled with filter material. The trench would be excavated the width of the flow from the northeastern side, down flow, in a southwestern direction through the older depositional lobes and drain into the intermittent stream leading to a highway culvert (Fig. 8 in the map pocket).

However, although such a network is technically feasible it may be of questionible value and very difficult to implement. Problems anticipated with a system of counterfort drains include:

1. Trench stability during construction; the collapse of side walls could be a substantial problem. This was evident during excavations for this study, as the trench walls were prone to sudden failure or bulging at the sides. Once support was removed digging became difficult as the bulging hampered the backhoe shovel entering the trench. Shoring would have to be immediate (refer to Chapter Four, section 4.3.3).

2. There would be no guarantee that the scheme would intercept enough water to substantially increase stability. Because of the impermeable nature of the materials interception of substantial aquifers would be necessary to drain any water.

3. There are risks that continual slow creep or local failure planes developed within the Earthflow could damage any drains and ultimately render them ineffective.

5.7.4 Planting

Close planting of C. Macrocarpa is recomended by D. Mackay of the Marlborough Catchment Board for its adabtability to local soil conditions and to the salty air. Advantages and disadvantages are listed below.

1. Advantages

A) The root network would provide strength to the ridge-side slopes substantially eliminating or reducing shallow regolith failures. This would reduce or eliminate the source of debris which accumulates from the side slopes and in effect reduce the driving force.

B) The canopy effect of close planting would result in interception of up to 35% precipitation (Pearce et al. 1985).

C) Timber production from the trees could be realized with time.

2. Disadvantages

A) The loss of productive grazing land by the owner may mean the land would have to be purchased by the crown.

B) Trees would have to be established for at least 5-7 years before full potential is made upon stability.

5.7.5 Diversion of the Earthflow.

In a severe situation where movement of debris onto the road is imminent, it may be possible to divert the Earthflow into a small valley to the southwest by cutting a channel through the old earthflow deposits (lobe 2 and lobe 3). This diversion channel would substantially reduce the driving forces upon the active toe which would then be expected to stabilize. However, the diversion channel could prove to be a greater threat than the existing toe, because when the earthflow material reaches the valley, movement in the upper area could accelerate. This acceleration of movement would increase the debris flowing into the small valley which may not be large enough to contain this amount of material. The result of this could be another lobe encroaching on the highway.

5.7.6 Highway Relocation

Relocating the highway near the railway line would provide the most stable and permanent solution to the problem (Fig. 8 in the map pocket). However, this alternative probably would be the most expensive measure to adopt.

5.7.7 Coping With The Present Situation

To cope with the present situation without major

expenditures on remedial measures, several things should be done.

1. Maintainence of Drains. The maintainence of the existing drainage scheme should be kept up as it is normally in a state of disrepair. This would at least insure that some surface drainage was taking place during wet periods.

2. Monitoring. Monitoring the Earthflow should be undertaken at regular intervals to establish movement rates and patterns. As well as monitoring movement, groundwater levels should be observed in the installed piezometers. The frequency of monitoring should be increased during wetter years.

3. Warning Device. A warning device could be installed at the toe of the Earthflow to detect movement. An electrical warning device need not be expensive but could simply consist of a cable stretched between two points in front of the toe. Should movement occur it would send off an alarm by radio or phone link to the M.W.D. (Blenheim) or to the landholder who could notify the M.W.D. The system would need to be fenced off and maintained regularly.

5.7.8 Recommendations

At the conclusion of investigations, the following recommendations for treatment of the Wharanui earthflow are:

1. Installation of surface drainage trenches and upgrading the existing system.

2. Maintaining the system and frequent and regular inspections.

3. Monitoring of the earthflow so that the effectiveness of remedial measures may be assessed, or in the event of future movement the reasons for lack of success understood. Monitoring to include:

A) Groundwater level monitoring of piezometers in auger holes.

B) Continued monitoring of surface movement.

C) Measurement of discharge rates from all drainage systems so that drainage effectiveness can be appraised.

4. Close space planting of C. Macrocarpa along the sides of the catchment and along the earthflow itself.

CHAPTER SIX

SUMMARY AND CONCLUSIONS

6.1 SETTING

The Wharanui Earthflow is located at the southern end of the East Coast Deformed Belt. Within the belt fine grained lithologies have been complexly folded and faulted. The Earthflow has developed essentially along the axis of one of the minor faults (the Woodside Fault). Valley development along the Fault has resulted from the combination of weak lithologies, structure, weathering, and slope processes. The valley asymmetry reflects the attitude of the strata. The Grey Siltstone of the northeastern ridge dips from 35 to 45^{o} to the northeast, and strikes approximately parallel to the Earthflow. The southwestern ridge is composed of highly sheared and highly weathered Grey Argillites which have developed a regolith mantle. This side of the valley appears to have reached a stable angle of repose (approximately 15^{o}).

6.2 EARTHFLOW GEOMETRY AND MATERIALS

The Wharanui Earthflow is a long narrow deposit, descending 210 metres over a length of 1 km, ranging in width from 30 to 100 m within a narrow valley floor. Materials are derived from the headscarp area (zone of depletion), from feeder earthflows and shallow earth-slides (<1.5 m) occurring within the regolith of the ridges above the valley. The surface of the Earthflow is hummocky and crevassed, being marked by pressure ridges, bulges, gullies, and tension cracks. The boundaries of the Earthflow are clearly seen as prominent lateral shears, and are visible for most of the length of the flow.

Using seismic refraction techniques, hand augering, and back-hoe excavations, the deposits were found to overlie bedrock at depths of 2 to 7 metres. Materials within the Earthflow are fine grained soils with a high proportion of clay size fraction (up to 58%). Clay minerals identified include smectite, kaolinite, and illite. The sand and silt fraction consists predominantly of quartz and feldspar grains.

Within these fine-grained cohesive soils rubbly lenses occur. These act as confined aquifers containing significant

amounts of entrained water. Groundwater levels were measured using Casagrande type piezometers but the monitoring period did not cover a sufficient time span to ascertain a correlation of rainfall to groundwater levels. Groundwater levels varied considerably along the length of the flow, with some augerholes being dry at depths as great as 4 metres, and some indicating water levels within less than .5 metres of the ground surface.

The "zone of accumulation" is characterized by five distinct debris lobes resulting from successive phases of slope movement. The debris lobes are stratified, indicating that each lobe is made up of episodic movements. Only one of these lobes is currently active and it lies within 25 metres of State Highway 1.

6.3 MOVEMENT AND FAILURE MECHANISM(S)

6.3.1 Movement

Movement occurs primarily along distinct basal and lateral shears. The lateral shears are clearly visible at the margins of the Earthflow whilst the basal shears are seen only in trench excavations or in gullies. The movement since 1947 is approximately one metre/year, as interpreted from aerial photographs. However, the rate is variable, increasing when precipitation is high and decreasing when precipitation is low. Since installation of a monitoring network by the M.W.D., movement has been recorded as high as 4.6 m/year (1980), this following a period of six years with exceptionally high rainfall.

Two survey networks (primary and secondary) were installed and monitored in this study to delineate types and rates of movement. The primary network measured absolute movement along the Earthflow and the secondary network was employed to indicate relative movement across tension cracks and scarps. Movement over the study period has been mostly insignificant, with displacements commonly less than 100 mm. However, movements of up to 390 mm were recorded from localized reactivations of the Earthflow.

6.3.2 Failure Mechanism(s)

The mechanism of failure is a complex process involving several factors which include the geometry and nature of the materials. Precipitation is the triggering mechanism which

initiates movement of the mass. Two modes of failure within the valley catchment can occur depending on the duration and intensity of precipitation:

a) Rapid regolith failures on the valley sides are initiated by high intensity rainstorms. High rainfall associated with these storm events generates high pore-water pressure above a potential failure surface, and decreases the shear strength of the material;

b) Movement of the Earthflow at rates of up to 4.6 m/year can be correlated to cycles (5 + years) of higher than average rainfall. This happens when water infiltrates fissures, tension cracks, and boundary shears, increasing the unit weight of the mass. This decreases the shear strength until the threshold of stability is exceeded and movement is initiated.

6.4 FUTURE INSTABILITY AND RECOMMENDATIONS

Reactivation of the Earthflow will occur both locally and on a large scale given sufficient precipitation to initiate movement. As noted above movement has been correlated to high average precipitation occurring over years, but high precipitation over several months may be enough to initiate movement. The monitoring of the Earthflow has not been of sufficient duration or frequency to determine correlation of movement to short term increases in precipitation.

Past efforts to stabilize the Earthflow have not successfully arrested movement; this is at least in part due to lack of maintenance of the drainage and the severe storm events which destroyed many of the trees (refer to Appendix 10). Possible remedial measures aimed at stabilizing the Earthflow include:

(1) dewatering by counterfort drains,
(2) drainage of surface waters, and
(3) planting.

To design a correction scheme which will succeed, further geotechnical work must be carried out to provide adequate design information including triaxial strength testing and groundwater investigations. In the meantime regular monitoring should be carried out to provide an established record of movement which can be correlated with rainfall.

REFERENCES

ANDERSON, M.G., HUBBARD, M.G., KNEALE, P.E. (1982) The Influence of Shrinkage Cracks on Pore-Water Pressures within a Clay Embankment. Quarterly Journal of Engineering Geology. Vol. 15, no. 1 : 9-14.

BELL, D.H. (1976) High Intensity Rainstorms and Geological Hazards: Cyclone Alison, March 1975, Kaikoura, New Zealand. Bull. International Assoc. of Engineering Geologists no. 14 : 189-200.

BELL, D.H. and PETTINGA, J.R. (1983) Presentation of Geological Data, Part I Philosophy and Methods Used in New Zealand. Symposium on Engineering for Dams and Canals, Alexandra : 4.1-4.75.

BISHOP, D.G. (1968) The Geology of an area of Accelerated Erosion At Waerengaokuri, Near Gisborne. New Zealand Journal of Geology and Geophysics Vol. 11, no. 3 : 551-563.

BAILEY, R.G. (1972) Landslide Hazards Related to Land Use Planning in Teton National Forest, Northwest Wyoming. Ogden, Utah, U.S. Department of Agriculture, Forest Service, Intermountain Region : 131p.

BLONG, R.J. (1973) A numerical Classification of Selected Landslides of the Debris Slide-Avalanche-Flow Type. Engineering Geology, 7 : 99-114.

BORCHARDT, G.A. (1977) Clay Mineralogy and Slope Stability. California Division of Mines and Geology. Special report 133.

BRITISH GEOTECHNICAL SOCIETY (1974) Field Instrumentation In Geotechnical Engineering. Wiley, New York : 720p.

BULLOCK, S.J. (1978) The Case For Using Multichannel Seismic Refraction Equipment and Techniques for Site Investigation. Bull. Assoc. Engineering Geologists, Vol. 15 no. 1 : 19-35.

CAMPBELL, A.P. (1966) Measurment of Movement of an Earthflow. Soil and Water. Vol. 2, no. 3 : 23-24.

CARROLL, D. (1974) Clay Minerals : A Guide to their X-Ray Identification. The Geological Society of America , special paper 126 : 80p.

CARSON, M.A. and KIRKBY, M.J. (1972) Hillslope Form and Process. Cambridge University Press, London : 425p.

CHARBONEAU, R.G. et al. (1980) Stabilization of the Upper Portion of the Hat Creek Landslide. Proc. 18th Annual Symposium on Eng. Geol. and Soils Eng. Boise, Idaho : 61-80.

CZERNY T. and LANDA (1977) The Decisive Effect of Neotectonic Movements on the Origin of Gravitational Phenomena in the Zaranag Area, Northern Caucasus, U.S.S.R., Bull. International Assoc. of Engineering Geologists, no. 16 : 20-23.

DAVIS, S.N. and DeWIEST, R.J. (1966) Hydrogeology. John Wiley & Sons, Inc. New York. : 463p.

DURR, D.L. (1974) An Embankment Saved by Instrumentation. Transportation Research Record no. 482 Washington D.C. : 43-50.

DUTRO, H.B. (1974) Slope Instrumentation Using Multiple-Position Borehole Extensometers. Transportation Research Record no. 482 Washington D.C. : 9-17.

EL-SOHBY, M.A. (1981) Activity of Soils. Proc 10th Int. Conf. Soil Mechanics and Foundation Engineering, Vol. 1 : 587-591.

FERGUSSON, L.J. (1985) The Mineralogy, Geochemistry, and Origin of Lower Tertiary Smectite-Mudstones East Coast Deformed Belt, New Zealand. Unpubl. M.Sc. Thesis University of Canterbury.

FREEZE, R.A. and CHERRY, J.A. (1979) Groundwater. Prentice- Hall, Inc., Englewood Cliffs, N.J. : 604p.

FUKUOKA, M. (1980) Instrumentation: Its' Role in Landslide Prediction, Proc. Int. Symposium on Landslides. Vol. 2, New Delhi, India : 139-153.

GEDNEY, D.S. and WEBER, W.G. (1978) Design and Construction of Soil Slopes. In Landslides Analysis and Control. Transportation Research Board, Special Report 176 : 172-191.

GEOLOGICAL SOCIETY OF LONDON (1972) The Preparation of Maps and Plans in Terms of Engineering Geology. Quarterly Journal of Engineering Geology, Vol. 5 no. 4 : 295-382.

GILLOTT, Jack E. (1968) Clay in Engineering Geology. Elsevier Publishing Co. Amesterdam : 296p.

GRIM, R.E. (1962) Applied Clay Mineralogy. McGraw-Hill Book Co. New York : 422p.

HALL, W.D.M (1965) The Geology of Coverham and the Upper Waima Valley, Marlborough. Unpubl. M.Sc. Thesis, Victoria University of Wellington.

HARDEN, D.R., JANDA, R.J., AND NOLAN, K.M. (1978) Mass Movement And Storms In The Drainage Basin Of Redwood Creek, Humboldt County, California-a progress report. U.S. Geological Survey Open-File Report 78-486 : 161p.

HAWKINS, L.V. (1961) The Reciprocal Method of Routine Shallow Seismic Refraction Investigations. Geophysics, Vol. 26 no. 6 : 806-819.

HAWLEY, J.G., NORTHEY, R.D. (1981) Laboratory Permeability tests with Annular Seals. Proc 10th Int. Conf. Soil Mechanics and Foundation Engineering. Stockholm, Vol. 1 : 617-620.

HECTOR, Sir J. (1886) Reports of Geological Explorations. Colonial Museum & Geological Survey of N.Z. Reports, no. 17.

HILL, J.K. (1978) The La Clare Subdivision Landslide, Akaroa. Private Report, Christchurch.

HOLTZ, W.G. (1983) The influence of Vegetation on the Swelling And Shrinking of Clays in the U.S.A. Geotechnique Vol. 33, no. 2 : 159-163.

HUTCHINSON, J.N. (1968) Mass Movement. In Encyclopedia of Geomorphology. Reinhold Book Corp., New York : 688-695.

HUTCHINSON, J.N. (1970) A Coastal Mudflow On The London Clay Cliffs At Beltinge, North Kent (England). Geotechnique, Vol. 20, no. 4 : 412-438.

HUTCHINSON, J.N. (1977) Assessment of the Effectivness of Corrective Measures in Relation to Geological Conditions and Types of Slope Movement. Bull. International Assoc. Engineering Geologists no. 16 : 131-155.

HUTCHINSON, J.N. and BHANDARI, R.K. (1971) Undrained Loading, a Fundamental Mechanism of Mudflows and Other Mass Movements. Geotechnique, Vol. 21, no. 4 : 353-358.

HUTCHINSON, J.N., PRIOR, D.B., and STEPHENS, N. (1974) Potentially Dangerous Surges in an Antrim (Ireland) Mudslide. Quart. Jour. Eng. Geol. Vol. 7, no. 4 : 363-376.

HUTTON, F.W. (1874) Report on the Geology of Northeast Portion of the South Island, From Cook Straight to the Rakaia. N.Z. Geol. Surv. Rep. Geol. Expl. 1872-73.

KEEFER, D.K. (1984) Landslides Caused by Earthquakes. Geological Society of America Bulletin, no. 95 : 406-421.

KEEFER, D.K. and JOHNSON, A.M. (1978) Mobilization and Movement Mechanics of Earthflows. In Sierakowsky, R.L. ed., Recent Advances in Engineering Science, 15th Proc. Society of Engineering Science Annual Meeting, Gainsville, Fla. : 223-226.

KEEFER, D.K. and JOHNSON, A.M. (1983) Earthflows: Morphology, Mobilization, and Movement. U.S. Geological Survey Paper no. 1264. U.S. Govt. Printing Office, Washington D.C. : 56p.

LAMBE, T.W. and WHITMAN R.V. (1969) Soil Mechanics. John Wiley and Sons, New York : 553p.

LENSEN, G.J. (1962) Geological Map of New Zealand. Sheet 16, Kaikoura 1:250,000 DSIR, Wellington.

LEWIS, D.W. (1981) Practical Sedimentology. Apteryz.

McCAULEY, M.L. and KOSKO F. (1980) Monitoring a Slope to Failure. Proc. 18th Annual Eng. Geol. Soils Eng. Symp., Boise, Idaho : 45-60.

McGILL J.T. (1965) Landslide Problems and their Investigations. Landslides and Subsidence, Geologic Hazards Conference, Los Angeles, California : 13-19.

McKAY, A. (1886) On Geology of Eastern Part of Marlborough Provincial District. Rep. Geol. Expl. 1885 : 27-136.

MACPHERSON, E.O. (1952) The Stratigraphy and Bentonitic Shale Deposits of Kekerengu and Blue Slip, Marlborough. New Zealand Journal of Science and Technology. Sec B, Vol. 33 no. 4 : 258-286.

MARLBOROUGH CATCHMENT BOARD; D.J. Parsons and MWD, Slip Stabilization. File no. 194/S.390, courtesy of Mr. Don Mackay, Kaikoura.

MARTIN, W. (1932) The Vegetation of Marlborough. Published in the Marlborough Express : 46p.

MEYER, R. (1978) The Continous Seismic Refraction Method. Bull. Assoc. Engineering Geologists, Vol. 15 no. 1 : 37-49.

MOFFITT, F.H. and BOUCHARD, H. (1982) Surveying. 7th ed. Harper & Row Publishers, New York : 834p.

MORGENSTERN, N.R. and SANGREY, D.A. (1978) Methods of Stability Analysis. In Landslides Analysis and Control. Transportation Research Board, Special Report 176 : 155-171.

MUNOZ, A. (1974) The Role of Field Instrumentation in Correction of the "Fountain Slide". Transportation Research Record no. 482 Washington D.C. : 1-8.

NORTHEY, R.D., HAWLEY, J.G., and BARKER, P.R. (1974) Classification and Mechanisms of Slope Failures in Natural Ground. NZIE Proc. of Symposium on Stability of Slopes in Natural Ground, Nelson, Vol. 1, no. 5 : 3.1-3.8.

PATERSON, B.R. (1984) Engineering Geology Immediate Report 84/010 Geological Investigation of the Wharanui Slip, SH1, Kaikoura Coast.NZGS, DSIR report P30/921,924. Christchurh : 10p.

PETTINGA, J.R. (1980) Creeping Earthflows. University of Canterbury Geology Dept. unpublished paper ENCI 372 : 5p.

PREBBLE, W.M. (1976) The Geology of the Kekerengu-Waima River District Northeast Marlborough. Unpublished M.Sc. thesis. Victoria University, Wellington.

PREBBLE, W.M. (1980) Late Cainozoic Sedimentation and Tectonics of the East Coast Deformed Belt, in Marlborough, New Zealand. Int. Assoc. Sediment. Spec. publ. no. 4 : 217-218.

PRIOR, D.B., AND STEPHENS, N. (1972) Some Movement Patterns of Temperate Mudflows: Examples From Northeastern Ireland: Geological Society of America Bulletin, Vol. 83, no. 8: 2533-2543.

READ, H.H. (1970) Rutley's Elements of Mineralogy. Thomas Murby & Co. London 26th edition.

REAY, M.B. (1980) Cretaceous and Tertiary Stratigraphy of Part of the Middle Clarence Valley, Marlborough. Unpubl. M.Sc. Thesis, University of Canterbury.

RUSSEL, W.A.C. (1959) A Geological Reconnaissance of North-East Marlborough, Geol. Rep. no. 1, BP Oil Expl. Co. Ltd., N.Z., NZGS files.

SAAYMAN, C.M. (1978) Fundamentals of the Seismic Method-Important Factors Concerning its Engineering Applications and Prerequisites for Optimum Utilization. Bull. Assoc. Engineering Geologists, Vol. 15 no. 1 : 1-17.

SAVAGE, W. Z. and CHLEBORAD, A. F. (1982) A Model for Creeping Flow in Landslides. Bull. Assoc. of Engineering Geologists. Vol. 19 no. 4 : 333-338.

SCOTT, C.R. (1980) An Introduction to Soil Mechanics and Foundations. Applied Science Publishers LTD, London : 406p.

SHANNON, W.L., WILSON, S.D., and MEESE, R.H. (1962) Field Problems: Field Measurements. In Foundation Engineering, McGraw-Hill, New York : 1025-1080.

SHARP, C.F.S. (1938) Landslides and Related Phenomenon. A Study of Mass Movements of Soil and Rock. Columbia University Press, New York : 137p.

SHARP, J.C., LEY, G.M.M., and SAGE, R. (1977) Pit Slope Manuel, Chapter Four-Groundwater; Canadian Centre for Mineral and Energy Technology, Report 77-13 : 240p.

SIDLE, R.C., PEARCE, A.J., and O'LOUGHLIN, C.L. (1985) Hillslope Stability and Land Use. American Geophysical Union, Water Resources Monograph, Vol. 11 : 138p.

SKEMPTON, A.W. (1953) The Colloidal Activity of Clays. Proc. 3rd Int Conf. Soil Mechanics and Foundation Engineering, Vol. 1 : 57-61.

SMITH, R.K. (1974) Earthflows In The Poverty Bay-East Coast Region, Report on Project NA/HY/5. National Water and Soil Conservation Organisation, New Zealand, Hydrological Research: Progress Report No. 18 : 19p.

SMITH, W.D. and BERRYMAN, K.R. (1983) Revised Estimates of Earthquake Hazard in New Zealand. Bull N.Z. Nat. Soc. Earthquake Eng., 16 : 259-272.

SPORLI, K.B. (1980) New Zealand and Oblique Slip Margins: Tectonic Development Up To and During the Cainozoic. Int. Assoc.. Sediment. Spec. publ. no. 4 : 147-170.

STANDARDS ASSOCIATION OF NEW ZEALAND (1980) Methods of Testing Soils For Civil Engineering Purposes, Part 1, New Zealand Standards 4402, Wellington.

STEINER, A. (1977) The Wairakei Geothermal Area, North Island, New Zealand: Its Subsurface Geology and Hydrothermal Rock Alteration. New Zealand Geological Survey Bulletin no. 90. Wellington.

STRONG, C.P. (1977) Cretaceous-Tertiary boundary at Woodside Creek, Northeastern Marlborough. New Zealand Journal of Geology and Geophysics Vol. 20, no. 4 : 687-696.

SWANSTON, D.N. (1978) Effect of Geology on Soil Mass Movement Activity in the Pacific Northwest. In Proc. 5th North American Forest Soils Conf. Fort Collins: 89-115.

TERZAGHI, K. and PECK, R.B. (1967) Soil Mechanics in Engineering Practice. 2nd edition, John Wiley & Sons, New York : 729p.

THOMSON, S. (1975) The Little Smoky Landslide. Canadian Geotechnical Journal. Vol. 12, no. 3 : 379-392.

TICE, J.A. and SAMS, C.E. (1974) Experiences With Landslide Instrumentation in the Southeast. Transportation Research Record no. 482 Washington D.C. : 18-29.

TUELLER, D.O. (1965) Landslide Problems on California State Highways. Landslides and Subsidence Geologic Hazards Conference, Los Angeles, California : 21-30.

WILSON S.D. (1974) Landslide Instrumentation for the Minneapolis Freeway. Transportation Research Record no. 482 : 30-42.

VARNES D.J. (1958) Landslides Types and Processes. In Landslides and Engineering Practice. Highway Research Board Special Report 29 : 20-47.

---------- (1978) Slope Types and Processes. In Landslides Analysis and Control. Transportation Research Board, Special Report 176 : 112-138.

VOIGHT, B., and W.G. PARISEAU, (1978) Rockslides and Avalanches-An Introduction in Rockslides and Avalanches, Vol. 1 Natural Phenomena, edited by Voight, Developments in Geotech. Eng no. 14A, Elsevier, Amsterdam : 1-67.

WILSON, S.D. and MIKKELSEN, P.E. (1978) Field Instrumentation; In Landslides Analysis and Control. Transportation Research Board, Special Report 176 : 112-138.

WINTERMEYER, A.M. and KINTER,E.B. (1955) Dispersing Agents for Particle Size Analysis of Soils. Highway Research Board Bulletin 95, Washington D.C. : 1-14.

WU and SANGREY (1978) Strength Properties and Their Measurment. In Landslides Analysis and Control. Transportation Research Board, Special Report 176 : 112-138.

ZARUBA, Q. and MENCL, V. (1969) Landslides and Their Control. Elsevier Publishing Co., New York : 214pp.

APPENDIX ONE

GEOLOGICAL HISTORY

NEW ZEALAND GEOLOGIC TIME SCALE

UPPER MESOZOIC-QUATERNARY

SYSTEM	T (m.y.)	SERIES	STAGE	SUB STAGE	MAP SYMBOL	INTERNATIONAL EQUIVALENT	
QUATERNARY	0.001		ARANUIAN		Quor	HOLOCENE	
	0.07		OTIRAN		Quti	WURM	PLEISTOCENE
	0.16		OTURIAN		Qutu	NEOTYRRHENIAN	
			WAIMEAN			RISS	
	0.25	HAWERA	TERANGIAN			EUTYRRHENIAN	
			WAIMAUNGAN			MINDEL	
			WAIWHERAN			PALEOTYRRHENIAN	
	0.28		PORIKAN.			GUNZ	
	0.45		CASTLECLIFFIAN	PUTIKIAN	Wu Wc	SICILIAN	
	1.06	WANGANUI		OKEHUAN	Wk	DONAU	
	1.60		NUKUMARUAN	MARAHAUAN	Wa Wn	EMILIAN	
	1.79			HAUTAWAN	Wh	CALABRIAN	
TERTIARY			WAITOTARAN	MANGAPANIAN	Wm Ww	ASTIAN	PLIOCENE
				WAIPIPIAN	Wp		
	5.0		OPOITIAN		Wo	PLAISANCIAN	
		TARANAKI	KAPITEAN		Tk	MESSINIAN	UPPER MIOCENE
	10.5		TONGAPORUTUAN		Tt		
			WAIAUAN		Sw		
	14.0	SOUTHLAND	LILLBURNIAN		Sl	TORTONIAN	MID
			CLIFDENIAN		Sc	HELVETIAN	
		PAREORA	ALTONIAN		Pl	BURDIGALIAN	LOWER
	22.5		OTAIAN		Po	AQUITANIAN	
		LANDON	WAITAKIAN		Lw	CHATTIAN	OLIGOCENE
			DUNTROONIAN		Ld	RUPELIAN	
			WHAINGAROAN		Lwh	LATTORFIAN	
	36.0	ARNOLD	RUNANGAN		Ar	BARTONIAN	UPPER EOCENE
			KAIATAN		Ak		
			BORTONIAN		Ab	LUTETIAN	MID
	46.5	DANNEVIRKE	PORANGAN		Dp		
			HERETAUNGAN		Dh	YPRESIAN	LOWER
			MANGAORAPAN		Dm		
	53.5		WAIPAWAN		Dw	THANETIAN	PALEOCENE
			TEURIAN		Dt	DANIAN	
UPR MESOZOIC	65.0	MATA	HAUMURIAN		Mh	MAASTRICHTIAN	UPPER CRETACEOUS
			PIRIPAUAN		Mp	CAMPANIAN	
		RAUKUMARA	TERATAN		Rt	SANTONIAN	
			MANGAOTANEAN		Rm	CONIACIAN	
			AROWHANAN		Ra	TURONIAN	
						CENOMANIAN	
	95.0	CLARENCE	NGATERIAN		Cn	ALBIAN	LOWER
			MOTUAN		Cm		
			URUTAWAN		Cu	APTIAN	
			KORANGAN		Ck		
	135.0					NEOCOMIAN	

A1.2 GEOLOGICAL HISTORY

The following historical outline is based on Prebble (1976 & 1980). Prebble recognizes fifteen formations which are summarized in Table A1.

The geology of northeastern Marlborough consists of basement rocks of Jurassic and Lower Cretaceous age overlain by Upper Cretaceous and Tertiary covering strata (Fig 3.1). The break between the undermass and the covering strata is described by Prebble (1980) as,

"in part an unconformity, and in part a complex fault, the two merging into each other. The fault is interpreted as an undermass/cover decollement in the eastern half of the Ben More Block."

The undermass is comprised of Torlesse Greywacke (flysch turbidites) and the Good Creek Formation (proximal to distal turbidites) which dominated in the Jurassic through to Ngaterian and consist of well indurated coarse grained clastic detritus. The sequence was uplifted, eroded, and subsequently overlain by covering sediments which began deposition in the Teratan Stage (Upper Cretaceous). The basal members of the covering strata are proximal and distal turbidites and conglomerates (Burnt Creek Formation and Paton Sandstone).

During the Haumurian Stage there was a transgression and fine grained quartzose clastic sediments accumulated in the deep water (Whangai Shale). Deep water conditions persisted through to the Waitakian Stage as fine grained calcareous sediment accumulated (Amuri Limestone). As calcareous deposition progessively diminished in the far eastern part of the basin it was replaced by clastic quartzose turbidites which began in the Waipawan (Woodside Formation). However in much of the eastern part of the basin, calcareous deposition continued with clastic terrigenous turbidites interbedded. From the Whaingaroan to the Waitakian calcareous deposition is marked by the Whales Back Limestone which was superseeded by renewed fine grained

terrigenous sedimentation and grain-flow sands in the Otain to Altonian (Waima Siltstone/Tirohanga Sandstone). At this time extensive submarine lava flows and breccias were extruded (Cookson Volcanics).

Tectonic subsidence and normal faulting persisted into the Late Oligocene-Early Miocene and was concurrent with deposition. In the Mid-Miocene faulting continued with local rapid uplift and gave rise to the Great Marlborough Conglomerate (Southland Series). This conglomerate is massive, unsorted with large angular blocks and rafts up to hundreds of metres in length. Further offshore thick clastic turbidites, grainflow sands, thick mudstone, and rare marl continued through the Southland (Heavers Creek Formation). Sedimentation probably ceased in the Pliocene as their is no evidence of marine sedimentation during the Quaternary.

In the Late Miocene block faulting and differential uplift continued, but with less intensity. In the Pliocene the character of the deformation changed. The covering strata was subjected to imbricate thrust faulting along a northwest trend, and folding along a northeast trend. Subsequently major northeast striking dextral faults, the Kekerengu and the Clarance Faults, rotated the covering slab of the shallow thrust and fold belt which was uncoupled from the undermass as a tectonic decollement in the Ben More Block. Dextral Faulting continued on the Kekerengu and Clarance Fault through to Recent, with the northern side of each fault uplifted through thrusting.

Active Quaternary faulting is evident on all the major dextral faults from offset Pleistocene terraces and recent landforms.

Table A1

Formation Name and Ages recognized by Prebble (1976).

COVERING STRATA:

Heavers Creek Formation - Altonian, Clifdenian, Lillburnian, Waiuan.

Great Marlborough Conglomerate - Altonian, Clifdenian, and ?Lillburnian.

Tirohanga Sandstone - Otaian and ?Altonian.

Waima Siltstone - Waitakian, Otaian, Altonian.

Cookson Volcanics - Arnold to Landon.

Woodside Formation - Waipawan, Mangaorapan, Heretaungan.

Amuri Limestone - consisting of seven members from Haumurian to Whaingaroan.

Whangai Shale - Haumurian.

Flags Formation - Haumurian.

Wharanui Point Limestone - Haumurian and possibly Piripauan.

Paton Sandstone - Piripauan.

Burnt Creek Formation - Teratan.

Glencoe Siltstone - Ngaterian or Teratan.

UNDERMASS:

Good Creek Formation - Urutawan to Motuan and Ngaterian.

Greywacke - Puaroan, Mokoiwian, Korangan, Urutawan, Motuan.

APPENDIX TWO

TERMINOLOGY

A2.1 ROCK MATERIAL AND ROCK MASS DESCRIPTION

Rock material and rock mass descriptions as suggested by Bell and Pettinga (1984) are followed in this thesis. Figure A2.1 defines the nomenclature used.

A2.2 SOIL MATERIAL AND SOIL MASS DESCRIPTION

Soil material and soil mass descriptions as suggested by Bell and Pettinga (1984) are followed in this thesis. The following figures define the nomenclature used.

A2.3 SAMPLE NUMBERING SYSTEM

Samples were numbered as follows:

Augerhole samples - numbering system depicts the augerhole number and the sample number from the hole. The depth of the sample is listed on the auger log summary sheets (Figs. 6 & 7 map pocket) and in Table A2.1.

Trench samples - numbered with the trench number and the sample number, ie. T2-1 denotes Trench 2 sample 1. Location of trenches are shown in Fig. 3 (map pocket). Trench logs show location of samples extracted from trenches, (Fig. 7, map pocket).

Other Samples - any other samples are noted with a letter and a number denoting their location found within the field area, ie. S63 denotes a sample from location 63 on Fig. 1 (map pocket).

ENGINEERING GEOLOGICAL FIELD DESCRIPTION FOR ROCK MATERIAL

WEATHERING

	TERM	GRADE	ROCK DESCRIPTION
1.	residual soil (RW)	VI	discolouration and complete transformation to soil; original fabric destroyed
2.	completely weathered (CW)	V	discolouration and transformation to soil; original fabric largely preserved
3.	highly weathered (HW)	IV	discolouration; discontinuities open and rock fabric affected by deep alteration; lithorelicts present
4.	moderately weathered (MW)	III	discolouration; discontinuities; open with discolouration and alteration penetrating inwards; loss of strength
5.	slightly weathered (SW)	II	slight discolouration on open discontinuities; no loss of material strength
6.	unweathered (UW)	I	no discolouration or loss of strength, or any other effects due to weathering

STRENGTH

	TERM	POINT LOAD STRENGTH INDEX $I_s(50)$	FIELD ESTIMATION OF STRENGTH
1.	extremely strong (ES)	more than 10	can only be chipped with geological hammer
2.	very strong (VS)	3 to 10	several blows of hammer required to break hand specimen
3.	strong (S)	1 to 3	few firm blows of hammer required to break specimen
4.	moderately strong (MS)	0·3 to 1	breaks readily with one blow of hammer
5.	moderately weak (MW)	0·1 to 0·3	broken by hand only with difficulty, small thin pieces broken by finger pressure
6.	weak (W)	0·03 to 0·1	broken by hand; pieces 25 mm or more broken by finger pressure
7.	very weak (VW)	less than 0·03	crushed or remoulded by hand (includes hard soils)

GEOLOGICAL CLASSIFICATION

CRYSTAL OR GRAIN SIZE	SEDIMENTARY		IGNEOUS					METAMORPHIC	
	CLASTIC	CHEM/ORGANIC		Silicic	Intermed.	Mafic	Ultramaf.	FOLIATED	MASSIVE
very coarse 64	CONGLOMERATE (1)								
coarse 2	AGGLOMERATE (2)								
	BRECCIA (3)								
medium	SANDSTONE (4)	Calcareous: LIMESTONE (9)	Intrusive	GRANITE (27) GRANODIORITE (28)	SYENITE (29) DIORITE (30)	GABBRO (31)	PERIDOTITE (32) DUNITE (33)	GNEISS (34) SCHIST (35) PHYLLITE (36) SLATE (37) MYLONITE (38)	HORNFELS (39) MARBLE (40) QUARTZITE (41) AMPHIBOLITE (42)
		Siliceous: CHERT (10) OTHER (11)							
0·06		Carbonaceous: COAL (12) OTHER (13)							
fine TUFFS (7)	SILTSTONE (5)	Ferruginous: LATERITE (14) OTHER (15)	Extrusive	(19) RHYOLITE (20) OBSIDIAN (21) DACITE	(22) TRACHYTE (23) ANDESITE	(24) DOLERITE (25) BASALT	(26) SERPENTINITE		
	MUDSTONE (6)								
very fine 0·002 (mm)	CLAYSTONE (8)	Saline: ROCK SALT (16) GYPSITE (17) OTHER (18)							

Mode of Occurrence

WEATHERING TERM — STRENGTH TERM — COLOUR — FABRIC — ROCK NAME

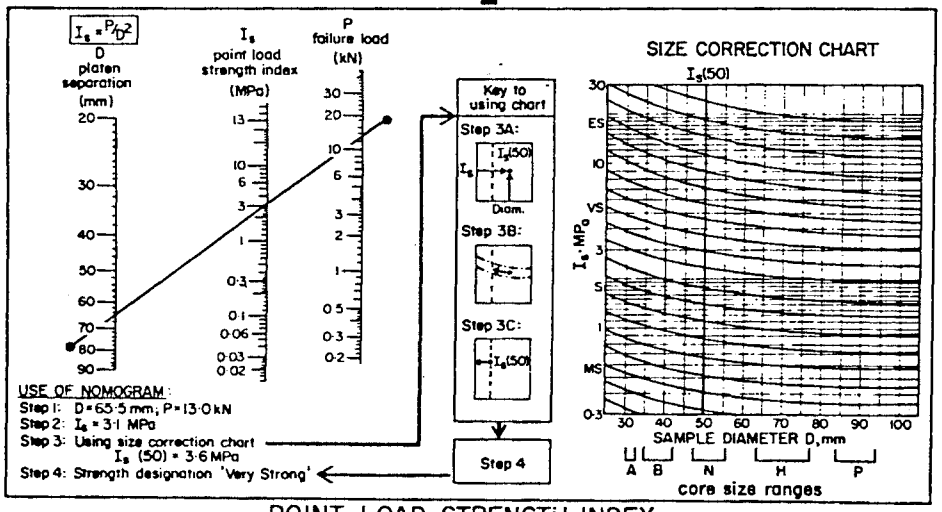

POINT LOAD STRENGTH INDEX

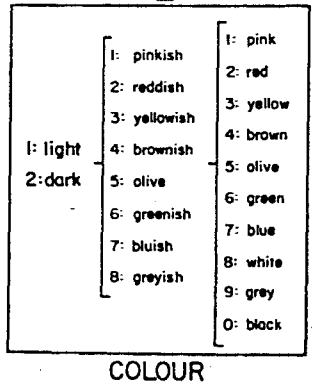

COLOUR

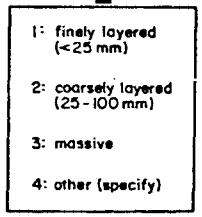

FABRIC

ENGINEERING GEOLOGICAL FIELD DESCRIPTION FOR SOIL MATERIAL

WEATHERING

	TERM	GRADE	SOIL DESCRIPTION
5	Completely Weathered (CW)	V	completely discoloured and altered, no trace of original fabric
4	Highly Weathered (HW)	IV	mostly altered and weakened, little trace of original fabric
3	Moderately Weathered (MW)	III	large discoloured portions of original soil separated by more altered material, significantly weakened
2	Slightly Weathered (SW)	II	minor discolouration of some parts of the original soil, no loss of strength
1	Unweathered (UW)	I	original soil with NO discolouration, loss of strength or other effects due to weathering
0	*		NOTE in coarse-grained soils record weathering grade of DOMINANT fraction here and qualify weathering grade of subordinate and/or minor fractions if appropriate

STRENGTH

	TERM	FIELD CRITERIA
1	loose	can be removed from exposure in disaggregated form by hand
2	compact	only removed from exposure by implement; material readily disaggregated by physical means
3	+cemented	only removed from exposure by implement; material does not disaggregate
4	hard	may be removed from exposure with difficulty by implement or hand; softened on immersion in water, may be remoulded
5	stiff	indented by thumb pressure, but not moulded by fingers; softened on immersion in water, and may be remoulded
6	firm	moulded or indented only by strong finger pressure; easily moulded after immersion in water
7	soft	easily indented or moulded by finger pressure
8	very soft	exudes between fingers when squeezed
9	spongy	readily compressed by finger pressure, but cannot be remoulded

+ may require description as rock material

UNIFIED SOIL CLASSIFICATION SYSTEM

			FIELD IDENTIFICATION	GROUP SYMBOL	TYPICAL NAMES
COARSE-GRAINED SOILS	GRAVELS (>50% larger than 2mm)	clean gravels	wide range in grain size and substantial amounts of all interm. sizes	GW	well graded GRAVELS
			predom. one size or a range of sizes with some interm. sizes missing	GP	poorly graded GRAVELS
		gravels with fines	non-plastic fines (see ML below)	GM	poorly graded SILTY-GRAVELS
			plastic fines (see CL below)	GC	poorly graded CLAYEY-GRAVELS
	SANDS (<50% smaller than 2mm)	clean sands	wide range in grain sizes and substantial amounts of all interm. sizes	SW	well graded SANDS
			predom. one size or a range of sizes with some interm. sizes missing	SP	poorly graded SANDS
		sands with fines	non-plastic fines (see ML below)	SM	poorly graded SILTY SANDS
			plastic fines (see CL below)	SC	poorly graded CLAYEY-SANDS

			SHINE	DILATANCY (1)	TOUGHNESS (2)		
FINE-GRAINED SOIL SILTS AND CLAYS	LIQUID LIMIT	<50	none to very dull	quick to slow	none	ML	INORGANIC SILTS with slight plasticity
			moderate	none to very slow	medium	CL	INORGANIC CLAYS of low to medium plasticity
			none to very dull	slow	slight	OL	ORGANIC SILTS & CLAYS of low plasticity
		>50	dull	slow to none	slight to medium	MH	INORGANIC SILTS of high plasticity
			very glossy	none	high	CH	INORGANIC CLAYS of high plasticity
			moderate to v. glossy	none to very slow	slight to medium	OH	ORGANIC CLAYS of medium to high plasticity
HIGHLY ORGANIC SOILS			identified by colour, odour, spongy feel and fibrous texture			Pt	PEAT and other highly organic soils

PROCEDURES FOR FINE-GRAINED SOILS OR FRACTIONS (1)

DILATANCY (reaction to shaking) -

1) Prepare pat of moist soil, adding water to make soft - but not sticky.

2) Place pat in palm of hand, shake horizontally by striking vigorously against other hand.

POSITIVE REACTION appearance of water on surface of pat, which becomes glossy. When squeezed between fingers, water and gloss disappear, pat stiffens and may crumble

TOUGHNESS (consistency near plastic limit) -

1) Mould sample to consistency of putty, adding water or air drying as required

2) Roll to thin (3mm) thread, fold and reroll repeatedly until thread crumbles at plastic limit

3) Knead together and continue until lump crumbles.

Diagnosis - a tough thread and stiff lump indicate high plasticity, a weak thread and lump low plasticity clays.

GROUP SYMBOL CODINGS FOR USCS

COLUMN 1		COLUMN 2	
G 1	C 4	W 1	C 4
S 2	O 5	P 2	L 5
M 3	Pt 6	M 3	H 6

BOUNDARY CLASSIFICATIONS specify, enter 0,0

WEATHERING TERM | WATER CONTENT TERM | STRENGTH TERM | COLOUR | FABRIC | SOIL NAME | USCS SYMBOL

	TERM	FIELD CRITERIA
1	Dry	looks and feels dry, fine-grained soils usually hard, powdery or friable, coarse-grained soils may run freely through hands
2	Moist	soil feels cool and may be darkened in colour, particles tend to adhere in coarse-grained materials, fine-grained soils may be softened
3	Wet	soils feel cold and are darkened in colour, free water forms on hands when sample is disturbed
4	Saturated	restricted to wet soils below the water table or the static water level in excavations or drill holes

WATER CONTENT

COLOUR

1: light	1 pinkish	1 pink	
	2 reddish	2 red	
	3 yellowish	3 yellow	
	4 brownish	4 brown	
	5 olive	5 olive	
	6 greenish	6 green	
	7 bluish	7 blue	
	8 greyish	8 white	
2: dark		9 grey	
		0 black	

FABRIC

1: finely layered (25 mm)
2: coarsely layered (25-100 mm)
3: massive
4: other (specify)

*SUBORDINATE FRACTION
20-50% volume visual estimate

DOMINANT FRACTION
>50% volume visual estimate

* MINOR FRACTION
<20% volume visual estimate

1	coarse	gravelly
2	medium	
3	fine	
4	coarse	sandy
5	medium	
6	fine	
7	silty	
8	clayey	
9	peaty	

PARTICLE SIZE

SOIL TYPE TERM		PARTICLE SIZE (mm)	GRAPHIC LOG
1 coarse	gravel	> 60	
2 medium		20-60	
3 fine		2-20	
4 coarse	sand	0·6-2·0	
5 medium		0·2-0·6	
6 fine		0·06-0·2	
7 silt		0·002-0·06	
8 clay		< 0·002	
9 peat		NA	

WITH SOME

1	coarse	gravel
2	medium	
3	fine	
4	coarse	sand
5	medium	
6	fine	
7	silt	
8	clay	
9	peat	

TABLE A2.1

Augerhole sample numbers and depths (metres)

Augerhole	Sample number	Sample depth
1	A1-1	0.5-0.55
	A1-2	1.0-1.05
	A1-3	1.5-1.55
	A1-4	2.1-2.24
	A1-5	2.5-2.60
	A1-6	2.9-3.00
	A1-7	3.0-3.2
	A1-8	3.2-3.3
	A1-9	3.3-3.4
	A1-10	3.4-3.55
	A1-11	3.9-4.1
2	A2-1	0.35-0.4
	A2-3	0.7-0.95
	A2-4	1.4-1.55
3	A3-1	0.3-0.4
	A3-2	0.9-1.0
	A3-3	1.1-1.2
	A3-4	1.65-1.8
	A3-5	2.1-2.5
	A3-6	3.1-3.3
	A3-7	5.0-5.4
	A3-8	5.5-5.8
	A3-9	5.8-6.3
4	A4-1	0.6-0.8
	A4-2	1.5-1.65
	A4-3	2.1-2.3
	A4-4	2.6-2.8
	A4-5	3.1-3.3
	A4-6	3.4-3.6
	A4-7	4.1-4.2
	A4-8	4.3-4.5
	A4-9	4.6-4.7
	A4-10	4.8-5.0
	A4-11	5.2-5.25
5	A5-1	0.05-0.2
	A5-2	0.7-0.9
	A5-3	1.3-1.5
	A5-4	1.9-2.1
	A5-5	2.5-2.7
	A5-6	3.0-3.2
	A5-7	3.4-3.6
	A5-8	3.7-3.8
6	A6-1	2.0-2.2
	A6-2	2.8-3.2
	A6-3	3.4-3.85
	A6-4	4.4-4.5
	A6-5	4.2-4.3

Augerhole	Sample number	Sample depth
7	A7-1	0.6-0.8
	A7-2	1.3-1.75
	A7-3	1.7-1.9
8	A8-1	0.4-0.9
	A8-2	1.4-1.7
	A8-3	1.9-2.4
9	A9-1	0.2-1.0
11	A11-1	0.2-1.0
	A11-2	1.8-2.5
	A11-3	3.0-4.0
12	A12-1	0.4-1.25
	A12-2	2.4-2.95
	A12-3	3.0-3.7
13	A13-1	0.2-1.0
	A13-2	1.2-1.6
	A13-3	1.9-2.3
	A13-4	2.5-2.7
	A13-5	2.5-2.7
14	A14-1	0.5-1.3
15	A15-1	0.5-1.5
	A15-2	1.5-2.0
	A15-3	3.2-4.0
18	A18-1	0.8-1.5
	A18-2	1.8-2.5
	A18-3	2.5-2.7
19	A19-1	2.2-2.3
20	A20-1	1.6-2.1
	A20-2	3.1-3.5
	A20-3	4.1-4.5

Trench number	Sample number	Sample depth (metres)
1	T1-1	4.0
2	T2-1	2.5
	T2-2	3.5
	T2-3	1.1
	T2-4	.95

APPENDIX THREE
GRAINSIZE ANALYSES

A3.1 METHODOLOGY

A3.2 RESULTS

A3.1 METHODOLOGY

Grainsize analyses of whole samples were carried out using techniques outlined in Lewis (1981). The sand fraction was determined by dry sieving (using 1/2 phi interval sieves in the 2 to 4 phi range) and the silt and clay fractions by hydrometer analyses.

There is a tendency for aggregates and partially weathered material to break down with continued sieving, therefore to avoid bias all samples were sieved for a standard period of 10 minutes.

Disaggregation for hydrometer analyses was done by hand in a solution of distilled water and calgon, then subjected to 10 minutes of ultrasound treatment. Two samples, A18-3 and S14 were treated with a double concentration of calgon, 20 minutes agitation, and 20 minutes of ultrasound, as flocculation was a problem.

A3.2 RESULTS

Grainsize analyses were carried out on 27 samples of earthflow material. Representative samples were chosen from the 4 main groups of colluvium, (see Chapter Four). In the following pages are representative grainsize distribution plots for;

1. Grey Clayey Silts,
2. Red silty Clays,
3. Yellowish-brown Clayey Silt, and
4. Cream sandy clays.

SEMI-LOG PLOT OF GRAINSIZE: CREAM SMECTITE CLAYS

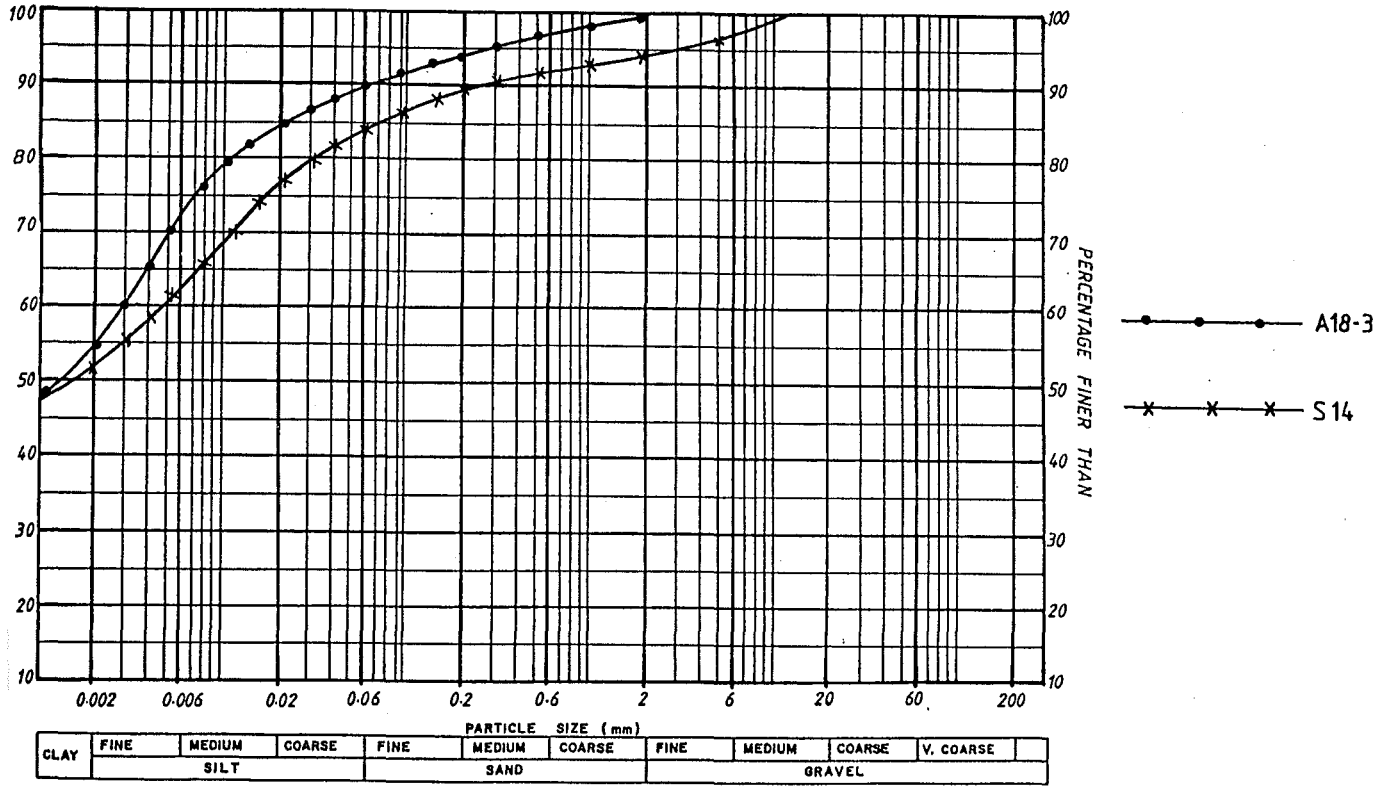

SEMI-LOG PLOT OF GRAINSIZE: YELLOWISH-BROWN CLAYEY SILTS

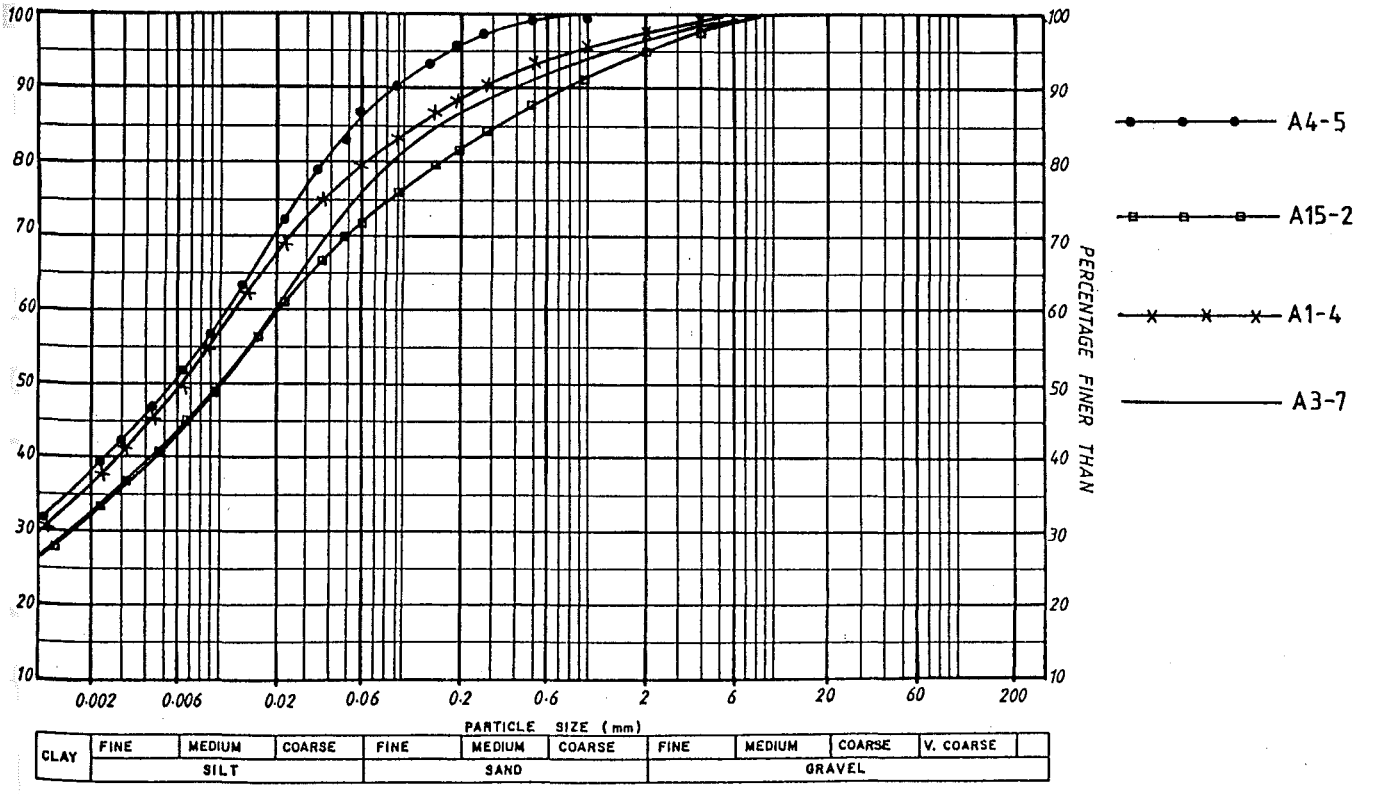

SEMI-LOG PLOT OF GRAINSIZE: RED SILTY CLAYS

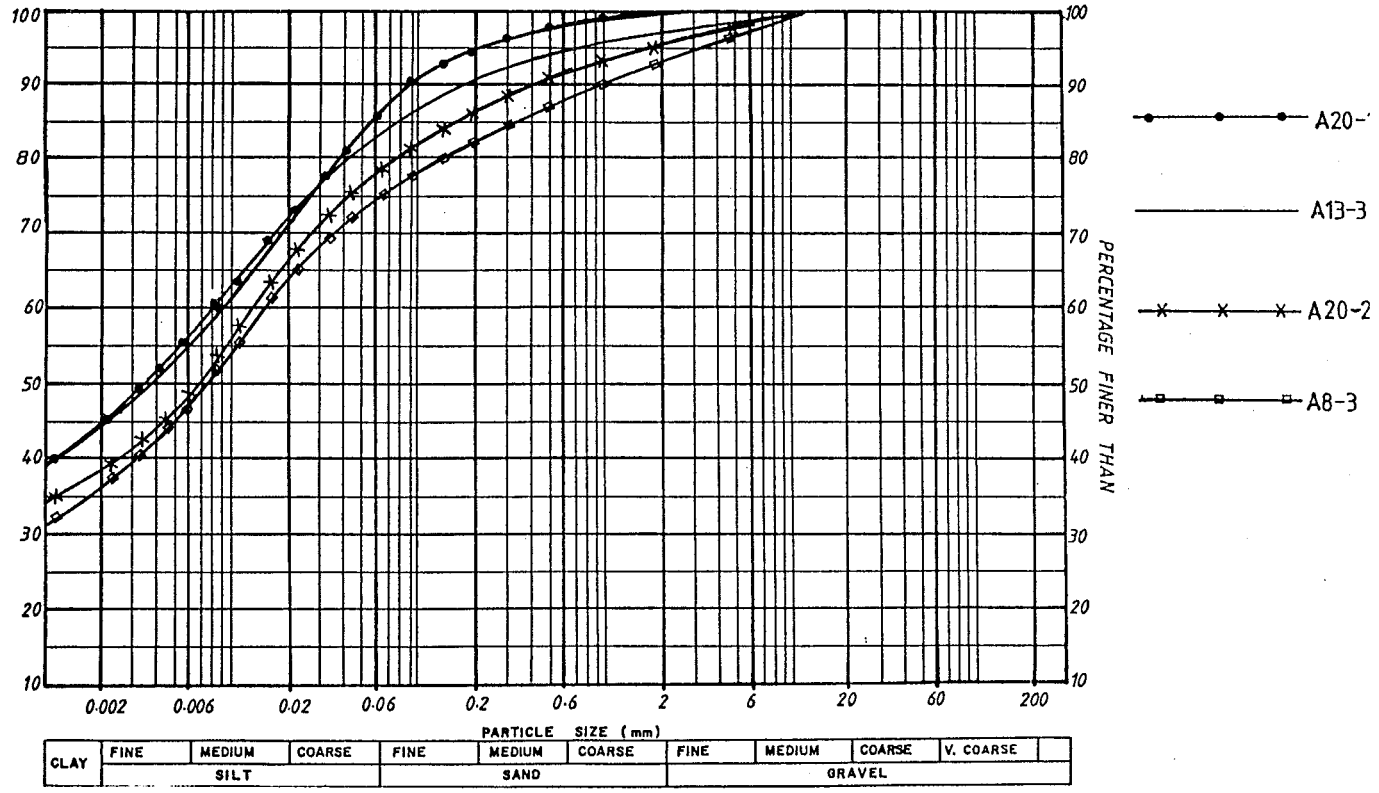

SEMI-LOG PLOT OF GRAINSIZE: GREY CLAYEY SILTS

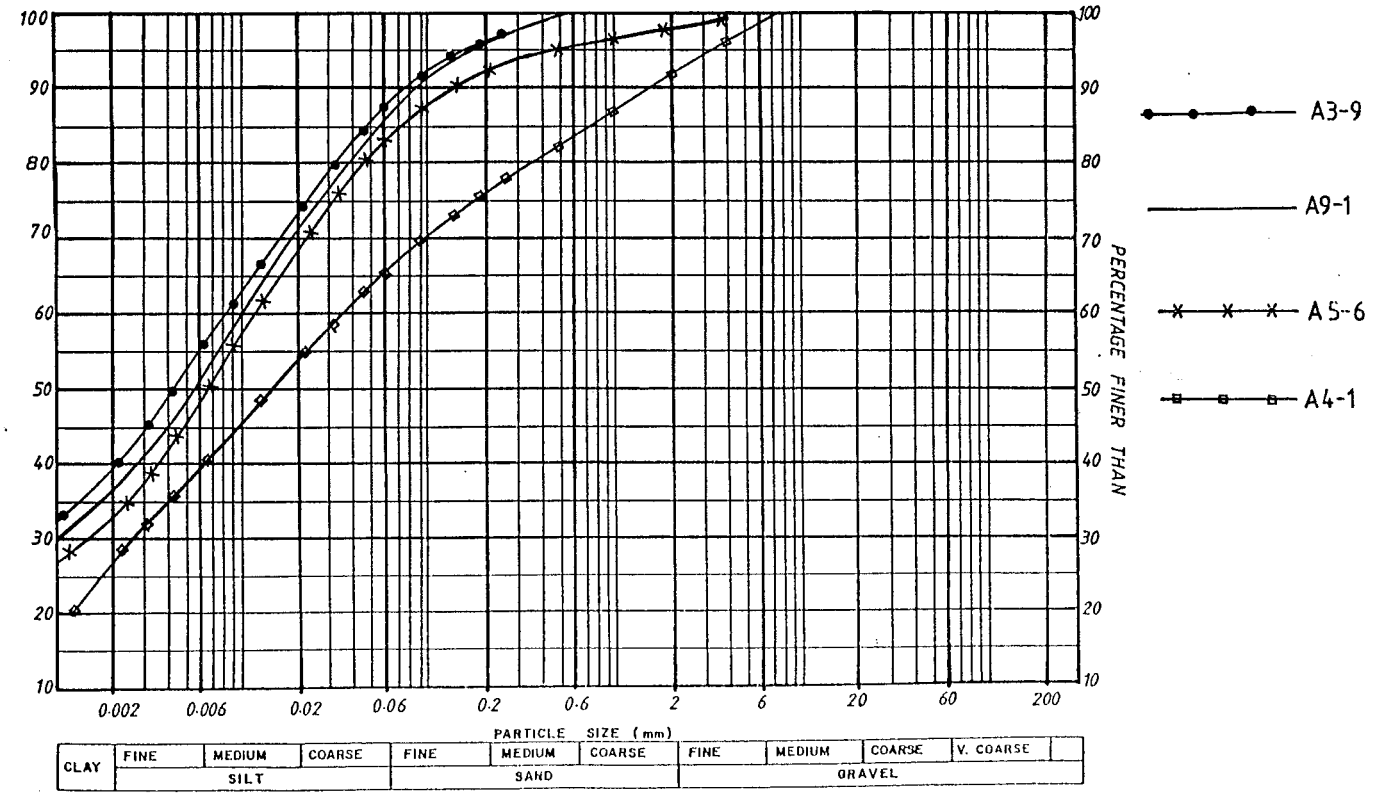

APPENDIX FOUR

CLAY MINERALOGY

A4.1 INTRODUCTION

Clay minerals by their nature give clay its plastic properties when wet, and hard and compact when dry. The clay fraction consists of clay and non-clay minerals ranging in size from .002 mm and less. In order to identify the clay fraction, X-ray diffraction techniques must be used on oriented mounts of the clay fraction. Orientation (settlement) of the clay fraction enhances the basal reflections (001) of the flaky clay minerals. The crystalline structure of clays is such that the most important diffractions from an X-ray beam occur within the 2-37° 2θ scanning distance. Overlapping of clay mineral patterns on diffractograms is common, so that treatment of the clay samples is used to distinguish between various clay minerals.

Clay minerals were identified using a Phillips X-ray diffractometer with CuK radiation maintained by a 1° divergence slit, a .2 mm receiving slit and a 1 antiscatter slit. A Norelco tube was run at 34 Kv and diffraction patterns recorded at a scan rate of 1 /min.

A4.2 METHODOLOGY

Oriented slide mounts were prepared by taking a sample of the .002 mm (2 microns) and finer fraction from settling columns during hydrometer analysis. These samples were allowed to air dry on a slide over-night. These untreated oriented mounts can give little more than preliminary identification of clay mineral assembledges and non-clay minerals such as feldspar and quartz so treatment was necessary. The mounts were treated with glycerol and re-run through the diffractometer. This treatment causes distinctive expansion of the C lattice dimension that is measurable on diffratograms.

After the glycerol treatment the mounts were subjected to heating at 550° C for 1 hour. Heating has the effect on certain clay minerals which causes a crystalline structure collapse and amorphous mineral matter results.

A4.3 CLAY MINERAL IDENTIFICATION

X-ray diffractograms were obtained for representative samples of the Grey Clayey-silts, the Red Silty-clays, the Yellowish-brown Silts, and the Whitish-cream Smectite Clays. Some whole fraction samples were also X-rayed to determine non-clay minerals.

Three types of clay minerals were identified during X-ray diffraction including smectite, kaolinite, and illite. These are briefly discussed below, and their diffractograms are shown in the following pages.

SMECTITES (swelling clays):

Smectites are 2:1 layer silicates including components which are not tightly bonded. The most distinctive feature of smectite is that water and organic liquids may penetrate between the layers so that basal spacings are varible. Water uptake is accompanied by a big increase in volume and large swelling pressures are generated. Glycerated oriented samples have a d spacing expansion from 12-14 Å, to 17-18 Å. Interlayer-water is removed by heating to 550° C and the original 12-14 Å reflection shifts to one at approximately 10 Å.

KAOLINITE:

Kaolinites are 1:1 layer silicates. The diffraction pattern is characterized by an integral series of d spacings based on (001) planes in oriented mounts; 7.15 Å (001), 3.57 Å (002), and 2.35 Å (003). Glyceration has no effect on the basal spacing but heating to 550°C completely destroys the structure, thereby making it amorphous to X-ray diffraction.

ILLITE:

Illite has a 2:1 layer structure and is structurally related to micas and includes all 10 Å non-expanding clay minerals including muscovite and illites. They are not affected by heating, but peaks generally become more intense upon heating if they are mixed layers as interlayer water is drawn off.

A4.4 NON-CLAY MINERALS

X-ray diffraction was performed on representative samples of whole rock samples as well as the clay fraction to determine the non-clay minerals present in the mixed colluvium. Minerals identified include quartz, feldspars, and hematite.

A4.5 QUANTITATIVE ANALYSIS

Quantitative analysis were not carried out on any samples as it is beyond the scope of this thesis.

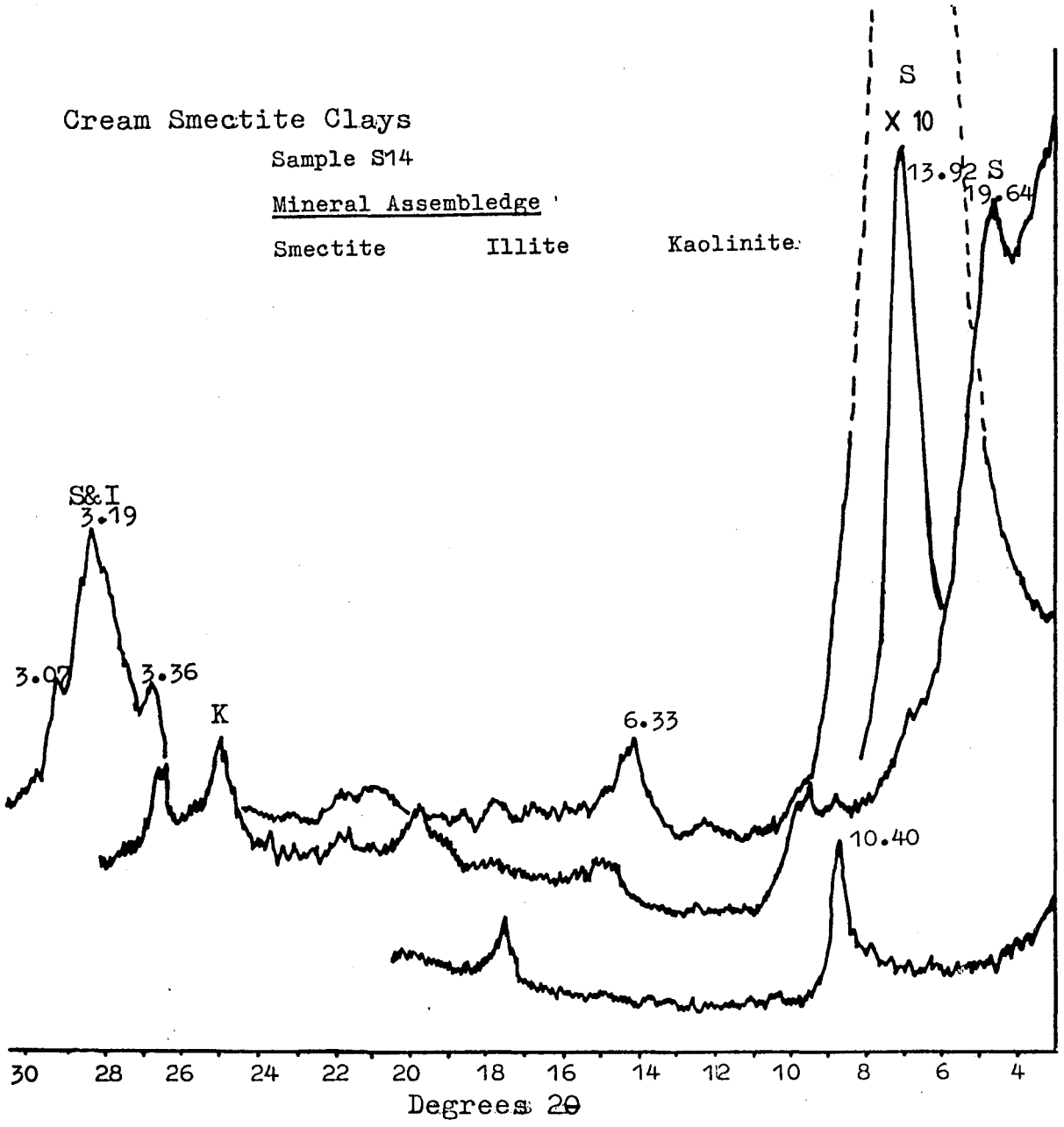
Cream Smectite Clays
Sample S14
Mineral Assembledge
Smectite
Illite
Kaolinite
S
X 10
13.92 S
19.64
S&I
3.19
3.07
3.36
K
6.33
10.40
30
28
26
24
22
20
18
16
14
12
10
8
6
4
Degrees 2θ

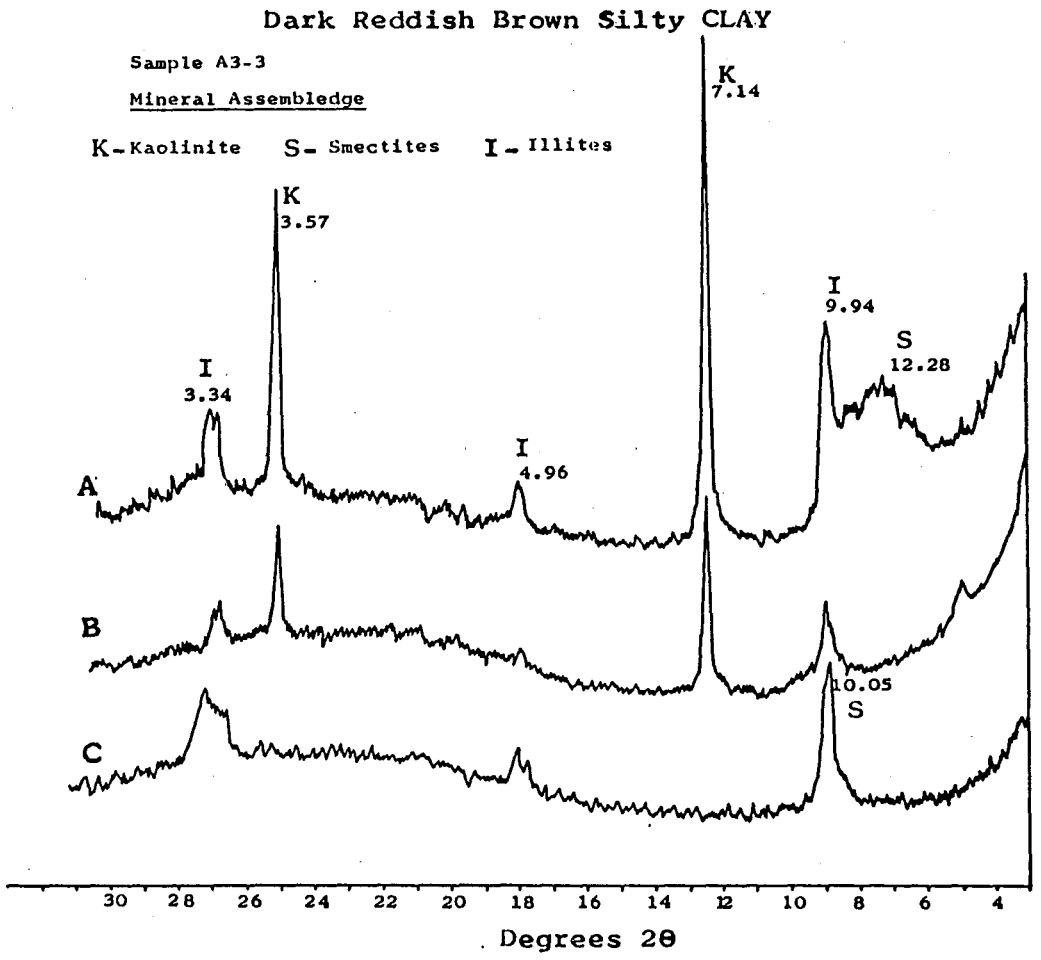
Dark Reddish Brown Silty CLAY
Sample A3-3
Mineral Assembledge
K-Kaolinite S- Smectites I- Illites
K 7.14
K 3.57
I 3.34
I 4.96
I 9.94
S 12.28
10.05 S
A
B
C
30 28 26 24 22 20 18 16 14 12 10 8 6 4
Degrees 2θ

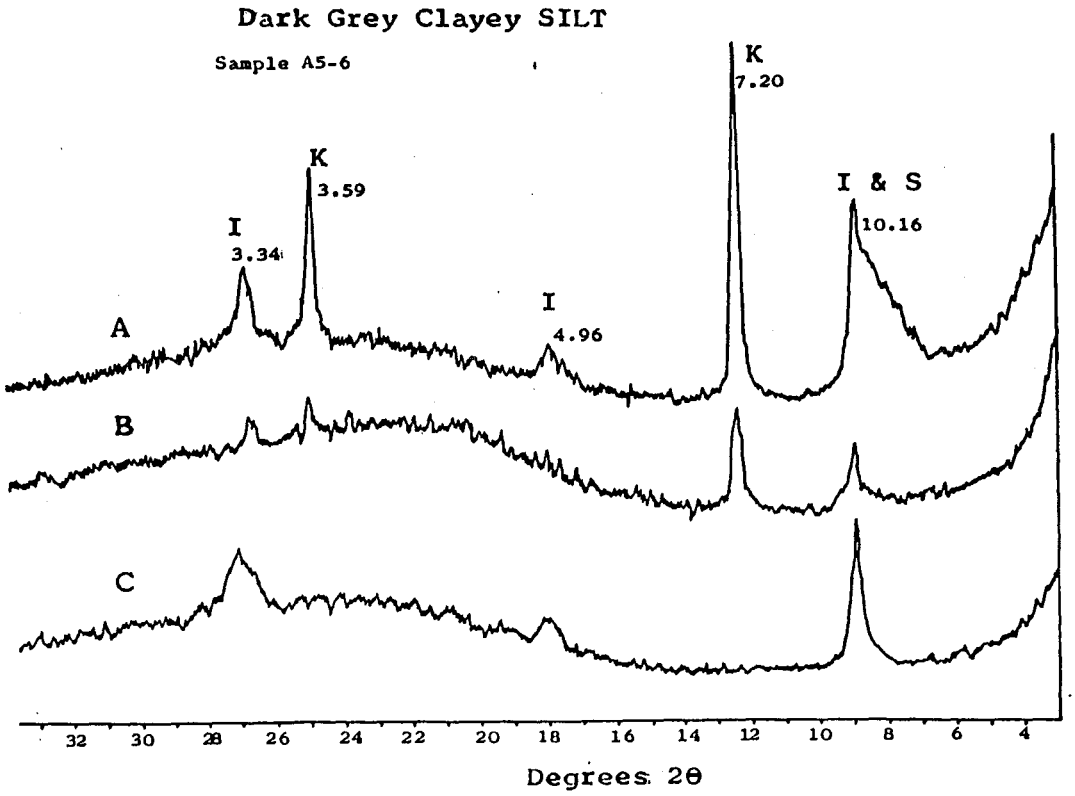
Dark Grey Clayey SILT
Sample A5-6
K 7.20
K 3.59
I 3.34
I 4.96
I & S 10.16
A
B
C
32 30 28 26 24 22 20 18 16 14 12 10 8 6 4
Degrees 2θ

Dark Brownish-Red Silty Clay

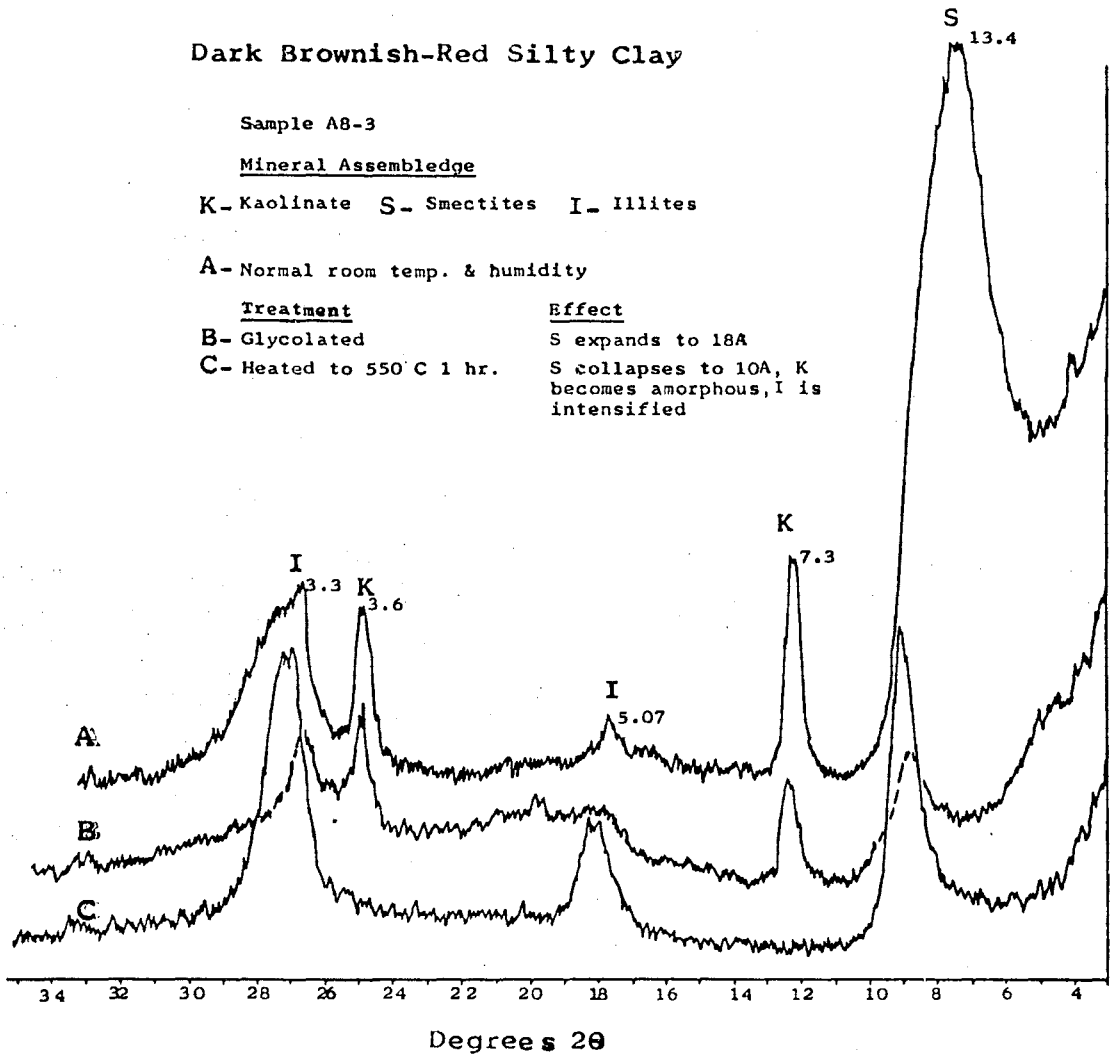

Dark Bluish-Grey Clayey Silt

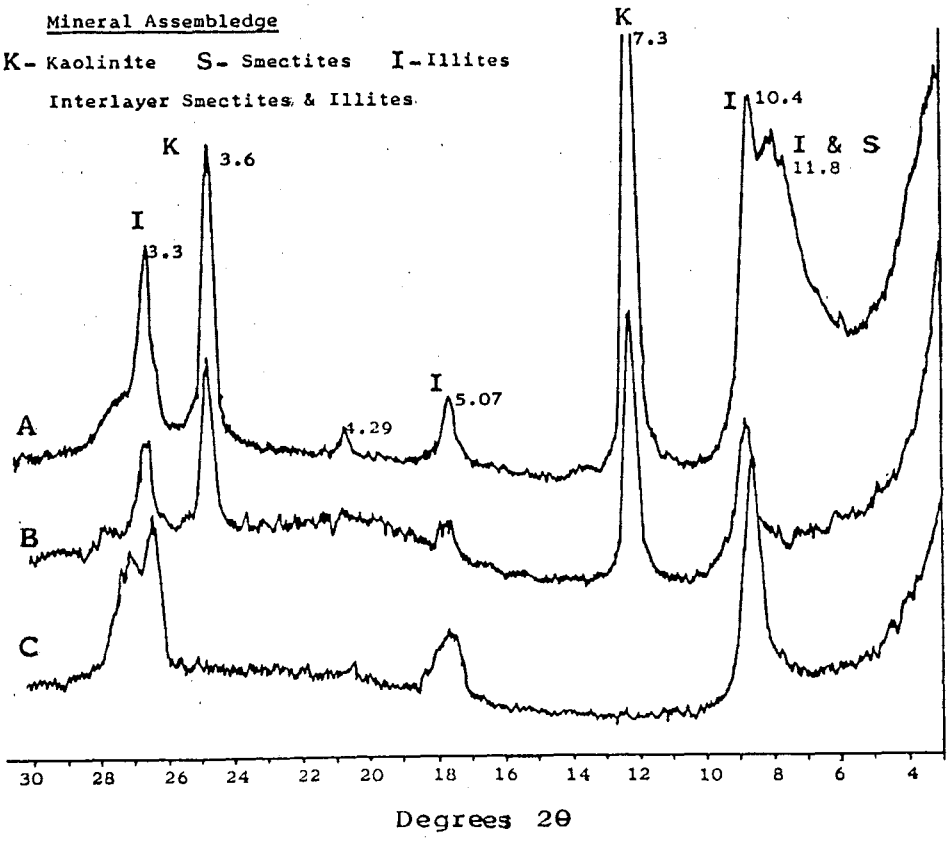

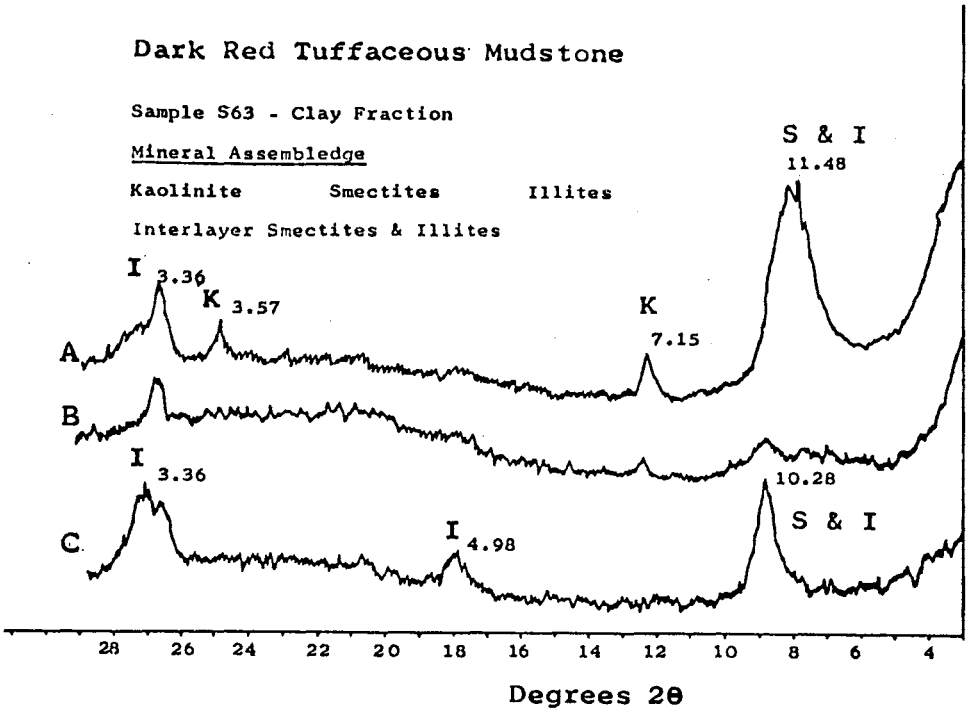
Dark Red Tuffaceous Mudstone
Sample S63 - Clay Fraction
Mineral Assembledge
Kaolinite Smectites Illites
Interlayer Smectites & Illites
I 3.36
K 3.57
K 7.15
S & I 11.48
A
B
I 3.36
10.28
S & I
C
I 4.98
28 26 24 22 20 18 16 14 12 10 8 6 4
Degrees 2θ

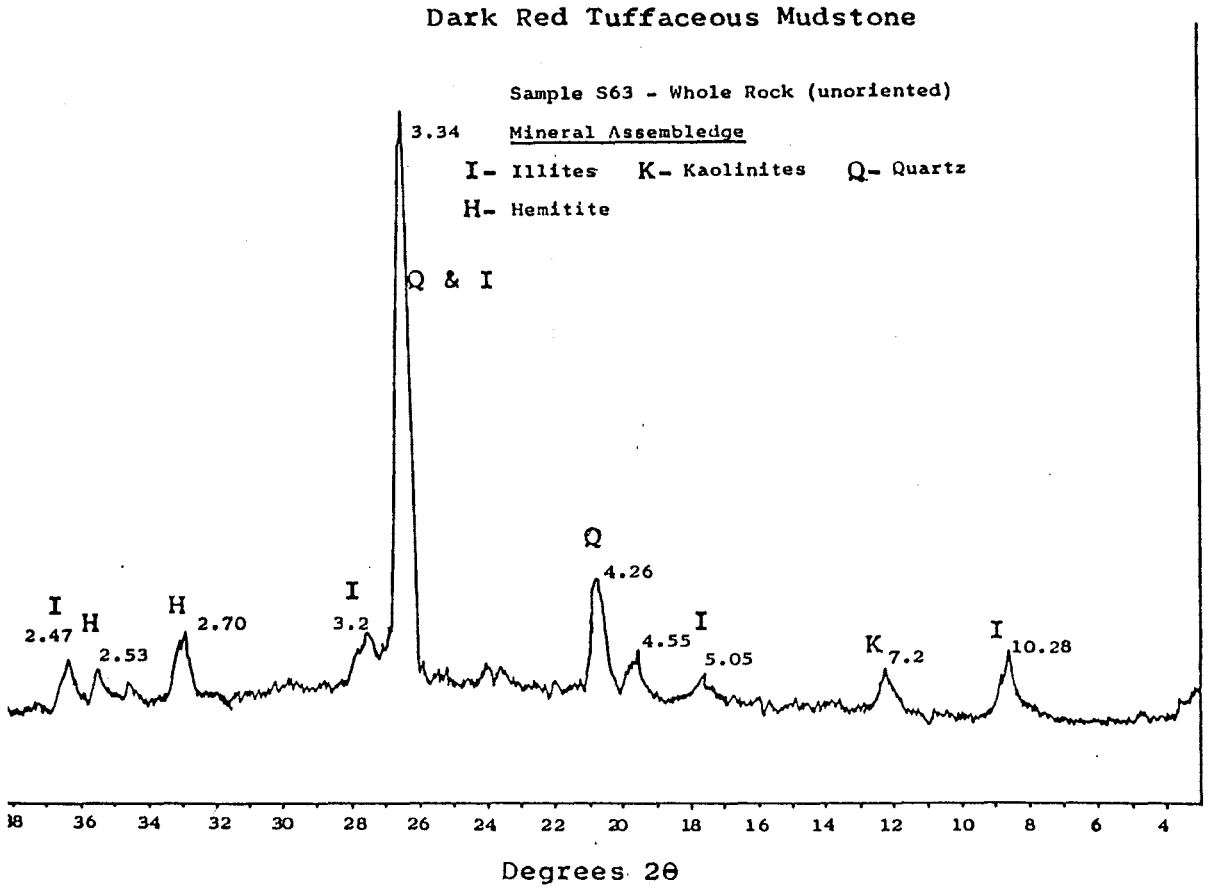
Dark Red Tuffaceous Mudstone
Sample S63 - Whole Rock (unoriented)
Mineral Assembledge
I- Illites K- Kaolinites Q- Quartz
H- Hemitite
3.34
Q & I
I 2.47
H 2.53
H 2.70
I 3.2
Q 4.26
I 4.55
I 5.05
K 7.2
I 10.28
38 36 34 32 30 28 26 24 22 20 18 16 14 12 10 8 6 4
Degrees 2θ

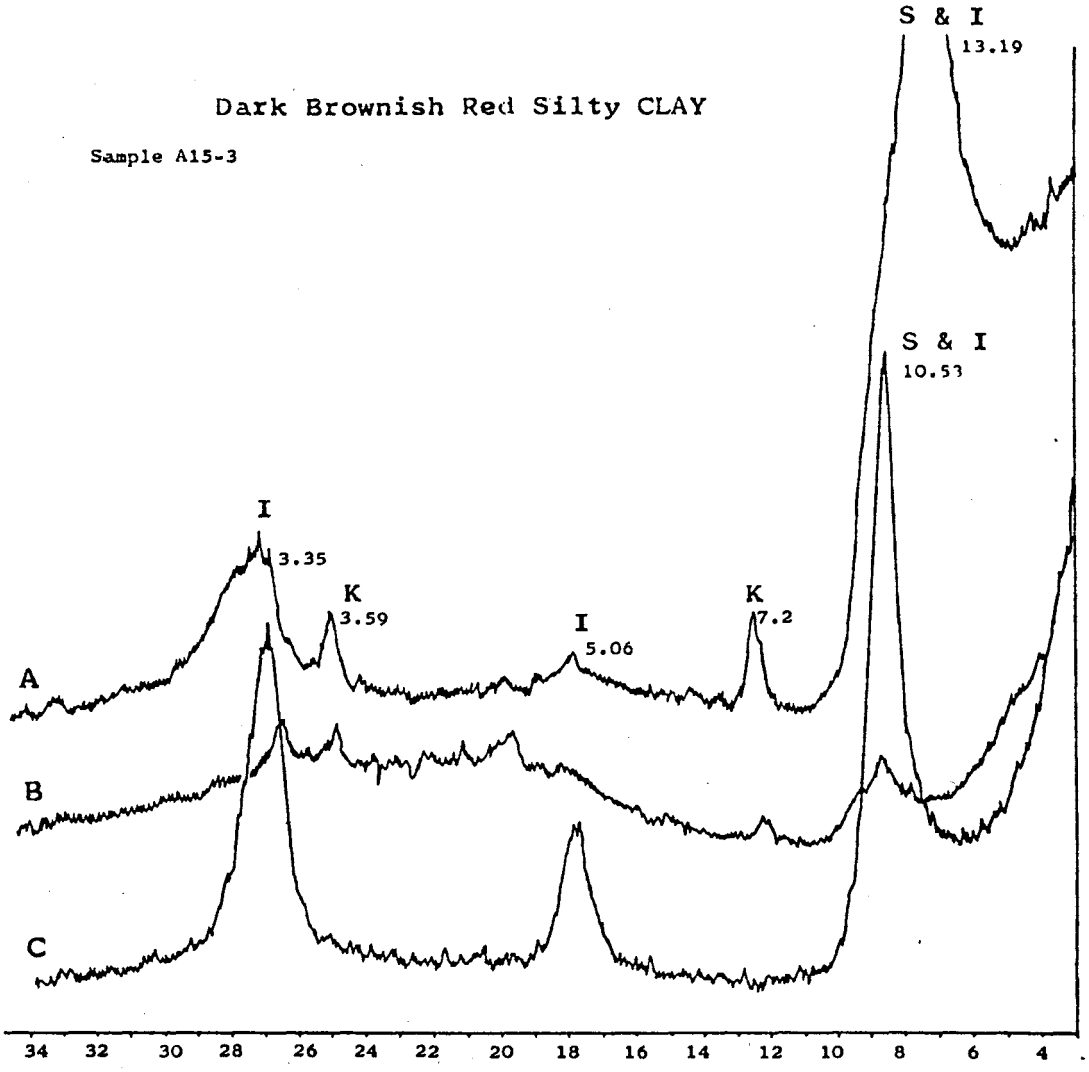
Dark Brownish Red Silty CLAY
Sample A15-3
S & I
13.19
S & I
10.53
I
3.35
K
3.59
I
5.06
K
7.2
A
B
C
34 32 30 28 26 24 22 20 18 16 14 12 10 8 6 4

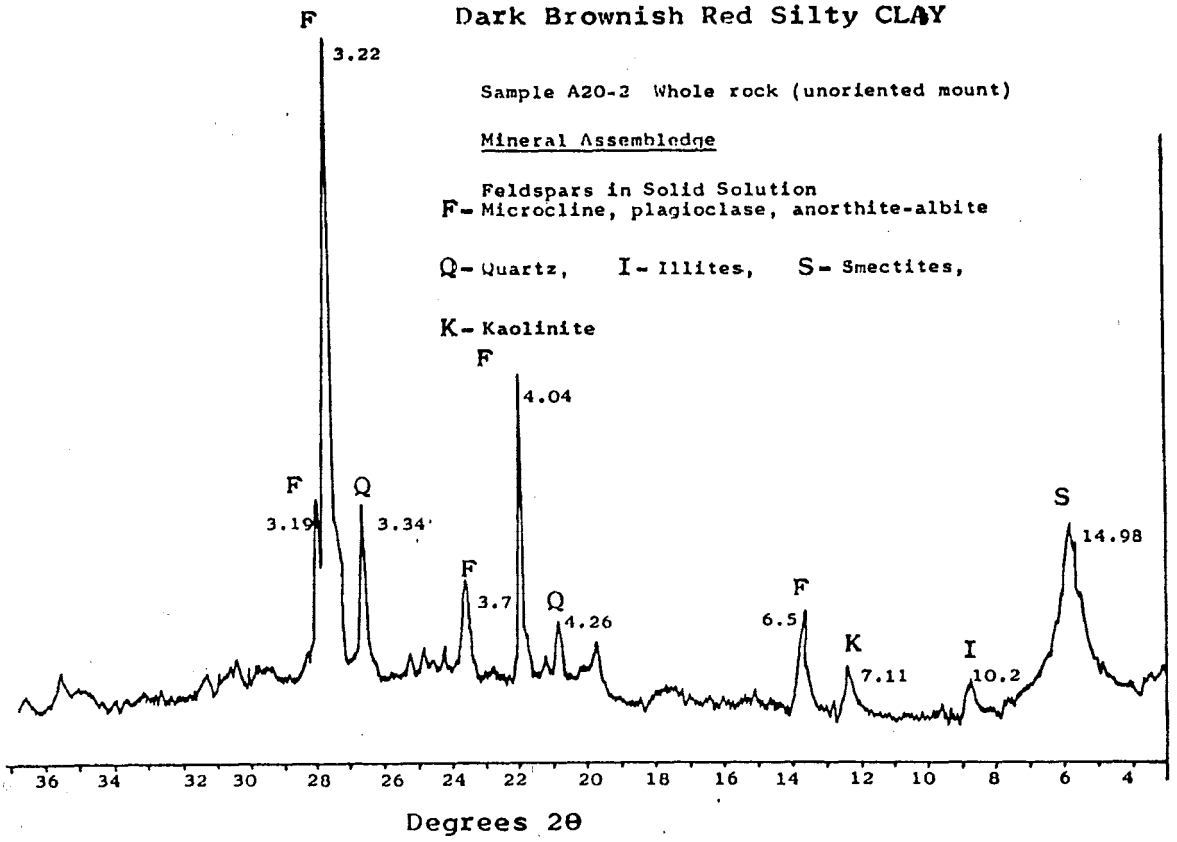
Dark Brownish Red Silty CLAY
Sample A20-2 Whole rock (unoriented mount)
Mineral Assemblage
Feldspars in Solid Solution
F- Microcline, plagioclase, anorthite-albite
Q- Quartz, I- Illites, S- Smectites,
K- Kaolinite
F
3.22
F
4.04
F
3.19
Q
3.34
F
3.7
Q
4.26
F
6.5
K
7.11
I
10.2
S
14.98
36 34 32 30 28 26 24 22 20 18 16 14 12 10 8 6 4
Degrees 2θ

APPENDIX FIVE

MISCELLANEOUS TESTS

DETERMINATION OF MOISTURE CONTENT

New Zealand Standard 4402 Part 1 (1980) Test 1, p. 15-17.

DETERMINATION OF ATTERBERG LIMITS

Liquid Limit NZS 4402 Part 1 (1980) Test 2, p. 18 - 23.
Plastic Limit NZS 4402 Part 1 (1980) Test 3, p. 24 - 26.
Plasticity Index NZS 4402 Part 1 (1980) Test 4, p. 24 - 26.

DETERMINATION OF LINEAR SHRINKAGE

Linear Shrinkage NZS 4402 Part 1 (1980) Test 6, p. 31.

DETERMINATION OF IN SITU DENSITY

NZS 4402 Part 2P (1981) Test 17(C) p. 40 - 42.

APPENDIX SIX

GROUNDWATER MONITORING

A6.1 INTRODUCTION

Casagrande piezometers were installed in five auger holes (A1, A3, A4, A5, & A8) in May, 1985, to monitor groundwater pressures and seasonal variations. Several open (uncased) holes which had water flowing into them were monitored as well as the piezometers. These give unconfined water levels and are listed in Table A6.2.

Casagrande piezometers require a sufficient volume of water in order to obtain a realistic value of groundwater pressure (see Chapter Two). As the earthflow material is very cohesive and fine grained, it was difficult to intercept zones with sufficient volumes of water which would enable true readings. However, water flowing into boreholes, while drilling, delineated several aquifers which could supply enough water volume to give indications of groundwater fluctuations. It was in these zones that the piezometers were installed and sealed.

A6.2 PIEZOMETER CONSTRUCTION

All five piezometers consist of pervious ceramic tips with 17 mm dia. PVC riser pipes. The filter tips are embedded in medium grained beach sand. Above the sand are a few cm of pea gravels, and above this is a bentonite plug which is used to seal the piezometers in their respective zones. Fig A6.1 shows the generalized construction. Refer to Fig. 7 in the Map pocket for details of specific piezometers.

A6.3 GROUNDWATER MEASURMENT

Groundwater levels were measured using a simple device. The device consists of a cable with two wires bared, glued to a brass weight, and connected to a multimeter. This was lowered into the piezometer riser pipe and when water is encountered there is a sudden resistivity change. This simple construction proved very accurate in determining water levels in the piezometer.

A6.4 DATA

PIEZOMETER READINGS

Date	Water Level Below Ground Surface (metres)				
	A1	A3	A4	A5	A8
8/3/85	3.46	1.09	1.35	1.16	1.80
24/5/85	3.1	1.32	2.37	2.09	1.33
28/8/85	2.75	0.85	1.20	1.98	0.88

Table A6.1 Piezometric Level Measurements.

OPEN HOLE READINGS

Date	Water Level Below Ground Surface (metres)				
	A20	A11	A12	A13	A15
8/3/85	3.72	2.06	3.24	0.30	3.64
24/5/85	1.2	1.75	0	0.48	2.60

Table A6.2 Open Hole Water Level Measurements.

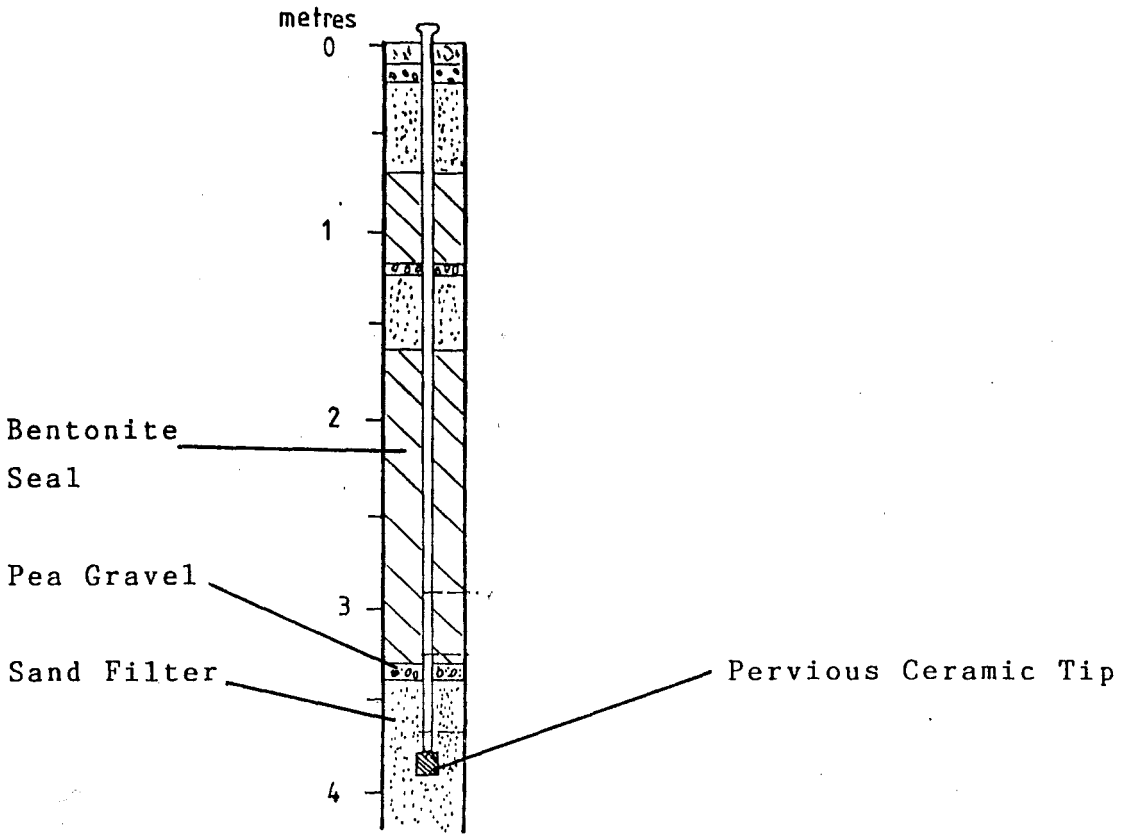

Figure A6.1 General construction of piezometers.

APPENDIX SEVEN

PERMEABILITY TESTS

A7.1 INTRODUCTION

Soil mass and soil material permeabilities were determined in the field and laboratory, respectively, by falling head permeability tests. Permeabilities were determined in the laboratory by using a falling head permeameter with annular seals. The device was built at the University of Canterbury after a design by Hawley and Northey (1981).

A7.2 FIELD TESTS

Falling head tests were performed for the zones where the piezometers were installed in boreholes. In this test, a section of the borehole is subjected to an increased pressure head above the static groundwater pressure. The head is then allowed to fall and measurement of the loss of head with time are taken from this, a relationship between flow and pressure is determined from which permeability is calculated (See Fig A7.1) (Sharp et al.,1977).

A7.3 FIELD RESULTS

Results of the falling head tests are shown below. A1 and A4 are used as examples for the method of obtaining results. (Fig. A7.2)

A1, $k = 4.2 \times 10^{-8}$

A3, $k = 1.5 \times 10^{-8}$

A4, $k = 2.0 \times 10^{-8}$

A5, $k = 4.0 \times 10^{-9}$

A8, $k = 6.0 \times 10^{-9}$

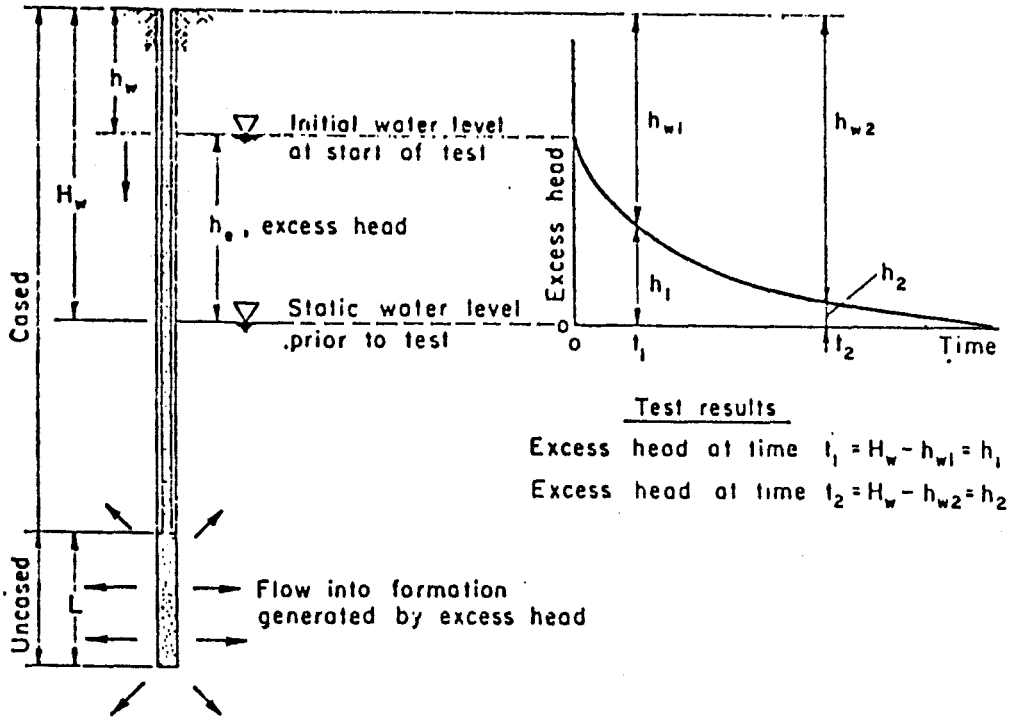

$$\text{Permeability, } k = \frac{2.3 \log_{10}(h_1/h_2)}{t_2 - t_1} \cdot \frac{r_c^2}{2L} \cdot \ln(R/r) \text{ m/min.}$$

ln (R/r) may be taken as 7

in which case

$$k = 0.133\ S\ \frac{r_c^2}{L} \text{ m/sec}$$

where S is the gradient of the log head time graph (Fig. B-3)

Figure A7.1 Principal of falling head test (from Sharp et al., 1977).

A7.4 LABORATORY TESTS

Laboratory permeability tests are most commonly conducted by measuring flow through a cylindrical sample. Samples must fit very well to minimise any leakage as errors of magnitudes are possible with leakage.

Laboratory falling head permeability tests were carried out on "undisturbed" core samples extracted from trench 2. These tests were conducted on an apparatus modified from Hawley and Northey (1981). The essential feature of this design is that it exposes a reduced central portion of the sample to the pressure difference. This apparatus minimises the chance of leakage around the sides

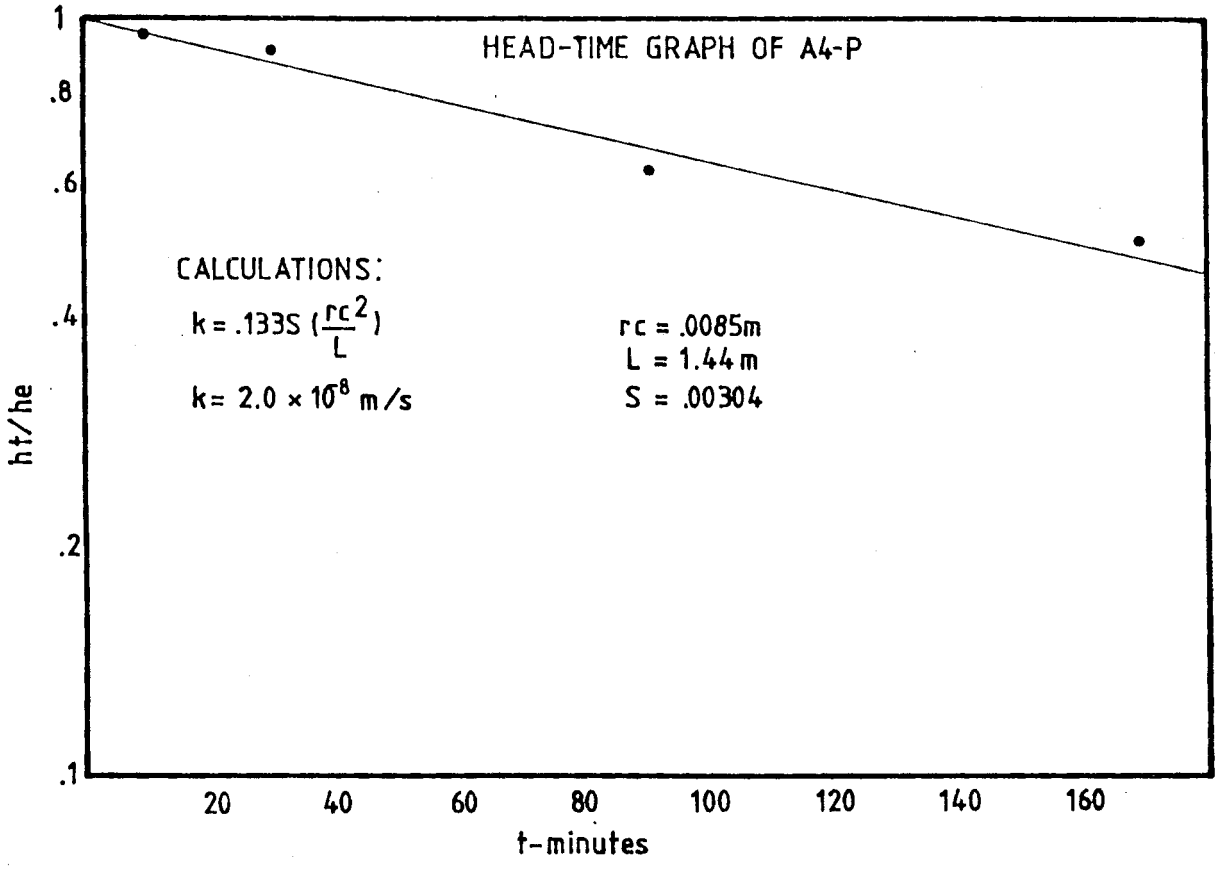
HEAD-TIME GRAPH OF A4-P
CALCULATIONS:
k = .133S (rc2/L)
k= 2.0 × 10⁻⁸ m/s
rc = .0085m
L = 1.44 m
S = .00304
ht/he
1
.8
.6
.4
.2
.1
20
40
60
80
100
120
140
160
t-minutes

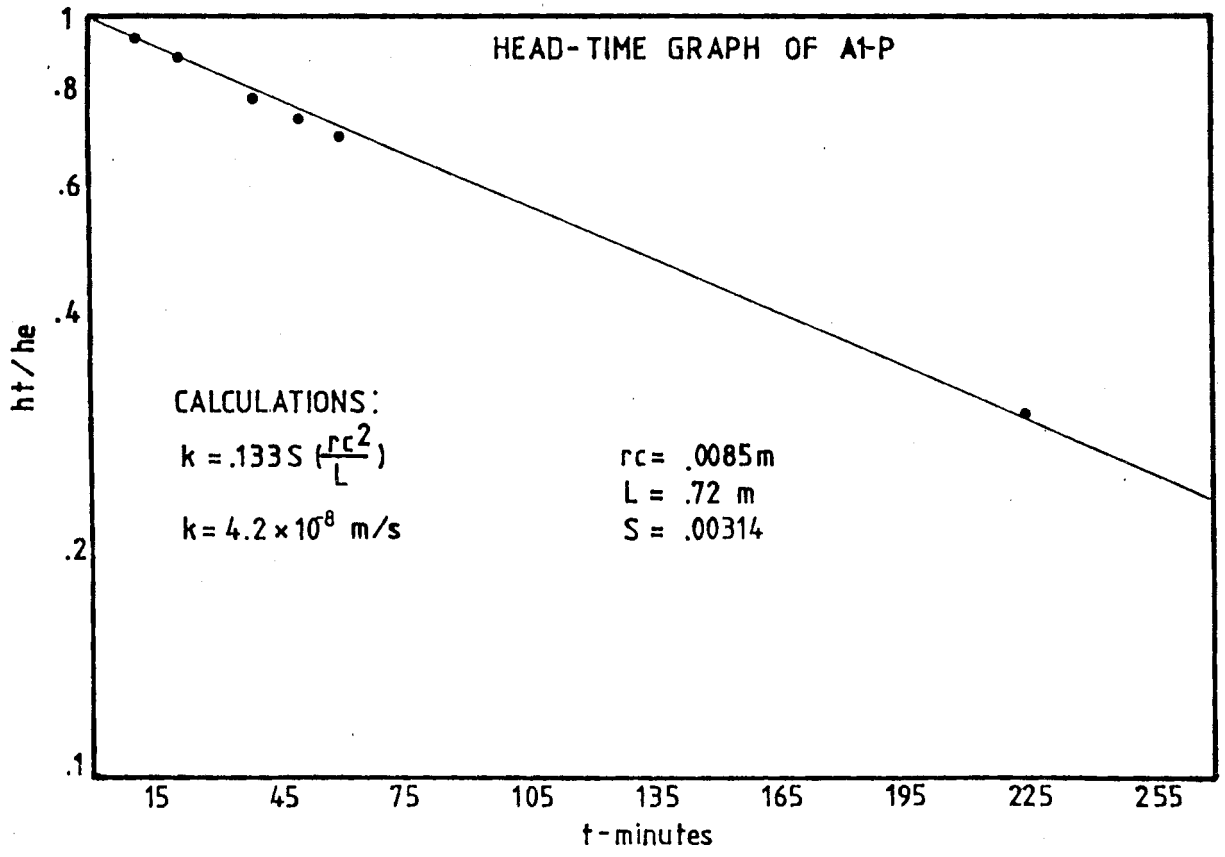
HEAD-TIME GRAPH OF A1-P
CALCULATIONS:
k = .133S (rc2/L)
k= 4.2 × 10⁻⁸ m/s
rc= .0085m
L = .72 m
S = .00314
ht/he
1
.8
.6
.4
.2
.1
15
45
75
105
135
165
195
225
255
t-minutes

Figure A7.1

so that errors (especially over-estimates of permeability are substantially reduced.

The device was constructed, at the University of Canterbury, Geology Dept., to fit the core sample tubes available at the University.

Flow Calculations

The permeability (k) of the soil material is given by the equation:

$$k = \frac{F \times QH}{\Delta pA}$$

where Q = measured flow

H = the axial length of the cell

Δp = the applied pressure potential difference

A = the full cross-sectional area of the cell

and F = 1.6 - 1.45 according to how well the sample fits in the cell. (See Hawley and Northey, 1983 for full details and description of apparatus.

A10.5 LABORATORY RESULTS

Laboratory permeability tests were performed on representative samples of the Red Silty Clay and the Grey Clayey Silts. These samples were extracted from trench 2, but as has been discussed in Chapter Four, very few samples were taken. Therefore only two permeability tests were performed.

Results of the laboratory falling head tests are shown below.

Sample T2-1, $k = 1.337 \times 10^{-10}$

Sample T2-3, $k = 1.350 \times 10^{-10}$

APPENDIX EIGHT

SEISMIC REFRACTION TRAVERSES

A8.1 INTRODUCTION

A total of five seismic refraction traverses were carried out on the Wharanui Earthflow to determine depth to bedrock and the subsurface profile (see Fig. 3 in the map pocket for location of each traverse). A Bison single channel Signal Enhancement Seismograph (Model 1570C), which uses a sledge hammer and steel plate as the energy source, was used to carry out the traverses. Augerholes and backhoe trenches were used to supplement information and provide control for the final interpretation.

Only one of the seismic traverses will be discussed in this section as an example of the methods employed.

A8.2 THEORY

Seismic waves travel at different speeds in materials with different elastic properties. In a two layer case where unconsolidated material overlies bedrock, the seismic waves travel more slowly in the overburden than in the bedrock.

At small horizontal distances from the hammer point, the direct wave travelling through the overburden is recorded as a first arrival. As the distance between the hammer position and the geophone increases (spread length), the first arrivals are transmitted through the bedrock and the overburden because of the higher bedrock velocity (fig. A8.1).

The refraction traverse is repeated in the reverse direction to ensure that in areas where the overburden thicknesses are changing the true velocity of bedrock may be calculated.

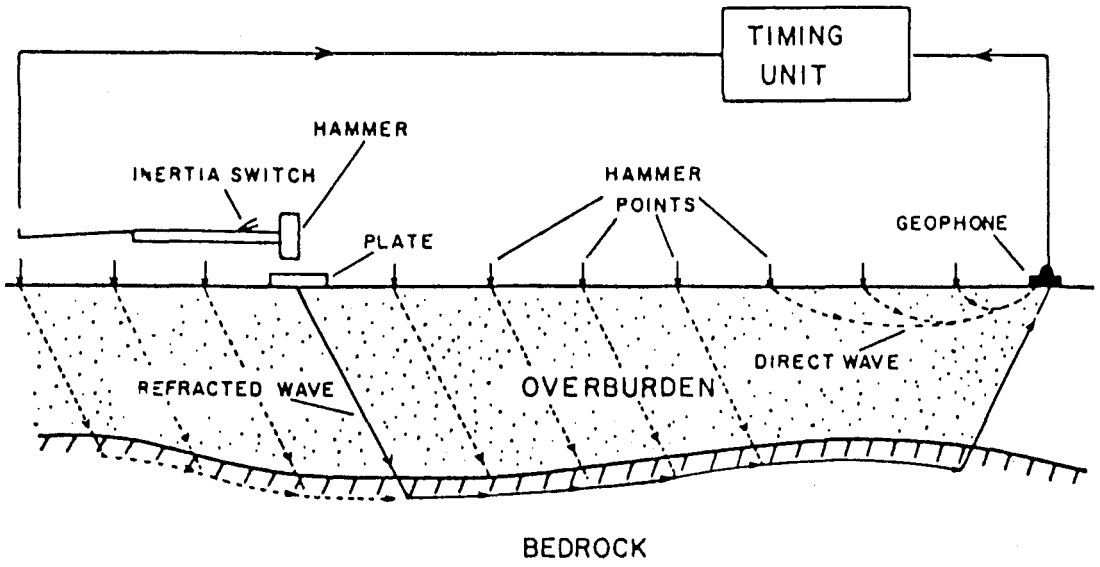

Figure A8.1 Principle of the hammer seismic method. Two layer case. (Bullock, 1978).

A graph is plotted of the seismic wave velocity from which the seismic velocity of the overburden is obtained. The actual seismic velocity of the bedrock must be calculated from the "time-depth" to the refractor. The time depth is defined as, "the time delay associated with the critical ray in travelling between the refractor and the surface" (Hawkins, 1961). (See fig A8.2).

The time-depth is calculated as follows:

$$td = \frac{tf + tr - TR}{2}$$

where td = time depth, tf = time forward, tr = time reverse, and TR = reciprocal time.

A corrected travel-time graph is plotted so the actual seismic wave velocity of both bedrock and overburden is known. The depth conversion factor and the radial depth to bedrock below each hammer point can then be determined (see Table A8.3), and the bedrock profile can be plotted (Fig A8.4).

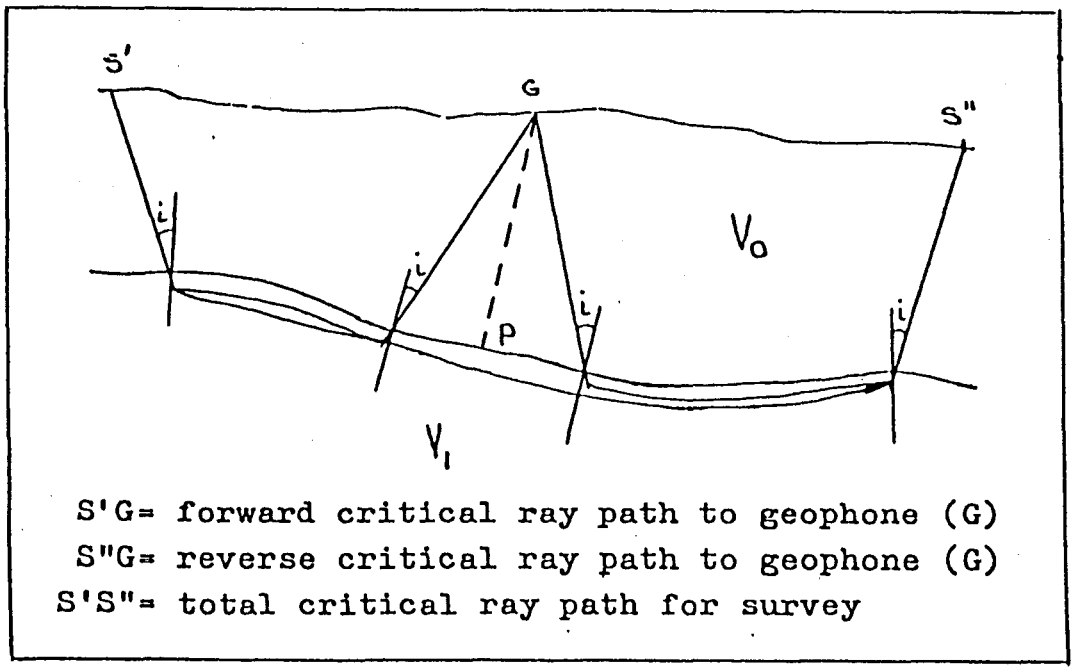

Fig. A8.2 Time-depth definition diagram (from Hawkins, 1961).

A8.3 DISCUSSION OF TRAVERSE X - Z

Section X - Z was completed with two traverses. The first one (0 - 34 m) is used as an illustration of the method of obtaining the bedrock profile. As can be seen by the time-distance graph, there are minor velocity changes on both the forward and reverse corrected plots for the V_1 refractor. However the average velocity is relatively constant so for this example V_1 is taken as 1785 m/s. The average forward and reverse times for V_0 was 333 m/s.

There needs to be some control for both the depth to bedrock, and for interpretation of lithologic changes in the bedrock. This control has been obtained by mapping of adjacent outcrops and by augering along the seismic traverses. Augering indicated that depths to bedrock were within 0.5-0.7 metres of the seismic interpretation.

A8.4 RESULTS

An example of the traverse data and calculation sheet, the time distance graph, and the final profile is shown for a section (0 - 34 m) of traverse X - Z and for traverse C - C'. The remainder of the seismic traverses (B, D, and E) are only shown as bedrock profiles.

Portion of seismic traverse X - Z along axis of flow. T_R= 38.8 ms.

Station	Ground R.l.	Forward Time	Reverse Time	$\frac{tf + tr - T_R}{2}$	tf - td	tr - td	F	td x F
m	m	ms	ms	ms	ms	ms	m/s	m
0	101	0	38.7	-.05	.05	38.75	------	-------
1	100.5	2.8	38.4	2.40	.40	36.00	------	-------
2	100.3	6.0	37.8	2.54	3.46	35.26	------	-------
3	100.0	8.5	38.9	4.30	4.20	34.70	------	-------
5	99.0	14.3	36.2	5.85	8.45	30.35	343.21	2.01
7	98.3	20.6	33.5	7.65	12.95	25.85	"	2.63
10	97.8	23.3	30.5	7.50	15.80	23.00	"	2.57
13	96.8	23.9	30.5	7.75	16.15	22.65	"	2.66
16	96.1	23.9	27.8	6.45	17.45	21.35	"	2.21
19	95.2	24.3	24.0	4.75	19.55	19.25	"	1.63
22	94.	30.7	25.9	8.90	21.80	17.00	"	3.05
25	94.8	32.1	24.5	8.90	23.20	15.60	"	3.04
28	94.2	31.2	18.7	5.55	25.65	13.15	"	1.90
30	92.8	32.8	12.6	3.30	29.50	9.30	------	-------
32	92.6	32.9	7.0	.55	32.35	6.45	------	-------
33	92.4	37.0	3.2	.70	36.30	2.5	------	-------
34	92.4	38.9	0.0	.05	38.85	-.05	------	-------

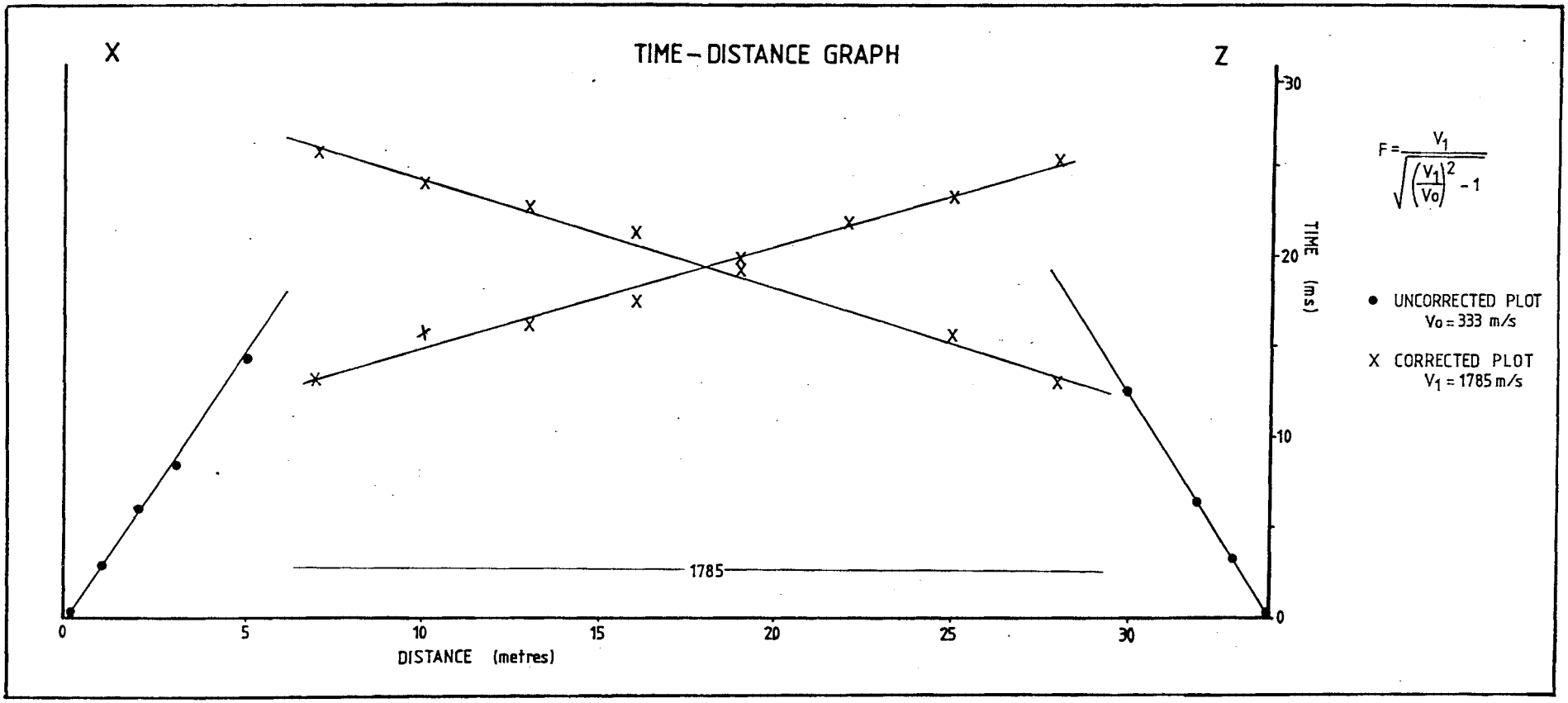
X
TIME – DISTANCE GRAPH
Z
30
20
10
0
TIME (ms)
1785
0
5
10
15
20
25
30
DISTANCE (metres)
$F = \frac{V_1}{\sqrt{\left(\frac{V_1}{V_0}\right)^2 - 1}}$
● UNCORRECTED PLOT
$V_0 = 333$ m/s
X CORRECTED PLOT
$V_1 = 1785$ m/s

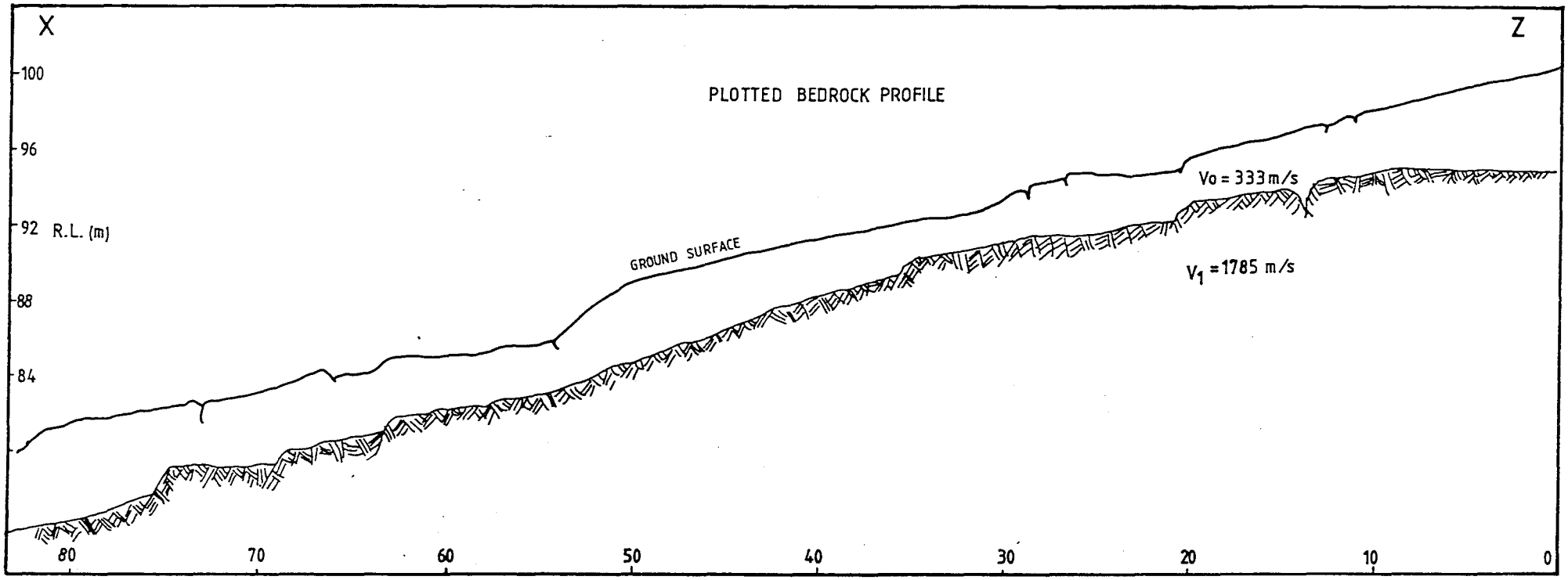
X
Z
PLOTTED BEDROCK PROFILE
100
96
92
88
84
R.L. (m)
GROUND SURFACE
Vo = 333 m/s
V1 = 1785 m/s
80
70
60
50
40
30
20
10
0

Profile C - C' T_R = 45

Station	Ground R.L.	Forward Time	Reverse Time	$\frac{td}{\frac{tf + tr - TR}{2}}$	tf - td	tr - td	F	td x F
m	m	ms	ms	ms	ms	ms	m/s	m
0	168	0	44.9	-.05	0	-	-	-
2	167.5	10.8	43.4	4.6	6.2	38.8	-	-
4	166.8	18.7	42.8	8.25	10.45	34.55	446.47	
6	166.0	20.0	41.8	8.40	11.5	33.40	"	3.75
8	165.2	20.6	41.3	8.45	12.15	32.85	"	3.77
10	165.2	24.2	40.5	9.85	14.35	30.65	"	4.40
12	164.8	24.6	39.7	9.65	14.95	30.05	"	4.31
14	164.4	24.6	38.2	8.90	15.7	29.30	"	3.97
16	164.2	24.8	38.8	9.30	15.5	29.50	"	4.15
18	164.2	29.4	38.1	11.25	18.15	26.85	"	5.02
20	164.3	32.1	39.2	13.15	18.60	25.70	"	5.87
22	164.6	33.4	36.2	12.30	21.10	23.9	"	5.49
24	164.4	33.0	34.1	11.05	21.95	23.05	"	4.93
26	164.4	33.0	33.6	10.80	22.20	22.8	"	4.84
28	164.2	34.5	32.6	11.05	23.45	21.55	"	4.93
30	163.6	35.4	31.3	10.85	23.65	20.45	"	4.84
32	163.6	37.5	31.5	12.00	25.50	19.50	467.06	5.98
34	163.0	39.9	30.7	12.80	27.10	17.90	"	5.98
36	163.0	42.0	29.2	13.10	28.90	16.10	"	6.12
38	163.4	41.6	26.0	11.30	30.30	14.70	"	5.28
40	163.6	41.6	24.9	10.75	30.85	14.15	440.00	4.73
42	163.4	41.8	23.5	10.15	31.65	13.35	"	4.47
44	162.8	42.6	22.9	10.25	32.35	12.65	"	
46	163.6	43.0	20.1	9.05	33.95	11.05	"	
48	164.4	43.6	15.0	6.80	36.80	8.20	"	-
50	166.4	45.1	0.0	.05	45.05	.05	"	-

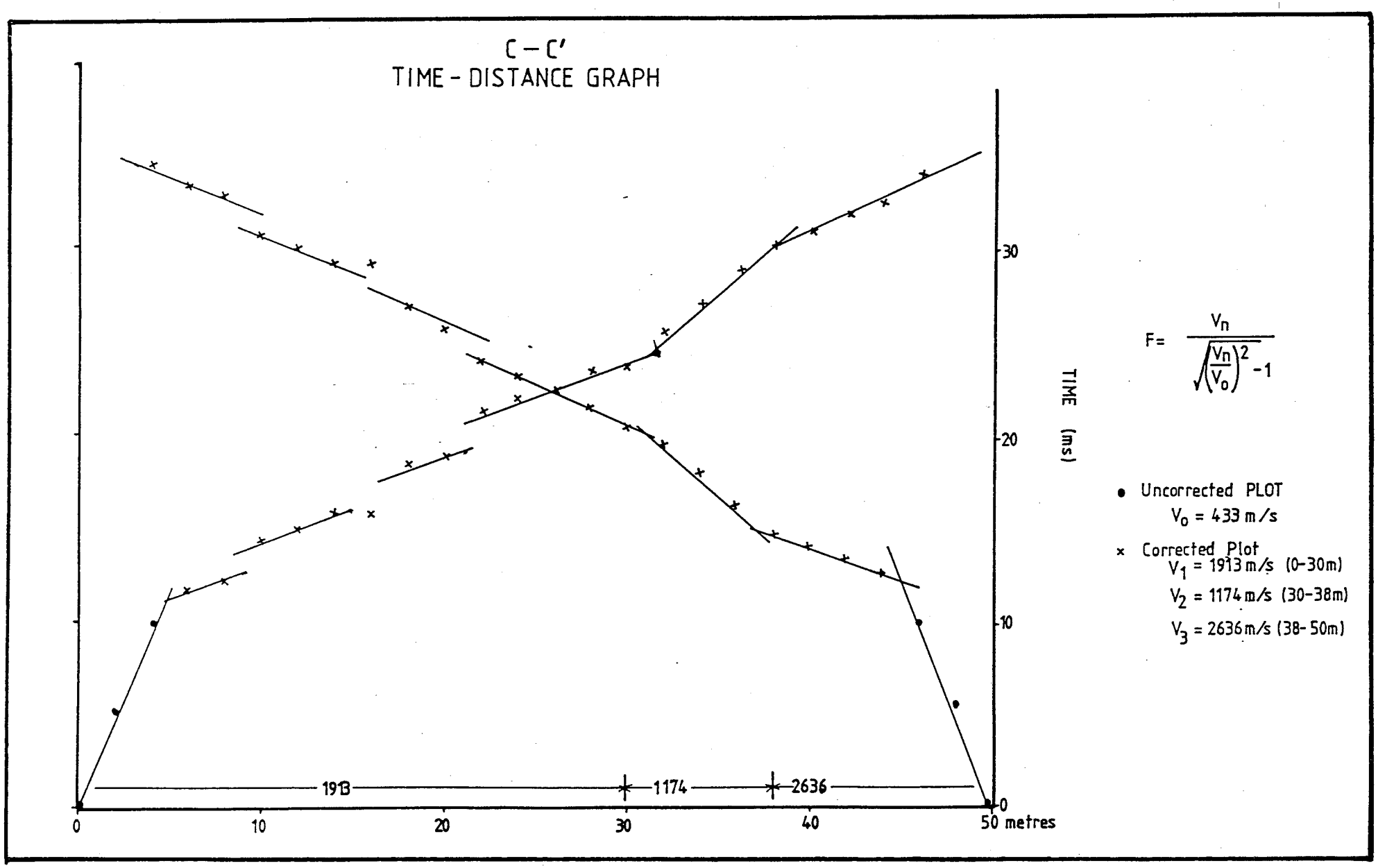
C – C′
TIME - DISTANCE GRAPH
TIME (ms)
0
10
20
30
1913
1174
2636
0
10
20
30
40
50 metres
F= Vn / √((Vn/Vo)² - 1)
• Uncorrected PLOT
Vo = 433 m/s
× Corrected Plot
V1 = 1913 m/s (0-30m)
V2 = 1174 m/s (30-38m)
V3 = 2636 m/s (38-50m)

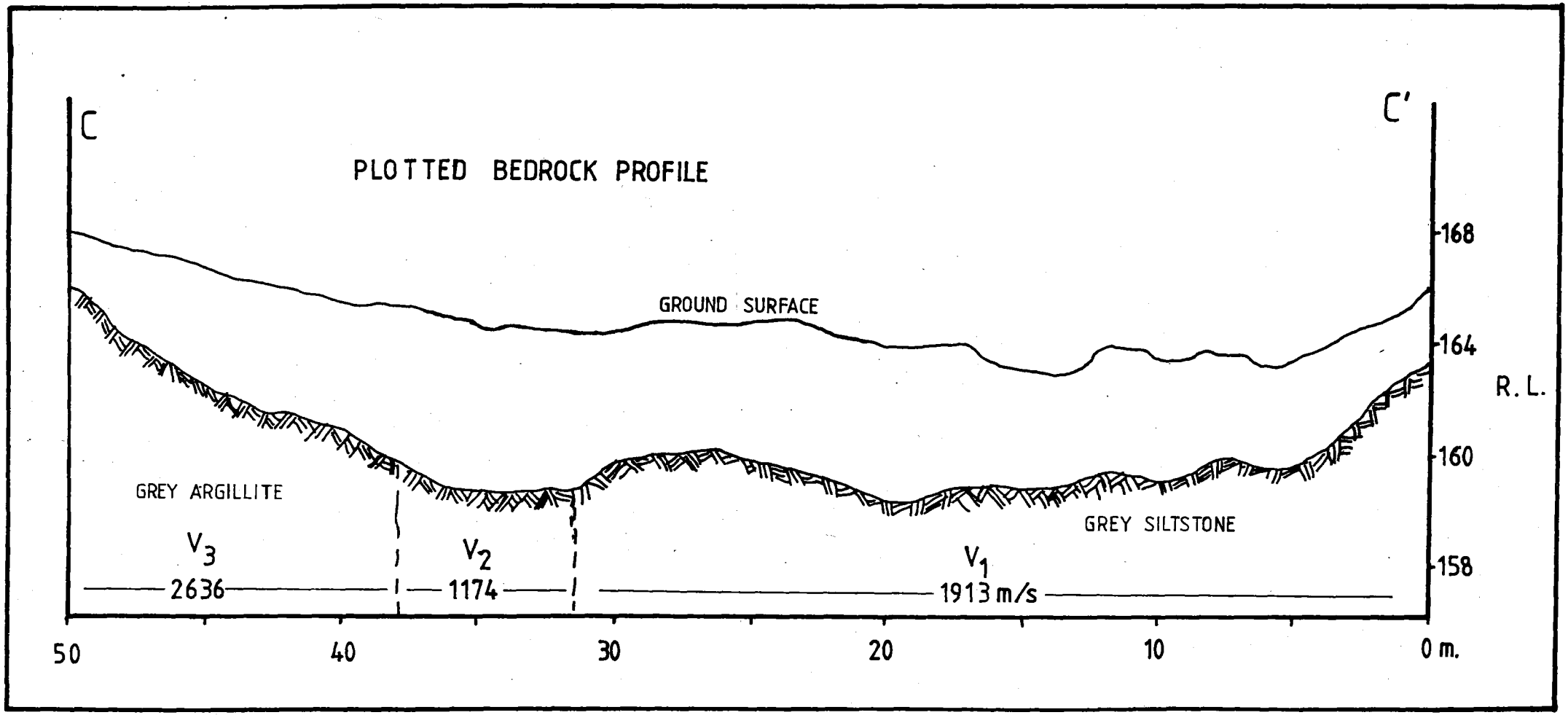
C
C'
PLOTTED BEDROCK PROFILE
GROUND SURFACE
GREY ARGILLITE
GREY SILTSTONE
V_3
2636
V_2
1174
V_1
1913 m/s
168
164
160
158
R. L.
50
40
30
20
10
0 m.

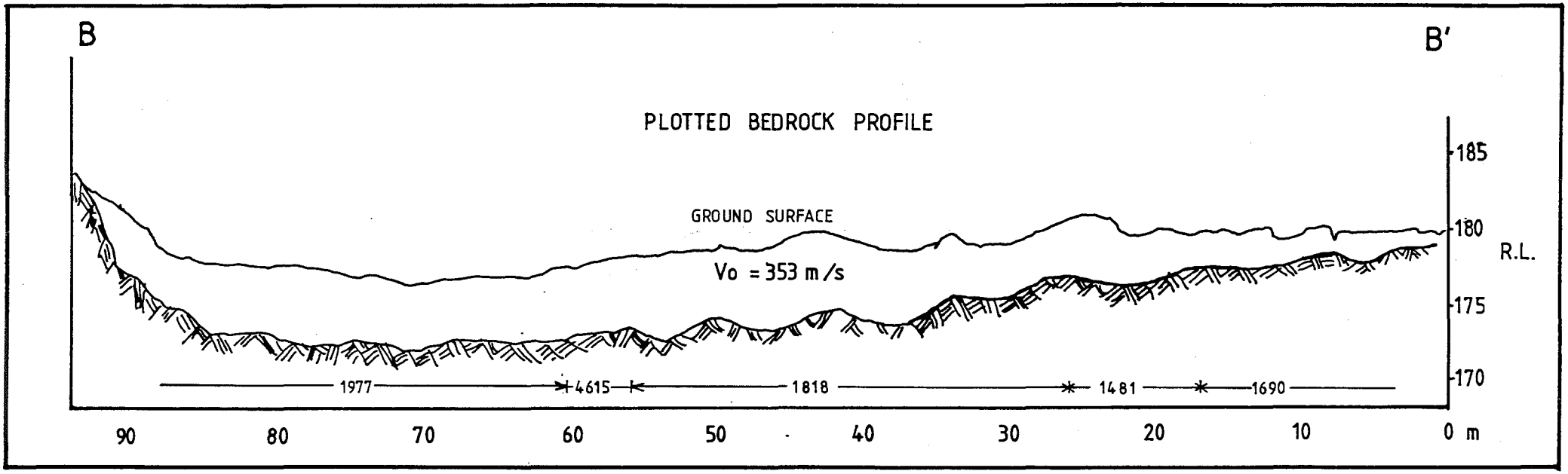
B
B'
PLOTTED BEDROCK PROFILE
GROUND SURFACE
Vo = 353 m/s
1977
4615
1818
1481
1690
185
180
175
170
R.L.
90
80
70
60
50
40
30
20
10
0 m

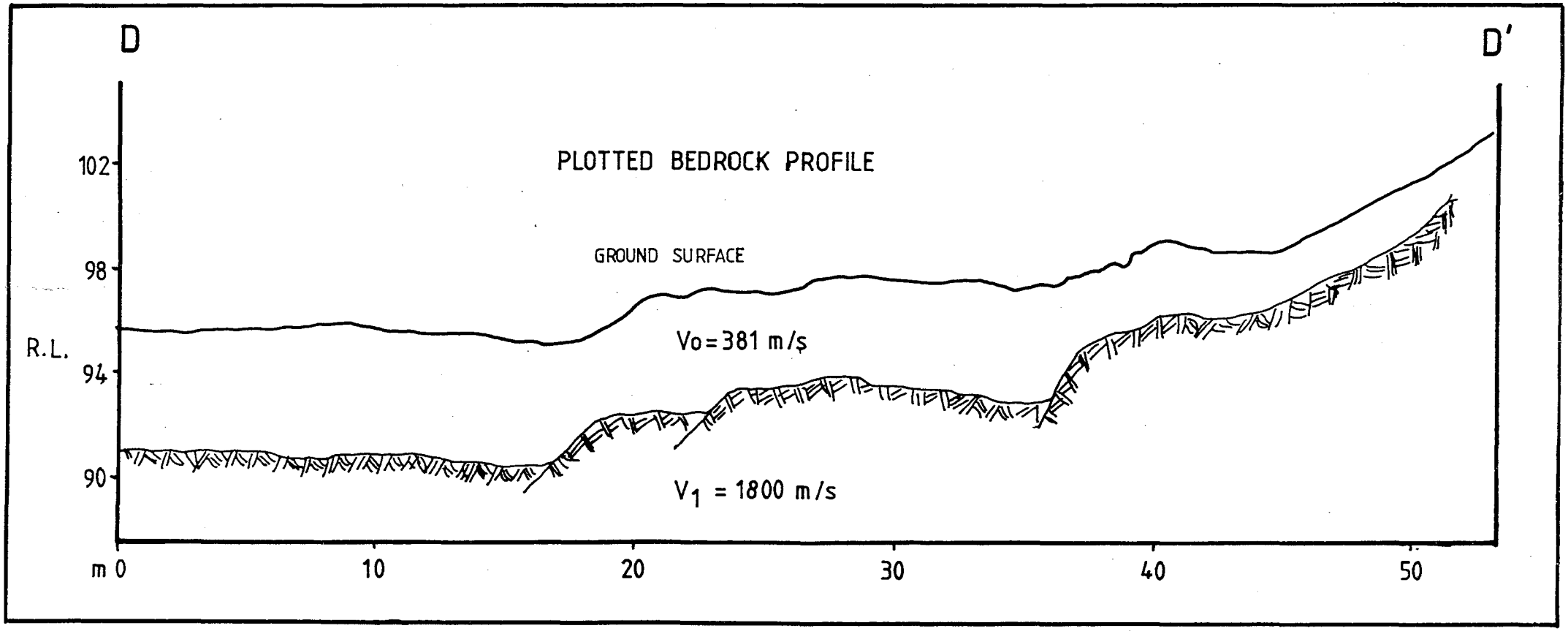
D
D'
PLOTTED BEDROCK PROFILE
GROUND SURFACE
Vo=381 m/s
V1 = 1800 m/s
R.L.
102
98
94
90
m 0
10
20
30
40
50

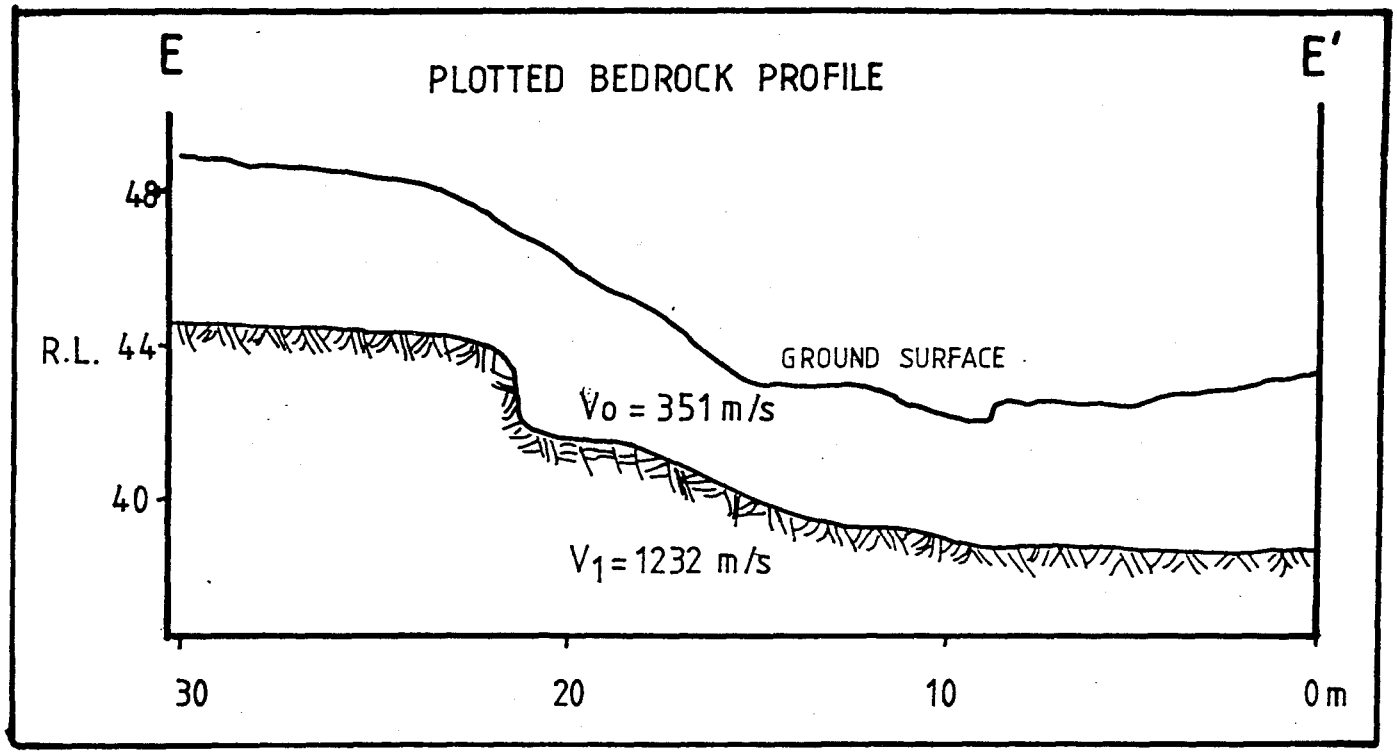
E
PLOTTED BEDROCK PROFILE
E'
48
R.L. 44
40
GROUND SURFACE
Vo = 351 m/s
V1 = 1232 m/s
30
20
10
0 m

APPENDIX NINE

SURVEY SYSTEMS

A9.1 INTRODUCTION

Two survey systems were installed on the Wharanui Earthflow to monitor movement. The first system, refered to here as the "primary network" was installed in August 1984. The primary network was designed to monitor absolute movement on the Earthflow with points placed parallel and perpendicular to the axis of the flow (see Fig. A9.1 or Fig. 1 in the map pocket). This primary network was resurveyed twice in the following year, first in March, 1985 and then in September 1985.

The second system refered to here as the secondary network was installed in November 1984. The secondary network was designed to monitor relative movement across tension cracks and small scarps on the flow, particularly in the toe area (see Fig. A9.4). This network was re-surveyed 3 times in 1985.

A9.2 PRIMARY NETWORK METHODOLOGY

The primary network consists of seven stable points (A - G) installed around the perimeter of the Earthflow, from which the monitoring points were surveyed. Station "A" is designated as the "control" station and the others as "base" stations.

The control station was constructed using a 0.3m x 1.8m concrete culvert, with the lower 1.2m buried in a concrete base. Concrete was also poured inside the pipe, and a stainless steel pin inserted as the survey mark. The remaining six base stations consist of 0.5m long 3/4 inch diameter galvanized pipe driven into "stable" ground. Survey markers, built at the University of Canterbury, Geology Dept., with fittings for the EDM single prism were used to survey the base stations in.

The control point has been coordinated using Flags trig and trig 3671, being adjusted from NZMS 1 to NZMS 260 using the University of Canterbury coordinate conversion

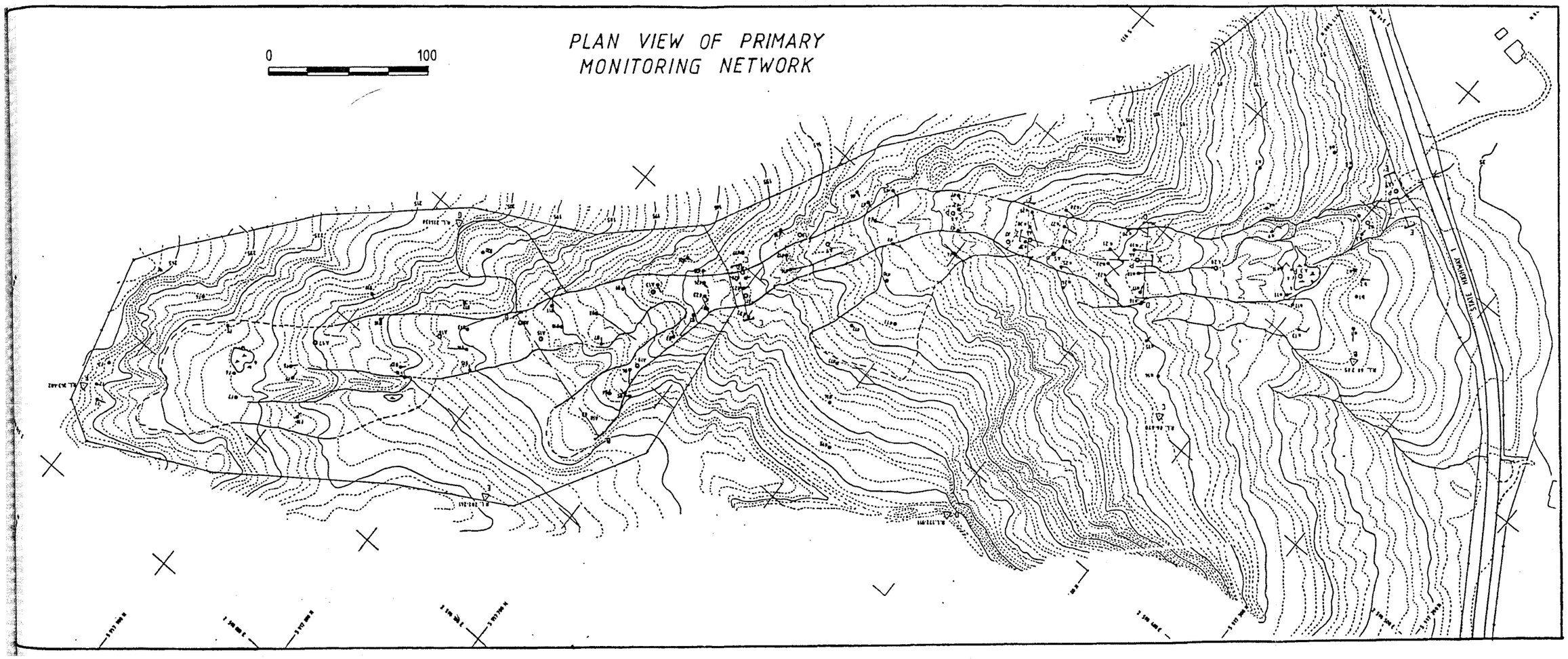

Fig. A9.1 Topographic plan of primary monitoring network, (Reduced from Fig. 5, map pocket) monitoring points show vectors of movement.

programme. Each station has been occupied and distances and angles measured with a Wild DI3 EDM and a T16 theodolite: distances and bearings have been adjusted using the MWD (Christchurch) Surtrig programme to obtain corrected coordinates for the base points. Fig A9.2 shows the triangulation network used for fixing the control and base stations.

Monitoring points were placed along the main flow and in several "feeder" zones. The monitoring points consist of 1/2 and 3/4 inch galvanized pipe cut to approximately 0.4 m in length and driven to leave about 75mm projecting above ground. Monitoring points were surveyed from the base stations or control point, and coordinated using the University of Canterburys' triangular grid coordinate program. Each monitoring point is numbered according to the station from where it was surveyed and the order from which it was surveyed. For example, A-1 refers to the first monitoring point surveyed from station A, D-1 refers to the first monitoring point surveyed from station D and so forth.

In the final survey, all points were surveyed from station A, B, D, F, or G to make the number of station set-ups as few as possible. This enabled all monitoring points to be surveyed in one day. Fig A9.3 shows the distances and angles of the monitoring points from their respective stations of observation. This figure highlights the distribution of points from the various stations.

A9.3 ACCURACY

The stated accuracy of the EDM is $\pm$ 5 mm, however meteorological conditions can limit the accuracy of EDM measurements at the time of measurment [Moffitt & Bouchard 1982].

The actual accuracies obtained with the DI3 were less than those stated as windy conditions prevailed during survey days which had a detrimental effect. For instance two consecutive readings of the same point could vary as much as 20 mm. In addition the T16 theodolite is accurate

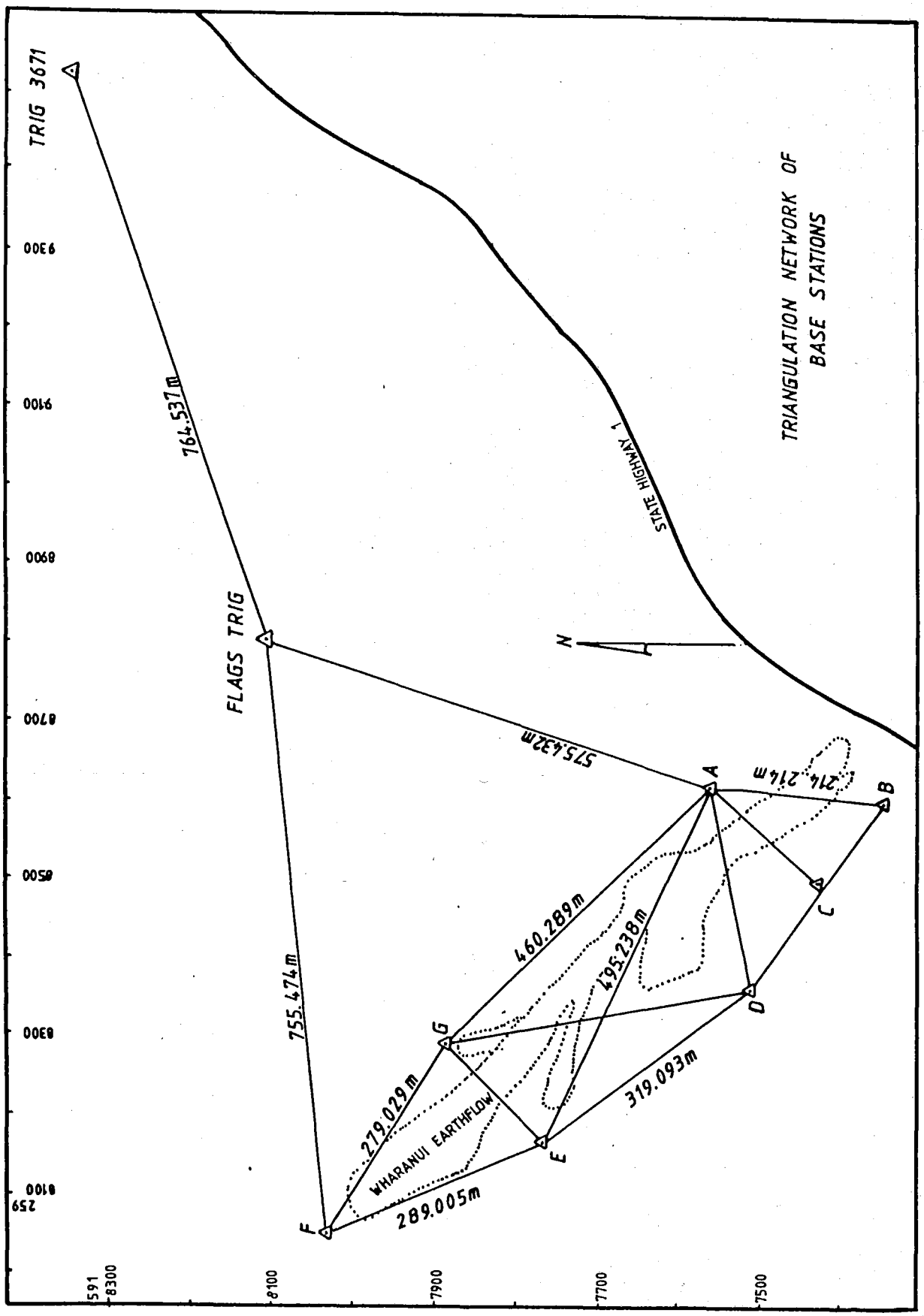

Fig. A9.2 Survey network plan showing Flags Trig and Trig 3671 from which contros station A was fixed and base stations B - G were coordinated.

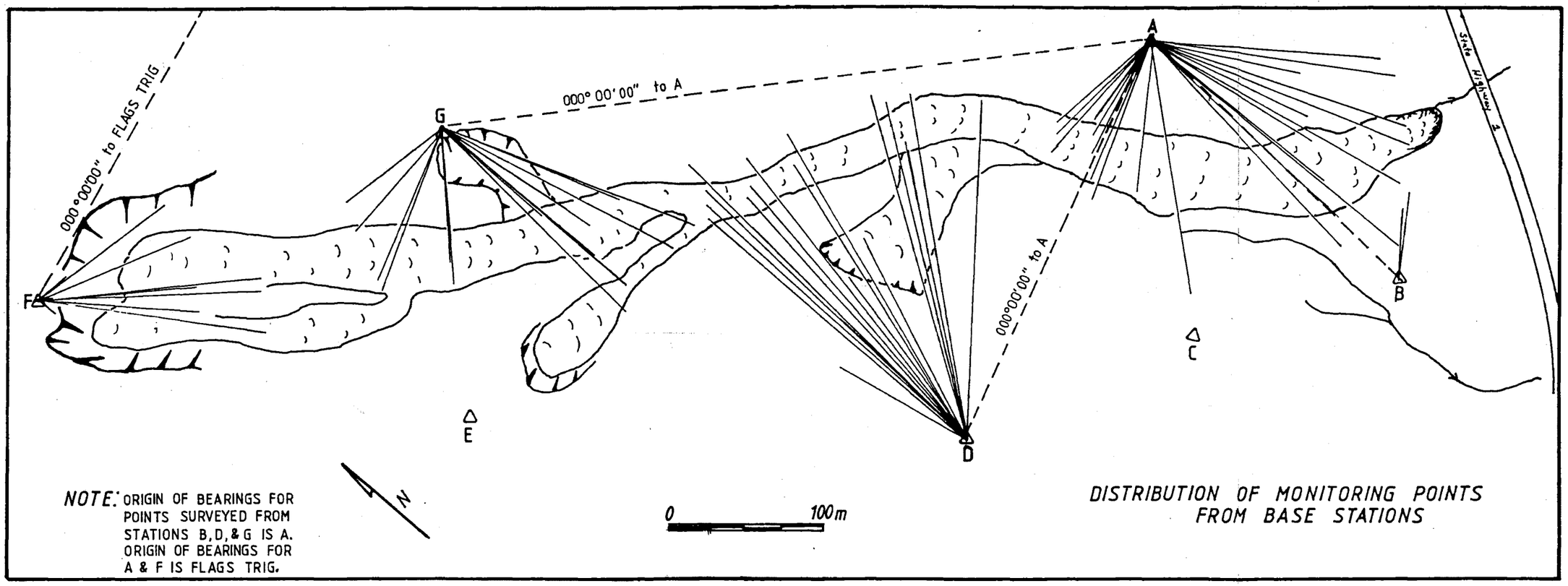

Fig. A9.3 Survey methodology of monitoring points. Each monitoring point was surveyed from A, B, D, F, or G. The sketch shows the ray of each point which was surveyed.

to 10 seconds yeilding an error of + 5 mm/100 m. Since most of the lines of survey were greater than 100m there was the possibility of considerable error, therefore only those monitoring points showing more than 30mm of change were considered a reliable indication of movement.

A9.4 RESULTS

The following pages show the initial and final coordinates for each point, the total movement, and the direction of movement (from north) .

A9.5 FUTURE MONITORING

Survey data sheets are provided for future use. These will aid in simplifying the locating of the monitoring points. The use of two-way radios is highly recommended for use on re-surveying as distances are relatively long and hearing directions to a point can be very difficult.

COORDINATES FOR CONTROL BASE POINTS (FIXED STATIONS)
GRID REFERENCES FROM NZMS 260 SHEET P30

Station	Northings	Eastings	R.L.
Flags Trig 591	8108.513	259 8803.816	
Trig 3671	8360.311	9525.699	
A	7560.569	8628.091	117.506
B	7346.670	8616.473	60.285
C	7425.839	8508.434	86.608
D	7501.699	8367.929	172.511
E	7753.559	8172.004	202.443
F	8017.315	8053.867	243.402

*NOTES: 1) All monitoring points were surveyed from one of these fixed stations, hence the points are numbered by the station from which they were surveyed and the order of their survey.
2) The direction of movement is listed only for those points which have moved more than 30 mm.

COORDINATES AND MOVEMENT FOR INITIAL AND FINAL SURVEY OF PRIMARY NETWORK

Movement Summary of Wharanui Earthflow from September 1984-September 1985

Monitor point	Northings	Eastings	Direction	Horizontal Change mm.
A-1	7360.729	8634.333		
	7360.685	8634.264	230	82
A-2	7382.223	8665.024		
	7382.222	8665.025	092	01
A-3	7394.662	8685.551		
	7394.662	8685.580		29
A-4	7402.893	8691.652		
	7402.897	8691.667		16
A-5	7429.605	8713.231		
	7429.611	8713.224		09
A-6	7444.353	8714.573		
	7444.358	8714.558		16
A-7	7477.209	8675.164		
	7477.211	8675.154		10
A-8	7456.570	8656.938		
	7456.565	8656.924		15
A-9	7443.163	8646.972		
	7443.147	8646.998	120	31
A-10	7422.882	8634.276		
	7422.853	8634.306	126	42
A-11	7409.046	8622.593		
	7409.026	8622.606		24

Monitor point	Northings	Eastings	Direction	Horizontal Change
A-12	7401.611	8619.941		
	7401.637	8620.001	072	65
A-13	7387.724	8610.159		
	7387.674	8610.209	138	71
A-14	7443.685	8527.739		
	lost peg			
A-15	7463.792	8540.662		
	7463.773	8540.692	094	36
A-16	7480.780	8556.586		
	7480.780	8556.611	120	25
A-17	7486.363	8561.495		
	7486.374	8561.611	070	117
A-18	7494.826	8570.373		
	7494.754	8570.446	138	102
A-19	7506.431	8580.310		
	7506.339	8580.368	144	108
A-20	7517.327	8587.796		
	7517.237	8587.851	150	105
A-21	7519.240	8569.755		
	7519.143	8569.752	182	97
A-22	7513.988	8562.319		
	7513.903	8562.309	188	86
A-23	7509.690	8552.788		
	7509.643	8552.786	188	47
A-24	7528.578	8530.520		
	7528.552	8530.531		28
A-25	7537.117	8540.071		
	7537.035	8540.089	168	84
A-26	7544.514	8550.317		
	7544.398	8550.347	172	120
A-27	7552.350	8560.935		
	7552.263	8560.953	173	89
A-28	7557.969	8570.147		
	7557.907	8570.146	175	62
A-29	7574.858	8554.259		
	7574.771	8554.195	212	108
A-30	7570.305	8545.880		
	7570.196	8545.834	202	118
A-31	7566.724	8536.516		
	7566.673	8536.562	161	69

End of points surveyed from Station A.

Monitor point	Northings	Eastings	Direction	Horizontal Change
B-1	7372.108	8651.431		
	7372.097	8651.417		18
B-2	7376.077	8662.328		
	7376.038	8662.347	142	43
End of points surveyed from Station B.				
D-1	7622.350	8530.337		
	7622.320	8530.314	191	38
D-2	7616.680	8523.032		
	7616.636	8523.007	191	15
D-3	7608.202	8512.369		
	7608.188	8512.365	161	15
D-4	7599.781	8500.827		
	7599.774	8500.832		09
D-5	7659.939	8503.556		
	7659.858	8503.486	198	107
D-6	7678.051	8487.403		
	7678.024	8487.403	196	27
D-7	7667.945	8486.983		
	7667.917	8486.967	190	32
D-8	7656.928	8481.459		
	7656.879	8481.469	157	50
D-9	7637.954	8477.950		
	7637.931	8477.939		25
D-10	7626.835	8456.575		
	7626.830	8456.582		09
D-11	7605.058	8438.787		
	7605.056	8438.802		15
D-12	7628.041	8418.462		
	7628.040	8418.476		14
D-13	7620.462	8393.352		
	7620.448	8393.359		16
D-14	7608.308	8371.160		
	7608.315	8371.171		13
D-15	7589.781	8348.432		
	7589.777	8348.425		08
D-16	7683.156	8419.227		
	7682.949	8419.558	120	390
D-17	7690.715	8423.888		
	7690.707	8423.864	216	25

Monitor point	Northings	Eastings	Direction	Horizontal Change
D-18	7703.728	8433.275		
	7703.733	8433.249		26
D-19	7715.907	8405.891		
	7715.901	8405.879		13
D-20	7703.674	8395.477		
	7703.654	8395.474		20
D-21	7700.102	8389.569		
	7700.082	8389.598	133	35
D-22	7686.320	8377.642		
	7686.324	8377.685	074	43
D-23	7717.181	8368.045		
	7717.162	8367.729	263	316
D-24	7724.097	8374.012		
	7724.068	8374.011		29
D-25	7728.994	8378.858		
	7728.980	8378.845		19
D-26	7742.890	8379.256		
	7742.887	8379.230		26
End of points surveyed at Station D.				
G-1	7711.724	8362.449		
	7711.811	8362.493	201	97
G-2	7717.001	8353.835		
	lost peg			
G-3	7717.959	8334.698		
	7717.977	8334.730	218	37
G-4	7728.346	8298.745		
	7728.293	8298.658	232	101
G-5	7718.549	8285.452		
	7718.611	8285.451	170	62
G-6	7728.992	8278.279		
	7729.021	8278.291	061	31
G-7	7753.557	8299.538		
	7753.587	8299.562	224	38
G-8	7768.416	8312.052		
	7768.085	8312.083	172	332
G-9	7764.961	8336.107		
	7764.946	8336.111		15
G-10	7782.472	8291.021		
	7782.467	8291.043		22

Monitor point	Northings	Eastings	Direction	Horizontal Change
G-11	7796.220	8296.174		
	7796.226	8296.194		21
G-12	7844.418	8259.997		
	7844.439	8259.977		29
G-13	7832.476	8247.884		
	7832.484	8247.883		08
G-14	7823.238	8238.562		
	7823.340	8238.493	320	123
G-15	7814.178	8228.987		
	7814.199	8229.003		26
G-16	7846.287	8196.637		
	7846.305	8196.653	132	24
G-17	7852.220	8200.525		
	7852.236	8200.538	134	21
G-18	7881.912	8214.478		
	7881.907	8214.481		06
G-19	7898.210	8222.720		
	7898.177	8222.714	194	34
G-20	7854.886	8293.734		
	7854.905	8293.751		25
End of points surveyed from Station G.				
F-1	8004.167	8053.115		
	8004,115	8053.125	158	53
F-2	8009.949	8059.903		
	8009.940	8059.911		12
F-3	8013.373	8075.635		
	8013.358	8075.639		16
F-4	7988.033	8150.278		
	7988.040	8150.290		14
F-5	7963.248	8145.444		
	7963.232	8145.438		17
F-6	7940.857	8125.291		
	7940.848	8125.299		12
F-7	7929.459	8113.937		
	7929.460	8113.954		17
F-8	7911.912	8153.158		
	7911.887	8153.187	126	38
F-9	7907.242	8147.604		
	7907.253	8147.648	082	45
F-10	7888.293	8130.836		
	7888.309	8130.863	096	31

WHARANUI EARTHFLOW PRIMARY MONITORING NETWORK
SURVEY POINTS' BEARING, DISTANCE, & VERTICAL ANGLE
(TO BE USED FOR LOCATION OF POINTS)

Survey points from station "A". Origin of bearings Flags trig.

Height of Instrument_____ Staff Height_____

R.L. of A 117.505m

SURVEY POINT	BEARING	VERTICAL ANGLE	SLOPE DIST.	HORIZ DIST.	FINAL R.L.
A-1	160 27 00	253 58 00	208.042	199.949	
	160 27 00	253 57 00	208.090	199.979	59.389
A-2	150 29 55	252 42 40	190.731	182.113	
	150 31 05	252 41 00	190.778	182.131	60.134
A-3	143 07 40	250 25 50	186.338	175.574	
	143 06 25	250 24 00	186.385	175.585	54.397
A-4	140 16 00	249 24 50	181.598	170.002	
	140 15 30	248 36 05	181.640	170.007	52.926
A-5	129 11 30	248 35 00	167.792	156.206	
	129 11 30	249 23 50	167.762	156.197	55.711
A-6	125 33 30	248 33 00	155.632	144.852	
	125 34 05	248 31 00	155.665	144.850	59.912
A-7	132 46 00	247 00 00	103.989	95.722	
	132 46 10	246 57 50	104.021	95.726	76.216
A-8	146 42 30	246 30 00	117.679	107.919	
	146 43 25	246 27 55	117.719	107.927	69.915
A-9	153 03 30	247 14 00	128.975	118.926	
	153 04 20	247 11 55	129.016	118.934	66.922
A-10	159 37 50	249 41 20	146.967	137.829	
	159 38 05	249 39 50	147.020	137.856	65.827
A-11	164 17 30	250 50 00	160.521	151.623	
	164 17 30	250 48 35	160.564	151.642	64.143
A-12	165 09 15	252 32 20	166.843	159.155	
	165 08 00	252 30 00	166.861	159.138	66.335

SURVEY POINT	BEARING	VERTICAL ANGLE	SLOPE DIST.	HORIZ DIST.	FINAL R.L.
A-13	168 08 00	253 49 00	180.991	173.819	
	168 07 25	253 46 25	181.029	173.817	66.415
A-14	202 51 50	258 12 00	157.361	154.036	84.741
	point not located				
A-15	204 18 10	256 23 00	134.164	130.393	
	204 18 00	256 20 30	134.206	130.411	85.231
A-16	204 04 30	252 41 20	112.218	107.135	
	204 04 30	252 39 00	112.231	107.124	83.453
A-17	204 07 10	250 28 50	105.749	99.671	
	204 07 00	250 25 00	105.798	99.678	81.460
A-18	203 27 00	247 44 10	94.522	87.475	
	203 26 00	247 41 00	94.595	87.491	81.000
A-19	203 37 10	244 54 40	79.721	72.199	
	203 34 00	244 51 00	79.803	72.238	83.005
A-20	205 09 00	241 49 00	67.051	59.101	
	205 06 00	241 44 30	67.136	59.135	85.135
A-21	216 52 00	247 04 00	77.661	71.522	
	216 50 30	247 00 30	77.726	71.551	86.561
A-22	216 53 10	248 27 30	86.682	80.627	
	216 52 00	248 24 00	86.744	80.653	84.988
A-23	218 10 00	250 44 00	96.273	90.881	
	218 09 00	250 41 00	96.332	90.908	85.055
A-24	234 03 50	257 39 00	105.097	102.665	
	234 03 00	257 36 00	105.132	102.679	94.872
A-25	237 16 50	254 56 20	94.303	91.064	
	237 14 50	254 53 30	94.355	91.094	92.328
A-26	240 31 00	253 38 00	82.751	79.398	
	240 28 10	253 34 30	82.787	79.408	93.512

SURVEY POINT	BEARING	VERTICAL ANGLE	SLOPE DIST.	HORIZ DIST.	FINAL R.L.
A-27	245 13 00	252 02 00	71.096	67.629	
	245 10 00	251 58 30	71.142	67.650	94.907
A-28	249 38 00	251 51 00	61.018	57.982	
	249 35 20	251 46 30	61.070	58.006	97.821
A-29	263 08 50	258 19 00	76.810	75.219	
	263 05 55	258 15 00	76.859	75.248	101.269
A-30	258 56 50	258 59 10	84.342	82.788	
	258 53 40	258 56 00	84.388	82.818	100.722
A-31	256 02 00	259 34 40	93.315	91.775	
	255 59 50	259 31 00	93.348	91.788	99.936

END OF POINTS SURVEYED FROM STATION "A".

MONITORING POINTS SURVEYED FROM STATION "D". ORIGIN OF BEARINGS STATION A

Height of Instrument_____ Staff Height_____

R.L. of D 172.51m

SURVEY POINT	BEARING	VERTICAL ANGLE	SLOPE DIST.	HORIZ DIST.	FINAL R.L.
D-1	336 08 30	253 14 50	211.245	202.279	
	336 08 40	253 15 30	211.237	202.283	111.662
D-2	336 12 20	252 15 10	202.676	193.031	
	336 12 40	252 16 10	202.673	193.028	110.789
D-3	336 21 00	251 17 00	189.438	179.420	
	336 21 00	251 18 10	189.446	179.448	111.781
D-4	336 19 30	250 29 10	175.219	165.154	
	336 19 30	250 30 30	175.215	165.173	114.047
D-5	323 21 20	256 23 00	214.395	208.369	
	323 21 00	256 24 00	214.394	208.383	122.098
D-6	316 52 10	258 52 00	217.058	212.973	
	316 52 15	258 53 00	217.063	212.990	130.659

SURVEY POINT	BEARING	VERTICAL ANGLE	SLOPE DIST.	HORIZ DIST.	FINAL R.L.
D-7	318 21 40	257 23 10	209.494	204.438	
	318 21 50	257 24 00	209.497	204.452	126.810
D-8	318 57 00	255 36 30	198.505	192.275	
	318 56 30	255 37 00	198.503	192.281	123.201
D-9	321 41 00	253 42 00	182.436	175.103	
	321 40 20	253 42 50	182.424	175.104	121.353
D-10	318 03 00	253 10 00	160.205	153.340	
	318 04 00	253 11 10	160.202	153.353	126.170
D-11	317 11 00	251 53 50	131.832	125.306	
	317 11 00	251 55 00	131.834	125.322	131.589
D-12	304 33 00	254 59 00	140.873	136.062	
	304 33 20	254 59 50	140.879	136.077	136.042
D-13	294 49 30	256 48 15	124.727	121.434	
	294 50 15	256 49 50	124.721	121.441	144.095
D-14	284 29 00	259 53 30	108.335	106.653	
	284 29 30	259 55 00	108.339	106.665	153.543
D-15	270 15 00	264 01 10	90.695	90.201	
	270 15 50	264 03 00	90.704	90.212	163.108
D-16	298 34 00	260 28 00	191.163	188.523	
	298 39 00	260 28 20	191.096	188.460	140.850
D-17	299 14 10	260 55 00	199.592	197.089	
	299 14 10	260 56 00	199.605	197.111	141.056
D-18	300 40 30	262 55 00	213.950	212.317	
	300 40 00	262 55 25	213.961	212.331	146.153
D-19	292 47 00	264 06 50	218.674	217.521	
	292 47 50	264 07 30	218.687	217.538	150.126
D-20	290 30 00	263 01 00	205.348	203.825	
	290 31 00	263 02 00	205.341	203.825	147.604

SURVEY POINT	BEARING	VERTICAL ANGLE	SLOPE DIST.	HORIZ DIST.	FINAL R.L.
D-21	288 58 00	263 15 00	200.937	199.544	148.902
	288 59 00	263 15 50	200.956	199.563	148.939
D-22	285 45 40	263 14 30	186.170	184.876	150.611
	285 46 30	263 15 00	186.173	184.883	150.629
D-23	282 46 40	264 41 00	216.389	215.389	152.469
	282 41 50	264 41 30	216.391	215.463	152.491
D-24	284 19 00	264 47 00	223.362	222.437	152.212
	284 19 00	264 47 30	223.374	222.452	152.233
D-25	285 29 40	265 16 40	228.303	227.528	153.725
	285 30 00	265 17 00	228.316	227.543	153.737
D-26	285 26 30	266 37 40	241.845	241.845	158.294
	285 26 00	266 38 25	241.869	241.453	158.336

END OF POINTS SURVEYED FROM STATION "D"

MONITORING POINTS SURVEYED FROM STATION "G".
ORIGINS OF BEARINGS STATION A.

Height of Instrument_____ Staff Height_____
R.L. of G 211.138

SURVEY POINT	BEARING	VERTICAL ANGLE	SLOPE DIST.	HORIZ DIST.	FINAL R.L.
G-1	024 44 00	252 33 15	189.443	180.728	154.347
G-2	026 47 00	252 33 00	181.199	172.860	156.806
G-3	032 54 10	253 22 05	173.848	166.575	
	032 53 20	253 22 00	173.865	166.589	161.375
G-4	045 21 20	254 53 55	157.360	151.926	
	045 21 00	254 53 30	157.368	151.928	170.126
G-5	050 04 00	257 26 00	165.980	162.004	175.029
G-6	053 02 00	256 28 00	156.683	152.332	
	053 01 50	256 27 10	156.689	152.329	174.439

SURVEY POINT	BEARING	VERTICAL ANGLE	SLOPE DIST.	HORIZ DIST.	FINAL R.L.
G-7	044 50 00	253 25 00	132.162	126.665	
	044 48 30	253 24 00	132.160	126.652	173.386
G-8	038 18 00	250 35 00	119.975	113.151	171.259
G-9	027 13 30	249 48 00	129.731	121.752	
	027 13 30	249 44 10	129.789	121.756	166.191
G-10	049 29 00	250 34 20	103.818	097.907	
	049 26 25	250 33 30	103.840	97.919	176.580
G-11	046 30 00	247 09 30	91.144	83.996	
	046 29 30	247 08 50	91.143	83.988	175.746
G-12	091 52 30	247 56 40	55.414	51.359	
	091 54 00	247 56 00	55.448	51.386	190.312
G-13	091 46 00	250 52 10	72.395	68.397	
	091 46 30	250 52 00	72.406	68.406	187.411
G-14	091 40 00	253 37 20	84.963	81.515	
	091 41 00	253 37 00	84.962	81.512	187.178
G-15	091 48 55	256 04 00	97.589	94.717	
	091 49 10	256 03 00	97.567	94.689	187.622
G-16	117 18 20	262 21 00	106.767	105.817	
	117 19 40	262 19 40	106.766	105.810	196.889
G-17	119 48 30	261 33 30	101.344	100.331	
	119 49 40	261 52 00	101.349	100.329	196.804
G-18	137 10 50	260 01 00	83.694	82.427	
	137 11 50	259 59 15	83.699	82.424	196.591
G-19	149 37 50	265 34 30	76.541	76.313	
	149 38 00	265 33 00	76.550	76.319	205.204
G-20	053 07 00	238 12 00	30.004	25.500	
	053 05 00	238 11 30	30.007	25.500	195.327

END OF MONITORING POINTS SURVEYED FROM STATION "G".

MONITORING POINTS SURVEYED FROM STATION "F"

Height of Instrument_____ Staff Height_____

R.L. of F 243.402

Origin of Bearings is Flags Trig.

SURVEY POINT	BEARING	VERTICAL ANGLE	SLOPE DIST.	HORIZ DIST.	FILAL R.L.
F-1	100 12 30	246 55 10	14.316	13.170	
	100 09 05	247 02 00	14.359	13.221	237.764
F-2	057 36 10	254 18 15	9.891	9.523	
	057 36 00	254 30 05	9.895	9.535	240.691
F-3	017 11 50	260 20 00	22.441	22.122	
	017 14 00	260 15 40	22.453	22.129	239.568
F-4	023 49 40	263 53 00	101.337	100.760	
	023 49 20	263 54 00	101.343	100.769	232.598
F-5	037 29 40	259 17 50	108.229	106.346	
	037 30 00	259 19 00	108.225	106.349	223.304
F-6	053 53 00	255 39 30	107.995	104.629	
	053 53 00	255 41 00	107.995	104.641	216.928
F-7	062 34 20	256 02 00	109.671	106.429	
	062 33 50	256 03 00	109.672	106.437	216.928
F-8	053 38 40	257 04 00	148.574	144.805	
	053 38 30	257 25 40	148.151	144.843	210.149
F-9	056 31 00	257 25 00	148.136	144.578	
	056 30 00	257 25 40	148.151	144.598	211.119
F-10	066 06 55	257 09 00	154.095	150.236	
	066 06 10	257 09 55	154.086	150.236	209.138

END OF MONITORING POINTS SURVEYED FROM STATION "F"

MONITORING POINTS SURVEYED FROM STATION "B" AND "C"
ORIGIN OF BEARINGS STATION "A"

Height of Instrument_____ Staff Height_____

R.L. of B 60.285m

SURVEY POINT	BEARING	VERTICAL ANGLE	SLOPE DIST.	HORIZ DIST.	FILAL R.L.
B-1	050 50 00	265 01 10	43.371	43.207	56.542
	050 51 00	265 05 00	43.376	43.216	56.527
B-2	054 13 10	266 38 00	54.568	54.474	57.103
	054 15 50	266 41 00	54.561	54.469	57.088

END OF ALL POINTS SURVEYED

A9.6 SECONDARY NETWORK METHODOLOGY

The secondary monitoring network consists of monitoring points (pipes), driven in place on each side of a tension crack or across small scarps. The purpose is to measure the relative movement across the cracks in the horizontal and vertical directions. Monitoring points were placed perpendicular to cracks, and installed in lines across multiple tension cracks so that there is a successive set of points. This enables strain to be measured. (See Fig. A9.4 map of network lines).

A system was devised at the University of Canterbury to measure the relative displacement to within 1mm. The device is shown in photo A9.1. Monitoring points are measured periodically and movement recorded. This gives an indication of the type of movement occurring, either tensional or compressional, and the rates at which movement is occurring across the cracks.

A9.7 EXPOSITION OF SECONDARY MONITORING METHODS

A9.7.1 Introduction

The device used for the measurement of tension cracks has been designed at the University Canterbury Geology Dept. and is new to the Geology Dept., therefore it is appropriate that a description of the device, its use, and an evaluation of the problems associated with its use are discussed. At the end of the section the author makes a few personal recomendations for improvements to the device for easier use and for practicality. (As there is no instruction manual for this device, this section is an attempt to provide some guidance for a new user. It is written with the assumption that the reader has seen the device, and may be partially familiar with it.)

Photo A9.2 Crack width monitor designed and built at the University of Canterbury

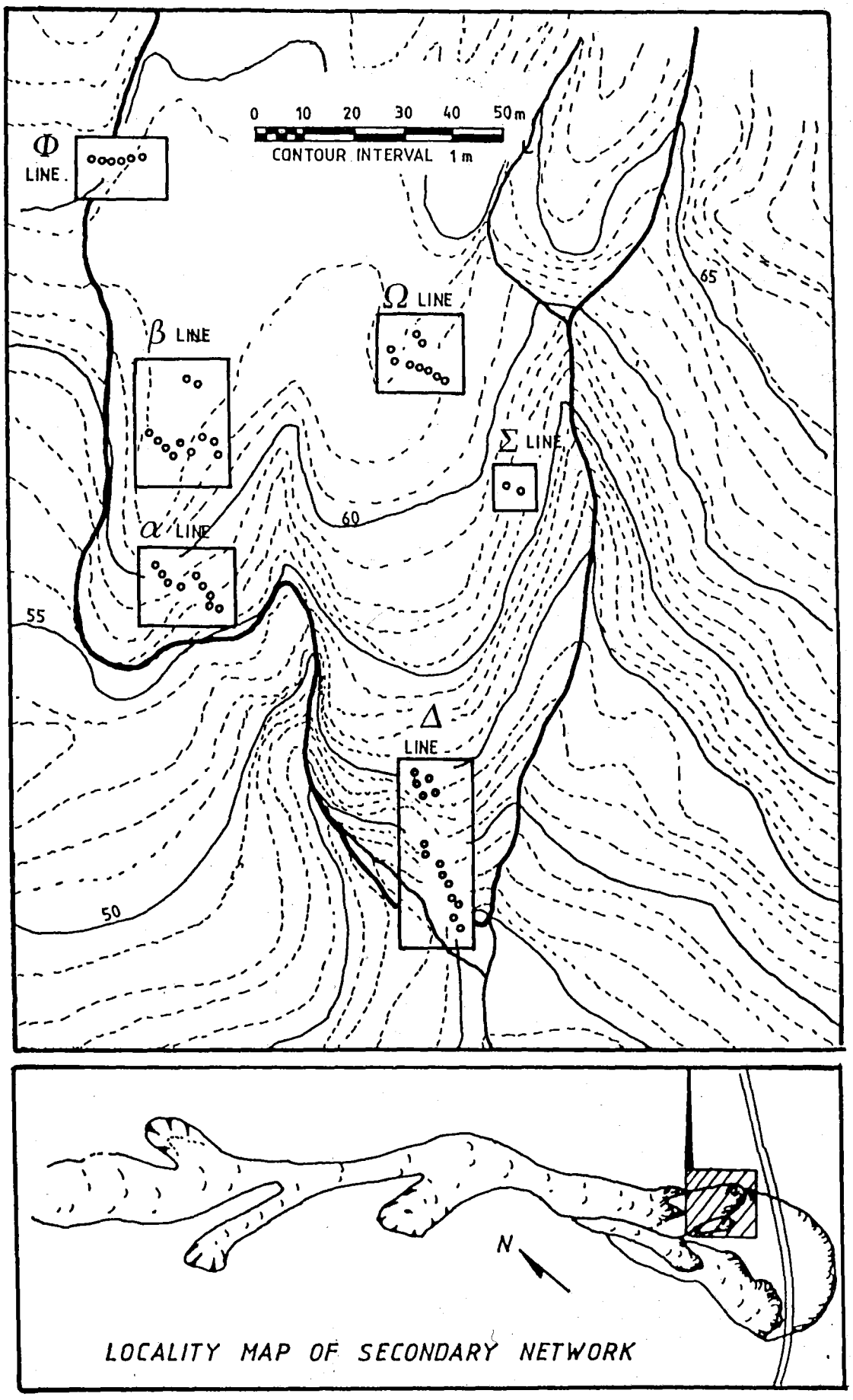

Fig. A9.4 Secondary monitoring network plan showing locations of each line of points.

A9.7.2 Crack Monitor Description

The crack width monitor is a simple device, constructed of aluminum alloy, which is intended to measure the vertical and horizontal components of movement between two fixed points (3/4 inch pipes), (see photo A9.2). The device is made up of 3 components consisting of a horizontal arm, a vertical arm, and a central "hub" which has nylon sleeves into which the two arms are inserted.

The two arms are extendable (telescoping) up to 1040 mm. At the end of each arm are machined fittings (end pieces) which are intended to sit flush in the pipes.

Readings are taken from the hub, which has vertical and horizontal scales. The device must be horizontally level and vertically plumb to give accurate measurements, as the distances are measured at the intersection of the vertical and horizontal arms. To accomplish this there is a level bubble mounted upon the hub.

A9.7.3 Use of Device

Use of the device is relatively straight forward and is outlined herein.

1. Assembly. Assemble the tool by inserting the horizontal arm into the horizontal aperture of the hub and the vertical arm through the vertical aperture. The horizontal arm is differentiated from the vertical arm by the end piece which is perpendicular to the arm.

2. Extension of the arms. The arms are telescoping and may, or may not, need to be extended to full length depending on the distance between the two points, however they must be either fully extended or completely retracted. This is so that readings are accurate. The arms are extended by pulling the telescoping ends until a red mark appears, then a spring loaded ball snaps into place to "lock" it there. It must not be extended past the red mark as the

ball may fly out and be injurious (ie. to eyes) or lost.

3. Placement of the device. The device is then placed on the monitoring points so that both the vertical and horizontal end pieces are fitting in their respective points. The monitoring points have machined tops which allows the end pieces to be inserted into them. The fit must not be binding to the device.

4. Leveling. The leveling of the bubble can be difficult and care is needed to obtain accurate results. As the there is only a single bubble, movement of either horizontal or vertical arms will move the bubble with the possibility of a "false leveling". This can occur when one of the arms is not the true length between points, but because of binding the bubble can be leveled. The best way to adjust the level is to move the arms in unison with the hub. This avoids binding, which can cause the vertical or horizontal arm to be too short or too long. Once the device is properly level, it should lift in and out of the points freely without binding. (This procedure takes practice).

5. Reading the tool. Each arm is marked every 10 mm and the hub has a scale which alows the measurment to be read to 0.5 mm. Reading the distance requires some practice as the scale can easily be misread. It must also be noted, while measuring, if the arms are fully extended or retracted, as the scale is read as if the arms are fully extended. If the arms are not extended, then a subtraction of 423.5 mm must be made to compensate for the retracted position.

A9.7.4 Problems

There are several problems which surfaced when the tool was used, primarilly because it is a new device and needs a few "bugs" worked out.

1. The Level Bubble. Whilst the single level bubble is adequate for obtaining accurate measurements, it may take

the user an unnecessary length of time to get it properly level. The problem is that either a vertical or horizontal adjustment can be made to centre the bubble, and the user may not know which movement is necessary; this problem is particularly noticable on long lengths.

2. End Pieces. The end pieces are designed to fit flush and square on the top of the monitoring points. This requires that the pipes are installed plumb, and that movement will not alter this. Driving the pipes in the ground to be reasonably plumb may be possible, but can be very difficult. Even if a point is installed plumb, movement can certainly alter it.

3. Scale. Markings for the horizontal distance are not correct even if read fully extended. This is because the scale is 50 mm to the left (short) of the centre of the hub (see Fig. A.9.5). Therefore 50 mm must be added to all readings if a true horizontal distance is required.

4. Length of Arms. The length of the telescoping arms have been adequate for this study, as movement was small, but where greater movement occurs there may be a need to add more length to the arms.

A9.7.5 Recomendations

The device could be improved in several ways to make it easier to use and more practical. The recomendations address the problems summarized above and are made from a users point of view. The author does not assume to have a technical expertise to advise the actual modifications necessary.

1. A vertical plumb and a horizontal level bubble should be added. This would enable fine adjustments to be made on the vertical and/or horizontal arms independantly, thus making the level procedure much faster as well as more accurate.

2. The end pieces of the arm could be converted from a "flush fit type" to a "ball-joint" type (see Fig. A9.5). Thus movement of the point or installation off plumb would not affect how the device rests on the monitoring points.

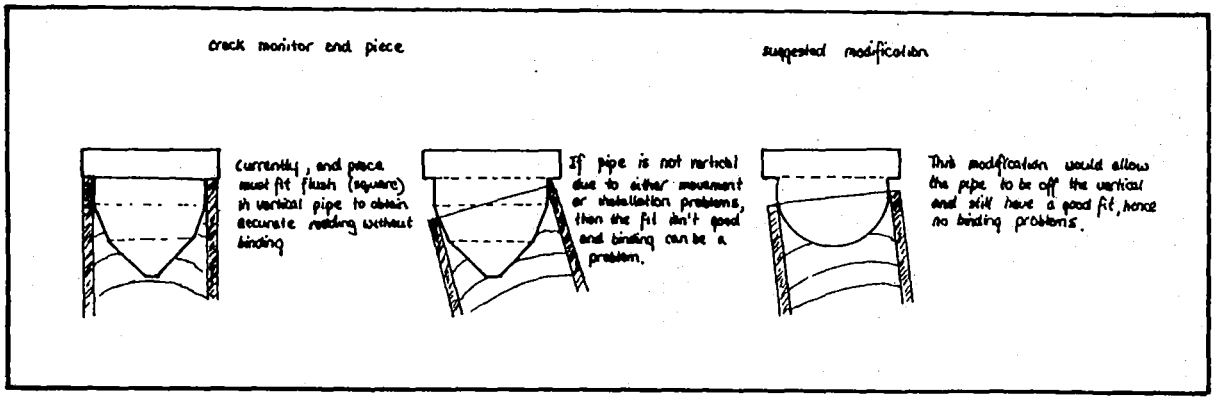

Figure A9.5 Recommended change to end piece.

3. The horizontal scale should either be moved to the centre of the hub, or the graduations on the arm be changed to compensate for the 50 mm offset.

4. Another telescoping section could be added to the arms to increase the length of measurable movement.

A9.7.6 Discussion

The Crack Width Monitor is basically a good design, as it is simple to use and is extremely accurate for measuring horizontal and vertical distances between two points. The modifications suggested above would only serve to enhance the performance and viability of the device.

There are many applications where the device could be very useful for monitoring movement. This is especially true when it is only possible for one person to take measurements, or where conventional survey systems are not warranted. Uses may include, areas with road or housing subsidence and movement, mining subsidence, or movement on landslides which are threatening to life and/or property.

Concerning the Wharanui Earthflow, the device will be useful for indicating an increase in activity without having to use conventional surveying methods (see Chapter Five).

A9.8 RESULTS

The results are shown in tabular form on the following pages. The monitoring points are organised by the line which they are on (Alpha, Beta, Sigma, Phi, Omega, or Delta). Refer to Fig. A9.4 for the locality of each line and point.

The table shows the original horizontal and vertical distance measured across a set of points on November, 1984 (survey 0). Each point was then re-measured in March, 1985 (survey 1); May, 1985 (survey 2); and August, 1985 (survey 3). The horizontal and vertical change from the prior survey are shown, and then the cumulative change from the initial measurement. The final cumulative change is in bold point for the horizontal and vertical changes.

The numbers are shown as a + or -, indicating a lengthing or shortening of the horizontal or vertical distance between the points. For example, on Alpha line between points 1 & 2, the original horizontal length was 1005.5 mm and the final length was 990.0 mm, which shows a length shortened by 15.5 mm (-15.5). The original vertical length is 832.5 mm and the final vertical length is 843.5 mm or a lengthening of 11.0 mm (+11.0). For interpretation of the results, see Chapter Four.

CRACK WIDTH MONITORING

ALPHA LINE ALL MEASUREMENTS IN MILLIMETERS

Point span	Survey no.	Horiz. length	Horiz. chg.	Cum. chg.	Vert. length	Vert. chg.	Cum. chg.
1-2	0	1005.5	----	----	832.5	----	----
	1	1003.5	-2.0	-2.0	835.5	+3.0	+3.0
	2	996.0	-7.5	-9.5	832.5	-3.0	0.0
	3	990.0	-6.0	-15.5	843.5	+11.0	+11.0
2-3	0	978.0	----	----	263.5	----	----
	1	974.0	-4.0	-4.0	262.5	-1.0	-1.0
	3	980.0	+6.0	+2.0	258.5	-4.0	-5.0
3-4	0	878.5	----	----	314.5	----	----
	1	883.0	+4.5	+4.5	315.5	+1.0	+1.0
	3	880.0	-3.0	+1.5	320.5	+5.0	+6.0
5-6	0	846.0	----	----	290.5	----	----
	1	848.0	+2.0	+2.0	288.5	-2.0	-2.0
	3	851.0	+3.0	+5.0	284.5	-4.0	-6.0
6-7	0	946.0	----	----	484.5	----	----
	1	944.0	-2.0	-2.0	481.5	-3.0	-3.0
	3	947.0	+3.0	+1.0	489.5	+8.0	+5.0
7-8	0	843.0	----	----	89.5	----	----
	1	848.5	+5.5	+5.5	89.5	0.0	0.0
	3	857.0	+8.5	+14.0	95.5	+6.0	+6.0
8-9	0	907.0	----	----	532.5	----	----
	1	904.0	-3.0	-3.0	534.5	+2.0	+2.0
	3	898.5	-5.5	-8.5	533.5	-1.0	+1.0

END OF ALPHA LINE

BETA LINE

Point span	Survey no.	Horiz. length	Horiz. chg.	Cum. chg.	Vert. length	Vert. chg.	Cum. chg.
1-2	0	961.5	----	----	263.5	----	----
	1	960.0	-1.5	-1.5	262.5	-1.0	-1.0
	3	957.0	-3.0	-4.5	263.5	+1.0	0.0
2-3	0	963.0	----	----	103.0	----	----
	1	962.0	-1.0	-1.0	100.5	-2.5	-2.5
	3	969.0	+7.0	+6.0	103.5	+3.0	+0.5
3-4	0	974.5	----	----	167.0	----	----
	1	975.0	+0.5	+0.5	169.5	+2.5	+2.5
	3	977.0	+2.0	+2.5	172.5	+3.0	+5.5
4-5	0	948.0	----	----	367.5	----	----
	1	929.0	-19.0	-19.0	364.5	-3.0	-3.0
	3	926.0	-3.0	-22.0	365.5	+1.0	-2.0

5-6	0	843.0	----	----	367.5	----	----
	1	843.0	0.0	0.0	299.5	+3.0	+3.0
	3	841.0	-2.0	**-2.0**	291.5	-8.0	**-5.0**
7-8	0	886.0	----	----	324.5	----	----
	1	890.0	+4.0	+4.0	328.5	+4.0	+4.0
	3	893.0	+3.0	**+7.0**	331.5	+3.0	**+7.0**
8-9	0	900.5	----	----	380.0	----	----
	1	891.0	-9.5	-9.5	383.5	+3.5	+3.5
	2	883.5	-7.5	-17.0	380.0	-3.5	0.0
	3	869.0	-14.5	**-31.5**	377.5	-2.5	-2.5
10-11	0	846.0	----	----	489.5	----	----
	1	847.0	+1.0	+1.0	489.0	-0.5	-0.5
	3	833.0	-14.0	**-13.0**	491.5	+2.5	**+2.0**

END OF BETA LINE

SIGMA LINE

Point span	Survey no.	Horiz. length	Horiz. chg.	Cum. chg.	Vert. length	Vert. chg.	Cum. chg.
1-2	0	865.5	----	----	651.0	----	----
	1	864.0	-1.5	-1.5	654.5	+3.5	+3.5
	2	859.0	-5.0	-6.5	645.0	-9.5	-6.0
	3	851.0	-8.0	**-14.5**	650.0	+5.0	**-1.0**

END OF SIGMA LINE

PHI LINE

Point span	Survey no.	Horiz. length	Horiz. chg.	Cum. chg.	Vert. length	Vert. chg.	Cum. chg.
1-2	0	930.5	----	----	694.5	----	----
	1	940.0	+9.5	+9.5	693.0	-1.5	-1.5
	2	939.0	-1.0	+8.5	693.5	+0.5	-1.0
	3	930.0	-9.0	**-0.5**	697.0	+3.5	**+2.5**
2-3	0	966.5	----	----	346.0	----	----
	1	979.5	+13.0	+13.0	383.0	+37.0	+37.0
	2	978.0	-1.5	+11.5	381.5	-1.5	+35.5
	3	973.0	-5.0	**+6.5**	373.5	-8.0	**+27.5**
3-4	0	898.5	----	----	223.0	----	----
	1	886.0	-12.5	-12.5	200.5	-22.5	-22.5
	2	889.0	+3.0	-9.5	201.5	+1.0	-21.5
	3	897.0	+8.0	**-1.5**	193.5	-8.0	**-29.5**
4-5	0	1018.0	----	----	364.5	----	----
	1	1008.0	-10.0	-10.0	363.5	-1.0	-1.0
	2	1007.0	-1.0	-11.0	-----		
	3	1020.0	+13.0	**+ 2.0**	373.5	+9.0	**+9.0**

5-6	0	997.0	----	----	247.5	----	----
	1	994.0	-3.0	-3.0	237.5	-10.0	-10.0
	2	992.5	-1.5	-4.5	238.5	+1.0	-9.0
	3	993.0	+0.5	**-4.0**	254.5	+16.0	**+7.0**

END OF PHI LINE

OMEGA LINE

Point span	Survey no.	Horiz. length	Horiz. chg.	Cum. chg.	Vert. length	Vert. chg.	Cum. chg.
1-2	0	868.0	----	----	418.5	----	----
	1	860.5	-7.5	-7.5	420.0	+1.5	+1.5
	2	860.0	-0.5	-8.0	419.0	-1.0	+0.5
	3	855.0	-5.0	**-13.0**	420.5	+1.5	**+2.0**
3-4	0	986.0	----	----	513.5	----	----
	1	971.0	-15.0	-15.0	499.0	-14.5	-14.5
	2	965.0	-6.0	-21.0	497.5	-1.5	-16.0
	3	943.0	-22.0	**-43.0**	492.5	-5.0	**-21.0**
4-5	0	729.5	----	----	337.5	----	----
	1	736.0	+6.5	+6.5	343.5	+6.0	+6.0
	2	735.5	-0.5	+6.0	339.5	-4.0	+2.0
	3	743.0	+8.0	**+14.0**	359.5	+20.0	**+22.0**
5-6	0	765.0	----	----	130.5	----	----
	1	759.5	-5.5	-5.5	128.5	-2.0	-2.0
	2	751.0	-8.5	-14.0	127.5	-1.0	-3.0
	3	767.0	+16.0	**+2.0**	116.5	-11.0	**-14.0**
6-7	0	804.0	----	----	118.5	----	----
	1	793.5	-10.5	-10.5	117.5	-1.0	-1.0
	2	792.5	-1.0	-11.5	110.0	-7.5	-8.5
	3	777.0	-15.5	**-27.0**	112.5	+2.5	**-6.0**
8-9	0	904.5	----	----	444.5	----	----
	1	902.0	-2.5	-2.5	447.5	+3.0	+3.0
	2	897.0	-5.0	-7.5	446.0	-1.5	+1.5
	3	894.0	-3.0	**-10.5**	450.5	+4.5	**+6.0**

END OF OMEGA LINE

DELTA LINE

Point span	Survey no.	Horiz. length	Horiz. chg.	Cum. chg.	Vert. length	Vert. chg.	Cum. chg.
1-2	0	824.0	----	----	765.5	----	----
	1	826.0	+2.0	+2.0	766.0	+0.5	+0.5
	2	826.5	+0.5	+2.5	766.0	0.0	+0.5
	3	PEG NO. 1 DISAPEARED					
3-4	0	889.0	----	----	703.0	----	----
	1	890.0	+1.0	+1.0	700.0	-3.0	-3.0
	2	888.0	-2.0	-1.0	703.0	+3.0	0.0
	3	893.0	+5.0	**+4.0**	704.0	+1.0	**+1.0**

4-5	0	891.5	----	----	760.5	----	----
	1	870.5	-21.0	-21.0	760.0	-0.5	-0.5
	2	874.0	+4.0	-17.0	760.0	0.0	-0.5
	3	866.0	-18.0	**-35.0**	757.0	-3.0	**-0.5**
5-6	0	824.0	----	----	518.5	----	----
	1	839.5	+15.5	+15.5	521.0	+2.5	+2.5
	2	843.5	+4.0	+19.5	518.0	-3.0	-0.5
	3	851.0	+7.5	**+27.0**	420.5	+2.5	**+2.0**
6-7	0	954.5	----	----	779.5	----	----
	1	939.0	-15.5	-15.5	780.0	-0.5	-0.5
	2	935.0	-4.0	-19.5	778.0	-2.0	-1.5
	3	930.0	-5.0	**-24.5**	779.0	+1.0	**-0.5**
8-9	0	917.0	----	----	560.0	----	----
	1	915.5	-1.5	-1.5	564.0	+4.0	+4.0
	2	914.0	-1.5	-3.0	561.5	-2.5	+1.5
	3	918.0	+4.0	**+1.0**	559.0	-2.5	**-1.0**
10-12	0	866.0	----	----	505.5	----	----
	1	866.0	0.0	0.0	504.5	-1.0	-1.0
	2	866.0	0.0	0.0	502.5	-2.0	-3.0
	3	872.6	+6.0	**+6.0**	502.5	0.0	**-3.0**
12-14	0	996.5	----	----	540.0	----	----
	1	1002.5	+6.0	+6.0	541.5	+1.5	+1.5
	2	1000.0	-2.5	+3.5	540.5	-1.0	+0.5
	3	996.0	-4.0	**-0.5**	539.5	-1.0	**-0.5**
11-13	0	793.0	----	----	508.5	----	----
	1	790.0	-3.0	-3.0	509.5	+1.0	+1.0
	2	788.0	-2.0	-5.0	508.5	-1.0	0.0
	3	791.0	+3.0	**-2.0**	510.5	+2.0	**+2.0**

END OF DELTA LINE

APPENDIX TEN

HISTORY OF REMEDIAL MEASURES ON THE WHARANUI EARTHFLOW

A10.1 INTRODUCTION

Remedial measures began on the Wharanui earthflow in 1974 with the installation of drains in the toe area. At the time, this drainage scheme seemed to be slowing down movement but it was desired by the MWD to stabilize the whole earthflow.

In October 1976, proposals were made by the MWD to stabilize the "slip" by a drainage scheme and by "close" planting. Installation of new drainage works consisted of a cut-off "Vee" drain, and 44 gallon drums buried and used as collection points. The Vee drain was made using a 37mm slotted pipe in filter gravel to collect surface and subsurface water. The drums and Vee drain were linked to one another by 37mm PVC pipe and water was to be disposed of through the pipe to the highway culvert. The close planting of 8 ha of Pinas Radiata in the upper catchment (upper half of the slip) was proposed. The existing drainage system in the toe area was to be upgraded (see Fig. A10.1).

The Marlborough Catchment Board was asked to undertake planting and management of the proposed planting, but there was opposition to close planting from the owner, Mr. D.J. Parsons, as it was prime grazing land. Space planting was permitted. It was agreed that the upper half of the catchment was to be fenced off and grazing denied to cattle for up to 5 years, with sheep allowed to graze sooner.

A10.2 INSTALLATION OF WORKS AND PLANTING

The MWD installed the "up-graded" drainage scheme in summer of 1976-1977, and the Parsons fenced off the upper catchment. In July of 1977 space planting of trees began. Poplars were planted on the flow itself and eucalyptus on the sides of the catchment.

A10.3 SCHEME HISTORY

1977-

Heavy rains late in July damaged the drainage system. The Vee drain became only 1/3 functional as the filter gravel was washed out by tributary gully flows. In October the MWD modified the dewatering system by digging in 2 additional 44 gallon drums. The Vee drain was not repaired.

1978-

In August-September the Catchment Board planted additional Eucalyptus and Poplars.

1980-

In February a severe hailstorm reduced foliage of the trees by up to 90%, and on March 2, 3, & 4 during a high intensity storm it rained 500 mm triggering severe slipping on both sides of the catchment. Continual movement of the flow resulted in the Parsons abandoning the fence across the slip, as it kept breaking, in favour of a "floodgate", (a fence suspended from across the flow as opposed to conventional posts in the ground).

The Catchment Board found results of the planting so poor that they recomended acquiring the land, and close planting the whole in P. Radiata or C. Macrocarpa.

1981-

In September the MWD was unsatisfied with drainage scheme and they were interested in doing something else. Suggestions were made for design of a deeper drainage scheme but there were uncertainties as to the depth and shape of the slip plane. Recomendations were made for a backhoe pits to be dug to investigate the slip, but nothing further came of this and the existing drainage scheme was repaired and reconnected.

1982-

In April of the year the drainage pipes again had to be reconnected.

1984-

In February Brian Paterson of the New Zealand Geological Survey, (Christchurch) was requested to look at the slip. His recomendations included reinstating the drainage scheme (as it had again come apart), and further investigations of the slip. In June the System was once again repaired by the MWD, but in a matter of months the pipes were broken at the joints again.

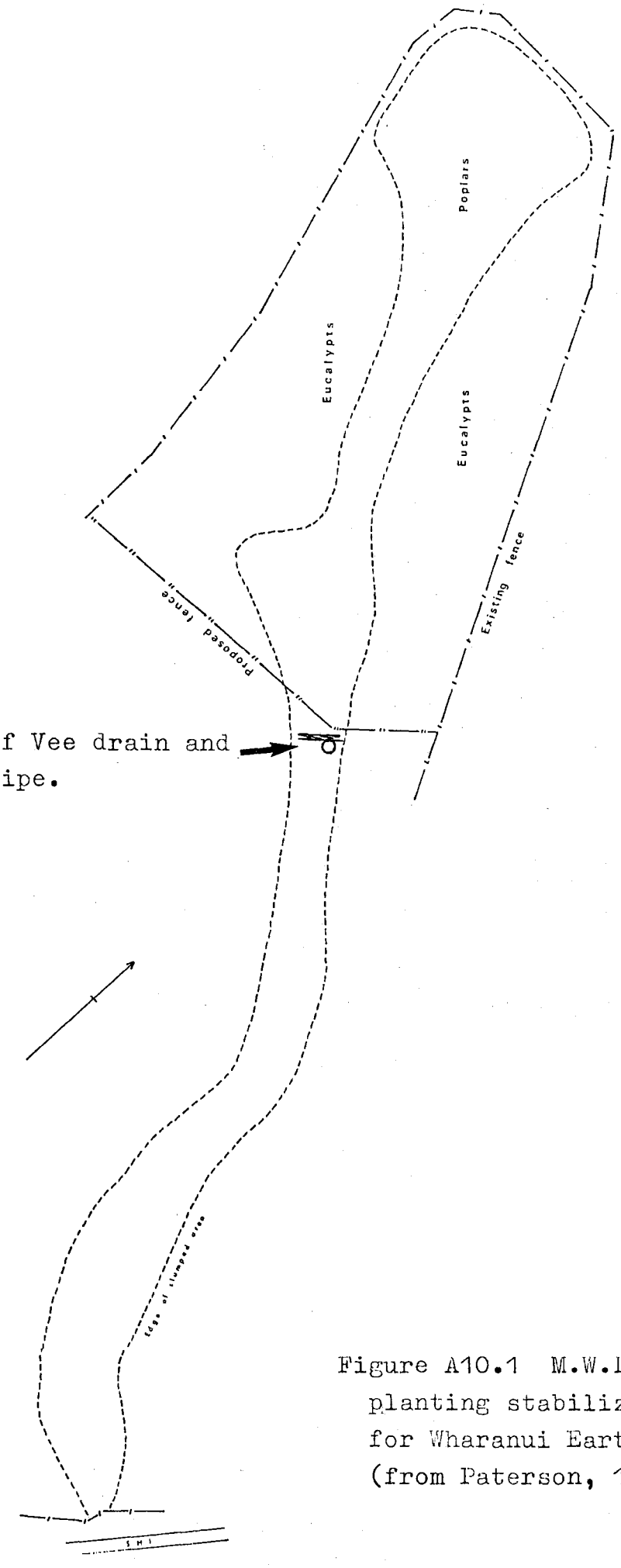

Figure A10.1 M.W.D. proposed planting stabilization scheme for Wharanui Earthflow, 1976 (from Paterson, 1984)